



Università degli Studi di Torino

Doctoral School of the University of Torino

PhD Programme in Chemical and Materials Sciences, XXXIII Cycle

Lewis and Brønsted acid-catalysed synthetic transformations: new avenues for C-C bond formation



Stefano Nejrotti

Supervisor:
Prof. Cristina Prandi



Università degli Studi di Torino

Doctoral School of the University of Torino

PhD Programme in Chemical and Materials Sciences, XXXIII cycle

**Lewis and Brønsted acid-catalysed synthetic transformations: new
avenues for C-C bond formation**

Candidate: **Stefano Nejrotti**

Supervisor: Prof. **Cristina Prandi**

Jury Members: Prof. **Vittorio Pace**
Università degli Studi di Torino
Dipartimento di Chimica

Prof. **Elisabetta Rossi**
Università degli Studi di Milano
Dipartimento di Scienze Farmaceutiche

Prof. **Antonio M. Echavarren**
Institut Català d'Investigació Química

Head of the Doctoral School: Prof. Alberto Rizzuti

PhD Programme Coordinator: Prof. Bartolomeo Civalieri

Torino, 2021

Acknowledgements

A PhD is not only a job and a significant step in the professional growth of the student, it is not only a three-years-long travel, but it truly is a life experience that affects you and determines what person you are at the end of it. In this perspective, I feel that this dissertation should begin by acknowledging the people who contributed the most to my PhD.

First of all, I would like to acknowledge Cristina, my supervisor. She has always believed in me and never made me feel alone or unsupported, even in the most critical moments of these three years. She has advised me wisely and I could learn a lot from her, and not just from a scientific point of view. I am grateful to her for giving me her trust and the freedom to experiment my own research ideas.

I would like to acknowledge prof. Antonio Echavarren, who hosted me in his group in Tarragona for my abroad period. I am grateful to him for our discussions and for the scientific and human growth that I experienced during my stay in Tarragona. On this regard, dr. Allegra Franchino is deeply acknowledged too.

I would then like to thank all the colleagues with whom I shared these three years: MSc students, PhD students, post-docs and professors. In our academic world, the people around you often change, and in the timespan of a PhD I have made acquaintance with many. Some of them have passed, some of them have stayed, some of them, even if we do not share the laboratory anymore, have turned into a loyal and affectionate companion.

Lastly, I would like to acknowledge my family, primarily my parents, Andrea and Roberta, and my brother, Davide. They have put me in condition to express myself in the way I saw fit, and they have always supported me and helped to face adversities, even those on which they could not have any direct influence. I am grateful to them for their critical voice on my approach to work and related matters.

*I suppose it is tempting, if the only tool you have is a hammer,
to treat everything as if it were a nail.*
Abraham Maslow

Table of content

Abstract	1
List of abbreviations	3
Chapter 1: Gold(I)-catalysed activation of alkynes	4
1.1 Au(I) complexes	4
1.1.1 <i>Neutral [LAuCl] complexes</i>	4
1.1.2 <i>Neutral [LAuX] and cationic [LAuL]⁺X⁻ complexes</i>	5
1.2 Reactivity of Au(I) complexes	7
1.2.1 <i>Activation of alkynes</i>	7
1.2.2 <i>Effect of the ligand</i>	9
1.2.3 <i>Effect of the counterion</i>	12
1.3 Hydroarylation of alkynes	14
1.3.1 <i>Friedel-Crafts-type electrophilic aromatic substitution</i>	14
1.3.2 <i>The furan-yne hydroarylation pathway</i>	17
1.3.3 <i>Arenes functionalisation through oxidative gold catalysis with nucleophilic oxidants</i>	18
References	21
Chapter 2: Gold(I)-catalysed intramolecular hydroarylation of lactam-derived 1,3-enynes	24
2.1 Lactam and lactone-derived triflates and phosphates as versatile building blocks in synthesis	24
2.2 Synthesis of the substrates	26
2.3 Study of the reaction conditions	27
2.4 Regioselectivity	30
2.5 Reaction substrate scope	32
2.6 Structural analysis of the tetrahydrobenzo[<i>g</i>]quinolines	33
2.7 Conclusion	36
2.8 Experimental section	36
References	58
Chapter 3: Gold(I)-catalysed divergent reactivity of furan-ynes with <i>N</i>-oxides	60

3.1	Reactions of furans with gold(I) carbenes	60
3.2	Study of the reaction conditions	62
3.2.1	<i>Optimisation of the divergent reactivity</i>	62
3.2.2	<i>Mechanistic hypothesis</i>	66
3.3	Reaction substrate scope	67
3.4	Conclusion	69
3.5	Experimental section	69
	References	81
Chapter 4: Bifunctional ligands for the silver-free activation of gold(I) chloride complexes		82
4.1	Silver-free activation of Au complexes	82
4.2	Synthesis of the complexes	84
4.2.1	<i>Synthesis of the ligands</i>	84
4.2.2	<i>Complexation</i>	86
4.3	Preliminary results on catalytic activity	86
4.4	Conclusion	88
4.5	Experimental section	88
	References	95
Chapter 5: Deep eutectic solvents in organic synthesis		96
5.1	Deep eutectic solvents: general features	96
5.1.1	<i>Composition</i>	96
5.1.2	<i>Green credentials</i>	98
5.2	Deep eutectic solvents in organic synthesis	99
5.2.1	<i>Acid- and base-catalysed reactions</i>	99
5.2.2	<i>Transition metal-catalysed reactions</i>	101
5.2.3	<i>Operational aspects</i>	103
	References	106
Chapter 6: The Nazarov cyclisation in natural deep eutectic solvents		109
6.1	The Nazarov cyclisation	109
6.1.1	<i>General features</i>	109
6.1.2	<i>Improving sustainability of the Nazarov cyclisation</i>	110

6.2	Study of the reaction conditions	112
6.3	Reaction substrate scope	115
6.4	Recycling of the eutectic mixture	117
6.5	Conclusion	120
6.6	Experimental section	121
	References	134
	Appendix: Gold(I)-catalysed hydroarylation reactions in deep eutectic solvents	136
	Experimental section	138
	References	140

Abstract

One of the main goals of modern synthetic chemistry is to develop new and efficient chemical processes under sustainable conditions. During my PhD I undertook the project of developing new synthetic strategies based on two independent but ultimately not unrelated research lines: homogeneous gold(I) catalysis and reactivity in unconventional solvents.

Homogeneous catalysis is an incredibly large and diversified area of organic chemistry. New synthetic methodologies taking advantage of catalytic reactions are continuously reported. The efforts in developing new methodologies are generally oriented towards three main aims, all of which relate with attaining a better understanding of the underlying mechanistic picture, in view of further and improved efficiency of catalysis as a key aspect of chemical processes:

- 1) Discovering unprecedented reactions or applying known reactivities to new substrates.
- 2) Improving an already known reaction in terms of yield and selectivity.
- 3) Enhancing the sustainability of a reaction by reducing both its environmental and economic impact.

A large part of catalytic methodologies is represented by reactions that are catalysed by transition metal salts and complexes. Among these, gold plays a significant role because of its peculiar reactivity. The exploitation of the unique properties of gold as a soft Lewis acid has disclosed several organic transformations that are in general characterised by their excellent selectivity and the mild conditions required.

In the first part of this thesis, the investigation on gold(I)-catalysed synthetic methodologies is presented. My work mainly focused on the manipulation and functionalization of *O*- and *N*-heterocycles through gold(I) catalysis. Indeed, the possibility to access structurally diversified heterocyclic molecular scaffolds from easily accessible common precursors is of high synthetic value, given the relevance of these structures among natural and pharmaceutical compounds. Gold(I) catalysis is addressed in Chapters 2–4. More in detail, the gold(I)-catalysed hydroarylation of lactam-derived heterocyclic alkynes for the synthesis of tetrahydrobenzo[*g*]quinolines is reported in Chapter 2, and the divergent gold(I)-catalysed reactivity of furans with *N*-oxides is reported in Chapter 3. Alongside with this, the development of new gold(I) complexes possessing bifunctional ligands is presented in Chapter 4. This part of the project was carried out during a visiting period in the group of prof. Antonio Echavarren at the Institute of Chemical Research of Catalonia (ICIQ) in Tarragona, Spain.

Furthermore, as previously said, significant advances in the field of organic methodology are also being done to improve sustainability. This issue has seen growing attention from the scientific community since the formulation of the 12 principles of green chemistry in 1998. Among the main topics are the replacement of hazardous reagents and solvents with safer ones. In this direction, deep eutectic solvents are of particular interest, because of their green credentials and their effectiveness in promoting several organic reactions without the need of additional additives or catalysts. Chapter 6 reports the study on the application of deep eutectic solvents as active reaction media for a Brønsted acid catalysed reaction, the Nazarov cyclisation. Lastly, an Appendix is dedicated to the preliminary investigation on the gold(I)-catalysed hydroarylation reaction in deep eutectic solvents.

List of abbreviations

Ad	1-adamantyl
Bn	benzyl
Boc	<i>tert</i> -butoxycarbonyl
Ch	choline
CPME	cyclopentyl methyl ether
DCE	1,2-dichloroethane
DCM	dichloromethane
DES	deep eutectic solvent
Dipp	2,6-diisopropylphenyl
dippf	1,1'-bis(diisopropylphosphino)ferrocene
DMF	<i>N,N</i> -dimethylformamide
DMS	dimethylsulfide
DMSO	dimethylsulfoxide
DMU	1,3-dimethylurea
DTBP	di- <i>tert</i> -butylphenol
Gly	glycerol
HBA	hydrogen bond acceptor
HBD	hydrogen bond donor
HFIP	1,1,1,3,3,3,-hexafluoropropan-2-ol
IL	ionic liquid
IMes	1,3-bis(2,4,6-trimethylphenyl)-1,3-dihydro-2 <i>H</i> -imidazol-2-ylidene
IPr	1,3-bis(2,6-diisopropylphenyl)-1,3-dihydro-2 <i>H</i> -imidazol-2-ylidene
LA	Lewis acid
Mes	2,4,6-trimethylphenyl
mp	melting point
Ms	methanesulfonyl
NaDES	natural deep eutectic solvent
NHC	<i>N</i> -heterocyclic carbene
PE	petroleum ether
PG	protecting group
Tf	trifluoromethanesulfonyl
TFA	trifluoroacetic acid
TFAA	trifluoroacetic anhydride
THT	tetrahydrothiophene
TMS	trimethylsilyl
Tol	tolyl
TON	turnover number
Ts	<i>p</i> -toluenesulfonyl
VOC	volatile organic compound
XBD	halogen bond donor

Chapter 1: Gold(I)-catalysed activation of alkynes

The role of gold in organic chemistry has shifted in the last two decades from being considered as poorly useful, due to its redox inertness, to becoming a widely employed tool in synthesis. After the seminal reports by Teles on the hydroalkoxylation of alkynes^[1] and by Hashmi on the synthesis of furans,^[2] the new century has witnessed the flourish of novel synthetic methodologies involving gold catalysis, as well as a deeper understanding of their mechanistic features.^[3] The success of gold catalysis relies in some characteristics that make Au(I) and Au(III) unique among other soft Lewis acids: notably, their peculiar affinity for π -systems, which has been attributed to relativistic effects,^[4] their good tolerance for other electron-rich functional groups and the possibility to tune the reactivity by the appropriate choice of the ligands on the metal centre.

In the present chapter some relevant features of Au(I) complexes and of their catalytic activity towards alkynes will be discussed, with the exception of asymmetric gold catalysis.

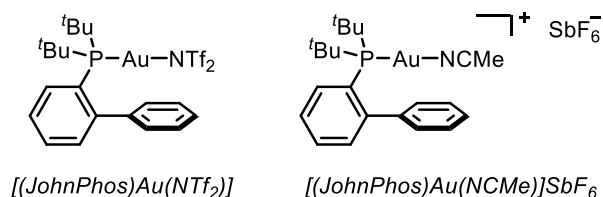
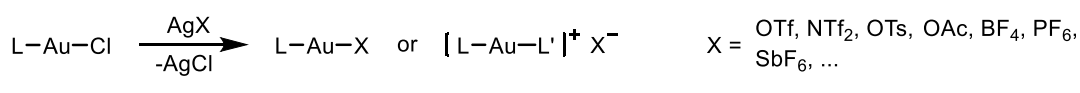
1.1 Au(I) complexes

1.1.1 Neutral [LAuCl] complexes

Gold(I) complexes are usually linear dicoordinated [LAuL']-type complexes. The ancillary ligand L can be a phosphorus-based ligand or a *N*-heterocyclic carbene (NHC) and tightly coordinates the metal centre, effecting the electronic and steric features of the complex. The further coordination position can be occupied by an anionic ligand, as in the case of gold(I) chlorides [LAuCl] or other neutral [LAuX] complexes, or by a second neutral ligand, giving rise to cationic [LAuL']⁺X⁻ complexes.

Gold(I) chloride complexes are commonly employed because they are bench-stable, their synthesis is feasible and many of them are commercially available. However, [LAuCl] complexes are usually not active as catalysts and are regarded as pre-catalysts, because the chloride ligand is too coordinating and thus prevents the interaction with the substrate. As shown in Figure 1.1, common ligands include phosphines, phosphites and NHCs.

of the gold(I) chloride precursor and the silver(I) salt, or alternatively the active complex can be synthesised and isolated after removal of AgCl by filtration.^[5] Neutral [LAuX] complexes are isolated if the anion X⁻ is sufficiently coordinating, such as triflate (TfO⁻) or triflimide (Tf₂N⁻), while very weakly coordinating anions, such as BF₄⁻, PF₆⁻ or SbF₆⁻ lead to the isolation of [LAuL']⁺X⁻ complexes in which L' is a weak neutral ligand, usually acetonitrile or benzonitrile.^[6]



Scheme 1.2 Anion metathesis of LAuCl complexes. The coordinating strength of X⁻ determines the LAuX or [LAuL']⁺X⁻ nature of the JohnPhos gold complexes.

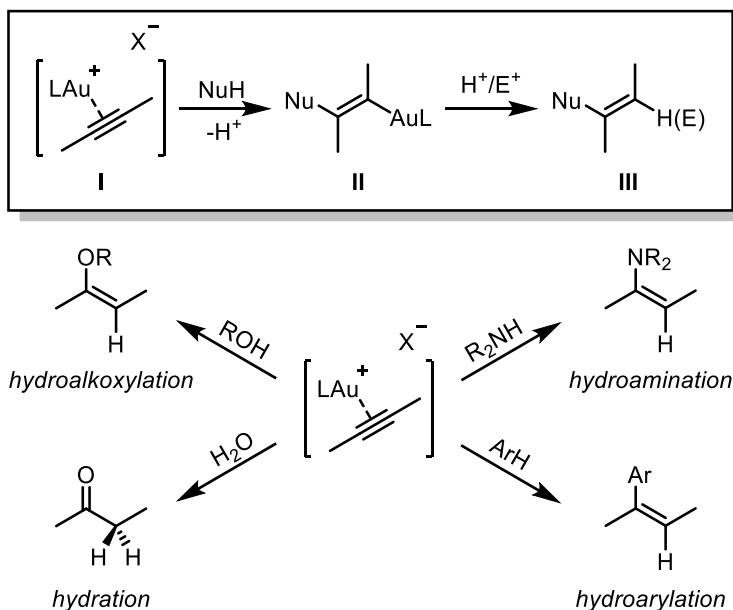
Both [LAuX] and [LAuL']⁺X⁻ are active electrophilic gold complexes that in solution can coordinate π-systems, thus affording [LAuL']⁺X⁻ species, in which L' is now a substrate molecule, and starting the catalytic cycle.

When the active species is generated *in situ* from a gold(I) chloride precursor, the presence of silver in the reaction medium is not always innocent towards the gold catalysis. A comparison of the outcome of different gold(I)-catalysed reactions, performed either with *in situ* generated or preformed Ag-free Au(I) catalysts, led Shi to propose a categorization into three classes: 1) “genuine” gold catalysis, in which the presence or absence of Ag(I) does not influence the yield of the reaction; 2) Au/Ag bimetallic catalysis, in which the Au(I) catalyst alone is not effective in promoting the reaction, and the presence of Ag(I) is required; 3) Ag(I)-assisted catalysis, in which the Au(I) catalyst alone is active, but the presence of silver significantly enhances the reaction yield.^[7] Some studies have tried to shed light on this so-called “silver effect”. The isolation of stable Au-Ag bimetallic or trimetallic complexes suggested that the Au/Ag ratio influences the speciation equilibria and consequently the formation of catalyst resting state and active species.^[8] Also, not all the unsaturated substrates display the same ability to cleave those polynuclear complexes and effectively start the catalytic cycle.^[9]

1.2 Reactivity of Au(I) complexes

1.2.1 Activation of alkynes

A remarkable feature of Au(I), as well as Au(III), is its ability to selectively coordinate and activate π -systems, especially alkynes, in the presence of other electron-rich functional groups, such as *O*- and *N*-based ones. The nucleophilic addition to a triple bond involves the *anti*-attack of the nucleophile onto the activated unsaturated system (Scheme 1.3, **I**), with gold shifting from π -coordination to a *trans*- σ -alkenyl complex **II**. The latter can undergo protodeauration, *i.e.* substitution of the coordinated gold with a proton, resulting in an overall addition of Nu-H to the triple bond (hydrofunctionalisation); alternatively, reaction with an electrophile is possible. Although π -activation is the most simple and common mode of action, dual σ,π -activation has also been proposed to account for a number of gold-catalysed transformations of terminal alkynes.^[10]



Scheme 1.3 Au(I)-catalysed nucleophilic addition to alkynes. General examples of hydrofunctionalisation reactions.

Beyond nucleophilic addition, more complicated reaction pathways involving rearrangements, eliminations and fragmentations can take place, depending on the substrate and the gold catalyst. Among those, a wide range of methodologies involving gold(I) carbenes of general structure [LAu(CR₂)]⁺ have been reported throughout the years.^[11]

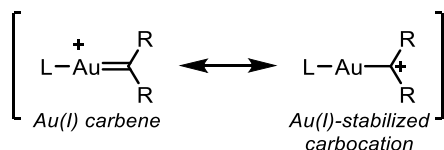
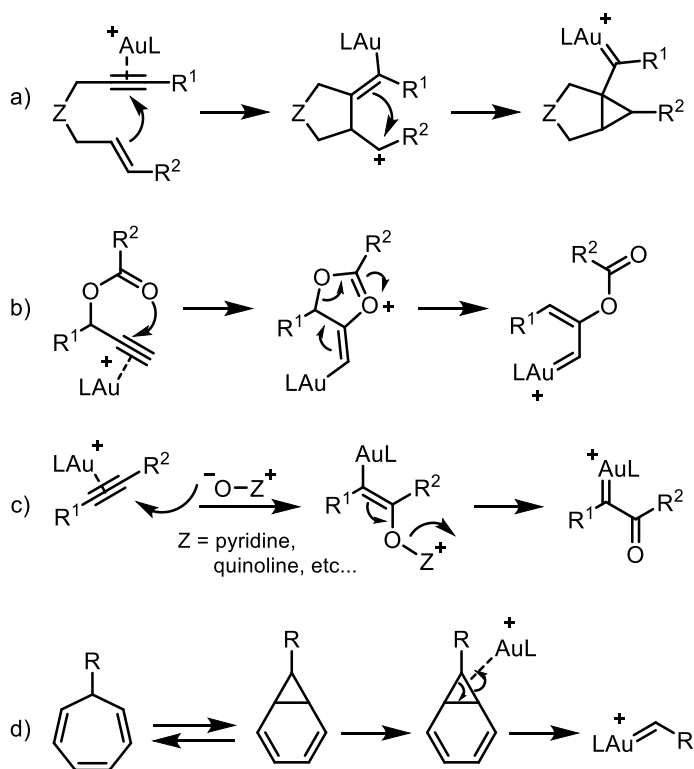


Figure 1.2 Resonance structures for gold(I) carbenes.

These intermediates can be described by two resonance structures, as gold(I) carbenes or gold(I)-stabilized carbocations (Figure 1.2). Their generation can take place through different reaction pathways, including but not limited to cycloisomerisation of 1,*n*-enynes (Scheme 1.4, a),^[12] 1,2-acyloxy migration of propargyl esters (Scheme 1.4, b),^[13] oxidation of alkynes with *N*-oxides species (Scheme 1.4, c)^[14] and *retro*-Buchner reaction (Scheme 1.4, d).^[15]



Scheme 1.4 Examples of the generation of Au(I) carbene intermediates.

Once formed, the electrophilic gold(I) carbene intermediates can undergo common carbene reactivity, such as cyclopropanations, insertions, rearrangements and reactions with nucleophiles.

1.2.2 Effect of the ligand

The reactivity of an Au(I) complex is strongly influenced by the electronic and steric features of its ancillary ligand. The selectivity of a gold(I)-catalysed transformation, as well as its efficiency, can be tuned by the appropriate choice of the ligand.^[16] A wide body of experimental and theoretical investigation has led to a better understanding of this influence, thus allowing for general guidelines to help direct the trial-and-error approach that is generally adopted for the optimisation of a gold-catalysed reaction.

The bonding model for gold(I) carbenes proposed by Toste and Goddard in 2009 involves the contribution of σ -donation from the ligand and the carbene moiety to the metal centre, and backdonation from the filled π orbitals of gold (Figure 1.3).^[17] Both the ligand and the substrate compete for electron density: therefore, a carbene-like structure is favoured by more σ -donating ligands, such as *N*-heterocyclic carbenes, while ligands with a stronger π -acidity, such as phosphites, favour a carbocation-like structure.^[11]

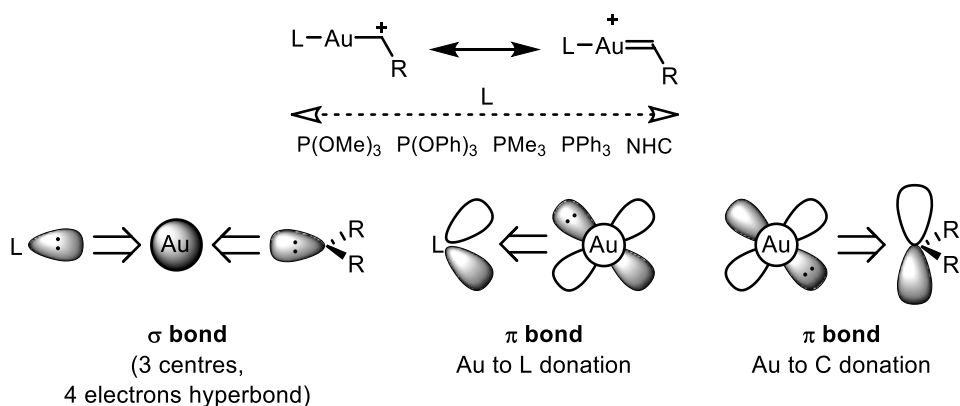
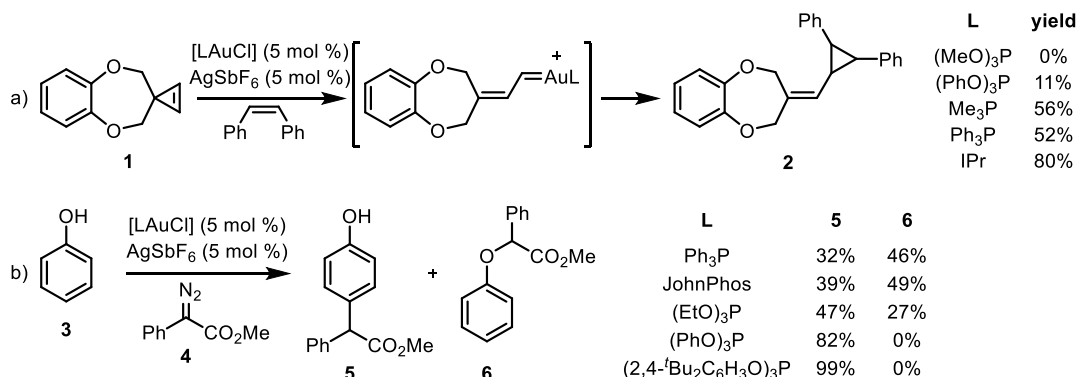


Figure 1.3 Bonding model for gold(I) carbenes and influence of the electronic features of the ligand.

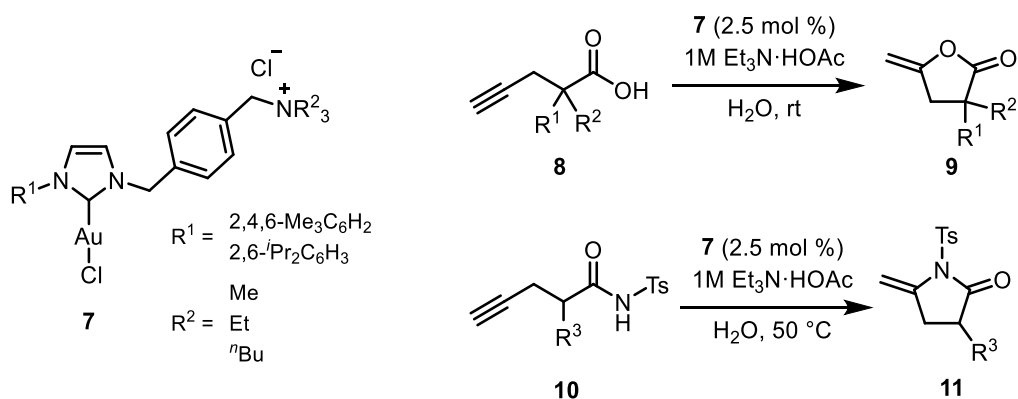
The tendency is well exemplified by the ring opening of cyclopropene **1**, followed by cyclopropanation of the gold(I) carbene with *cis*-stilbene to product **2**. As shown in Scheme 1.5, a, the *N*-heterocyclic carbene IPr proved to be the best ligand for this carbene reactivity.^[17] When the gold(I) carbene generated upon treatment of α -diazoacetate **4** with Au(I) catalysts was reacted with phenol **3**, two products were observed: *para*-substituted phenol **5**, resulting from electrophilic aromatic substitution, a typical carbocation reaction, as well as phenyl ether **6** from O-H insertion, a carbene reaction (Scheme 1.5, b). With electrophilic phosphite ligands, the selectivity for the carbocation-like reactivity was complete.^[18] It should

be remarked that with other metals, such as Pd(II), Cu(I), Rh(II) and Re(VII) the reaction was selective for the O-H insertion.^[19]



Scheme 1.5 Effect of the ligand on the carbene *vs* carbocation reactivity.

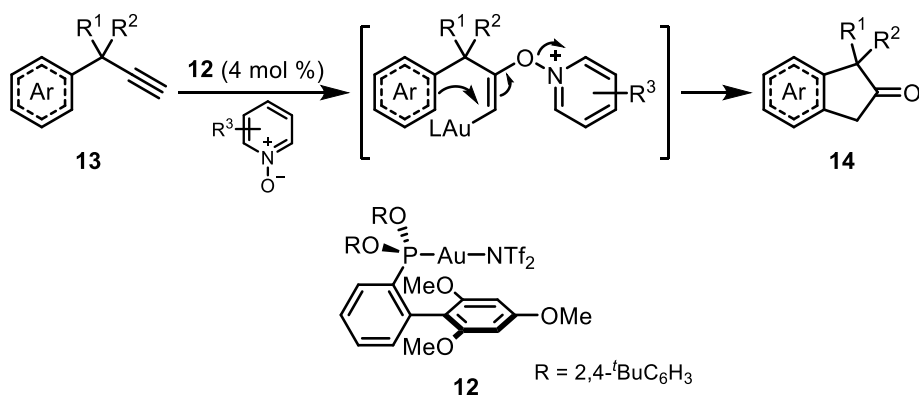
In light of these considerations, NHCs are often privileged ligands for catalytic transformations involving gold(I) carbene species.^[20] Water soluble Au(I) complexes have been synthesised by modification of the NHC core through functionalisation with charged functional groups^[21] or even biotin and cyclodextrins,^[22] thus extending the field of application and allowing for more sustainable methodologies (Scheme 1.6). Interestingly, complexes **7** were all able to selectively promote the cycloisomerisation of γ -alkynoic acids **8** and lactams **10** against hydration in the aqueous medium, and no activation of the [LAuCl] species with Ag(I) salts was required.^[21d]



Scheme 1.6 Cycloisomerisation of γ -alkynoic acids and amides with ammonium-tagged water soluble NHC Au(I) complexes.

Buchwald-type dialkyl biarylphosphines (Figure 1.1) represent another relevant class of ligands for Au(I) catalysis.^[23] They are more electron-rich than triarylphosphines and their steric properties can be modulated by functionalisation

of the biaryl moiety. An interesting combination of biarylphosphine steric bulkiness and phosphite electron-poor character was proposed by Gagosz with his biarylphosphonite Au(I) complex **12**, which was able to successfully promote the oxidative synthesis of indan-2-ones **14** from propynyl arenes **13** (Scheme 1.7).^[24] The same catalyst was later applied to the parent synthesis of isochroman-4-ones and 2*H*-pyran-3(6*H*)-ones.^[25]



Scheme 1.7 Biarylphosphonite gold(I) complex for the synthesis of indan-2-ones.

The geometry of the biaryl scaffold has been exploited to introduce bifunctional ligands able to increase the efficiency of the gold catalyst. Indeed, the orientation of the linearly dicoordinated metal centre is forced by the two bulky adamantyl or *tert*-butyl groups and the substrate is located close to the second aryl ring upon coordination, as shown in Figure 1.4 by the Au(I) complex **15** developed by Zhang.^[26] In this case, the distal amide functional group assists the intermolecular nucleophilic addition onto the Au-coordinated alkyne by directing the attack of the nucleophile and enhancing its nucleophilicity by general base catalysis. Moreover, in the process the amide gets protonated and constitutes a proton source that accelerates the protodeauration step, further increasing the reaction rate. This allowed to dramatically improve the TON of the process with different nucleophiles. The addition of benzoic acid to 1-dodecyne was performed with a TON as high as 24'000 at a 40 ppm loading of catalyst: by comparison, in the same conditions JohnPhosAuNTf₂ afforded a TON of 40 at a 500 ppm loading.^[26] Not only the amide, but also cyclic and acyclic amine groups have been employed by Zhang in a similar manner for both general base catalysis and directing effects.^[27]

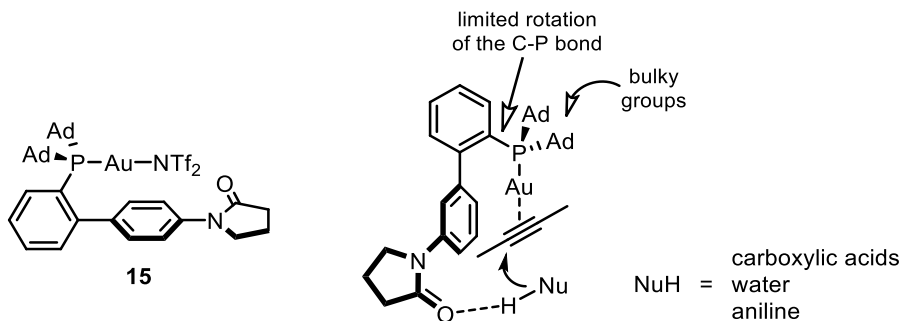


Figure 1.4 Ligand-directed nucleophilic attack through the use of a bifunctional Buchwald-type phosphine.

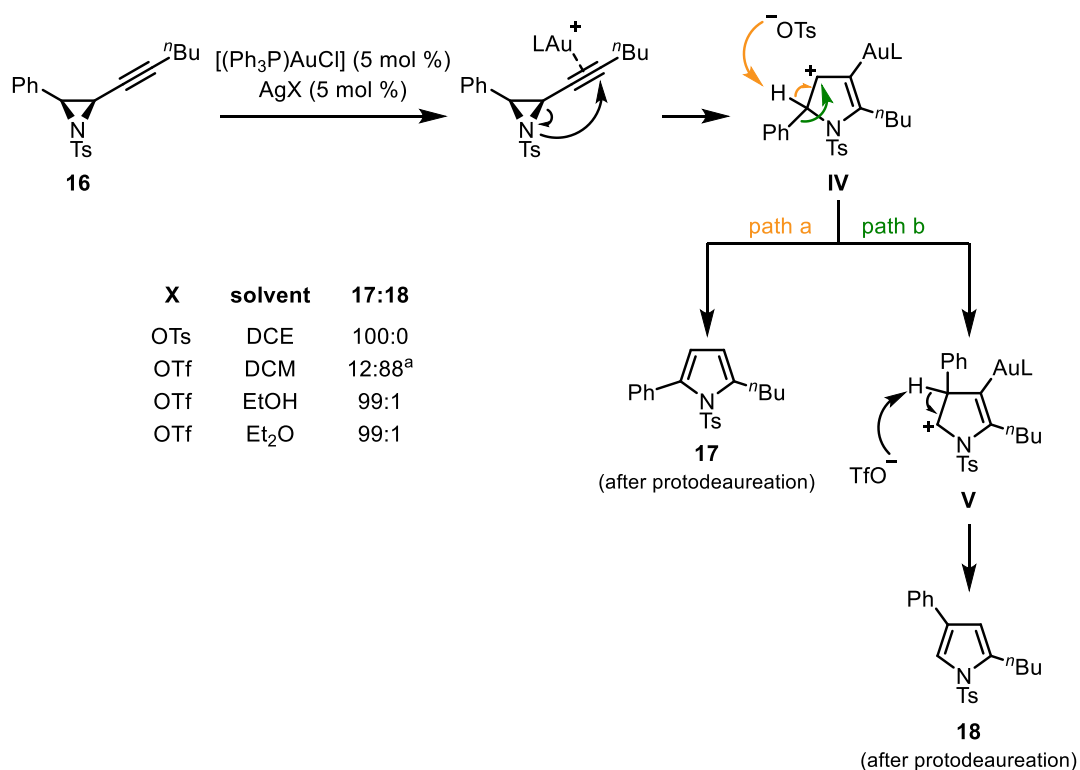
1.2.3 Effect of the counterion

The role of the counterion X^- in gold catalysis has been long overlooked, compared to other factors such as the ligand, considering it to be a mere spectator in the catalytic process. However, experimental evidence on the influence of the anion on the outcome of the reaction prompted the investigation on its role, which is not as immediately understandable and predictable.^[28]

A first parameter to be taken into account is the coordinating strength, because of the competition with the substrate for the coordination vacancy. Based on computational^[29] and NMR^[30] studies, a scale of affinity for the gold centre places spherical, poorly nucleophilic BF_4^- , SbF_6^- and ClO_4^- anions as very weakly coordinating. Triflate (TfO^-) and triflimide (Tf_2N^-), the most popular counterions for gold catalysis together with SbF_6^- , are considered of intermediate strength, with the first being more coordinating than the latter. The strongest counterions are tosylate (TsO^-), CF_3COO^- and NO_3^- .

The relative position of the LAu^+ fragment and the anion needs to be considered too. A series of studies from Macchioni and Zuccaccia revealed that, upon complexation of the unsaturated substrate, the counterion is preferentially located close to the ancillary ligand, when the latter is a NHC, while in the case of phosphines and phosphites the counterion tends to reside in proximity of the unsaturated substrate.^[31] This was found to affect the catalytic performance of Au(I) complexes in the hydroalkoxylation of alkynes, since the anion, when close to the coordinated substrate, can activate the approaching nucleophile through hydrogen bonding.^[32] The extent of these ion pairing effects strongly depends on which are the rate-determining steps of each reaction, as well as on the solvent in which the reaction is performed.^[28b, 33]

Finally, secondary interactions between the counterion and the substrate, such as hydrogen bonding, can play a significant role.^[28a] On this regard, the basicity of the anion is an important parameter, as shown by the regiodivergent gold(I) catalysed pyrrole synthesis reported by Davies.^[34] As shown in Scheme 1.8, treatment of alkynyl aziridine **16** with [(Ph₃P)Au(OTs)] led to 2,5-disubstituted pyrrole **17** after ring expansion and deprotonation of the cationic intermediate **IV** (path a). Switching the counterion from TsO⁻ to less basic TfO⁻ afforded 2,4-disubstituted pyrrole **18** instead (path b). The formation of this product was attributed to the kinetically favoured 1,2-aryl shift towards intermediate **V** in the absence of an efficient proton abstractor. Again, the reaction medium played a crucial role: when the reaction was performed with AgOTf in a Brønsted or Lewis basic solvent, the selectivity switched back to **17**.

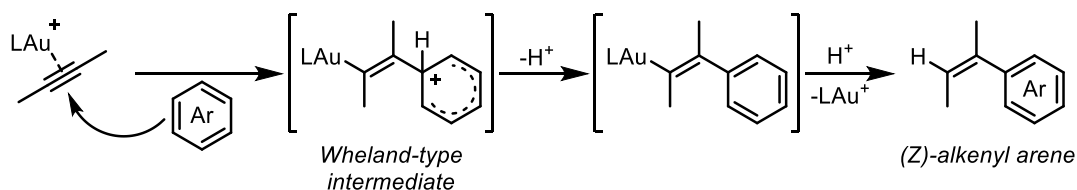


Scheme 1.8 Effect of the basicity of the counterion in the regiodivergent synthesis of pyrroles. ^a 4:96 in DCE, but with slightly reduced yield.

1.3 Hydroarylation of alkynes

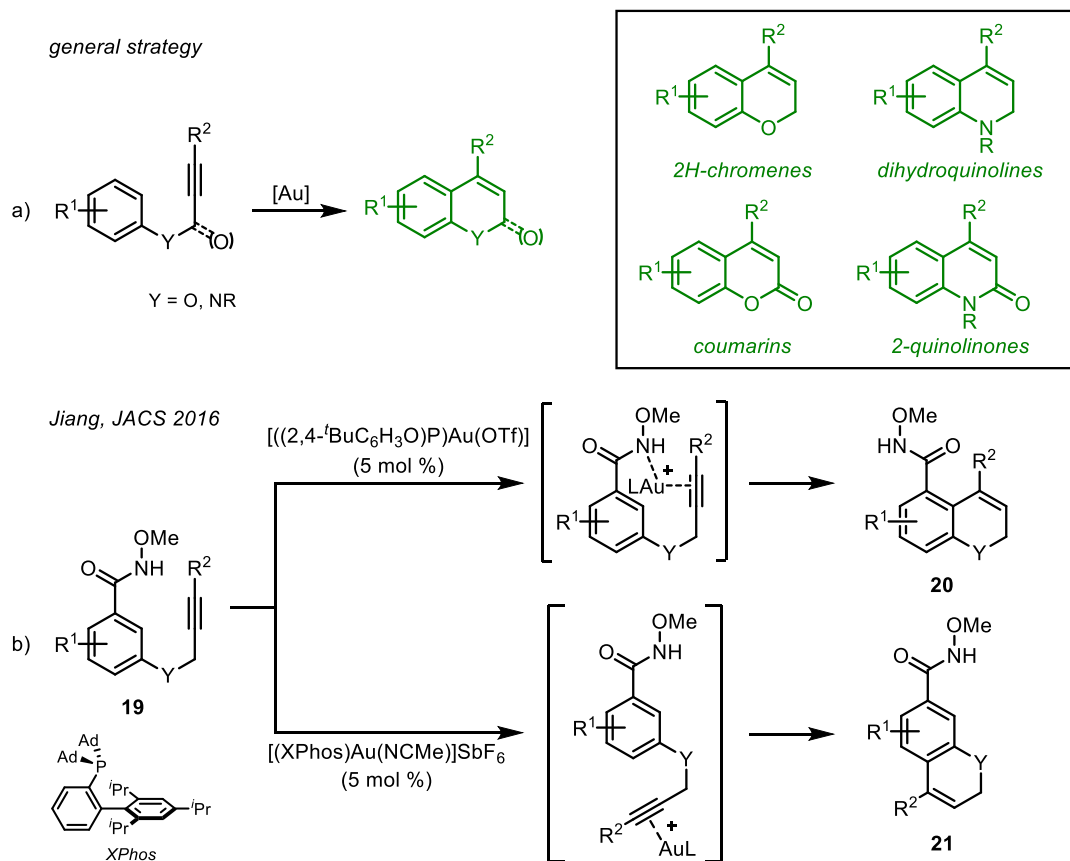
1.3.1 Friedel-Crafts-type electrophilic aromatic substitution

The gold-catalysed hydroarylation reaction consists in the addition of Ar-H to an alkyne, affording an alkenyl arene as the product. A plausible mechanism involves the attack of the (hetero)aryl ring on the activated π -system, followed by rearomatisation of the so-formed Wheland-type intermediate. The final protodeauration step affords the final hydroarylation product (Scheme 1.9). From the point of view of the arene, the process is analogous to a Friedel-Crafts-type alkenylation, representing a valuable synthetic alternative to the Heck cross-coupling, which however requires pre-functionalisation of the arene; moreover, the Heck product is generally an (*E*)-alkene, while in the Au(I)-catalysed hydroarylation (*Z*)-alkenes are obtained.



Scheme 1.9 Au(I)-catalysed Friedel-Crafts-type hydroarylation of alkynes.

Since the first report from Reetz in 2003,^[35] advances in both inter- and intramolecular gold-catalysed hydroarylation of alkynes have disclosed several synthetic applications of the general methodology.^[36] Among them, the intramolecular hydroarylation of electron-rich phenyl propargyl ethers and propargyl anilines, as well as their ester and amide analogues, has been widely studied (Scheme 1.10, a).^[37] The reaction, which has been performed employing phosphine complexes such as [(JohnPhos)Au(NCMe)]SbF₆, [(XPhos)Au(NCMe)]SbF₆ and [(Ph₃P)AuCl]/AgX, affords partially saturated heterobicyclic scaffolds and has been exploited for the synthesis of natural compounds^[37c, 37d] as well as fluorescent dyes for materials applications (Figure 1.5).^[37e, 37h] In a recent work, the presence of a *N*-methoxyamide group in *meta* position on the aryl ring of propargyl derivatives **19** enabled a ligand-controlled regioselectivity (Scheme 1.10, b).^[37g] Indeed, with the electron-poor phosphite ligand, the amide nitrogen was able to act as a directing group and favour the cyclisation at its *ortho* position by coordinating the Au centre, affording products **20**. On the other hand, less electrophilic and more sterically demanding XPhos ligand induced the opposite selectivity, pushing the coordinated π -system far away from the amide substituent, which eventually resulted in products **21**. The mechanistic hypothesis was later confirmed by DFT calculations.^[38]



Scheme 1.10 a) Au(I)-catalysed intramolecular hydroarylation of electron-rich arenes.
b) Ligand-controlled regiodivergence in the presence of a directing group.

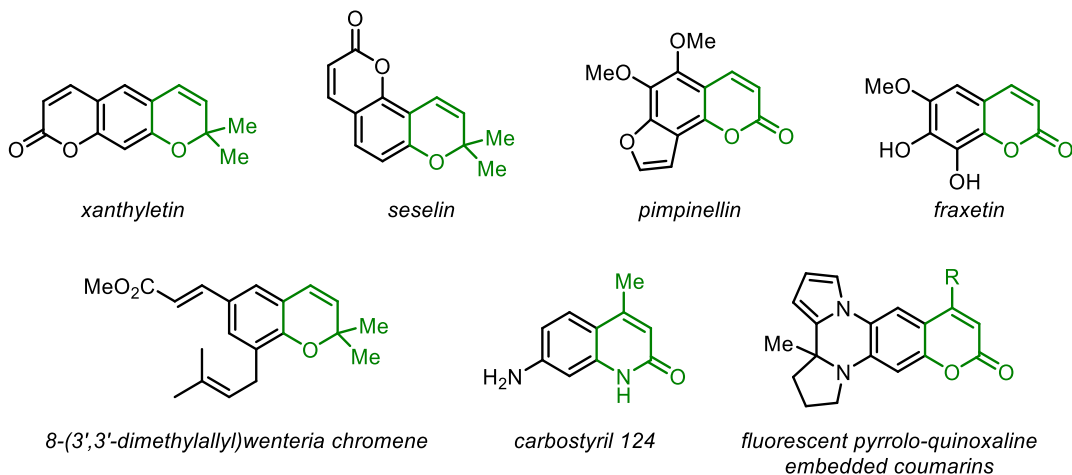
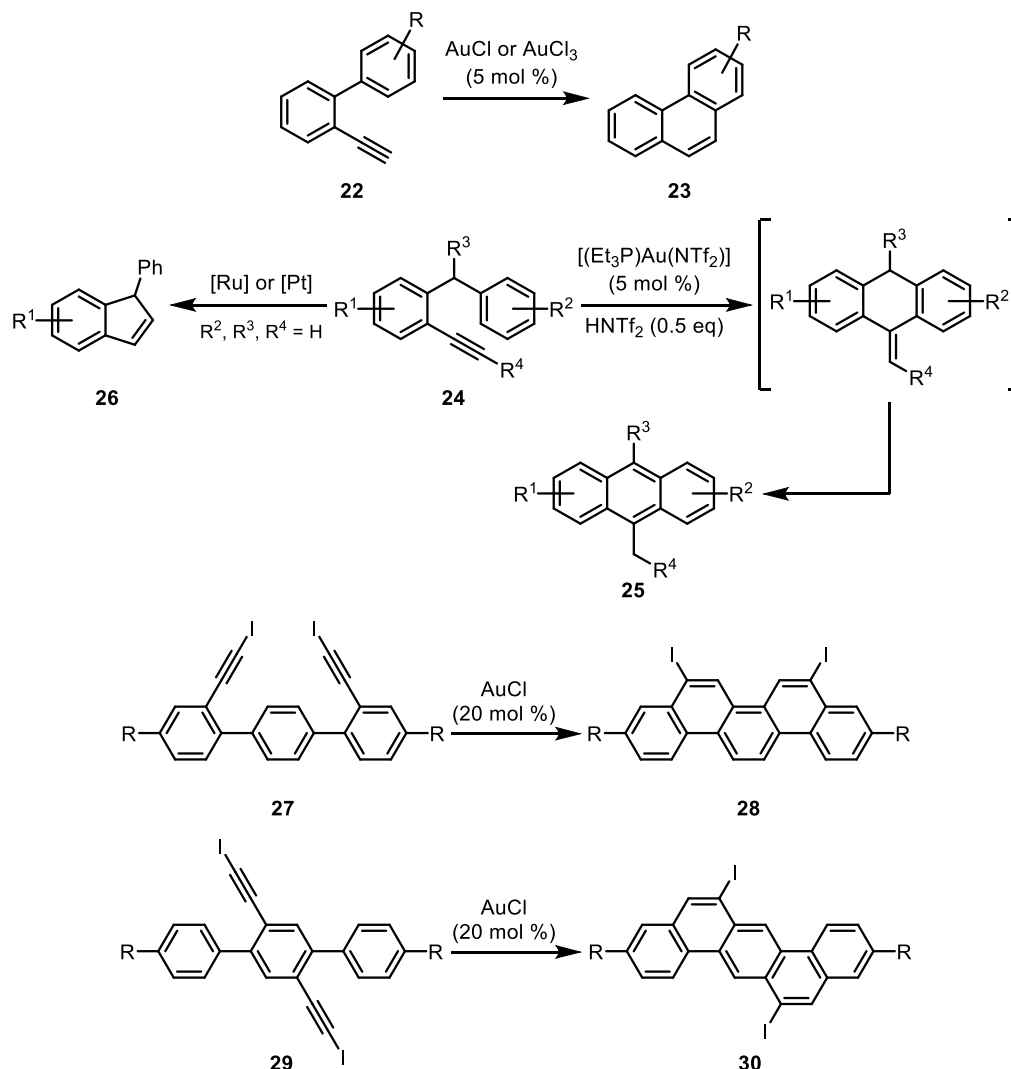


Figure 1.5 Examples of natural or technologically relevant compounds accessible through intramolecular Au(I)-catalysed hydroarylation of electron-rich arenes.

The gold-catalysed hydroarylation of alkynes has also been applied to the synthesis of poly(hetero)aromatic compounds. Phenanthrenes **23** were obtained through the 6-*endo-dig* cyclisation of *o*-alkynylbiaryls **22** both with Au(I) and Au(III) (Scheme 1.11).^[39] Anthracenes **25** were synthesised from *o*-alkynyldiarylmethanes **24** by 6-*exo-dig* cyclisation and spontaneous aromatisation through *exo-endo* migration of the double bond.^[40] Interestingly, other transition metals such as Ru and Pt afforded indenenes **26** instead (Scheme 1.11).^[41]



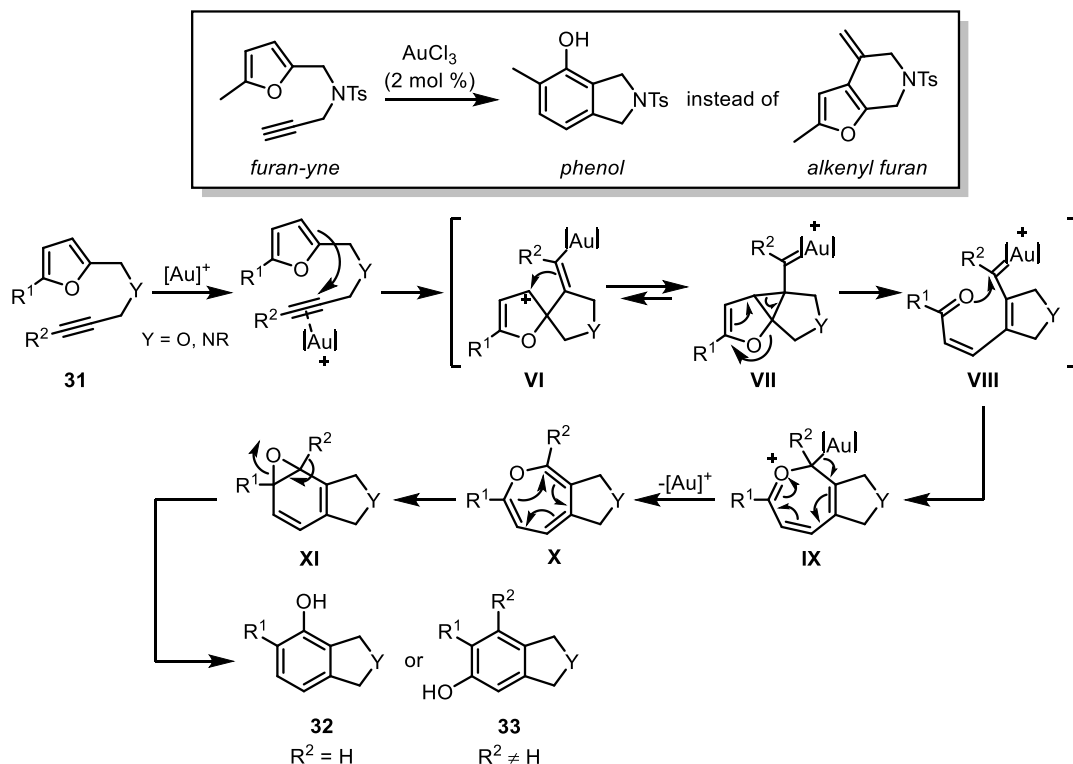
Scheme 1.11 Synthesis of polyaromatic compounds through Au-catalysed intramolecular hydroarylation.

The application of the same strategy on *o*-propargylbiaryl afforded phenanthrenes.^[42] Looking at larger polyaromatics, the synthesis of diiodinated

picones **28** and dibenzo[*a,h*]anthracenes **30** was achieved starting from diynes **27** and **29** respectively, through a sequential hydroarylation/1,2-iodine migration (Scheme 1.11).^[43]

1.3.2 The furan-yne hydroarylation pathway

The gold-catalysed hydroarylation of furan-tethered alkynes (“furan-ynes”) does not follow the classical pathway shown in Scheme 1.9. First reported by Hashmi in 2000,^[2] the reaction indeed affords phenols rather than the expected alkenylated furans (Scheme 1.12).^[36a, 36c] The mechanism was later elucidated by theoretical studies and experimental evidences,^[44] also in analogy with the related Pt(II)-catalysed reaction.^[45] Upon coordination of gold, the alkyne moiety of the 2-substituted furan **31** is attacked by the furan *ipso* carbon, forming the *spiro* intermediate **VI**, which then evolves into the cyclopropyl gold carbene **VII** (Scheme 1.12). A ring opening/cyclisation/demetalation sequence leads to oxepine **X**, which further evolves into the arene oxide **XI**. The latter undergoes aromatisation through epoxide opening, eventually affording phenol **32** or **33**, depending on the substitution of the starting alkyne, as the reaction product.



Scheme 1.12 Phenol synthesis through Au-catalysed hydroarylation of furan-ynes.

Following the early reports, the gold-catalysed reactivity of furan and alkynes has been widely explored in several works, mainly from the Hashmi group.^[46] Variations on the alkyne tether and different substitution patterns on the furan ring, as well as the extension to the intermolecular version of the reaction, allowed for the construction of a number of structurally diversified molecular scaffolds, including the natural product jungianol (Figure 1.6).

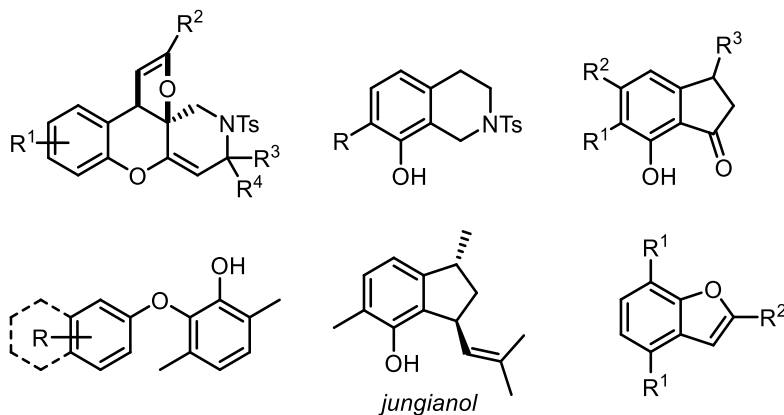


Figure 1.6 Examples of molecular scaffolds accessible through inter- and intramolecular versions of the furan-yne hydroarylation pathway.

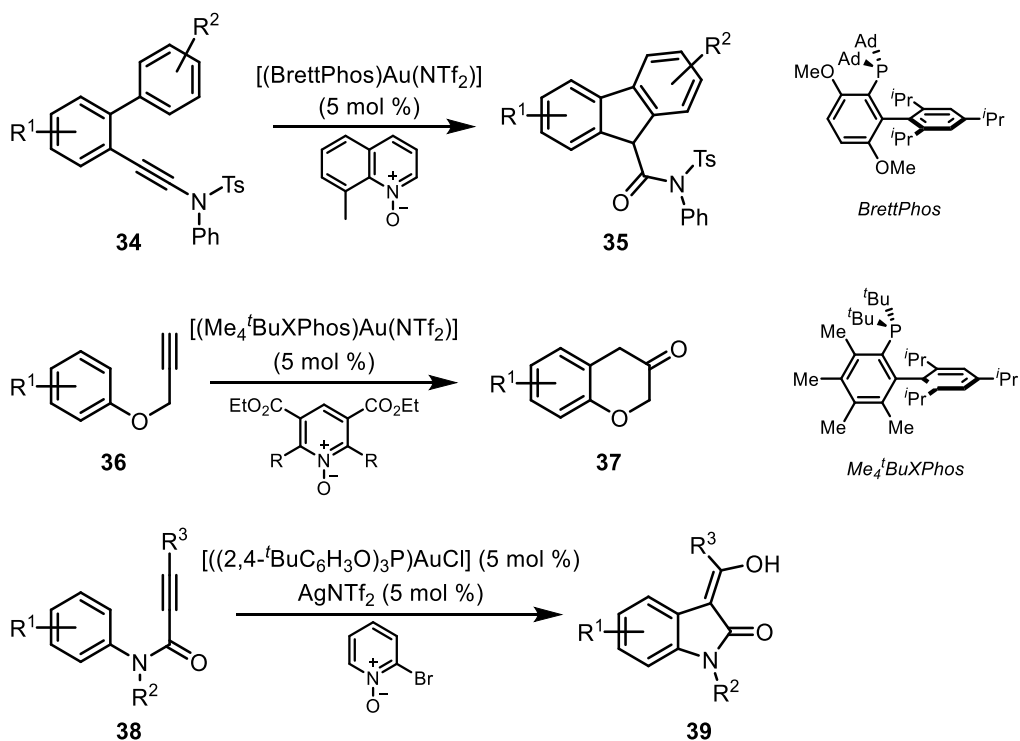
1.3.3 Arenes functionalisation through oxidative gold(I) catalysis with nucleophilic oxidants

The generation of α -oxo gold(I) carbenes through gold(I)-catalysed oxidation of alkynes (see Section 1.2.1) was first reported in 2007 by two independent works from Toste^[47] and Zhang.^[48] Since then, one of the most attractive features to prompt the investigation on the methodology has been that it prevents the use of α -diazo carbonyl compounds as precursors to α -oxo metal carbenes.^[14b] Indeed, alkynes are considerably cheaper, more available, less hazardous and allow for more flexible synthesis, compared to α -diazo carbonyls.

The general mechanism involves the attack of a nucleophilic species Z^+O^- , such as a pyridine or quinoline *N*-oxide, or a sulfoxide, onto the Au(I)-coordinated alkyne. Subsequent cleavage of the Z-O bond affords the reactive metal carbene intermediate and releases the free Z species (Scheme 1.4, c). The actual structure of these carbenes has been object of debate, and they have also been described as gold(I) carbenoids rather than carbenes, with pyridine coordinated to the same carbon atom as gold after the Z-O bond cleavage.^[49]

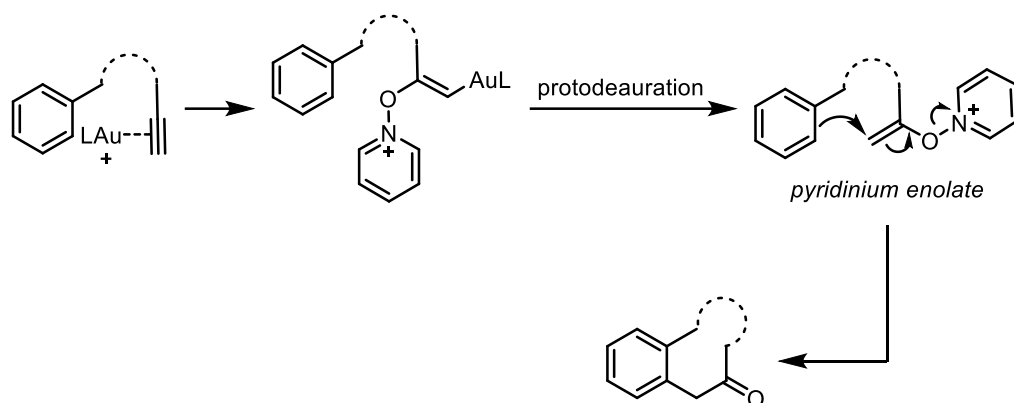
Among the wide number of reactions that have been reported on this chemistry, trapping of the α -oxo gold(I) carbene with carbon nucleophiles such as

aryl moieties has disclosed new opportunities for the Au(I)-catalysed functionalisation of arenes. The arylation of the electrophilic carbene is complementary to the direct hydroarylation of the alkyne: this is well exemplified by the oxidative synthesis of fluorenes **35**,^[50] chroman-3-ones **37**^[51] and 3-acyloxindoles **39**^[52] shown in Scheme 1.13, if compared with the reactions presented in Section 1.3.1 (Schemes 1.10 and 1.11), which feature analogous substrates. An intermolecular version of the reaction, employing electron-rich arenes such as indoles and anilines, was also successfully performed in water as the reaction medium.^[53]



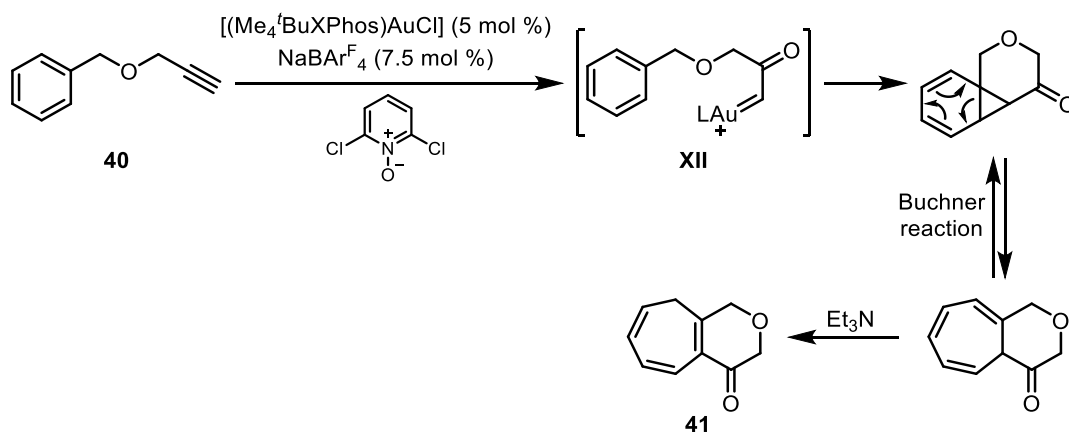
Scheme 1.13 Functionalisation of arenes through oxidative gold(I) catalysis.

From the mechanistic point of view, the actual formation of a gold carbene species has been questioned, as the reaction might as well proceed *via* a pyridinium enolate intermediate through $\text{S}_{\text{N}}2'$ mechanism (Scheme 1.14).^[24, 54] The pyridinium enolate shows *umpolung* reactivity and is electrophilic at the terminal alkene end, even in the absence of a coordinated metal, as was demonstrated by its generation with protic acids instead of gold.^[55]



Scheme 1.14 Alternative reaction pathway involving an *umpolung* pyridinium enolate intermediate.

However, other examples such as the ring expansion of benzyl propargyl ethers **40** (Scheme 1.15) account for a more likely involvement of a gold(I) carbene species. Indeed, the reaction is supposed to proceed through a key cyclopropanation step of carbene **XII**.^[56] It seems reasonable to presume that, after the initial attack of the pyridine *N*-oxide, the evolution into either the gold(I) carbene or the pyridinium enolate should depend on the features of the substrate, the ligand of the Au(I) complex and the nucleofugacity of the pyridine/quinoline species.



Scheme 1.15 Gold(I)-catalysed ring expansion of benzyl propargyl ethers.

References

- [1] J. H. Teles, S. Brode, M. Chabanas, *Angew. Chem. Int. Ed.* **1998**, *37*, 1415-1418.
- [2] A. S. K. Hashmi, T. M. Frost, J. Bats, *J. Am. Chem. Soc.* **2000**, *122*, 11553-11554.
- [3] a) A. M. Echavarren, A. S. K. Hashmi, F. D. Toste, *Adv. Synth. Catal.* **2016**, *358*, 1347-1347; b) R. Dorel, A. M. Echavarren, *Chem. Rev.* **2015**, *115*, 9028-9072; c) D. Pflaesterer, A. S. K. Hashmi, *Chem. Soc. Rev.* **2016**, *45*, 1331-1367; d) Z. Li, C. Brouwer, C. He, *Chem. Rev.* **2008**, *108*, 3239-3265; e) H. C. Shen, *Tetrahedron* **2008**, *18*, 3885-3903; f) H. C. Shen, *Tetrahedron* **2008**, *34*, 7847-7870.
- [4] D. J. Gorin, F. D. Toste, *Nature* **2007**, *446*, 395-403.
- [5] Active Au(I) species can also be generated by protonolysis of [LAu(OH)] or [LAu(CH₃)] complexes, but the case is much less common.
- [6] B. Ranieri, I. Escofet, A. M. Echavarren, *Org. Biomol. Chem.* **2015**, *13*, 7103-7118.
- [7] D. Wang, R. Cai, S. Sharma, J. Jirak, S. K. Thummanapelli, N. G. Akhmedov, H. Zhang, X. Liu, J. L. Petersen, X. Shi, *J. Am. Chem. Soc.* **2012**, *134*, 9012-9019.
- [8] a) D. Weber, M. R. Gagné, *Org. Lett.* **2009**, *11*, 4962-4965; b) Y. Zhu, C. S. Day, L. Zhang, K. J. Hauser, A. C. Jones, *Chem. Eur. J.* **2013**, *19*, 12264-12271; c) Z. Lu, J. Han, G. B. Hammond, B. Xu, *Org. Lett.* **2015**, *17*, 4534-4537.
- [9] A. Homs, I. Escofet, A. M. Echavarren, *Org. Lett.* **2013**, *15*, 5782-5785.
- [10] a) A. Gómez-Suárez, S. P. Nolan, *Angew. Chem. Int. Ed.* **2012**, *51*, 8156-8159; b) A. S. K. Hashmi, *Acc. Chem. Res.* **2014**, *47*, 864-876.
- [11] a) R. Harris, R. Widenhoefer, *Chem. Soc. Rev.* **2016**, *45*, 4533-4551; b) Y. Wang, M. E. Muratore, A. M. Echavarren, *Chem. Eur. J.* **2015**, *21*, 7332-7339.
- [12] a) E. s. Jiménez-Núñez, A. M. Echavarren, *Chem. Rev.* **2008**, *108*, 3326-3350; b) C. Obradors, A. M. Echavarren, *Acc. Chem. Res.* **2014**, *47*, 902-912.
- [13] S. Wang, G. Zhang, L. Zhang, *Synlett* **2010**, *2010*, 692-706.
- [14] a) J. Xiao, X. Li, *Angew. Chem. Int. Ed.* **2011**, *50*, 7226-7236; b) L. Zhang, *Acc. Chem. Res.* **2014**, *47*, 877-888; c) H.-S. Yeom, S. Shin, *Acc. Chem. Res.* **2014**, *47*, 966-977.
- [15] M. Mato, C. García-Morales, A. M. Echavarren, *ChemCatChem* **2019**, *11*, 53-72.
- [16] a) D. J. Gorin, B. D. Sherry, F. D. Toste, *Chem. Rev.* **2008**, *108*, 3351-3378; b) Y. Wei, M. Shi, *ACS Catal.* **2016**, *6*, 2515-2524; c) W. Wang, G. B. Hammond, B. Xu, *J. Am. Chem. Soc.* **2012**, *134*, 5697-5705.
- [17] D. Benitez, N. D. Shapiro, E. Tkatchouk, Y. Wang, W. A. Goddard III, F. D. Toste, *Nat. Chem.* **2009**, *1*, 482.
- [18] Z. Yu, B. Ma, M. Chen, H.-H. Wu, L. Liu, J. Zhang, *J. Am. Chem. Soc.* **2014**, *136*, 6904-6907.
- [19] See for example: a) X. L. Xie, S. F. Zhu, J. X. Guo, Y. Cai, Q. L. Zhou, *Angew. Chem. Int. Ed.* **2014**, *53*, 2978-2981; b) T. Osako, D. Panichakul, Y. Uozumi, *Org. Lett.* **2012**, *14*, 194-197; c) Z. Qu, W. Shi, J. Wang, *J. Org. Chem.* **2004**, *69*, 217-219; d) Z. Zhu, J. H. Espenson, *J. Am. Chem. Soc.* **1996**, *118*, 9901-9907.
- [20] S. P. Nolan, *Acc. Chem. Res.* **2011**, *44*, 91-100.
- [21] a) A. Almássy, C. E. Nagy, A. C. Bényei, F. Joó, *Organometallics* **2010**, *29*, 2484-2490; b) E. Tomás-Mendivil, P. Y. Toullec, J. Borge, S. Conejero, V. Michelet, V. Cadierno, *ACS Catal.* **2013**, *3*, 3086-3098; c) K. Belger, N. Krause, *Eur. J. Org. Chem.* **2015**, *2015*, 220-225; d) K. Belger, N. Krause, *Org. Biomol. Chem.* **2015**, *13*, 8556-8560.
- [22] a) V. Breker, H. Sak, G. Baracchi-Krause, N. Krause, *Tetrahedron Lett.* **2015**, *56*, 3390-3392; b) H. Sak, M. Mawick, N. Krause, *ChemCatChem* **2019**, *11*, 5821-5829.

- [23] G. Zuccarello, M. Zanini, A. M. Echavarren, *Isr. J. Chem.* **2020**, *60*, 360-372.
- [24] G. Henrion, T. E. Chavas, X. Le Goff, F. Gagosz, *Angew. Chem. Int. Ed.* **2013**, *52*, 6277-6282.
- [25] Q. Zhao, G. Henrion, F. Gagosz, *Bioorg. Med. Chem.* **2019**, *27*, 2616-2620.
- [26] Y. Wang, Z. Wang, Y. Li, G. Wu, Z. Cao, L. Zhang, *Nat. Commun.* **2014**, *5*, 1-8.
- [27] Some selected examples: a) X. Li, Z. Wang, X. Ma, P.-n. Liu, L. Zhang, *Org. Lett.* **2017**, *19*, 5744-5747; b) T. Li, L. Zhang, *J. Am. Chem. Soc.* **2018**, *140*, 17439-17443; c) S. Liao, A. Porta, X. Cheng, X. Ma, G. Zanoni, L. Zhang, *Angew. Chem. Int. Ed.* **2018**, *57*, 8250-8254; d) H. Wang, T. Li, Z. Zheng, L. Zhang, *ACS Catal.* **2019**, *9*, 10339-10342; e) T. Li, Y. Yang, B. Luo, B. Li, L. Zong, W. Kong, H. Yang, X. Cheng, L. Zhang, *Org. Lett.* **2020**, *22*, 6045-6049.
- [28] a) M. Jia, M. Bandini, *ACS Catal.* **2015**, *5*, 1638-1652; b) D. Zuccaccia, A. Del Zotto, W. Baratta, *Coord. Chem. Rev.* **2019**, *396*, 103-116; c) J. Schießl, J. Schulmeister, A. Doppiu, E. Wörner, M. Rudolph, R. Karch, A. S. K. Hashmi, *Adv. Synth. Catal.* **2018**, *360*, 2493-2502.
- [29] G. Kovács, G. Ujaque, A. Lledós, *J. Am. Chem. Soc.* **2008**, *130*, 853-864.
- [30] a) A. Zhdanko, M. Ströbele, M. E. Maier, *Chem. Eur. J.* **2012**, *18*, 14732-14744; b) A. Zhdanko, M. E. Maier, *ACS Catal.* **2014**, *4*, 2770-2775.
- [31] a) D. Zuccaccia, L. Belpassi, F. Tarantelli, A. Macchioni, *J. Am. Chem. Soc.* **2009**, *131*, 3170-3171; b) N. Salvi, L. Belpassi, D. Zuccaccia, F. Tarantelli, A. Macchioni, *J. Organomet. Chem.* **2010**, *695*, 2679-2686; c) D. Zuccaccia, L. Belpassi, L. Rocchigiani, F. Tarantelli, A. Macchioni, *Inorg. Chem.* **2010**, *49*, 3080-3082. See also: T. J. Brown, M. G. Dickens, R. A. Widenhoefer, *Chem. Commun.* **2009**, 6451-6453.
- [32] a) L. Biasiolo, G. Ciancaleoni, L. Belpassi, G. Bistoni, A. Macchioni, F. Tarantelli, D. Zuccaccia, *Catal. Sci. Technol.* **2015**, *5*, 1558-1567; b) L. Biasiolo, M. Trinchillo, P. Belanzoni, L. Belpassi, V. Busico, G. Ciancaleoni, A. D'Amora, A. Macchioni, F. Tarantelli, D. Zuccaccia, *Chem. Eur. J.* **2014**, *20*, 14594-14598.
- [33] M. Gatto, P. Belanzoni, L. Belpassi, L. Biasiolo, A. Del Zotto, F. Tarantelli, D. Zuccaccia, *ACS Catal.* **2016**, *6*, 7363-7376.
- [34] a) P. W. Davies, N. Martin, *Org. Lett.* **2009**, *11*, 2293-2296; b) P. W. Davies, N. Martin, *J. Organomet. Chem.* **2011**, *696*, 159-164.
- [35] M. T. Reetz, K. Sommer, *Eur. J. Org. Chem.* **2003**, *2003*, 3485-3496.
- [36] a) M. E. Muratore, A. M. Echavarren, *Gold-catalyzed hydroarylation of alkynes in PATAI'S Chemistry of Functional Groups* (Ed.: Wiley), **2009**, pp. 1-96; b) M. Bandini, *Chem. Soc. Rev.* **2011**, *40*, 1358-1367; c) M. S. Kirillova, F. M. Miloserdov, A. M. Echavarren, *Hydroarylation of Alkynes using Cu, Ag, and Au Catalysts in Catalytic Hydroarylation of Carbon-Carbon Multiple Bonds* (Ed.: Wiley), **2017**, pp. 217-303; d) V. P. Boyarskiy, D. S. Ryabukhin, N. A. Bokach, A. V. Vasilyev, *Chem. Rev.* **2016**, *116*, 5894-5986.
- [37] a) C. Nevado, A. M. Echavarren, *Chem. Eur. J.* **2005**, *11*, 3155-3164; b) R. S. Menon, A. D. Findlay, A. C. Bissember, M. G. Banwell, *J. Org. Chem.* **2009**, *74*, 8901-8903; c) I. N. Lykakis, C. Efe, C. Gryparis, M. Stratakis, *Eur. J. Org. Chem.* **2011**, *2011*, 2334-2338; d) A. Cervi, P. Aillard, N. Hazeri, L. Petit, C. L. Chai, A. C. Willis, M. G. Banwell, *J. Org. Chem.* **2013**, *78*, 9876-9882; e) A. C. Shaikh, S. Shalini, R. Vaidhyanathan, M. V. Mane, A. K. Barui, C. R. Patra, Y. Venkatesh, P. R. Bangal, N. T. Patil, *Eur. J. Org. Chem.* **2015**, *2015*, 4860-4867; f) S. A. Sharif, E. D. Calder, A. H. Harkiss, M. Maduro, A. Sutherland, *J. Org. Chem.* **2016**, *81*, 9810-9819; g) D. Ding, T. Mou, M. Feng, X. Jiang, *J. Am. Chem. Soc.* **2016**, *138*, 5218-5221; h) T.

- Vacala, L. P. Bejcek, C. G. Williams, A. C. Williamson, P. A. Vadola, *J. Org. Chem.* **2017**, *82*, 2558-2569.
- [38] Y. Yang, Y. Liu, P. Lv, R. Zhu, C. Liu, D. Zhang, *J. Org. Chem.* **2018**, *83*, 2763-2772.
- [39] a) V. Mamane, P. Hannen, A. Fürstner, *Chem. Eur. J.* **2004**, *10*, 4556-4575; b) E. Soriano, J. Marco-Contelles, *Organometallics* **2006**, *25*, 4542-4553.
- [40] C. Shu, C.-B. Chen, W.-X. Chen, L.-W. Ye, *Org. Lett.* **2013**, *15*, 5542-5545.
- [41] a) A. Odedra, S. Datta, R.-S. Liu, *J. Org. Chem.* **2007**, *72*, 3289-3292; b) M. Tobisu, H. Nakai, N. Chatani, *J. Org. Chem.* **2009**, *74*, 5471-5475.
- [42] C. Shu, L. Li, C. B. Chen, H. C. Shen, L. W. Ye, *Chem. Asian J.* **2014**, *9*, 1525-1529.
- [43] T. Nakae, R. Ohnishi, Y. Kitahata, T. Soukawa, H. Sato, S. Mori, T. Okujima, H. Uno, H. Sakaguchi, *Tetrahedron Lett.* **2012**, *53*, 1617-1619.
- [44] a) A. S. K. Hashmi, M. Rudolph, J. P. Weyrauch, M. Wölfle, W. Frey, J. W. Bats, *Angew. Chem. Int. Ed.* **2005**, *44*, 2798-2801; b) A. M. Echavarren, M. Méndez, M. P. Muñoz, C. Nevado, B. Martín-Matute, C. Nieto-Oberhuber, D. J. Cárdenas, *Pure Appl. Chem.* **2004**, *76*, 453-463; c) A. S. K. Hashmi, M. Rudolph, H. U. Siehl, M. Tanaka, J. W. Bats, W. Frey, *Chem. Eur. J.* **2008**, *14*, 3703-3708.
- [45] a) B. Martín-Matute, D. J. Cárdenas, A. M. Echavarren, *Angew. Chem. Int. Ed.* **2001**, *40*, 4754-4757; b) B. Martín-Matute, C. Nevado, D. J. Cárdenas, A. M. Echavarren, *J. Am. Chem. Soc.* **2003**, *125*, 5757-5766.
- [46] Some examples: a) A. S. K. Hashmi, L. Ding, J. W. Bats, P. Fischer, W. Frey, *Chem. Eur. J.* **2003**, *9*, 4339-4345; b) A. S. K. Hashmi, L. Grundl, *Tetrahedron* **2005**, *61*, 6231-6236; c) A. S. K. Hashmi, J. P. Weyrauch, E. Kurpejović, T. M. Frost, B. Miehlich, W. Frey, J. W. Bats, *Chem. Eur. J.* **2006**, *12*, 5806-5814; d) A. S. K. Hashmi, R. Salathé, W. Frey, *Chem. Eur. J.* **2006**, *12*, 6991-6996; e) A. S. K. Hashmi, E. Kurpejović, M. Wölfle, W. Frey, J. W. Bats, *Adv. Synth. Catal.* **2007**, *349*, 1743-1750; f) A. S. K. Hashmi, M. Rudolph, J. Huck, W. Frey, J. W. Bats, M. Hamzić, *Angew. Chem. Int. Ed.* **2009**, *48*, 5848-5852; g) M. Rudolph, M. Q. McCreery, W. Frey, A. S. K. Hashmi, *Beilstein J. Org. Chem.* **2011**, *7*, 794-801; h) A. S. K. Hashmi, T. Häffner, M. Rudolph, F. Rominger, *Chem. Eur. J.* **2011**, *17*, 8195-8201; i) A. Zeiler, M. J. Ziegler, M. Rudolph, F. Rominger, A. S. K. Hashmi, *Adv. Synth. Catal.* **2015**, *357*, 1507-1514.
- [47] N. D. Shapiro, F. D. Toste, *J. Am. Chem. Soc.* **2007**, *129*, 4160-4161.
- [48] G. Li, L. Zhang, *Angew. Chem. Int. Ed.* **2007**, *46*, 5156-5159.
- [49] a) J. Schulz, L. Jasikova, A. Skriba, J. Roithova, *J. Am. Chem. Soc.* **2014**, *136*, 11513-11523; b) J. Schulz, J. Jašík, A. Gray, J. Roithová, *Chem. Eur. J.* **2016**, *22*, 9827-9834.
- [50] F. Pan, S. Liu, C. Shu, R.-K. Lin, Y.-F. Yu, J.-M. Zhou, L.-W. Ye, *Chem. Commun.* **2014**, *50*, 10726-10729.
- [51] Y. Wang, K. Ji, S. Lan, L. Zhang, *Angew. Chem. Int. Ed.* **2012**, *51*, 1915-1918.
- [52] D. Qian, J. Zhang, *Chem. Commun.* **2012**, *48*, 7082-7084.
- [53] L. Li, C. Shu, B. Zhou, Y.-F. Yu, X.-Y. Xiao, L.-W. Ye, *Chem. Sci.* **2014**, *5*, 4057-4064.
- [54] Z. Xu, H. Chen, Z. Wang, A. Ying, L. Zhang, *J. Am. Chem. Soc.* **2016**, *138*, 5515-5518.
- [55] a) D. F. Chen, Z. Y. Han, Y. P. He, J. Yu, L. Z. Gong, *Angew. Chem. Int. Ed.* **2012**, *51*, 12307-12310; b) K. Graf, C. L. Ruehl, M. Rudolph, F. Rominger, A. S. K. Hashmi, *Angew. Chem. Int. Ed.* **2013**, *52*, 12727-12731.
- [56] K. Ji, L. Zhang, *Adv. Synth. Catal.* **2018**, *360*, 647-651.

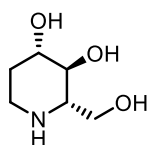
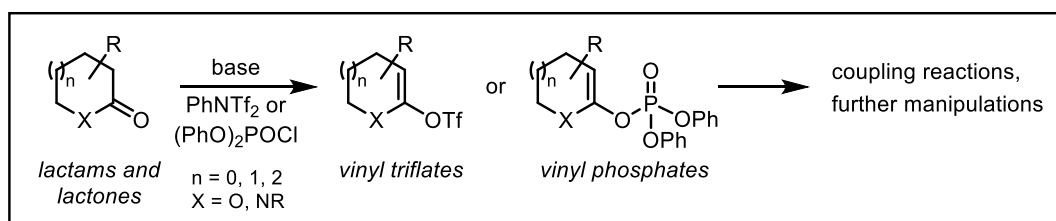
Chapter 2: Gold(I)-catalysed intramolecular hydroarylation of lactam-derived 1,3-enynes

Part of the results presented in this chapter are published in *Eur. J. Org. Chem.* **2020**, 646-653.

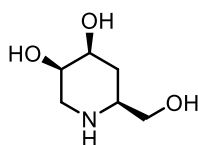
2.1 Lactam- and lactone-derived triflates and phosphates as versatile building blocks in synthesis

In the search for novel methodologies for the synthesis of natural or pharmaceutically active compounds, our research group, in collaboration with the Occhiato group at the University of Firenze, has long focused on the functionalisation of *N*- and *O*-heterocycles.

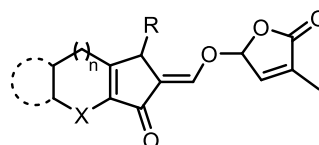
In particular, the synthetic versatility of lactams and lactones as readily available starting material has been disclosed by the chemistry of the corresponding vinyl triflates and phosphates.^[1] Those are indeed easily accessible and relatively stable intermediates for several cross-coupling reactions.^[2]



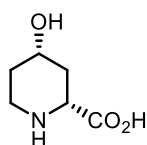
L-fagomine



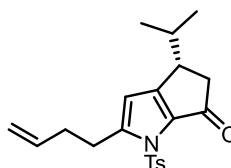
1,4-dideoxymannojirimycin



heterocyclic strigolactone analogues



(2*R*,4*S*)-4-hydroxypipercolic acid



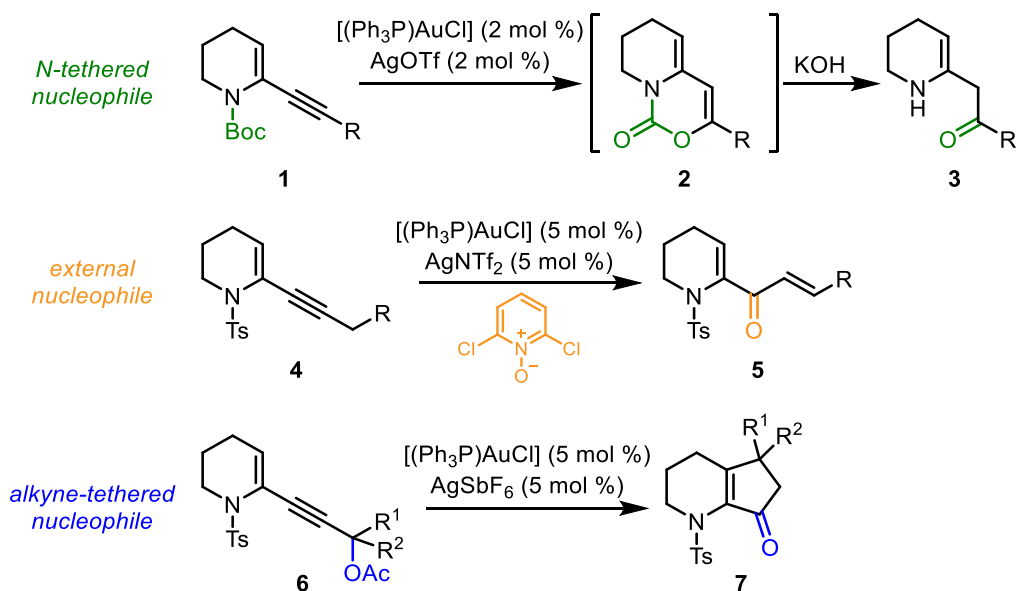
key intermediate in the formal synthesis of roseophilin

Scheme 2.1 Preparation and synthetic applications of lactam- and lactone-derived triflates and phosphates.

Some achievements in the synthesis of biologically relevant compounds through lactam triflates and phosphates are represented by the synthesis of

hydroxypiperidine alkaloids,^[3] heterocyclic strigolactone analogues^[4] and the key intermediate for the synthesis of roseophilin^[5] (Scheme 2.1).

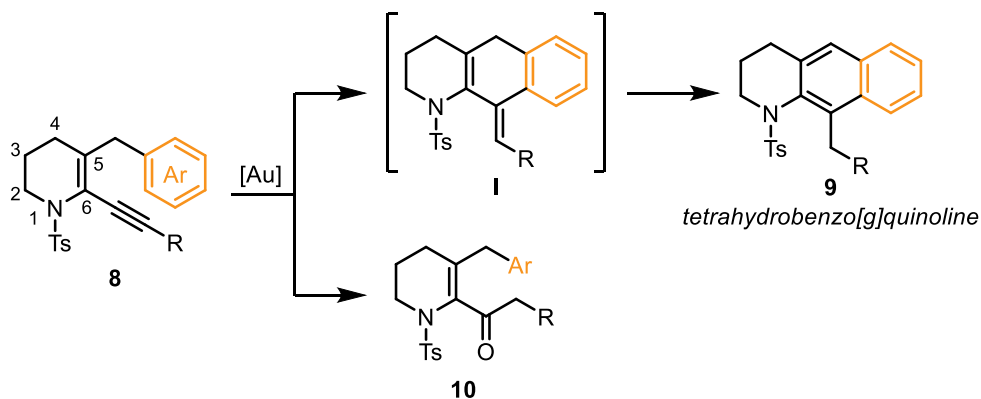
More recently, the application of gold(I) catalysis on lactam- and lactone-derived 1,3-enynes, obtained by Sonogashira coupling of the corresponding triflates and phosphates, further increased the synthetic possibilities in terms of accessible functionalized heterocyclic scaffolds. The activation of the triple bond by means of Au(I) complexes enabled the intramolecular reaction with tethered nucleophiles or the intermolecular reaction with external nucleophiles (Scheme 2.2). For example, *N*-Boc derivatives **1** undergo Au(I)-catalysed cyclisation to carbamates **2**, eventually affording vinylogous amides **3** after hydrolysis;^[6] if the *N*-protecting group is not nucleophilic, such as in the case of *N*-tosyl derivatives **4**, dienones **5** are obtained through oxidative gold(I) catalysis.^[7] The nucleophile may as well be tethered to the alkyne side chain, as in the case of propargyl acetates **6**, which afford bicyclic ketones **7** upon tandem 1,3-acyl migration/Nazarov cyclisation.^[8]



Scheme 2.2 Gold(I)-catalysed reactions of lactam-derived alkynes.

On this basis, we aimed at extending the synthetic possibilities offered by this versatile molecular scaffold and we envisaged that a gold(I)-catalysed intramolecular hydroarylation reaction could take place upon instalment of a benzylic side chain on the position 5 on the heterocyclic ring (**8**, Scheme 2.3). Substrate **8** could be converted into intermediate **I** featuring an exocyclic double bond, which could undergo *exo-endo* aromatisation to product **9** (Scheme 2.3). Based on the work of Ye,^[9] we also took into account the possibility of an Au(I)-catalysed hydration of the triple bond to ketone **10**.

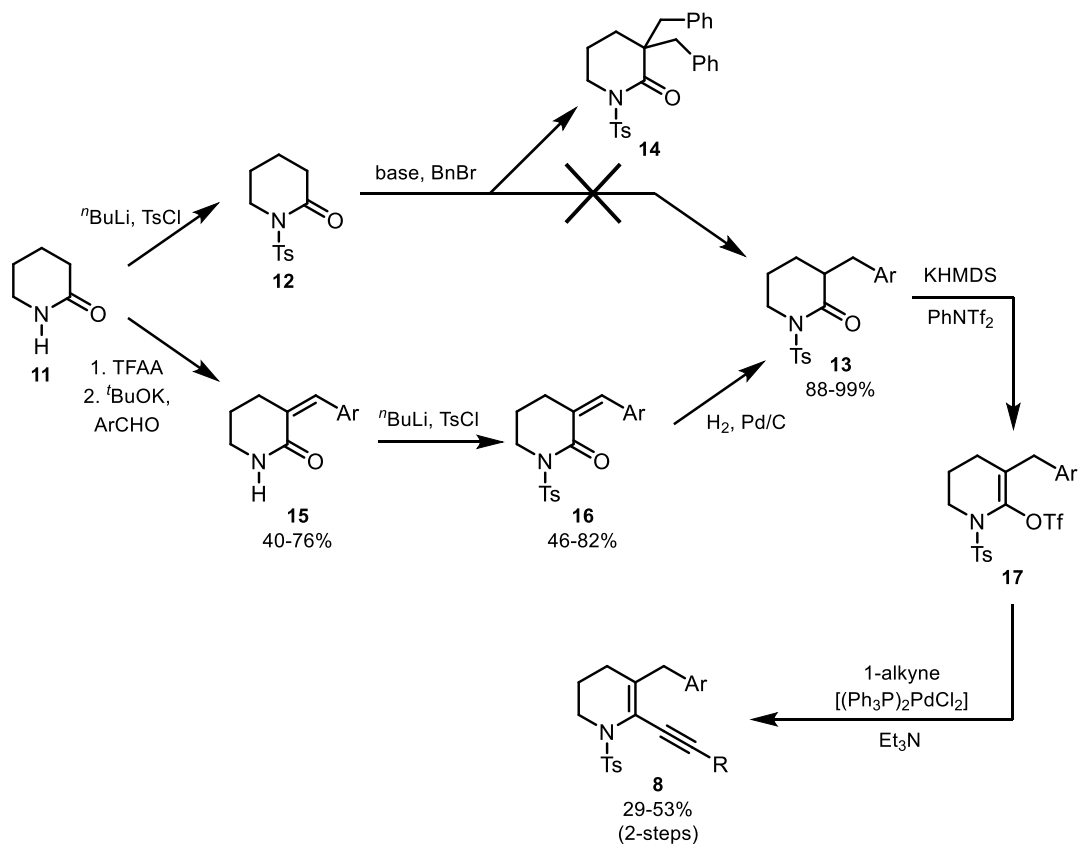
The heterocyclic aromatic skeleton of **9** is a tetrahydrobenzo[*g*]quinoline. The tetrahydroquinoline and tetrahydroisoquinoline scaffolds, decorated with different substituents or fused with carbo- and heterocycles, are found in a wide variety of bioactive compounds used as drugs and agrochemicals.^[10] Tetrahydrobenzoquinoline scaffolds have been synthesised through nucleophilic cycloaromatisation,^[11] decarboxylative cyclisation/ring expansion,^[12] Co(II)-catalysed hydrogenation^[13] and Au(I)-catalysed formal [4+2] cycloaddition.^[14] This chapter will present the gold(I)-catalysed intramolecular hydroarylation of lactam-derived alkynes for the synthesis of tetrahydrobenzo[*g*]quinolines.



Scheme 2.3 Gold(I)-catalysed hydroarylation of heterocyclic alkynes **8** into tetrahydrobenzo[*g*]quinolines **9** and hydration side-reaction into ketone **10**.

2.2 Synthesis of the substrates

At first, we approached the synthesis of substrates **8**, bearing a benzyl side arm on the heterocyclic ring. The introduction of this substituent was initially attempted through reaction of the enolate of *N*-tosyl δ -valerolactam **12** with benzyl bromide to afford lactam **13** (with Ar = Ph), but the only product recovered was the double-alkylated derivative **14** (Scheme 2.4). We varied the base used, the reaction temperature and times, the stoichiometric ratios and we also performed the reaction under Barbier conditions, but we were unable to obtain a satisfactory yield of the desired product. On the other hand, the same reaction using MeI as electrophile is reported to proceed smoothly.^[15] A possible explanation lies in the slightly higher stability of the enolate formed from **13** towards the enolate formed from **12**, which we calculated to be 3.0 kcal mol⁻¹.^[16] This difference might be enough to shift the equilibrium towards the formation of **13**-enolate, which then reacts with BnBr to afford **14**.



Scheme 2.4 Synthetic pathway towards alkyne **8**.

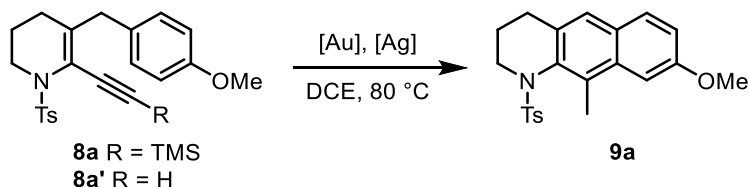
We then changed the synthetic approach towards alkyne **8** and introduced the aryl group through an aldol condensation between δ -valerolactam **12** and an aromatic aldehyde,^[17] followed by *N*-tosyl protection^[18] and hydrogenation of the double bond (Scheme 2.4). The so-obtained lactam **13** was converted into the corresponding vinyl triflate **17**, which was then reacted through Sonogashira coupling with an appropriate terminal alkyne to obtain 1,3-enynes **8**. This synthetic strategy allows to employ cheap and available benzaldehydes as starting material: thus, we were able to obtain a set of substrates with different substituents on the aryl ring, to be tested for the Au(I)-catalysed hydroarylation reaction.

2.3 Study of the reaction conditions

To start our investigation, we chose enyne **8a** as a model substrate for the intramolecular gold(I)-catalysed hydroarylation (Table 2.1). The aryl ring of this derivative bears a methoxy group in the position *para* to the tether, which makes it moderately activated as a nucleophile. Moreover, a trimethylsilyl group (TMS) on

the alkyne moiety was selected, in order to easily access the corresponding terminal alkyne by deprotection, if needed.

Table 2.1 Reaction conditions for the hydroarylation of **8a**.^a



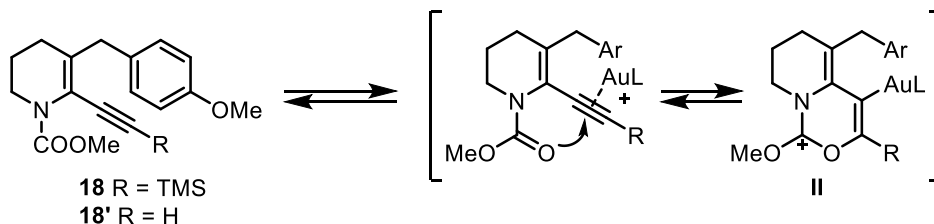
entry	[Au]	[Ag]	time	additive	yield ^b
1	[(Ph ₃ P)AuCl]	AgNTf ₂	4.5 h	–	–
2	[(JohnPhos)AuCl]	AgNTf ₂	7 h	–	9%
3	[(JohnPhos)Au(NCMe)]SbF ₆	–	6 h	–	–
4	[((2,4- ^t Bu ₂ C ₆ H ₃ O) ₃ P)AuCl]	AgNTf ₂	4 h	–	38% (37%)
5	[((MeO) ₃ P)AuCl]	AgNTf ₂	2 h	–	52% (45%)
6	[((MeO) ₃ P)AuCl]	AgOTf	23 h	–	17%
7	[((C ₆ F ₅) ₃ P)AuCl]	AgNTf ₂	2 h	–	62% (57%)
8	[((C ₆ F ₅) ₃ P)AuCl]	AgOTf	17 h	–	10%
9	[((C ₆ F ₅) ₃ P)AuCl]	AgNTf ₂	0.5 h	HNTf ₂ (0.5 eq)	16%
10	–	–	0.5 h	HNTf ₂ (0.5 eq)	15%
11	–	AgNTf ₂	5 h	–	–
12	[((C ₆ F ₅) ₃ P)AuCl]	–	5 h	–	– ^c
13 ^d	[((C ₆ F ₅) ₃ P)AuCl]	AgNTf ₂	3 h	–	39%
14 ^e	[((C ₆ F ₅) ₃ P)AuCl]	AgNTf ₂	3 h	–	18%

^a All reactions were performed at 80 °C in 1,2-dichloroethane (DCE) with 5 mol % [LAuCl] and 5 mol % AgX. ^b Determined by ¹H NMR at 600 MHz, using nitromethane as internal standard (yields of isolated product in brackets). If not otherwise specified, quantitative removal of the TMS group was observed. ^c No desilylation was observed. ^d Toluene as solvent. ^e Cyclopentyl methyl ether (CPME) as solvent.

When we reacted enyne **8a** in the presence of [(Ph₃P)AuCl] and AgNTf₂ (Table 2.1, entry 1), we did not observe any hydroarylation product. Instead, we recovered the terminal alkyne **8a'**, deriving from the desilylation of the starting material: this reaction has indeed been reported to be catalysed by silver(I) salts,^[19]

and we observed it when we reacted **8a** with AgNTf₂ alone (entry 11), while it did not take place in the presence of the [LAuCl] complex alone (entry 12). We then moved to complexes with different ligands and found that the combination [(JohnPhos)AuCl]/AgNTf₂ was able to directly convert **8a** into product **9a**, upon TMS removal and hydroarylation, even if with a low yield (entry 2). On the other hand, the cationic complex [(JohnPhos)Au(NCMe)]SbF₆ was not effective (entry 3). With the electron-poor phosphite ligand tris(2,4-di-*tert*-butylphenyl)phosphite the yield improved (entry 4). We then envisaged that a complex with reduced bulkiness, keeping the electron-withdrawing character, could be a better candidate, and we tested trimethylphosphite as a ligand, obtaining an increased yield in shorter reaction times (entry 5). Steric hindrance may indeed play a role in the cyclisation of these encumbered substrates. Aiming to further increase the electrophilicity of the Au(I) complex, we synthesised [((C₆F₅)₃P)AuCl], a complex which was also reported to perform well in the intramolecular hydroarylation of *o*-propargylbiaryls.^[9b] As reported in entry 7, this gold(I) chloride complex, in combination with AgNTf₂, led to an improvement in the reaction yield. On the other hand, both [((C₆F₅)₃P)AuCl] and [(MeO)₃P)AuCl] were significantly less active when AgOTf was used as co-catalyst (entries 6 and 8). We then verified if the addition of a strong Brønsted acid, such as HNTf₂, could further improve the yield. Indeed, as reported by Ye in the synthesis of anthracenes,^[9a] ketone **10** (Scheme 2.3), possibly formed as a by-product deriving from Au(I)-catalysed hydration, is converted into **9** in the presence of a strong acid catalyst. When we added 0.5 eq of HNTf₂, we observed a fast consumption of the starting material, but with lower yield (entry 9): this suggests that **8a** mainly undergoes decomposition under acidic conditions, even if some of it is converted into the hydroarylation product, also in the absence of the gold(I) catalyst (entry 10). It is noteworthy that we actually never observed the formation of ketone **10**, even if the reactions were performed using non-anhydrous solvents and under air. Finally, switching the solvent from DCE to toluene (entry 13) or CPME (entry 14) resulted in a decrease of the reaction yield.

Parallel to the investigation of the reactivity of **8a**, we synthesised and tested enyne **18**, in which the *N*-protecting group is a methoxycarbonyl (Scheme 2.5). Indeed, while *N*-Boc and *N*-Cbz groups were active as nucleophiles for a gold(I)-catalysed intramolecular attack in the work previously reported by our group, the same reactivity had not been observed for *N*-COOMe, which could then represent a good candidate for the hydroarylation process.^[6]



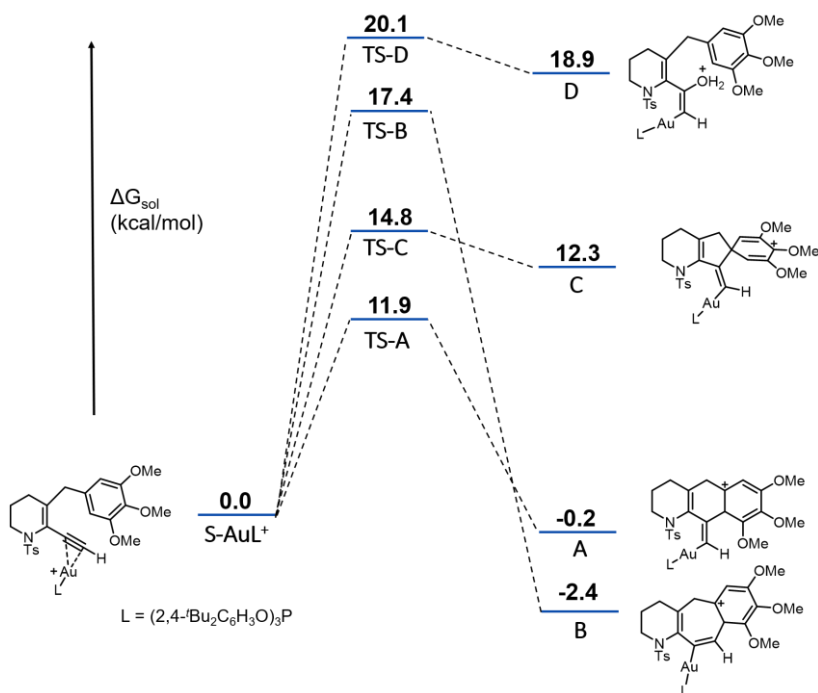
Scheme 2.5 Attempted hydroarylation of *N*-COOMe derivative **18**. Conditions: $[\text{((MeO)}_3\text{P)AuCl}]$ or $[\text{((C}_6\text{F}_5)_3\text{P)AuCl}]$ 5 mol %, AgNTf_2 5 mol %, DCE, 80 °C.

Unfortunately, when we reacted **18** in the presence of the gold catalyst we recovered the desilylation product **18'** only. We hypothesized that the COOMe group, a better nucleophile than the aryl ring, could indeed be able to attack the Au(I)-activated triple bond, but the intermediate **II** deriving from this attack could not evolve towards any product, so the reaction would just go back to the starting material (Scheme 2.5). This process would continue until degradation of the gold catalyst, hampering any conversion into the hydroarylation product.

2.4 Regioselectivity

The hydroarylation reaction can in principle occur on both carbon atoms of the triple bond of substrates **8** and, as previously discussed, possible Au(I)-catalysed hydration has also to be taken into account, as the reactions were not performed under anhydrous conditions.^[20] Since we observed instead complete regioselectivity for the 6-*exo-dig* cyclisation over the 7-*endo-dig*, we investigated the mechanism by DFT calculations. The reaction profile for the cyclisation of substrate 6-ethynyl-1-tosyl-5-(3,4,5-trimethoxybenzyl)-1,2,3,4-tetrahydropyridine, by interaction with the gold(I) complex (L = tris(2,4-di-*tert*-butylphenyl)phosphite), is shown in Scheme 2.6. The π -complex with the alkyne is slightly asymmetrical, as the Au-C distance is 2.19 Å for the terminal carbon, while it is 2.53 Å for the other carbon. According to the Natural Bond Orbital analysis, the charges are -0.41 on the terminal carbon and +0.13 on the internal carbon (Figure 2.1). The reaction with the lowest free energy barrier is the 6-*exo-dig* cyclisation towards intermediate **A** (Scheme 2.6), a result which is in line with the observed regioselectivity. The 7-*endo-dig* cyclisation leads to the thermodynamically most stable intermediate **B**, but the barrier for this process is quite high compared to **TS-A**, which makes the process about 1000 times slower. We hypothesized that the high barrier is due to the deformation energy required to move the Au(I) complex from the terminal to the adjacent carbon of the triple bond. Moreover, as indicated from the NBO charges, -0.41 for the terminal carbon and +0.13 for the internal carbon (Figure 2.1), the latter is more electrophilic. These results are consistent with the theoretical study

on transition metal-catalysed cycloisomerisations of propargyl biphenyls to anthracenes.^[21] A 5-*exo-dig* cyclisation on the *ipso* carbon of the aryl ring is also possible, leading to the *spiro* intermediate **C**. The transition state **TS-C** for this reaction is slightly higher in energy than **TS-B**. Furthermore, **C** is thermodynamically less stable than the reactant, it has a very low barrier of only 2.5 kcal mol⁻¹ for the reverse reaction (*i.e.* from **C** to the reactant) and it does not have any hydrogen that may be lost to form a stable compound. Therefore, we hypothesize that, in case **C** is formed, it merely goes back to the starting material without forming any detectable product. Finally, the barrier for the hydration reaction (**TS-D**) is the highest one, 20.1 kcal mol⁻¹, due to a significant entropic contribution for this bimolecular step ($\Delta S^\ddagger(353\text{ K}) = -57.9\text{ kcal mol}^{-1}$), that raises the free energy barrier by about 11 kcal mol⁻¹, compared to the potential energy. The rate for this reaction is estimated to be very slow even considering the adventitious water in the non-anhydrous solvent.



Scheme 2.6 Free energy profile for the possible reaction steps. Energetics were calculated at M06/def2TZVP-PCM level, at M06/6-31G(d) geometries.

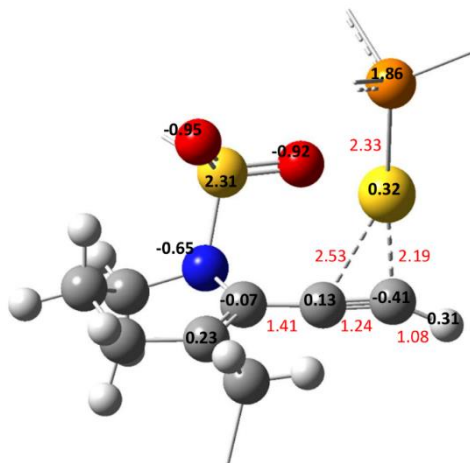
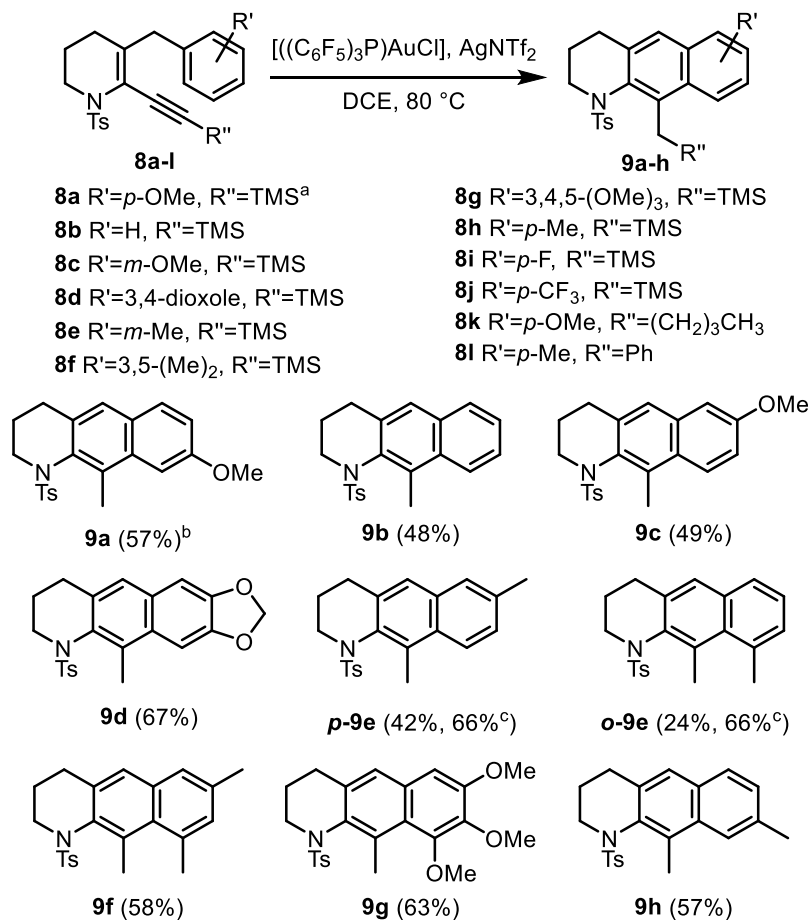


Figure 2.1 NBO charges (black) and bond lengths (red, in Angstrom) for S-AuL⁺ reactant in Scheme 2.6. For sake of clarity, only part of the molecule is shown.

2.5 Reaction substrate scope

The best conditions for the gold(I)-catalysed hydroarylation were applied to the enynes **8b–l**, as reported in Scheme 2.7. Variations of the substituents on the aryl ring showed that the reaction works well with electron-donating methoxy and dioxole groups, as well as with less strong electron-donating methyl groups. The electron-neutral phenyl ring is also suitable. On the other hand, no hydroarylation products were observed when the methodology was applied to electron-poor *p*-fluorophenyl and *p*-(trifluoromethyl)phenyl derivatives **8i** and **8j**. Even substrates **8k** and **8l** bearing an alkyl and a phenyl group respectively on the alkyne moiety, failed to convert into the corresponding tetrahydrobenzo[*g*]quinolines. When the substitution pattern on the aryl ring allows for different regioisomers, the selectivity is dictated by both electronic and steric factors. Complete regioselectivity for the *para* position was observed with *m*-methoxy- and dioxole-substituted enyne **8c** and **8d**, while *m*-methyl derivative **8e** afforded a mixture of *para* and *ortho* products.

Having in mind to extend the reaction also to lactone-derived substrates, we tested an enyne in which the *N*-Ts group is replaced by an oxygen, but preliminary results were discouraging. The different electronic features of the *O*-heterocycles probably require a re-optimisation of the reaction conditions and a dedicated study, which we consider to be a possible future development to further enlarge the spectrum of accessible molecular scaffolds.



Scheme 2.7 Substrate scope. All reactions were performed with 5 mol % [LAuCl] and 5 mol % AgX. ^a TMS in the starting material is converted to H in the product. ^b Yields of isolated product. ^c Overall yield of the two regioisomers.

2.6 Structural analysis of the tetrahydrobenzo[*g*]quinolines

When we first recorded the ¹H NMR spectrum of **9a**, we found an unexpected pattern which is worth of deeper investigation. Indeed, the signals attributed to the methylene groups of the heterocyclic ring are split, indicating that the two protons of each -CH₂- are not equivalent (**a**, **b** and **c** in Figure 2.2, A). This feature is found in the spectra of the tetrahydrobenzo[*g*]quinolines only, as in all the intermediates the protons of every methylene group appear instead as a single peak integrating for two protons.

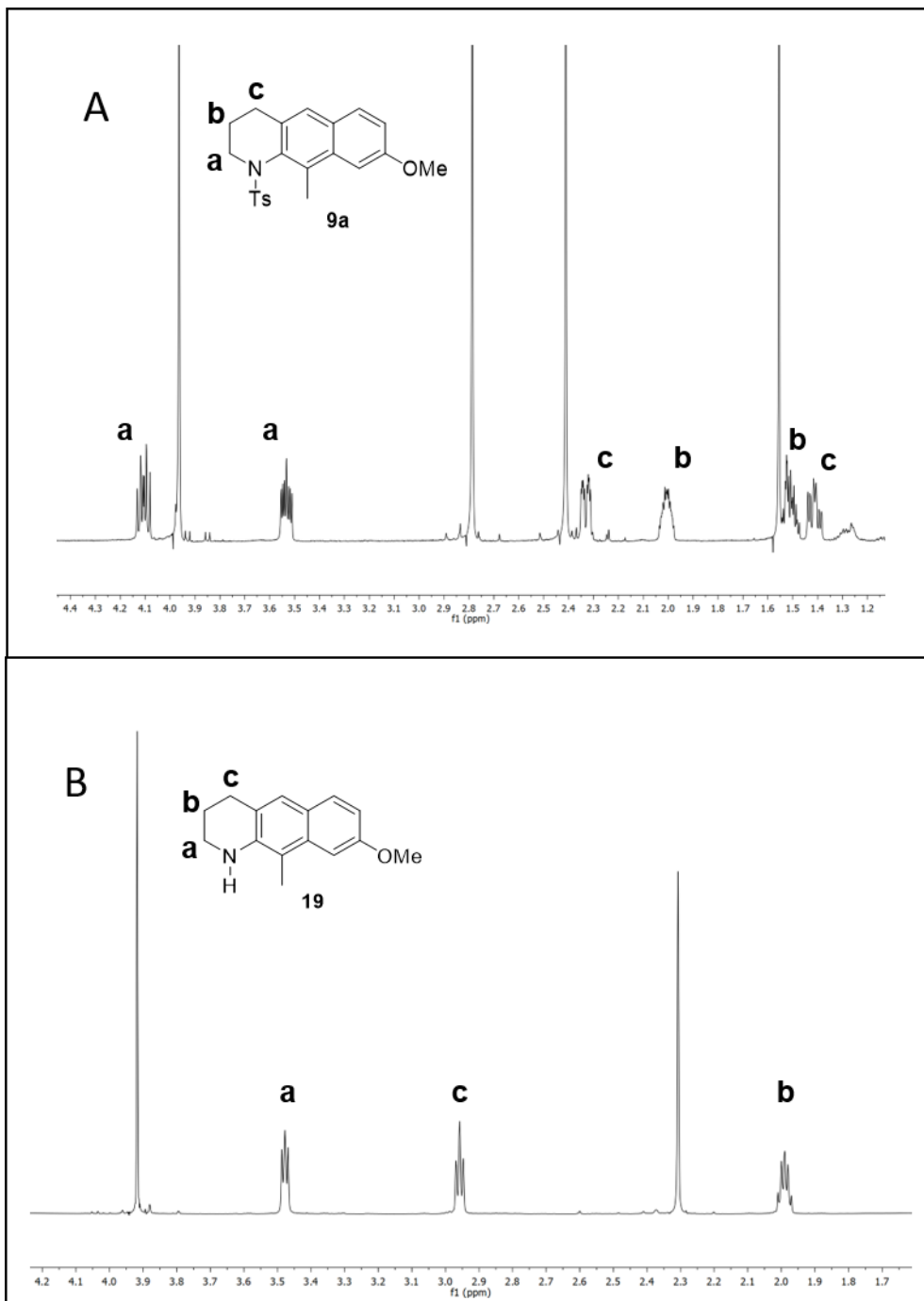


Figure 2.2 The aliphatic zone in the ^1H NMR spectra of **9a** (A) and **19** (B). The assignments were confirmed by COSY and HMQC analysis.

A possible explanation could rely in the rigidity of the fused aromatic scaffold, which may reduce the conformational freedom of the partially saturated *N*-ring. The steric clash between the *N*-tosyl group and the neighbouring methyl group may hamper the pyramidal inversion of the tri-substituted nitrogen atom, preventing the *N*-enantiomers from being averaged in the NMR timescale. Steric interactions have been reported even between the methyl group and the *peri*-hydrogen in 1-methylnaphthalene and 9-methylantracene.^[22] A dynamic NMR study on the slow pyramidal inversion of *N*-sulfonyl morpholines estimated a barrier of 9.2-10.3 kcal mol⁻¹ for the ring interconversion of these fully saturated monocyclic derivatives.^[23] When we calculated the free energy conformational barrier for **9a**, we found a value of 18.9 kcal mol⁻¹, with a $t_{1/2}$ of around 1.7 s. The calculated geometries of the two conformers were in agreement with the crystal structures obtained by X-ray diffraction, which are reported in Figure 2.3.^[24] Replacing the tosyl group with a hydrogen resulted in a calculated barrier of 4 kcal mol⁻¹, with a dramatically lower $t_{1/2}$ of 10⁻¹⁰ s. On this basis, we decided to remove the sulfonyl group of **9a** by means of the radical anion sodium naphthalenide,^[25] obtaining the secondary amine **19**. The ¹H NMR spectrum of **19** (Figure 2.2, B) shows that the signals of the -CH₂-groups are not split anymore, as rapid interconversion between the two enantiomers is now allowed.

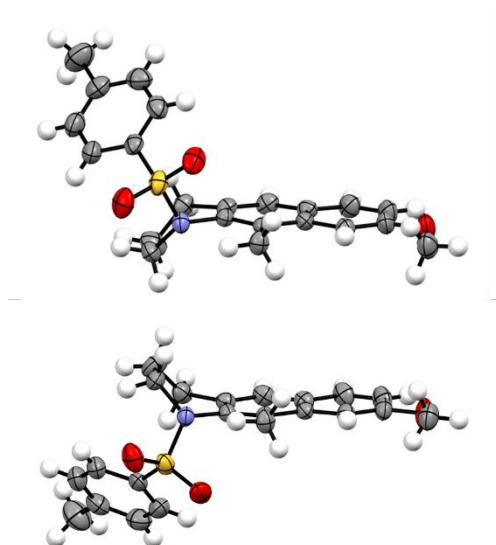


Figure 2.3 ORTEP diagram of the two enantiomers in the crystal structure of **9a**. Ellipsoids are displayed at a 50% probability level. Element colours: grey (C), white (H), red (O), violet (N), yellow (S).

2.7 Conclusion

The gold(I)-catalysed intramolecular hydroarylation of lactam-derived 1,3-enynes has been successfully employed for the synthesis of a series of tetrahydrobenzo[*g*]quinolines. This fused heteropolycyclic molecular scaffold is a structure of interest for the synthesis of natural and pharmaceutical compounds, and its structural rigidity, combined with the steric bulkiness of the *N*-tosyl group, is able to dramatically slow down the interconversion between the two enantiomers on the nitrogen atom. The tetrahydrobenzo[*g*]quinoline synthesis is performed without the exclusion of air and moisture, and it shows complete regio- and chemoselectivity. The selectivity for the 6-*exo-dig* cyclisation was investigated through DFT calculation.

This study extends the range of nitrogen-containing molecular scaffolds accessible in few steps from simple lactams as common precursors, adding a piece to the synthetic opportunities previously disclosed not only by our research group on this topic.

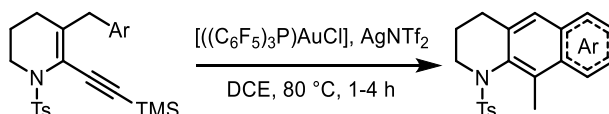
2.8 Experimental section

General information

Flasks and all equipment used for the generation and reaction of moisture-sensitive compounds were dried by electric heat gun under nitrogen. Anhydrous THF was obtained by distillation over LiAlH₄, followed by distillation over Na-benzophenone; anhydrous DME was obtained by distillation over Na-benzophenone; anhydrous toluene was purchased from Sigma Aldrich or Acros Organics; Et₃N was distilled over CaH₂; *t*-BuOK was sublimated under vacuum. All other reagents were used as received, without further purification. Flash column chromatography was performed over silica gel (40–63 μm, 230–400 mesh); *R_f* values refer to TLC carried out on silica gel plates. ¹H NMR and ¹³C NMR spectra were recorded on a Jeol ECZR600, on a Bruker AVIII400 UltraShield Plus or on a Bruker Avance 200, in CDCl₃, using residual solvent peak as an internal reference (CHCl₃, ¹H: 7.26 ppm, ¹³C: 77.16 ppm). Multiplicity is reported as follows: s (singlet), d (doublet), t (triplet), q (quartet), quin (quintet), sext (sextet), m (multiplet), br (broad). GC-MS spectra were recorded at an ionizing voltage of 70 eV. ESI-MS spectra were acquired on a Waters ZQ mass spectrometer equipped with ESCI source. All spectra were recorded in ESI+ mode, using appropriate values of capillary and cone voltages. HRMS analysis were run on a high resolving power hybrid mass spectrometer (HRMS) Orbitrap Fusion (Thermo Scientific, Rodano, Italy), equipped with an a ESI ion source. The samples were analysed in acetonitrile solution using a syringe pump at a flow rate of 5 μL/min. The tuning parameters adopted for the ESI source were: source voltage 4.0 kV. The heated capillary temperature was maintained at 275°C. The mass accuracy of the recorded ions (vs. the calculated ones) was ±2.5 mmu (milli-mass units). Microanalysis were carried out on an elemental analyser. Preparative HPLC was

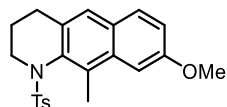
performed on a SunFire™ Prep C18 (5 μm, 10x150 mm) column, with a Waters 2998 photodiode array detector.

General procedure for gold-catalysed hydroarylation



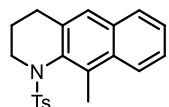
To a 0.1 M solution of the enyne (1.0 eq, 0.1–0.5 mmol) in 1,2-dichloroethane the gold(I) catalyst (5 mol %) and the silver(I) co-catalyst (5 mol %) were added. The mixture was stirred at 80 °C until complete conversion (TLC monitoring), then the solvent was removed under vacuum and the crude product was purified by flash column chromatography.

8-methoxy-10-methyl-1-tosyl-1,2,3,4-tetrahydrobenzo[g]quinoline, **9a**



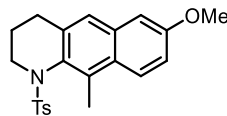
Synthesised according to the general procedure. White solid, 57% yield, **mp** 155–156 °C (PE). **R_f** 0.25 (8/2 PE/Et₂O). **¹H NMR** (600 MHz) δ (ppm): 7.64 (d, 1H, *J* = 8.8 Hz), 7.45 (d, 2H, *J* = 8.2 Hz), 7.32 (d, 1H, *J* = 2.3 Hz), 7.25 (s, 1H), 7.20 (d, 2H, *J* = 8.0 Hz), 7.16 (dd, 1H, *J* = 8.9 Hz, 2.4 Hz), 4.11 (dt, 1H, *J* = 13.8 Hz, 8.4 Hz), 3.96 (s, 3H), 3.55–3.51 (m, 1H), 2.79 (s, 3H), 2.41 (s, 3H), 2.33 (ddd, 1H, *J* = 14.6 Hz, 4.8 Hz, 2.8 Hz), 2.04–1.98 (m, 1H), 1.54–1.47 (m, 1H), 1.41 (td, 1H, *J* = 13.3 Hz, 5.5 Hz). **¹³C NMR** (150 MHz) δ (ppm): 157.5 (Cq), 143.6 (Cq), 137.0 (Cq), 134.1 (Cq), 133.9 (Cq), 133.5 (Cq), 133.4 (Cq), 129.7 (CH), 129.2 (CH), 127.7 (CH), 127.6 (Cq), 123.8 (CH), 118.6 (CH), 104.1 (CH), 55.5 (CH₃), 45.9 (CH₂), 26.4 (CH₂), 24.1 (CH₂), 21.7 (CH₃), 16.7 (CH₃). **HRMS** (ESI) *m/z*: calcd. for C₂₂H₂₃NO₃Na⁺ 404.1291; found 404.1297.

10-methyl-1-tosyl-1,2,3,4-tetrahydrobenzo[g]quinoline, **9b**



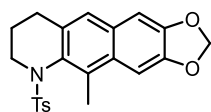
Synthesised according to the general procedure. White solid, 48% yield, **mp** 131–132 °C (MeOH). **R_f** 0.19 (9/1 PE/Et₂O). **¹H NMR** (600 MHz) δ (ppm): 8.08 (d, 1H, *J* = 8.3 Hz), 7.74 (d, 1H, *J* = 7.6 Hz), 7.54–7.47 (m, 2H) superimposed to 7.46 (d, 2H, *J* = 7.69 Hz), 7.32 (s, 1H), 7.20 (d, 2H, *J* = 7.6 Hz), 4.15–4.10 (m, 1H), 3.57–3.51 (m, 1H), 2.83 (s, 3H), 2.41 (s, 3H), 2.40–2.35 (m, 1H), 2.07–2.00 (m, 1H), 1.55–1.43 (m, 2H). **¹³C NMR** (150 MHz) δ (ppm): 143.7 (Cq), 137.0 (Cq), 136.0 (Cq), 134.8 (Cq), 133.5 (Cq), 132.9 (Cq), 132.3 (Cq), 129.7 (CH), 127.7 (CH), 127.7 (CH), 126.2 (CH), 125.6 (CH), 125.4 (CH), 124.0 (CH), 45.9 (CH₂), 26.7 (CH₂), 24.0 (CH₂), 21.7 (CH₃), 16.5 (CH₃). **HRMS** (ESI) *m/z*: calcd. for C₂₁H₂₁NO₂Na⁺ 374.1191; found 374.1186.

7-methoxy-10-methyl-1-tosyl-1,2,3,4-tetrahydrobenzo[g]quinoline, 9c



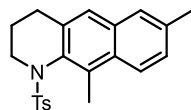
Synthesised according to the general procedure. White solid, 49% yield, **mp** 166–167 °C (MeOH). **R_f** 0.24 (8/2 hexane/EtOAc). **¹H NMR** (400 MHz) δ (ppm): 7.98 (d, 1H, J = 9.2 Hz), 7.46 (d, 2H, J = 8.0 Hz), 7.21–7.15 (m, 4H), 7.04 (d, 1H, J = 2.8 Hz), 4.15–4.05 (m, 1H), 3.92 (s, 3H), 3.55–3.48 (m, 1H), 2.79 (s, 3H), 2.41 (s, 3H), 2.36–2.31 (m, 1H), 2.06–1.98 (m, 1H), 1.56–1.41 (m, 2H). **¹³C NMR** (100 MHz) δ (ppm): 157.9 (Cq), 143.6 (Cq), 137.1 (Cq), 136.7 (Cq), 134.8 (Cq), 133.6 (Cq), 131.6 (Cq), 129.7 (2CH), 128.1 (CH), 127.7 (2CH), 127.1 (CH), 123.0 (CH), 117.8 (CH), 105.9 (CH), 55.4 (CH₃), 45.9 (CH₂), 26.7 (CH₂), 24.0 (CH₂), 21.7 (CH₃), 16.4 (CH₃). Elemental analysis (%): calcd for C₂₂H₂₃NO₃· $\frac{1}{4}$ H₂O C 68.46, H 6.14, N 3.63; found C 68.21, H 6.13, N 3.45.

5-methyl-6-tosyl-6,7,8,9-tetrahydro-[1,3]dioxolo[4',5':4,5]benzo[1,2-g]quinoline, 9d



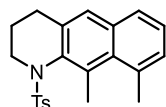
Synthesised according to the general procedure. White solid, 67% yield, **mp** 175–177 °C (hexane/EtOAc). **R_f** 0.14 (9/1 PE/EtOAc). **¹H NMR** (600 MHz) δ (ppm): 7.45 (d, 2H, J = 8.3 Hz), 7.36 (s, 1H), 7.20 (d, 2H, J = 8.3 Hz), 7.14 (s, 1H), 7.01 (s, 1H), 6.05 (s, 2H), 4.10 (dt, 1H, J = 13.8 Hz, 8.6 Hz), 3.50 (ddd, 1H, J = 13.4 Hz, 8.3 Hz, 4.5 Hz), 2.72 (s, 3H), 2.41 (s, 3H), 2.32–2.27 (m, 1H), 2.03–1.96 (m, 1H), 1.55–1.46 (m, 1H), 1.41 (td, 1H, J = 13.3 Hz, 5.4 Hz). **¹³C NMR** (150 MHz) δ (ppm): 147.7 (Cq), 147.6 (Cq), 143.6 (Cq), 137.0 (Cq), 134.3 (Cq), 133.7 (Cq), 132.5 (Cq), 129.6 (CH), 129.6 (Cq), 129.3 (Cq), 127.7 (CH), 123.3 (CH), 103.7 (CH), 102.1 (CH), 101.2 (CH₂), 45.8 (CH₂), 26.3 (CH₂), 24.0 (CH₂), 21.7 (CH₃), 16.8 (CH₃). **HRMS** (ESI) m/z : C₂₂H₂₁NO₄SN⁺ 418.1084; found 418.1087.

7,10-dimethyl-1-tosyl-1,2,3,4-tetrahydrobenzo[g]quinoline, p-9e



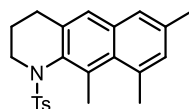
Synthesised according to the general procedure, separated from regioisomer **o-9e** by HPLC (9/1 MeCN/H₂O, 2.5 ml/min). White solid, 42% yield (66% total yield of two isomers), **mp** 188–190 °C. **R_f** 0.45 (8/2 PE/Et₂O). **¹H NMR** (600 MHz) δ (ppm): 7.97 (d, 1H, J = 8.6 Hz), 7.50 (s, 1H), 7.44 (d, 2H, J = 8.3 Hz), 7.35 (dd, 1H, J = 8.6 Hz, 1.4 Hz), 7.22 (s, 1H), 7.19 (d, 2H, J = 7.9 Hz), 4.11 (td, 1H, J = 13.8 Hz, 8.6 Hz), 3.53 (ddd, 1H, J = 13.1 Hz, 8.3 Hz, 4.1 Hz), 2.80 (s, 3H), 2.51 (s, 3H), 2.41 (s, 3H), 2.36–2.32 (m, 1H), 2.05–1.98 (m, 1H), 1.54–1.47 (m, 1H), 1.42 (td, 12.9 Hz, 4.8 Hz). **¹³C NMR** (150 MHz) δ (ppm): 143.6 (Cq), 137.0 (Cq), 136.1 (Cq), 135.8 (Cq), 134.7 (Cq), 132.7 (Cq), 132.5 (Cq), 131.1 (Cq), 129.7 (CH), 127.8 (CH), 127.7 (CH), 126.7 (CH), 125.3 (CH), 123.4 (CH), 45.9 (CH₂), 26.7 (CH₂), 24.0 (CH₂), 21.7 (CH₃), 21.7 (CH₃), 16.4 (CH₃). **HRMS** (ESI) m/z : calcd. for C₂₂H₂₃NO₂SN⁺ 388.1347, found 388.1345

9,10-dimethyl-1-tosyl-1,2,3,4-tetrahydrobenzo[g]quinoline, o-9e



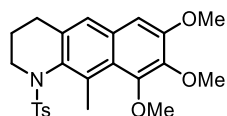
Synthesised according to the general procedure, separated from regioisomer **p-9e** by HPLC (9/1 MeCN/H₂O, 2.5 ml/min). White solid, 24% yield (66% total yield of two isomers). *R_f* 0.45 (8/2 PE/Et₂O). **¹H NMR** (600 MHz) δ (ppm): 7.55 (d, 1H, *J* = 8.3 Hz), 7.47 (d, 2H, *J* = 8.3 Hz), 7.33–7.29 (m, 1H), 7.28–7.26 (m, 2H), 7.20 (d, 2H, *J* = 7.6 Hz), 4.16–4.10 (m, 1H), 3.48 (ddd, 1H, *J* = 13.1 Hz, 8.3 Hz, 4.8 Hz), 2.97 (s, 3H) superimposed to 2.97 (s, 3H), 2.41 (s, 3H), 2.36 (ddd, 1H, *J* = 14.5 Hz, 5.2 Hz, 2.8 Hz), 1.54–1.48 (m, 1H), 1.43 (td, 1H, *J* = 13.2 Hz, 6.0 Hz). **¹³C NMR** (150 MHz) δ (ppm): 143.6 (Cq), 137.1 (Cq), 136.7 (Cq), 136.7 (Cq), 135.3 (Cq), 135.0 (Cq), 140.0 (Cq), 133.7 (Cq), 129.7 (CH), 129.6 (CH), 127.7 (CH), 126.8 (CH), 125.8 (CH), 125.1 (CH), 45.7 (CH₂), 26.6 (CH₂), 26.2 (CH₃), 24.0 (CH₂), 21.9 (CH₃), 21.8 (CH₃). **HRMS** (ESI) *m/z*: calcd. for C₂₂H₂₃NO₂SNa⁺ 388.1347, found 388.1343.

7,9,10-trimethyl-1-tosyl-1,2,3,4-tetrahydrobenzo[g]quinoline, 9f



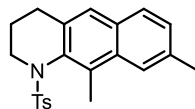
Synthesised according to the general procedure. White solid, 58% yield, **mp** 202–203 °C (MeCN). *R_f* 0.28 (9/1 PE/Et₂O). **¹H NMR** (600 MHz) δ (ppm): 7.46 (d, 2H, *J* = 8.2 Hz), 7.32 (s, 1H), 7.18 (d, 2H, *J* = 8.1 Hz) superimposed to 7.17 (s, 1H), 7.12 (s, 1H), 4.12 (ddd, 1H, *J* = 13.8 Hz, 8.8 Hz, 7.8 Hz), 3.50–3.45 (m, 1H), 2.95 (s, 3H), 2.93 (s, 3H), 2.43 (s, 3H), 2.40 (s, 3H), 2.33 (ddd, 1H, *J* = 14.5 Hz, 5.3 Hz, 2.8 Hz), 2.04–1.98 (m, 1H), 1.54–1.47 (m, 1H), 1.42–1.36 (m, 1H). **¹³C NMR** (150 MHz) δ (ppm): 143.5 (Cq), 137.1 (Cq), 136.5 (Cq), 136.4 (Cq), 135.4 (Cq), 135.2 (Cq), 134.3 (Cq), 134.2 (Cq), 131.9 (CH), 131.8 (Cq), 129.6 (CH), 127.7 (CH), 125.8 (CH), 124.5 (CH), 45.8 (CH₂), 26.6 (CH₂), 26.1 (CH₃), 24.0 (CH₂), 21.7 (CH₃), 21.2 (CH₃). **HRMS** (ESI) *m/z*: calcd. for C₂₃H₂₅NO₂SNa⁺ 402.1504; found 407.1500.

7,8,9-trimethoxy-10-methyl-1-tosyl-1,2,3,4-tetrahydrobenzo[g]quinoline, 9g



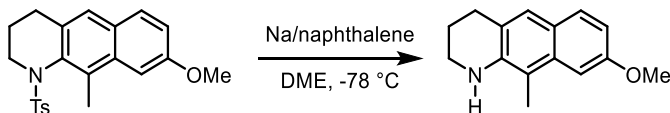
Synthesised according to the general procedure. White solid, 63% yield, **mp** 166–167 °C (*n*-Pr₂O). *R_f* 0.36 (8/2 PE/EtOAc). **¹H NMR** (600 MHz) δ (ppm): 7.51 (d, 2H, *J* = 7.9 Hz), 7.21 (d, 2H, *J* = 7.9 Hz), 7.14 (s, 1H), 6.83 (s, 1H), 4.14–4.08 (m, 1H), 3.96 (s, 3H), 3.96 (s, 6H), 3.49–3.44 (m, 1H), 2.92 (s, 3H), 2.41 (s, 3H), 2.34–2.30 (m, 1H), 2.06–1.99 (m, 1H), 1.52–1.47 (m, 2H). **¹³C NMR** (150 MHz) δ (ppm): 152.9 (Cq), 151.5 (Cq), 143.5 (Cq), 142.4 (Cq), 137.2 (Cq), 135.8 (Cq), 134.8 (Cq), 133.1 (Cq), 130.8 (Cq), 129.6 (CH), 127.7 (CH), 123.7 (Cq), 123.0 (CH), 102.8 (CH), 61.6 (CH₃), 61.2 (CH₃), 55.9 (CH₃), 45.7 (CH₂), 26.6 (CH₂), 24.0 (CH₂), 24.0 (CH₂), 21.7 (CH₃), 19.2 (CH₃). **HRMS** (ESI) *m/z*: calcd. for C₂₄H₂₇NO₅SNa⁺ 464.1508; found 464.1505.

8,10-dimethyl-1-tosyl-1,2,3,4-tetrahydrobenzo[g]quinoline, 9h



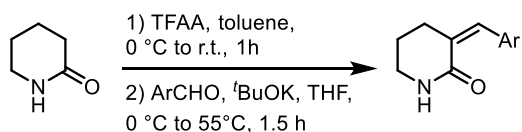
Synthesised according to the general procedure. White solid, 57% yield, **mp** 178–179 °C (hexane). **R_f** 0.36 (8/2 PE/Et₂O). **¹H NMR** (600 MHz) δ (ppm): 7.85 (s, 1H), 7.63 (d, 1H, *J* = 8.3 Hz), 7.45 (d, 2H, *J* = 8.3 Hz), 7.32 (dd, 1H, *J* = 8.3, 1.4 Hz), 7.27 (s, 1H), 7.19 (d, 2H, *J* = 8.3 Hz), 4.14–4.08 (m, 1H), 3.53 (ddd, 1H, *J* = 13.1, 7.9, 4.1 Hz), 2.80 (s, 3H), 2.56 (s, 3H), 2.41 (s, 3H), 2.37–2.33 (m, 1H), 2.05–1.98 (m, 1H), 1.55–1.48 (m, 1H), 1.44 (td, 1H, *J* = 13.1, 5.5 Hz). **¹³C NMR** (150 MHz) δ (ppm): 143.6 (Cq), 137.1 (Cq), 135.2 (Cq), 135.0 (Cq), 134.1 (Cq), 135.6 (Cq), 133.0 (Cq), 130.5 (Cq), 129.7 (CH), 128.3 (CH), 128.3 (CH), 127.7 (CH), 127.5 (CH), 124.6 (CH), 123.8 (CH), 45.9 (CH₂), 26.6 (CH₂), 24.1 (CH₂), 22.2 (CH₃), 21.7 (CH₃), 16.5 (CH₃). **HRMS** (ESI) *m/z*: calcd. for C₂₂H₂₃NO₂SNa⁺ 388.1347; found 388.1349.

Synthesis of 8-methoxy-10-methyl-1,2,3,4-tetrahydrobenzo[g]quinoline, 19



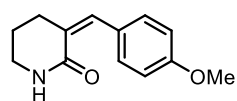
The *N*-tosyl deprotection was performed according to a literature procedure.^[25a] A solution of **9a** (1.0 eq, 0.2 mmol) in anhydrous DME (0.1 M) was cooled down to –78 °C. A 1.0 M solution of Na and naphthalene (6.0 eq) in anhydrous DME was prepared. The colour of sodium naphthalenide is dark green. The solution of sodium naphthalenide was slowly added to the solution of **9a** at –78 °C until the dark green colour was persistent. The mixture was stirred at –78 °C for 30 min, then it was allowed to warm to room temperature, H₂O was added and the mixture was extracted three times with EtOAc; the combined organic layers were dried over anhydrous Na₂SO₄, filtered and the solvent was removed under vacuum. The crude product was purified by flash column chromatography to afford pure **10a** as an off-white solid. 75% yield, **mp** 114–116 °C (hexane). **R_f** 0.40 (9/1 PE/EtOAc). **¹H NMR** (600 MHz) δ (ppm): 7.52 (d, 1H, *J* = 8.8 Hz), 7.28 (s, 1H), 7.08 (d, 1H, *J* = 2.1 Hz), 6.85 (dd, 1H, *J* = 8.8, 2.2 Hz), 3.92 (s, 3H), 3.49–3.47 (m, 2H), 2.96 (d, 2H, *J* = 6.4 Hz), 2.31 (s, 3H), 1.99 (quin, 2H, *J* = 6.2 Hz). **¹³C NMR** (150 MHz) δ (ppm): 157.6 (Cq), 141.2 (Cq), 133.5 (Cq), 129.5 (CH), 125.8 (CH), 122.8 (Cq), 122.0 (Cq), 113.4 (CH), 109.9 (Cq), 101.4 (CH), 55.3 (CH₂), 42.8 (CH₂), 28.3 (CH₂), 22.3 (CH₂), 11.5 (CH₃). **HRMS** *m/z*: calcd. for 250.1208, found 250.1211.

General procedure for aldol condensation of lactams^[17]



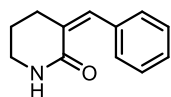
To a solution of lactam (1.0 eq, 10–30 mmol) in anhydrous toluene (1.5 M), at 0 °C under N₂ atmosphere, trifluoroacetic anhydride (1.1 eq) was slowly added. The mixture was stirred at 25 °C for 1 h, then the volatiles were removed under reduced pressure. To the resulting liquid, TFA-protected lactam, the aldehyde (0.9 eq) was added. The mixture was slowly added to a 1.0 M solution of *t*-BuOK (1.5 eq) in anhydrous THF, at 0 °C under N₂ atmosphere, then it was stirred at 55 °C until disappearance of the aldehyde; if necessary, another 0.5 eq of *t*-BuOK was added to complete the reaction. The mixture was concentrated to a slurry, then water (80–100 ml) was added, resulting in the precipitation of the solid product. The mixture was filtered and the solid was dried and precipitated from ethyl acetate/petroleum ether to afford pure α -benzylidene lactam.

3-(4-methoxybenzylidene)piperidin-2-one, **15a**^[17a]



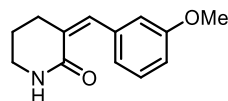
Synthesised according to the general procedure. White solid, 60% yield. **¹H NMR** (600 MHz) δ (ppm): 7.77 (br s, 1H), 7.37 (d, 2H, *J* = 8.7 Hz), 6.93–6.90 (m, 2H), 6.00 (br s, 1H), 3.83 (s, 3H), 3.43–3.41 (m, 2H), 2.83–2.81 (m, 2H), 1.88 (quin, 2H, *J* = 6.0 Hz). **GC-MS** *m/z* (%): 217 [M]⁺ (77), 216 (100), 174 (21).

3-benzylidenepiperidin-2-one, **15b**^[17b]



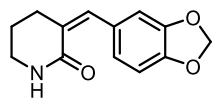
Synthesised according to the general procedure. White solid, 57% yield. **¹H NMR** (600 MHz) δ (ppm): 7.81 (t, 1H, *J* = 2.0 Hz), 7.39 (d, 4H, *J* = 4.5 Hz), 7.33–7.29 (m, 1H), 6.32 (br s, 1H), 3.45–3.42 (m, 2H), 2.83–2.81 (m, 2H), 1.87 (quin, 2H, *J* = 6.0 Hz). **GC-MS** *m/z* (%): 187 [M]⁺ (32), 186 (100), 129 (14), 115 (17).

3-(3-methoxybenzylidene)piperidin-2-one, **15c**^[26]



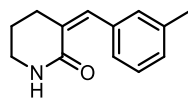
Synthesised according to the general procedure. White solid, 45% yield. **¹H NMR** (400 MHz) δ (ppm): 7.78 (s, 1H), 7.30 (t, 1H, *J* = 8.0 Hz), 6.98 (d, 1H, *J* = 7.9 Hz), 6.98 (d, 1H, *J* = 7.6 Hz), 6.92 (s, 1H), 6.87 (d, 1H, *J* = 8.0 Hz), 6.43 (br s, 1H), 3.82 (s, 3H), 3.45–3.41 (m, 2H), 2.83–2.79 (m, 2H), 1.90–1.83 (m, 2H).

3-(benzo[d][1,3]dioxol-5-ylmethylene)piperidin-2-one, 15d



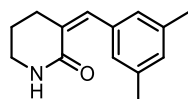
Synthesised according to the general procedure. White solid, 51% yield, **mp** 193–194 °C (MeOH). **¹H NMR** (600 MHz) δ (ppm): 7.71 (br s, 1H), 6.92–6.90 (m, 2H), 6.84–6.82 (m, 1H), 6.33 (br s, 1H), 5.99 (s, 2H), 3.43–3.41 (m, 2H), 2.81–2.78 (m, 2H), 1.87 (quin, 2H, $J = 6.0$ Hz). **¹³C NMR** (150 MHz) δ (ppm): 166.9 (Cq), 147.7 (Cq), 147.7 (Cq), 135.7 (CH), 130.0 (Cq), 128.0 (Cq), 124.9 (CH), 109.9 (CH), 108.5 (CH), 101.4 (CH₂), 42.2 (CH₂), 26.5 (CH₂), 23.2 (CH₂). **GC-MS** m/z (%): 231 [M]⁺ (100), 230 (91).

3-(3-methylbenzylidene)piperidin-2-one, 15e^[17b]



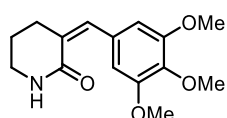
Synthesised according to the general procedure. White solid, 55% yield. **¹H NMR** (600 MHz) δ (ppm): 7.79 (br s, 1H), 7.29–7.25 (m, 2H), 7.21–7.18 (m, 2H), 7.13 (d, 1H, $J = 7.5$ Hz), 6.32 (br s, 1H), 3.45–3.42 (m, 2H), 2.84–2.80 (m, 2H), 2.37 (s 3H), 1.87 (quin, 2H, $J = 6.0$ Hz). **GC-MS** m/z (%): 201 [M]⁺ (36), 200 (100), 186 (11).

3-(3,5-dimethylbenzylidene)piperidin-2-one, 15f



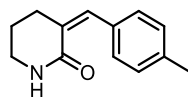
Synthesised according to the general procedure. White solid, 50% yield, **mp** 174–176 °C (MeOH). **¹H NMR** (600 MHz) δ (ppm): 7.75 (br s, 1H), 7.00 (s, 2H), 6.95 (s, 1H), 6.33 (br s, 1H), 3.44–3.41 (m, 2H), 2.82–2.80 (m, 2H), 2.33 (s, 3H), 1.86 (quin, 2H, $J = 6.0$ Hz). **¹³C NMR** (150 MHz) δ (ppm): 166.9 (Cq), 137.9 (Cq), 136.2 (CH), 135.9 (Cq), 130.0 (CH), 129.2 (Cq), 127.7 (CH), 42.3 (CH₂), 26.5 (CH₂), 23.2 (CH₂), 21.5 (CH₃). **GC-MS** m/z (%): 215 [M]⁺ (40), 214 (100), 200 (26).

3-(3,4,5-trimethoxybenzylidene)piperidin-2-one, 15g



Synthesised according to the general procedure. The product did not precipitate after addition of water, so it was extracted with ethyl acetate, then it was precipitated from ethyl acetate/petroleum ether. White solid, 76% yield, **mp** 145–147 °C (MeOH). **¹H NMR** (200 MHz) δ (ppm): 7.73 (br s, 1H), 6.62 (s, 2H), 6.50 (br s, 1H), 3.87 (s, 3H) superimposed to 3.86 (s, 6H), 3.48–3.38 (m, 2H), 2.89–2.80 (m, 2H), 1.88 (quin, 2H, $J = 6.2$ Hz). **¹³C NMR** (50 MHz) δ (ppm): 166.9 (Cq), 153.1 (Cq), 138.4 (Cq), 135.8 (CH), 131.4 (Cq), 129.0 (Cq), 107.4 (CH), 61.0 (CH₃), 56.3 (CH₃), 42.1 (CH₂), 26.4 (CH₂), 23.2 (CH₂). **GC-MS** m/z (%): 277 [M]⁺ (100), 262 (19), 230 (23), 246 (17).

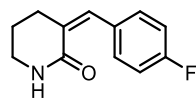
3-(4-methylbenzylidene)piperidin-2-one, 15h^[17b]



Synthesised according to the general procedure. White solid, 40% yield. **¹H NMR** (600 MHz) δ (ppm): 7.79 (br s, 1H), 7.30 (d, 2H, $J = 8.0$ Hz), 7.19 (d, 2H, $J = 7.9$ Hz), 6.06 (br s, 1H), 3.44–3.41 (m, 2H), 2.84–2.81

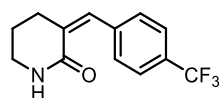
(m, 2H), 2.37 (s, 3H), 1.89–1.84 (m, 2H). **GC-MS** m/z (%): 201 [M]⁺ (37), 200 (100), 128 (15), 115 (15).

3-(4-fluorobenzylidene)piperidin-2-one, **15i**^[17b]



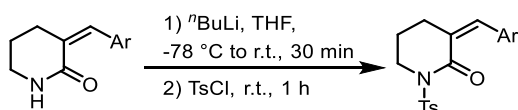
Synthesised according to the general procedure. White solid, 64% yield. **¹H NMR** (600 MHz) δ (ppm): 7.77 (br s, 1H), 7.38–7.35 (m, 2H), 7.10–7.06 (m, 2H), 5.89 (br s, 1H), 3.45–3.42 (m, 2H), 2.80–2.70 (m, 2H), 2.17 (s, 3H), 1.91–1.86 (m, 2H). **GC-MS** m/z (%): 205 [M]⁺ (38), 204 (100), 147 (19), 133 (22).

3-(4-(trifluoromethyl)benzylidene)piperidin-2-one, **15j**^[17b]



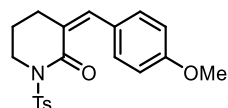
Synthesised according to the general procedure. White solid, 44% yield. **¹H NMR** (600 MHz) δ (ppm): 7.81 (br s, 1H), 7.64 (d, 2H, $J = 8.1$ Hz), 7.47 (d, 2H, $J = 8.3$ Hz), 6.42 (br s, 1H), 3.46–3.43 (m, 2H), 2.80–2.77 (m, 2H), 1.91–1.86 (m, 2H). **GC-MS** m/z (%): 255 [M]⁺ (36), 254 (100), 227 (12).

General procedure for *N*-tosyl protection of lactams^[7]



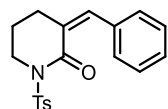
A 0.2 M suspension of α -benzylidene lactam (1.0 eq, 3–5 mmol) in anhydrous THF, under N₂ atmosphere, was cooled to –78 °C and *n*-BuLi (1.1 eq, 1.6 M or 2.5 M solution in hexane) was slowly added. The mixture was stirred below –70 °C for 15 min, then the cold bath was removed and the solution was stirred for 30 min. A solution of *p*-toluenesulfonyl chloride (1.2 eq) in anhydrous THF was added and the mixture was stirred for 1 h at room temperature. A 10% solution of NaOH was added and the mixture was extracted with ethyl acetate; the combined organic layers were dried over Na₂SO₄, filtered and the solvent was removed under reduced pressure. The crude product was purified by flash chromatography.

3-(4-methoxybenzylidene)-1-tosylpiperidin-2-one, **16a**



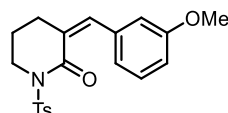
Synthesised according to the general procedure. White solid, 61% yield, **mp** 159–161 °C (EtOAc). **R_f** 0.38 (99/1 DCM/EtOAc). **¹H NMR** (600 MHz) δ (ppm): 7.95 (d, 2H, $J = 8.4$ Hz), 7.73 (s, 1H), 7.33–7.31 (m, 4H), 6.89 (d, 2H, $J = 8.9$ Hz), 4.06–4.04 (m, 2H), 3.82 (s, 3H), 2.81–2.78 (m, 2H), 2.42 (s, 3H), 1.98 (quin, 2H, $J = 6.0$ Hz). **¹³C NMR** (150 MHz) δ (ppm): 165.3 (Cq), 160.4 (Cq), 144.6 (Cq), 139.4 (CH), 136.8 (Cq), 132.2 (CH), 129.5 (CH), 128.7 (CH), 127.9 (Cq), 126.4 (Cq), 114.1 (CH), 55.5 (CH₃), 46.5 (CH₂), 26.5 (CH₂), 23.6 (CH₂), 21.8 (CH₃). **ESI-MS** m/z : 394 [M+Na]⁺, 372 [M+H]⁺.

3-benzylidene-1-tosylpiperidin-2-one, 16b



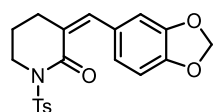
Synthesised according to the general procedure. White solid, 80% yield, **mp** 170–171 °C (EtOAc). **R_f** 0.44 (9/1 DCM/PE). **¹H NMR** (600 MHz) δ (ppm): 7.96 (d, 2H, J = 8.3 Hz), 7.78 (s, 1H), 7.38–7.36 (m, 2H), 7.34–7.32 (m, 5H), 4.06–4.04 (m, 2H), 2.80–2.78 (m, 2H), 2.43 (s, 3H), 1.99–1.95 (m, 2H). **¹³C NMR** (150 MHz) δ (ppm): 165.0 (Cq), 144.8 (Cq), 139.6 (CH), 136.7 (Cq), 135.3 (Cq), 130.2 (CH), 129.5 (CH), 129.1 (CH), 128.9 (Cq), 128.8 (CH), 128.6 (CH), 46.7 (CH₂), 26.3 (CH₂), 23.5 (CH₂), 21.8 (CH₃). **GC-MS** m/z (%): 277 (65), 276 (100), 129 (11), 115 (18) 91 (23).

3-(3-methoxybenzylidene)-1-tosylpiperidin-2-one, 16c



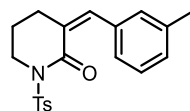
Synthesised according to the general procedure. White solid, 64% yield, **mp** 134–135 °C (toluene). **¹H NMR** (400 MHz) δ (ppm): 7.95 (d, 2H, J = 8.0 Hz), 7.74 (t, 1H, J = 2.0 Hz), 7.33 (d, 2H, J = 8.0 Hz), 7.28 (t, 1H, J = 8.0 Hz), 6.91 (d, 1H, J = 7.6 Hz), 6.89–6.83 (m, 2H), 4.06–4.02 (m, 2H), 3.79 (s, 3H), 2.80–2.76 (m, 2H), 2.43 (s, 3H), 1.99–1.92 (m, 2H). **¹³C NMR** (100 MHz) δ (ppm): 164.9 (Cq), 159.6 (Cq), 144.8 (Cq), 139.4 (CH), 136.6 (Cq), 136.5 (Cq), 129.6 (Cq), 129.5 (CH), 129.1 (CH), 128.7 (CH), 122.5 (CH), 115.7 (CH), 114.5 (CH), 55.4 (CH₃), 46.7 (CH₂), 26.3 (CH₂), 23.5 (CH₂), 21.8 (CH₃). **ESI-MS** m/z : 765 [2M+Na]⁺, 394 [M+Na]⁺, 372 [M+H]⁺.

3-(benzo[d][1,3]dioxol-5-ylmethylene)-1-tosylpiperidin-2-one, 16d



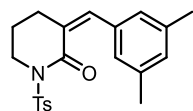
Synthesised according to the general procedure. White solid, 59% yield, **mp** 190–191 °C (EtOAc). **R_f** 0.30 (99/1 DCM/EtOAc). **¹H NMR** (600 MHz) δ (ppm): 7.94 (d, 2H, J = 8.3 Hz), 7.68 (s, 1H), 7.33 (d, 2H, J = 8.4 Hz), 7.87–7.84 (m, 2H), 6.81 (d, 1H, J = 8.0 Hz), 5.99 (d, 2H, J = 0.7 Hz), 4.05–4.03 (m, 2H), 2.78–2.76 (m, 2H), 2.43 (s, 3H), 1.98 (quin, 2H, J = 6.1 Hz). **¹³C NMR** (150 MHz) δ (ppm): 165.1 (Cq), 148.5 (Cq), 147.9 (Cq), 144.7 (Cq), 139.4 (CH), 136.8 (Cq), 129.5 (CH), 129.4 (Cq), 128.7 (CH), 127.0 (Cq), 125.8 (CH), 109.9 (CH), 108.6 (CH), 101.6 (CH₂), 46.5 (CH₂), 26.5 (CH₂), 23.5 (CH₂), 21.8 (CH₃). **ESI-MS** m/z : 408 [M+Na]⁺, 386 [M+H]⁺.

3-(3-methylbenzylidene)-1-tosylpiperidin-2-one, 16e



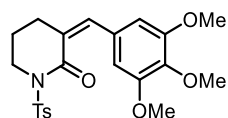
Synthesised according to the general procedure. White solid, 75% yield, **mp** 110–111 °C (*i*-Pr₂O). **R_f** 0.46 (8/2 PE/EA). **¹H NMR** (600 MHz) δ (ppm): 7.95 (d, 2H, J = 8.4 Hz), 7.75 (s, 1H), 7.33 (d, 2H, J = 8.3 Hz), 7.26 (t, 1H, J = 7.9 Hz), 7.15–7.12 (m, 3H), 4.06–4.03 (m, 2H), 2.80–2.77 (m, 2H), 2.43 (s, 3H), 2.35 (s, 3H), 1.98–1.94 (m, 2H). **¹³C NMR** (150 MHz) δ (ppm): 165.0 (Cq), 144.8 (Cq), 139.8 (CH), 138.3 (Cq), 136.7 (Cq), 135.2 (Cq), 130.8 (CH), 129.9 (CH), 129.5 (CH), 128.8 (CH), 128.7 (Cq), 128.5 (CH), 127.2 (CH), 46.7 (CH₂), 26.3 (CH₂), 23.5 (CH₂), 21.8 (CH₃), 21.6 (CH₃). **ESI-MS** m/z : 378 [M+Na]⁺, 356 [M+H]⁺.

3-(3,5-dimethylbenzylidene)-1-tosylpiperidin-2-one, **16f**



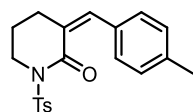
Synthesised according to the general procedure. White solid, 71% yield, **mp** 131–132 °C (*i*-Pr₂O). **R_f** 0.31 (DCM). **¹H NMR** (600 MHz) δ (ppm): 7.95 (d, 2H, *J* = 8.4 Hz), 7.72 (s, 1H), 7.33 (d, 2H, *J* = 8.1 Hz), 6.97 (s, 1H), 6.93 (s, 2H), 4.05–4.03 (m, 2H), 2.79–2.77 (m, 2H), 2.43 (s, 3H), 2.30 (s, 6H), 1.96 (quin, 2H, *J* = 6.0 Hz). **¹³C NMR** (150 MHz) δ (ppm): 165.1 (Cq), 144.7 (Cq), 139.9 (CH), 138.1 (Cq), 136.7 (Cq), 135.2 (Cq), 130.9 (CH), 129.5 (CH), 128.7 (CH), 128.5 (Cq), 128.0 (CH), 46.7 (CH₂), 26.4 (CH₂), 23.5 (CH₂), 21.8 (CH₃), 21.4 (CH₃). **ESI-MS** *m/z*: 392 [M+Na]⁺, 370 [M+H]⁺.

1-tosyl-3-(3,4,5-trimethoxybenzylidene)piperidin-2-one, **16g**



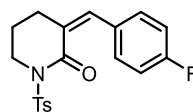
Synthesised according to the general procedure. White solid, 82% yield, **mp** 56–58 °C (hexane). **R_f** 0.33 (6/4 PE/EtOAc). **¹H NMR** (200 MHz) δ (ppm): 7.99–7.91 (m, 2H), 7.70 (br s, 1H), 7.33 (d, 2H, *J* = 8.1 Hz), 6.55 (s, 2H), 4.09–4.01 (m, 2H), 3.86 (s, 3H), 3.83 (s, 6H), 2.86–2.77 (m, 2H), 2.43 (s, 3H), 1.98 (quin, 2H, *J* = 6.0 Hz). **¹³C NMR** (50 MHz) δ (ppm): 164.9 (Cq), 153.1 (Cq), 144.7 (Cq), 139.6 (CH), 139.1 (Cq), 136.7 (Cq), 130.7 (Cq), 129.4 (CH), 128.7 (CH), 128.1 (Cq), 107.7 (CH), 61.0 (CH₃), 56.7 (CH₃), 46.5 (CH₂), 26.5 (CH₂), 23.5 (CH₂), 21.8 (CH₃). **ESI-MS** *m/z*: 454 [M+Na]⁺, 432 [M+H]⁺.

3-(4-methylbenzylidene)-1-tosylpiperidin-2-one, **16h**



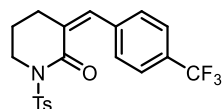
Synthesised according to the general procedure. White solid, 46% yield, **mp** 161–163 °C (*i*-Pr₂O). **R_f** 0.31 (8/2 DCM/PE). **¹H NMR** (600 MHz) δ (ppm): 7.96–7.94 (m, 2H), 7.75 (br s, 1H), 7.33 (d, 2H, *J* = 8.1 Hz), 7.24 (d, 2H, *J* = 8.2 Hz), 7.17 (d, 2H, *J* = 8.0 Hz), 4.06–4.03 (m, 2H), 2.80–2.77 (m, 2H), 2.43 (s, 3H), 2.35 (s, 3H), 1.99–1.94 (m, 2H). **¹³C NMR** (150 MHz) δ (ppm): 165.2 (Cq), 144.7 (Cq), 139.7 (CH), 139.5 (Cq), 136.7 (Cq), 132.4 (Cq), 130.3 (CH), 129.5 (CH), 129.4 (CH), 128.8 (CH), 127.9 (Cq), 46.6 (CH₂), 26.4 (CH₂), 23.5 (CH₂), 21.8 (CH₃), 21.5 (CH₃). **ESI-MS** *m/z*: 378 [M+Na]⁺, 356 [M+H]⁺.

3-(4-fluorobenzylidene)-1-tosylpiperidin-2-one, **16i**



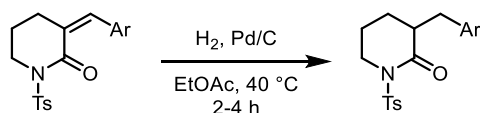
Synthesised according to the general procedure. White solid, 69% yield, **mp** 113–114 °C (*i*-Pr₂O). **R_f** 0.43 (DCM). **¹H NMR** (600 MHz) δ (ppm): 7.97–7.94 (m, 2H), 7.73 (br s, 1H), 7.35–7.30 (m, 4H), 7.08–7.04 (m, 2H), 4.06–4.04 (m, 2H), 2.77–2.74 (m, 2H), 2.43 (s, 3H), 2.00–1.95 (m, 2H). **¹³C NMR** (150 MHz) δ (ppm): 164.9 (Cq), 162.9 (Cq, *d*, *J* = 251.2 Hz), 144.8 (Cq), 138.3 (CH), 136.6 (Cq), 132.1 (CH, *d*, *J* = 7.9 Hz), 131.4 (Cq, *d*, *J* = 3.5 Hz), 129.5 (CH), 128.8 (CH), 128.6 (Cq), 115.8 (CH, *d*, *J* = 21.7 Hz), 46.6 (CH₂), 26.3 (CH₂), 23.5 (CH₂), 21.8 (CH₃). **¹⁹F NMR** (564 MHz) δ (ppm): –110.8 (m). **ESI-MS** *m/z*: 382 [M+Na]⁺, 360 [M+H]⁺.

1-tosyl-3-(4-(trifluoromethyl)benzylidene)piperidin-2-one, **16j**



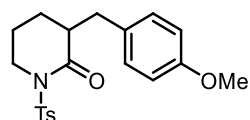
Synthesised according to the general procedure. White solid, 79% yield, **mp** 136–137 °C (*i*-Pr₂O). **R_f** 0.53 (DCM). **¹H NMR** (600 MHz) δ (ppm): 7.97–7.95 (m, 2H), 7.78 (br s, 1H), 7.62 (d, 2H, *J* = 8.1 Hz), 7.41 (d, 2H, *J* = 8.1 Hz), 7.34 (d, 2H, *J* = 8.1 Hz), 4.08–4.05 (m, 2H), 2.78–2.75 (m, 2H), 2.44 (s, 3H), 2.01–1.95 (m, 2H). **¹³C NMR** (150 MHz) δ (ppm): 164.4 (Cq), 145.0 (Cq), 138.7 (Cq), 137.7 (CH), 136.4 (Cq), 131.1 (Cq), 130.7 (Cq, *q*, *J* = 32.7), 130.1 (CH), 129.6 (CH), 128.8 (CH), 125.5 (CH, *q*, *J* = 3.7 Hz), 124.0 (Cq, *q*, *J* = 271.9 Hz), 46.7 (CH₂), 26.2 (CH₂), 23.4 (CH₂), 21.9 (CH₃). **¹⁹F NMR** (564 MHz) δ (ppm): –62.7 (s). **ESI-MS** *m/z*: 410 [M+H]⁺.

General procedure for hydrogenation



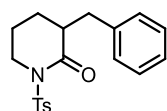
To a solution of α -benzylidene substrate (1.0 eq, 1–5 mmol) in ethyl acetate (0.1–0.2 M), Pd/C (10% w/w) was added. Air was removed and the flask was filled with H₂. The reaction mixture was stirred for 2–4 h under H₂ atmosphere at 40 °C (TLC monitoring), then it was cooled to room temperature and filtered over celite pad with dichloromethane. The volatiles were removed under reduced pressure, affording pure hydrogenation product.

3-(4-methoxybenzyl)-1-tosylpiperidin-2-one, **13a**



Synthesised according to the general procedure. White solid, 95% yield, **mp** 103–104 °C (*i*-Pr₂O). **R_f** 0.52 (7/3 PE/EtOAc) **¹H NMR** (600 MHz) δ (ppm): 7.92 (d, 2H, *J* = 8.3 Hz), 7.33 (d, 2H, *J* = 8.1 Hz), 6.94 (dt, 2H, *J* = 8.6 Hz, 3.0 Hz), 6.75 (dt, 2H, *J* = 8.7 Hz, 3.0 Hz), 3.99–3.95 (m, 1H), 3.80–3.76 (m, 1H) superimposed to 3.77 (s, 3H), 3.14 (dd, 1H, *J* = 13.8, 4.0 Hz), 2.61 (dd, 1H, *J* = 13.8 Hz, 9.3 Hz), 2.55–2.50 (m, 1H), 2.45 (s, 3H), 1.95–1.90 (m, 1H), 1.79–1.71 (m, 2H), 1.42–1.36 (m, 1H). **¹³C NMR** (150 MHz) δ (ppm): 172.8 (Cq), 158.3 (Cq), 144.8 (Cq), 136.4 (Cq), 130.9 (Cq), 130.2 (CH), 129.5 (CH), 128.8 (CH), 114.0 (CH), 55.3 (CH₃), 47.0 (CH₂), 45.5 (CH), 36.0 (CH₂), 25.0 (CH₂), 22.4 (CH₂), 21.8 (CH₂). **ESI-MS** *m/z*: 396 [M+Na]⁺, 374 [M+H]⁺.

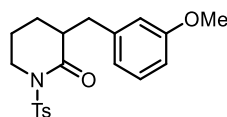
3-benzyl-1-tosylpiperidin-2-one, **13b**



Synthesised according to the general procedure. White solid, 96% yield, **mp** 128–129 °C (MeOH). **R_f** 0.27 (8/2 PE/EtOAc). **¹H NMR** (600 MHz) δ (ppm): 7.93–7.91 (m, 2H), 7.34 (d, 2H, *J* = 8.0 Hz), 7.23–7.17 (m, 3H), 7.04–7.03 (m, 2H), 4.00–3.96 (m, 1H), 3.80 (ddd, 1H, *J* = 12.3 Hz, 8.8 Hz, 4.7 Hz), 3.24 (dd, 1H, *J* = 13.5 Hz, 3.8 Hz), 2.63 (dd, 1H, *J* = 13.5 Hz, 9.5 Hz), 2.60–2.55 (m, 1H), 2.45 (s, 3H), 1.96–1.91 (m, 1H), 1.79–1.72 (m, 2H), 1.43–1.36 (m, 1H). **¹³C NMR** (150 MHz) δ (ppm): 172.7

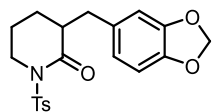
(Cq), 144.8 (Cq), 139.0 (Cq), 136.4 (Cq), 129.5 (CH), 129.3 (CH), 128.8 (CH), 128.6 (CH), 126.5 (CH), 46.9 (CH₂), 45.4 (CH), 36.9 (CH₂), 25.1 (CH₂), 22.4 (CH₂), 21.8 (CH₃). **GC-MS** *m/z* (%): 343 [M]⁺ (1), 279 (75), 188 (43), 160 (28), 117 (22), 91 (100), 65 (18).

3-(3-methoxybenzyl)-1-tosylpiperidin-2-one, **13c**



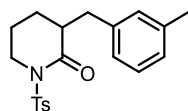
Synthesised according to the general procedure. White oil, quantitative yield. **¹H NMR** (400 MHz) δ (ppm): 7.92 (d, 2H, *J* = 8.0 Hz), 7.33 (d, 2H, *J* = 8.0 Hz), 7.13 (t, 1H, *J* = 8.0 Hz), 6.75–6.71 (m, 1H), 6.64–6.61 (m, 2H), 4.00–3.94 (m, 1H), 3.84–3.79 (m, 1H), 3.75 (s, 3H), 3.25–3.19 (m, 1H), 2.62–2.54 (m, 2H), 2.45 (s, 3H), 1.98–1.89 (m, 1H), 1.82–1.70 (m, 2H), 1.45–1.36 (m, 1H). **¹³C NMR** (100 MHz) δ (ppm): 172.7 (Cq), 159.8 (Cq), 144.8 (Cq), 140.6 (Cq), 136.4 (Cq), 129.5 (CH), 129.5 (CH), 128.7 (CH), 121.5 (CH), 114.9 (CH), 111.9 (CH), 55.2 (CH₃), 46.9 (CH₂), 45.4 (CH), 36.9 (CH₂), 25.2 (CH₂), 22.4 (CH₂), 21.8 (CH₃). **ESI-MS** *m/z*: 769 [2M+Na]⁺, 396 [M+Na]⁺, 374 [M+H]⁺.

3-(benzo[d][1,3]dioxol-5-ylmethyl)-1-tosylpiperidin-2-one, **13d**



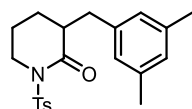
Synthesised according to the general procedure. White solid, 91% yield, **mp** 102–103 °C (*i*-Pr₂O). **R_f** 0.40 (7/3 PE/EtOAc) **¹H NMR** (600 MHz) δ (ppm): 7.91 (d, 2H, *J* = 8.6 Hz), 7.33 (d, 2H, *J* = 8.3 Hz), 6.65 (d, 1H, *J* = 7.9 Hz), 6.51 (d, 1H, *J* = 1.7 Hz), 6.47 (dd, 1H, *J* = 7.9 Hz, 1.7 Hz), 5.91 (s, 2H), 3.98 (dt, 1H, *J* = 11.0 Hz, 4.8 Hz), 3.82–3.77 (m, 1H), 3.12 (dd, 1H, *J* = 13.8 Hz, 4.1 Hz), 2.57 (dd, 1H, *J* = 13.8 Hz, 9.3 Hz), 2.54–2.48 (m, 1H), 2.45 (s, 3H), 1.98–1.91 (m, 1H), 1.81–1.73 (m, 2H), 1.43–1.36 (m, 1H). **¹³C NMR** (150 MHz) δ (ppm): 172.7 (Cq), 147.8 (Cq), 146.2 (Cq), 144.9 (Cq), 136.4 (Cq), 132.7 (Cq), 129.5 (CH), 128.7 (CH), 122.3 (CH), 109.5 (CH), 108.3 (CH), 101.0 (CH₂), 46.9 (CH₂), 45.5 (CH), 36.6 (CH₂), 25.1 (CH₂), 22.4 (CH₂), 21.8 (CH₃). **ESI-MS** *m/z*: 410 [M+Na]⁺, 388 [M+H]⁺.

3-(3-methylbenzyl)-1-tosylpiperidin-2-one, **13e**



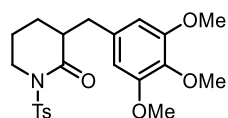
Synthesised according to the general procedure. White solid, quantitative yield, **mp** 77–78 °C (*i*-Pr₂O). **R_f** 0.40 (9/1 PE/EtOAc) **¹H NMR** (600 MHz) δ (ppm): 7.92 (d, 2H, *J* = 8.3 Hz), 7.33 (d, 2H, *J* = 8.3 Hz), 7.11 (t, 1H, *J* = 7.6 Hz), 7.00 (d, 1H, *J* = 7.6 Hz), 6.89 (s, 1H), 6.83 (d, 1H, *J* = 7.6 Hz), 3.97 (dt, 1H, *J* = 11.7 Hz, 5.5 Hz), 3.81 (ddd, 1H, *J* = 12.4 Hz, 8.6 Hz, 4.6 Hz), 3.22 (q, 1H, *J* = 9.0 Hz), 2.59–2.53 (m, 2H), 2.45 (s, 3H), 2.28 (s, 3H), 1.96–1.91 (m, 1H), 1.80–1.72 (m, 2H), 1.43–1.37 (m, 1H). **¹³C NMR** (150 MHz) δ (ppm): 172.8 (Cq), 144.8 (Cq), 139.0 (Cq), 138.2 (Cq), 136.4 (Cq), 130.1 (CH), 129.5 (CH), 128.8 (CH), 128.5 (CH), 127.3 (CH), 126.2 (CH), 46.9 (CH₂), 45.4 (CH), 36.8 (CH₂), 25.1 (CH₂), 22.4 (CH₂), 21.8 (CH₃), 21.5 (CH₃). **ESI-MS** *m/z*: 380 [M+Na]⁺, 358 [M+H]⁺.

3-(3,5-dimethylbenzyl)-1-tosylpiperidin-2-one, **13f**



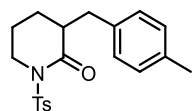
Synthesised according to the general procedure. White solid, 97% yield, **mp** 112–113 °C (*i*-Pr₂O). **R_f** 0.29 (9/1 PE/EtOAc) **¹H NMR** (600 MHz) δ (ppm): 7.93 (d, 2H, *J* = 8.3 Hz), 7.33 (d, 2H, *J* = 8.1 Hz), 6.82 (s, 1H), 6.69 (s, 2H), 3.99–3.93 (m, 1H), 3.83 (ddd, 1H, *J* = 12.3 Hz, 8.6 Hz, 4.7 Hz), 3.21 (dd, 1H, *J* = 13.0 Hz, 3.2 Hz), 2.57–2.51 (m, 1H) superimposed to 2.49 (dd, 1H, *J* = 13.1 Hz, 9.8 Hz), 2.44 (s, 3H), 2.24 (s, 6H), 1.97–1.91 (m, 1H), 1.80–1.72 (m, 2H), 1.43–1.36 (m, 1H). **¹³C NMR** (150 MHz) δ (ppm): 172.9 (Cq), 144.8 (Cq), 139.0 (Cq), 138.1 (Cq), 136.5 (Cq), 129.5 (CH), 128.8 (CH), 128.2 (CH), 127.0 (CH), 47.0 (CH₂), 45.5 (CH), 36.7 (CH₂), 25.2 (CH₂), 22.4 (CH₂), 21.8 (CH₃), 21.4 (CH₃). **ESI-MS** *m/z*: 394 [M+Na]⁺, 372 [M+H]⁺.

1-tosyl-3-(3,4,5-trimethoxybenzyl)piperidin-2-one, **13g**



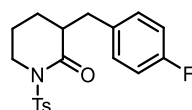
Synthesised according to the general procedure. White solid, 92% yield, **mp** 132–134 °C (*i*-Pr₂O/EtOAc). **R_f** 0.25 (7/3 PE/EtOAc). **¹H NMR** (600 MHz) δ (ppm): 7.92 (d, 2H, *J* = 8.3 Hz), 7.33 (d, 2H, *J* = 8.3 Hz), 6.31 (s, 1H), 3.99 (dt, 1H, *J* = 12.0 Hz, 5.9 Hz), 3.85–3.80 (m, 1H) superimposed to 3.81 (s, 3H), 3.79 (s, 6H), 3.17 (dd, 1H, *J* = 13.6 Hz, 4.0 Hz), 2.62 (dd, 1H, *J* = 13.6 Hz, 9.1 Hz), 2.58–2.52 (m, 1H), 2.44 (s, 3H), 1.99–1.94 (m, 1H), 1.85–1.74 (m, 2H), 1.48–1.41 (m, 1H). **¹³C NMR** (150 MHz) δ (ppm): 172.8 (Cq), 153.3 (Cq), 144.9 (Cq), 136.6 (Cq), 136.5 (Cq), 134.8 (Cq), 129.5 (CH), 128.8 (CH), 106.14 (CH), 61.0 (CH₃), 56.2 (CH₃), 47.01 (CH₂), 45.7 (CH), 37.3 (CH₂), 25.3 (CH₂), 22.5 (CH₂), 21.8 (CH₃). **ESI-MS** *m/z*: 456 [M+Na]⁺, 434 [M+H]⁺.

3-(4-methylbenzyl)-1-tosylpiperidin-2-one, **13h**



Synthesised according to the general procedure. White solid, 98% yield, **mp** 92–94 °C (*i*-Pr₂O). **R_f** 0.24 (9/1 PE/EtOAc). **¹H NMR** (600 MHz) δ (ppm): 7.94–7.91 (m, 2H), 7.34 (d, 2H, *J* = 7.9 Hz), 7.03 (d, 2H, *J* = 7.9 Hz), 6.92 (d, 2H, *J* = 7.9 Hz), 3.99–3.95 (m, 1H), 3.80 (ddd, 1H, *J* = 12.4 Hz, 8.8 Hz, 4.8 Hz), 3.19 (dd, 1H, *J* = 13.1 Hz, 3.4 Hz), 2.59 (dd, 1H, *J* = 13.3 Hz, 9.5 Hz) superimposed to 2.58–2.52 (m, 1H), 2.45 (s, 3H), 2.30 (s, 3H), 1.97–1.90 (m, 1H), 1.80–1.71 (m, 2H), 1.44–1.36 (m, 1H). **¹³C NMR** (150 MHz) δ (ppm): 172.8 (Cq), 144.8 (Cq), 136.4 (Cq), 136.0 (Cq), 135.8 (Cq), 129.4 (CH), 129.2 (CH), 129.1 (CH), 128.7 (CH), 46.9 (CH₂), 45.4 (CH), 36.4 (CH₂), 25.0 (CH₂), 22.3 (CH₂), 21.8 (CH₃), 21.0 (CH₃). **ESI-MS** *m/z*: 380 [M+Na]⁺, 358 [M+H]⁺.

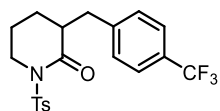
3-(4-fluorobenzyl)-1-tosylpiperidin-2-one, **13i**



Synthesised according to the general procedure. White solid, 97% yield, **mp** 120–121 °C (*i*-Pr₂O). **R_f** 0.13 (9/1 PE/EtOAc). **¹H NMR** (600 MHz) δ (ppm): 7.92–7.90 (m, 2H), 7.34 (d, 2H, *J* = 8.3 Hz), 6.99–6.95 (m, 2H), 6.90–6.86 (m, 2H), 4.01–3.96 (m, 1H), 3.77 (ddd, 1H, *J* = 12.4 Hz, 9.3 Hz, 4.6 Hz), 3.15 (dd, 1H, *J* = 13.9 Hz, 4.3 Hz), 2.67 (dd, 1H, *J* = 14.1 Hz, 9.0 Hz), 2.57–2.52 (m, 1H), 2.46

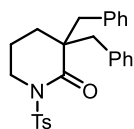
(s, 3H), 1.97–1.91 (m, 1H), 1.80–1.72 (m, 2H), 1.43–1.35 (m, 1H). **¹³C NMR** (150 MHz) δ (ppm): 172.4 (Cq), 161.6 (Cq, d, $J = 244.3$ Hz), 144.8 (Cq), 136.2 (Cq), 134.5 (Cq), 130.6 (CH, d, $J = 7.4$ Hz), 129.4 (CH), 128.7 (CH), 115.2 (CH, d, $J = 21.4$ Hz), 46.8 (CH₂), 45.3 (CH), 35.9 (CH₂), 25.0 (CH₂), 22.3 (CH₂), 21.7 (CH₃). **¹⁹F NMR** (564 MHz) δ (ppm): –116.5 (m). **ESI-MS** m/z : 384 [M+Na]⁺, 362 [M+H]⁺.

1-tosyl-3-(4-(trifluoromethyl)benzyl)piperidin-2-one, 13j



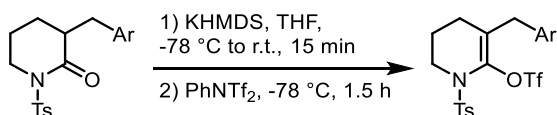
Synthesised according to the general procedure. White solid, 88% yield, **mp** 133–134 °C (*i*-Pr₂O). **R_f** 0.14 (9/1 PE/EtOAc). **¹H NMR** (600 MHz) δ (ppm): 7.92–7.89 (m, 2H), 7.44 (d, 2H, $J = 7.9$ Hz), 7.34 (d, 2H, $J = 8.3$ Hz), 7.13 (d, 2H, $J = 7.9$ Hz), 4.03–3.98 (m, 1H), 3.76 (ddd, 1H, $J = 12.4$ Hz, 9.3 Hz, 4.6 Hz), 3.22 (dd, 1H, $J = 13.9$ Hz, 4.3 Hz), 2.77 (dd, 1H, $J = 13.9$ Hz, 8.8 Hz), 2.63–2.57 (m, 1H), 2.46 (s, 3H), 1.99–1.93 (m, 1H), 1.82–1.74 (m, 2H), 1.43–1.35 (m, 1H). **¹³C NMR** (150 MHz) δ (ppm): 172.1 (Cq), 144.9 (Cq), 143.1 (Cq), 136.2 (Cq), 129.6 (CH), 129.5 (CH), 128.8 (Cq, q, $J = 32.9$ Hz), 128.7 (CH), 124.3 (Cq, q, $J = 272.1$ Hz), 125.4–125.3 (CH, m), 46.8 (CH₂), 45.0 (CH), 36.5 (CH₂), 25.1 (CH₂), 22.4 (CH₂), 21.7 (CH₃). **¹⁹F NMR** (564 MHz) δ (ppm): –62.3 (s). **ESI-MS** m/z : 412 [M+H]⁺.

3,3-dibenzyl-1-tosylpiperidin-2-one, 14



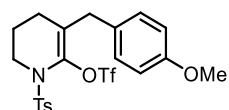
Obtained as the undesired product in the alkylation of *N*-tosyl δ -valerolactam with benzyl bromide. In a Schlenk tube, a solution of *N*-tosyl δ -valerolactam (1.0 eq, 1.0 mmol) in anhydrous THF (0.2 M) under N₂ was cooled down to –78 °C. KHMDS (1.1 eq, 1.0 M solution in THF) was added and the mixture was stirred below –70 °C for 1 h. Benzyl bromide (1.1 eq) was added and the reaction was allowed to warm to rt and stirred for 1 h. Water was added and the mixture was extracted three times with Et₂O; the combined organic layers were dried over anhydrous Na₂SO₄, filtered and the solvent was removed under vacuum. The crude product was purified by flash column chromatography to afford pure dibenzyl lactam. White solid, **mp** 171–172 °C (*i*-Pr₂O). **R_f** 0.37 (9/1 PE/EtOAc). **¹H NMR** (600 MHz) δ (ppm): 7.92–7.90 (m, 2H), 7.40 (d, 2H, $J = 7.9$ Hz), 7.19–7.16 (m, 2H), 7.13–7.09 (m, 4H), 6.90–6.88 (m, 2H), 3.41–3.36 (m, 4H), 2.53 (s, 3H), 2.48 (d, 2H, $J = 13.4$ Hz), 1.70–1.67 (m, 2H), 1.27–1.22 (m, 2H). **¹³C NMR** (150 MHz) δ (ppm): 175.0 (Cq), 144.6 (Cq), 137.1 (Cq), 136.6 (Cq), 130.4 (CH), 129.3 (CH), 129.2 (CH), 128.4 (CH), 126.8 (CH), 50.4 (Cq), 47.1 (CH₂), 46.7 (CH₂), 28.2 (CH₂), 21.9 (CH₂), 20.9 (CH₃). **GC-MS** m/z (%): 343 (17), 342 (73), 279 (21), 278 (100), 91 (80).

General procedure for lactam-derived vinyl triflates synthesis^[7]



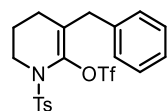
To a 1.0 M solution of KHMDS in THF (1.1 eq), at $-78\text{ }^{\circ}\text{C}$ under N_2 atmosphere, a 0.2 M solution of α -substituted lactam (1.0 eq, 2-3 mmol) in anhydrous THF was slowly added and the mixture was stirred below $-70\text{ }^{\circ}\text{C}$ for 15 min. Then, the cold bath was removed and the mixture was stirred for 15 min. The temperature was again lowered to $-78\text{ }^{\circ}\text{C}$ and a solution of *N*-phenyl-bis(trifluoromethanesulfonimide) (1.2 eq) in anhydrous THF was added. The mixture was stirred below $-60\text{ }^{\circ}\text{C}$ for 1.5 h (TLC monitoring), then it was allowed to reach room temperature. A 10% solution of NaOH was added and the mixture was extracted with Et_2O ; the combined organic layers were dried over Na_2SO_4 , filtered and the solvent was removed under reduced pressure to afford crude vinyl triflate, which was not isolated and used directly for the next step.

3-(4-methoxybenzyl)-1-tosyl-1,4,5,6-tetrahydropyridin-2-yl trifluoromethanesulfonate, 17a



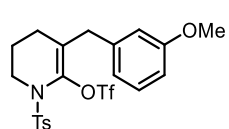
Synthesised according to the general procedure. Crude product is a yellow oil. R_f 0.60 (7/3 PE/EtOAc). $^1\text{H NMR}$ (600 MHz) δ (ppm): 7.69 (d, 2H, $J = 8.3$ Hz), 7.22 (d, 2H, $J = 8.0$ Hz), 7.05 (d, 2H, $J = 8.6$ Hz), 6.84 (d, 2H, $J = 8.6$ Hz), 3.81 (s, 3H), 3.60–3.58 (m, 2H), 3.47 (s, 2H), 2.41 (s, 3H), 1.78 (t, 2H, $J = 6.9$ Hz), 1.28–1.24 (m, 2H).

3-benzyl-1-tosyl-1,4,5,6-tetrahydropyridin-2-yl trifluoromethanesulfonate, 17b



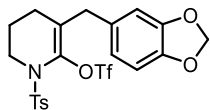
Synthesised according to the general procedure. Crude product is a yellow oil. R_f 0.66 (8/2 PE/EtOAc). $^1\text{H NMR}$ (600 MHz) δ (ppm): 7.70–7.67 (m, 2H), 7.33–7.30 (m, 2H), 2.28–2.25 (m, 1H), 7.20 (d, 2H, $J = 8.3$ Hz), 7.14 (d, 2H, $J = 6.9$ Hz), 3.62–3.59 (m, 2H), 3.53 (s, 2H), 2.40 (s, 3H), 1.79 (t, 2H, $J = 6.9$ Hz), 1.28–1.23 (m, 2H).

3-(3-methoxybenzyl)-1-tosyl-1,4,5,6-tetrahydropyridin-2-yl trifluoromethanesulfonate, 17c



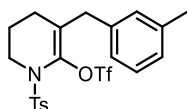
Synthesised according to the general procedure. Crude product is a yellow oil. $^1\text{H NMR}$ (400 MHz) δ (ppm): 7.70 (d, 2H, $J = 8.0$ Hz), 7.24–7.20 (m, 3H), 6.81–6.78 (m, 1H), 6.73–6.69 (m, 2H), 3.82 (s, 3H), 3.62–3.59 (m, 2H), 3.50 (s, 2H), 2.41 (s, 3H), 1.79 (t, 2H, $J = 7.2$ Hz), 1.30–1.23 (m, 2H).

3-(benzo[d][1,3]dioxol-5-ylmethyl)-1-tosyl-1,4,5,6-tetrahydropyridin-2-yl trifluoromethanesulfonate, 17d



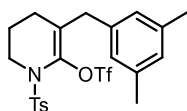
Synthesised according to the general procedure. Crude product is a dark yellow oil. R_f 0.58 (7/3 PE/EtOAc). $^1\text{H NMR}$ (600 MHz) δ (ppm): 7.721 (d, 2H, $J = 8.3$ Hz), 7.27 (d, 2H, $J = 8.1$ Hz), 6.74–6.72 (m, 1H), 6.59–6.58 (m, 2H), 5.96 (s, 2H), 3.62–3.60 (m, 2H), 3.43 (s, 2H), 2.42 (s, 3H), 1.78 (t, 2H, $J = 6.9$ Hz), 1.31–1.29 (m, 2H).

3-(3-methylbenzyl)-1-tosyl-1,4,5,6-tetrahydropyridin-2-yl trifluoromethanesulfonate, 17e



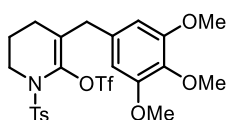
Synthesised according to the general procedure. Crude product is a yellow oil. R_f 0.18 (9/1 PE/Et₂O). $^1\text{H NMR}$ (600 MHz) δ (ppm): 7.71–7.69 (m, 2H), 7.22–7.18 (m, 3H), 7.07 (d, 1H, $J = 7.6$ Hz), 6.95 (s, 1H), 6.93 (d, 1H, $J = 7.6$ Hz), 3.62–3.59 (m, 2H), 3.49 (s, 2H), 2.40 (s, 3H), 2.36 (s, 3H), 1.78 (t, 2H, $J = 6.9$ Hz), 1.28–1.22 (m, 2H).

3-(3,5-dimethylbenzyl)-1-tosyl-1,4,5,6-tetrahydropyridin-2-yl trifluoromethanesulfonate, 17f



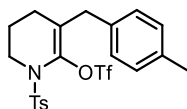
Synthesised according to the general procedure. Crude product is a yellow oil. R_f 0.43 (9/1 PE/EtOAc). $^1\text{H NMR}$ (600 MHz) δ (ppm): 7.71 (d, 2H, $J = 8.3$ Hz), 7.21 (d, 2H, $J = 8.1$ Hz), 6.89 (s, 1H), 6.75 (s, 2H), 3.61–3.59 (m, 2H), 3.46 (s, 2H), 2.40 (s, 3H), 2.31 (s, 6H), 1.77 (t, 2H, $J = 6.9$ Hz), 1.25–1.23 (m, 2H).

1-tosyl-3-(3,4,5-trimethoxybenzyl)-1,4,5,6-tetrahydropyridin-2-yl trifluoromethanesulfonate, 17g



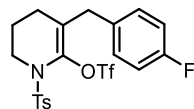
Synthesised according to the general procedure. Crude product is an orange oil. R_f 0.47 (7/3 PE/EtOAc). $^1\text{H NMR}$ (600 MHz) δ (ppm): 7.71 (d, 2H, $J = 8.3$ Hz), 7.24 (d, 2H, $J = 7.9$ Hz), 6.41 (s, 2H), 3.85 (s, 6H), 3.84 (s, 3H), 3.61–3.53 (m, 2H), 3.47 (s, 2H), 2.41 (s, 3H), 1.79 (t, 2H, $J = 6.9$ Hz), 1.42–1.30 (m, 2H).

3-(4-methylbenzyl)-1-tosyl-1,4,5,6-tetrahydropyridin-2-yl trifluoromethanesulfonate, 17h



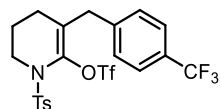
Synthesised according to the general procedure. Crude product is a yellow oil. R_f 0.16 (9/1 PE/Et₂O). $^1\text{H NMR}$ (600 MHz) δ (ppm): 7.71–7.68 (m, 2H), 7.21 (d, 2H, $J = 8.2$ Hz), 7.11 (d, 2H, $J = 7.8$ Hz), 7.02 (d, 2H, $J = 7.9$ Hz), 3.62–3.58 (m, 2H), 3.49 (s, 3H), 2.41 (s, 3H), 2.45 (s, 3H), 1.78 (t, 2H, $J = 6.9$ Hz), 1.28–1.23 (m, 2H).

3-(4-fluorobenzyl)-1-tosyl-1,4,5,6-tetrahydropyridin-2-yl trifluoromethanesulfonate, 17i



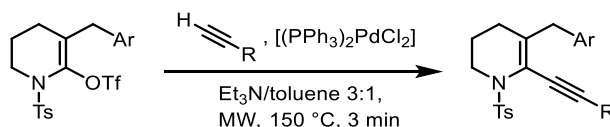
Synthesised according to the general procedure. Crude product is a yellow oil. **R_f** 0.23 (9/1 PE/EtOAc). **¹H NMR** (600 MHz) δ (ppm): 7.69 (d, 2H, $J = 8.3$ Hz), 7.23 (d, 2H, $J = 8.2$ Hz), 7.12–7.08 (m, 2H), 7.02–6.98 (m, 2H), 3.62–3.59 (m, 2H), 3.50 (s, 2H), 2.42 (s, 3H), 1.79 (t, 2H, $J = 6.9$ Hz), 1.30 (quin, 2H, $J = 6.9$ Hz).

1-tosyl-3-(4-(trifluoromethyl)benzyl)-1,4,5,6-tetrahydropyridin-2-yl trifluoromethanesulfonate, 17j



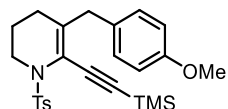
Synthesised according to the general procedure. Crude product is a yellow oil. **R_f** 0.24 (9/1 PE/EtOAc). **¹H NMR** (600 MHz) δ (ppm): 7.70–7.67 (m, 2H), 7.57 (d, 2H, $J = 8.0$ Hz), 7.28–7.25 (m, 2H), 7.21 (d, 2H, $J = 7.9$ Hz), 3.62–3.60 (m, 2H), 3.58 (s, 2H), 2.40 (s, 3H), 1.80 (t, 2H, $J = 6.9$ Hz), 1.36–1.31 (, 2H).

General procedure for Sonogashira coupling^[7]



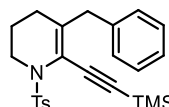
A microwave reaction vial under N₂ atmosphere was charged with [(Ph₃P)₂PdCl₂] (0.05 eq). A 0.13 M solution of crude vinyl triflate (1.0 eq) in anhydrous 1:3 toluene/Et₃N was degassed for 10 min, then it was added to the reaction tube. The mixture was degassed for another 10 min, then the alkyne (1.2 eq) was added. The vial was sealed and heated under MW irradiation at 150 °C for 3 min. The solvent was then removed under vacuum and the crude product was purified by flash column chromatography.

5-(4-methoxybenzyl)-1-tosyl-6-((trimethylsilyl)ethynyl)-1,2,3,4-tetrahydropyridine, 8a



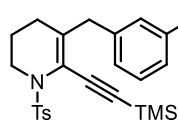
Synthesised according to the general procedure. Yellow oil, 35% yield (2-steps). **R_f** 0.23 (8/2 PE/Et₂O). **¹H NMR** (600 MHz) δ (ppm): 7.81 (d, 2H, $J = 8.2$ Hz), 7.25 (d, 2H, $J = 8.1$ Hz), 7.09 (d, 2H, $J = 8.4$ Hz), 6.80 (d, 2H, $J = 8.5$ Hz), 3.79 (s, 3H), 3.59–3.56 (m, 2H) superimposed to 3.56 (s, 2H), 2.42 (s, 3H), 1.96 (t, 2H, $J = 6.8$ Hz), 1.66–1.62 (m, 2H), 0.18 (s, 9H). **¹³C NMR** (150 MHz) δ (ppm): 156.3 (Cq), 143.3 (Cq), 138.0 (Cq), 137.7 (Cq), 131.7 (Cq), 129.7 (CH), 129.5 (CH), 127.7 (CH), 117.1 (Cq), 113.9 (CH), 99.6 (Cq), 99.5 (Cq), 55.4 (CH₃), 46.0 (CH₂), 40.2 (CH₂), 26.5 (CH₂), 22.0 (CH₂), 21.7 (CH₃), –0.2 (CH₃). **ESI-MS** m/z : 476 [M+Na]⁺, 454 [M+H]⁺.

5-benzyl-1-tosyl-6-((trimethylsilyl)ethynyl)-1,2,3,4-tetrahydropyridine, 8b



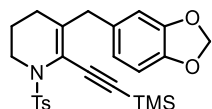
Synthesised according to the general procedure. Pale yellow oil, 36% yield (2-steps). *R_f* 0.21 (9/1 PE/Et₂O). **¹H NMR** (600 MHz) δ (ppm): 7.81 (d, 2H, *J* = 8.2 Hz), 7.26–7.24 (m, 4H), 7.22–7.18 (m, 1H), superimposed to 7.18 (d, 2H, *J* = 8.1 Hz), 3.63 (s, 2H), 3.60–3.57 (m, 2H), 2.42 (s, 3H), 1.96 (t, 2H, *J* = 6.9 Hz), 1.66–1.61 (m, 2H), 0.18 (s, 9H). **¹³C NMR** (150 MHz) δ (ppm): 143.4 (Cq), 139.6 (Cq), 138.0 (Cq), 137.3 (Cq), 129.5 (CH), 128.8 (CH), 128.5 (CH), 127.7 (CH), 126.5 (CH), 117.4 (Cq), 99.8 (Cq), 99.5 (Cq), 46.0 (CH₂), 41.1 (CH₂), 26.6 (CH₂), 21.9 (CH₂), 21.7 (CH₃), -0.2 (CH₃). **ESI-MS** *m/z*: 446 [M+Na]⁺, 424 [M+H]⁺.

5-(3-methoxybenzyl)-1-tosyl-6-((trimethylsilyl)ethynyl)-1,2,3,4-tetrahydropyridine, 8c



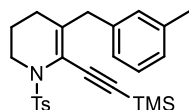
Synthesised according to the general procedure. Yellow oil, 29% yield (2-steps). *R_f* 0.24 (8/2 hexane/EtOAc). **¹H NMR** (400 MHz) δ (ppm): 7.80 (d, 2H, *J* = 8.0 Hz), 7.25 (d, 2H, *J* = 8.0 Hz), 7.17 (t, 1H, *J* = 8.0 Hz), 6.78–6.73 (m, 3H), 3.79 (s, 3H), 3.60 (s, 2H), 3.59–3.57 (m, 2H), 2.41 (s, 3H), 1.97 (t, 2H, *J* = 6.8 Hz), 1.67–1.60 (m, 2H), 0.17 (s, 9H). **¹³C NMR** (100 MHz) δ (ppm): 159.8 (Cq), 143.3 (Cq), 141.2 (Cq), 138.0 (Cq), 137.1 (Cq), 129.5 (CH), 129.4 (CH), 127.7 (CH), 121.2 (CH), 117.5 (Cq), 114.5 (CH), 111.7 (CH), 99.8 (Cq), 99.5 (Cq), 55.3 (CH₃), 46.0 (CH₂), 41.1 (CH₂), 26.6 (CH₂), 22.0 (CH₂), 21.7 (CH₃), -0.1 (CH₃). **ESI-MS** *m/z*: 929 [2M+Na]⁺, 476 [M+Na]⁺, 454 [M+1]⁺.

5-(benzo[d][1,3]dioxol-5-ylmethyl)-1-tosyl-6-((trimethylsilyl)ethynyl)-1,2,3,4-tetrahydropyridine, 8d



Synthesised according to the general procedure. Brown oil, 37% yield (2-steps). *R_f* 0.23 (8/2 PE/Et₂O). **¹H NMR** (600 MHz) δ (ppm): 7.81 (d, 2H, *J* = 8.4 Hz), 7.27 (d, 2H, *J* = 8.2 Hz), 6.69 (d, 1H, *J* = 8.0 Hz), 6.67 (d, 1H, *J* = 1.7 Hz), 6.61 (dd, 1H, *J* = 7.9 Hz, 1.7 Hz), 5.93 (s, 2H), 3.60–3.57 (m, 2H), 3.53 (s, 2H), 2.42 (s, 3H), 1.95 (t, 2H, *J* = 6.8 Hz), 1.67–1.62 (m, 2H), 0.18 (s, 9H). **¹³C NMR** (150 MHz) δ (ppm): 147.8 (Cq), 146.2 (Cq), 143.4 (Cq), 137.9 (Cq), 137.4 (Cq), 126.9 (Cq), 133.4 (Cq), 129.5 (CH), 127.7 (CH), 121.7 (CH), 117.3 (Cq), 109.1 (CH), 108.2 (CH), 101.0 (CH₂), 99.4 (Cq), 46.0 (CH₂), 40.7 (CH₂), 26.5 (CH₂), 21.9 (CH₂), 21.7 (CH₃), -0.2 (CH₃). **ESI-MS** *m/z*: 490 [M+Na]⁺, 468 [M+H]⁺.

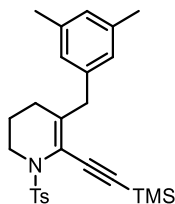
5-(3-methylbenzyl)-1-tosyl-6-((trimethylsilyl)ethynyl)-1,2,3,4-tetrahydropyridine, 8e



Synthesised according to the general procedure. Yellow oil, 35% yield (2-steps). *R_f* 0.18 (9/1 PE/Et₂O). **¹H NMR** (600 MHz) δ (ppm): 7.82–7.80 (m, 2H), 7.25 (d, 2H, *J* = 8.1 Hz), 7.16–7.13 (m, 1H), 7.03–7.00 (m, 2H), 6.97 (d, 1H, *J* = 7.4 Hz), 3.59 (s, 2H) superimposed to 3.60–3.57 (m, 2H), 2.42 (s, 3H), 2.32 (s, 3H), 1.96 (t, 2H, *J* = 6.7 Hz), 1.65–1.61 (m, 2H), 0.19 (s, 9H). **¹³C NMR** (150 MHz) δ (ppm): 143.3 (Cq), 139.6 (Cq), 138.1 (Cq), 138.0 (Cq), 137.4 (Cq), 129.6 (CH), 129.5 (CH), 128.4 (CH), 127.7 (CH), 127.2 (CH), 125.9 (CH), 117.3 (Cq), 99.7 (Cq), 99.6 (Cq),

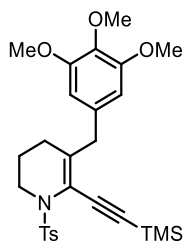
46.0 (CH₂), 41.1 (CH₂), 26.6 (CH₂), 21.9 (CH₂), 21.7 (CH₃), 21.6 (CH₃), -0.2 (CH₃). **ESI-MS** *m/z*: 460 [M+Na]⁺, 438 [M+H]⁺.

5-(3,5-dimethylbenzyl)-1-tosyl-6-((trimethylsilyl)ethynyl)-1,2,3,4-tetrahydropyridine, 8f



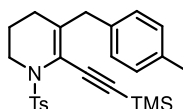
Synthesised according to the general procedure. Orange oil, 32% yield (2-steps). **R_f** 0.25 (9/1 PE/Et₂O). **¹H NMR** (600 MHz) δ (ppm): 7.82 (d, 2H, *J* = 8.3 Hz), 7.25 (d, 2H, *J* = 8.1 Hz), 6.85 (s, 1H), 6.82 (s, 2H), 3.59–3.57 (m, 2H) superimposed to 3.56 (s, 2H), 2.42 (s, 3H), 2.28 (s, 6H), 1.97 (t, 2H, *J* = 6.8 Hz), 1.64–1.60 (m, 2H), 0.20 (s, 9H). **¹³C NMR** (150 MHz) δ (ppm): 143.3 (Cq), 139.6 (Cq), 138.0 (Cq), 137.9 (Cq), 137.6 (Cq), 129.4 (CH), 128.1 (CH), 127.7 (CH), 126.7 (CH), 117.1 (Cq), 99.7 (Cq), 46.0 (CH₂), 41.0 (CH₂), 26.6 (CH₂), 21.9 (CH₂), 21.7 (CH₃), 21.4 (CH₃), -0.2 (CH₃). **ESI-MS** *m/z*: 474 [M+Na]⁺, 452 [M+H]⁺.

1-tosyl-5-(3,4,5-trimethoxybenzyl)-6-((trimethylsilyl)ethynyl)-1,2,3,4-tetrahydropyridine, 8g



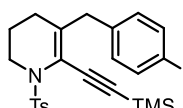
Synthesised according to the general procedure. Yellow oil, 33% yield (2-steps). **R_f** 0.31 (8/2 PE/EtOAc). **¹H NMR** (600 MHz) δ (ppm): 7.80 (d, 2H, *J* = 8.3 Hz), 7.25 (d, 2H, *J* = 8.5 Hz), 6.47 (s, 2H), 3.83 (s, 6H), 3.83 (s, 3H), 3.60–3.58 (m, 2H), 3.56 (s, 2H), 2.42 (s, 3H), 2.01 (t, 2H, *J* = 6.8 Hz), 1.72–1.66 (m, 2H), 0.16 (s, 9H). **¹³C NMR** (150 MHz) δ (ppm): 153.3 (Cq), 143.4 (Cq), 138.2 (Cq), 137.2 (Cq), 136.7 (Cq), 135.4 (Cq), 129.4 (CH), 127.6 (CH), 117.4 (Cq), 105.8 (CH), 99.6 (Cq), 99.6 (Cq), 61.0 (CH₃), 56.3 (CH₃), 46.0 (CH₂), 41.4 (CH₂), 26.6 (CH₂), 22.1 (CH₂), 21.7 (CH₃), -0.1 (CH₃). **ESI-MS** *m/z*: 514 [M+Na]⁺, 536 [M+H]⁺.

5-(4-methylbenzyl)-1-tosyl-6-((trimethylsilyl)ethynyl)-1,2,3,4-tetrahydropyridine, 8h



Synthesised according to the general procedure. Yellow oil, 39% yield (2-steps). **R_f** 0.40 (8/2 PE/Et₂O). **¹H NMR** (600 MHz) δ (ppm): 7.81 (d, 2H, *J* = 8.3 Hz), 7.25 (d, 2H, *J* = 7.9 Hz), 3.58 (s, 2H) superimposed to 3.59–3.56 (m, 2H), 2.42 (s, 3H), 2.32 (s, 3H), 1.95 (t, 2H, *J* = 6.7 Hz), 1.66–1.61 (m, 2H), 0.18 (s, 9H). **¹³C NMR** (150 MHz) δ (ppm): 143.3 (Cq), 138.0 (Cq), 137.6 (Cq), 136.5 (Cq), 136.0 (Cq), 129.5 (CH), 129.2 (CH), 128.7 (CH), 127.7 (CH), 117.2 (Cq), 99.7 (Cq), 99.5 (Cq), 46.0 (CH₂), 40.6 (CH₂), 26.6 (CH₂), 22.0 (CH₂), 21.7 (CH₃), 21.2 (CH₃), -0.2 (CH₃).

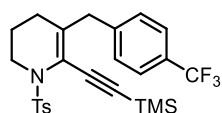
5-(4-fluorobenzyl)-1-tosyl-6-((trimethylsilyl)ethynyl)-1,2,3,4-tetrahydropyridine, 8i



Synthesised according to the general procedure. Yellow oil, 44% yield (2-steps). **R_f** 0.27 (9/1 PE/Et₂O). **¹H NMR** (600 MHz) δ (ppm): 7.81–7.79 (, 2H), 7.26 (d, 2H, *J* = 8.0 Hz), 7.15–7.11 (m, 2H), 6.96–6.91 (m, 2H), 3.59–3.57 (m, 2H), superimposed to 3.58 (s, 2H), 2.42 (s, 3H), 1.96 (t, 2H, *J* = 6.7 Hz), 1.69–1.64 (m, 2H), 0.17 (s, 9H). **¹³C NMR** (150 MHz) δ (ppm): 161.7 (Cq, *d*, *J* = 244.0 Hz),

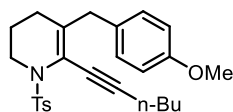
143.4 (Cq), 138.0 (Cq), 136.8 (Cq), 135.2 (Cq), 130.1 (CH, d, $J = 7.4$ Hz), 129.5 (CH), 127.7 (CH), 117.6 (Cq), 115.3 (CH, d, $J = 21.7$ Hz), 100.0 (Cq), 99.3 (Cq), 46.0 (CH₂), 40.2 (CH₂), 26.6 (CH₂), 22.0 (CH₂), 21.7 (CH₃), -0.2 (CH₃). **¹⁹F NMR** (564 MHz) δ (ppm): -116.8 (m). **ESI-MS** m/z : 442 [M+H]⁺.

1-tosyl-5-(4-(trifluoromethyl)benzyl)-6-((trimethylsilyl)ethynyl)-1,2,3,4-tetrahydropyridine, 8j



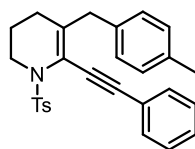
Synthesised according to the general procedure. Yellow oil 46% yield (2-steps). **R_f** 0.10 (9/1 PE/Et₂O). **¹H NMR** (600 MHz) δ (ppm): 7.81–7.79 (m, 2H), 7.51 (d, 2H, $J = 7.9$ Hz), 7.29 (d, 2H, $J = 7.9$ Hz), 7.27–7.24 (m, 2H), 3.67 (s, 2H), 3.61–3.59 (m, 2H), 2.42 (s, 3H), 1.96 (t, 2H, $J = 6.9$ Hz), 1.70–1.65 (m, 2H), 0.17 (s, 9H). **¹³C NMR** (150 MHz) δ (ppm): 143.8 (Cq), 143.5 (Cq), 137.9 (Cq), 135.7 (Cq), 129.5 (CH), 129.0 (CH), 127.7 (CH), 125.5 (CH), 118.2 (Cq), 100.4 (Cq), 99.2 (Cq), 46.0 (CH₂), 40.9 (CH₂), 26.8 (CH₂), 22.0 (CH₂), 21.7 (CH₃), -0.2 (CH₃). The CF₃ carbon and the carbon *ipso* to CF₃ are not visible. **¹⁹F NMR** (564 MHz) δ (ppm): -62.3 (s). **ESI-MS** m/z : 514 [M+Na]⁺, 492 [M+H]⁺.

6-(hex-1-yn-1-yl)-5-(4-methoxybenzyl)-1-tosyl-1,2,3,4-tetrahydropyridine, 8k



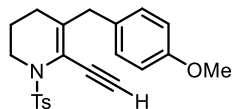
Synthesised according to the general procedure. Yellow oil, 43% yield (2-steps). **R_f** 0.24 (9/1 PE/EtOAc). **¹H NMR** (600 MHz) δ (ppm): 7.79–7.77 (m, 2H), 7.25 (d, 2H $J = 8.0$ Hz), 7.08–7.06 (m, 2H), 6.80–6.78 (m, 2H), 3.78 (s, 3H), 3.63–3.61 (m, 2H), 3.52 (s, 2H), 2.42 (s, 3H), 2.29 (t, 2H, $J = 7.1$ Hz), 1.91 (t, 2H, $J = 6.8$ Hz), 1.63–1.60 (m, 2H), 1.49–1.44 (m, 2H), 1.41–1.35 (m, 2H), 0.87 (t, 3H, $J = 7.3$ Hz). **¹³C NMR** (150 MHz) δ (ppm): 158.2 (Cq), 143.1 (Cq), 138.2 (Cq), 134.5 (Cq), 131.8 (Cq), 129.6 (CH), 129.3 (CH), 127.6 (CH), 117.3 (Cq), 113.8 (CH), 95.2 (Cq), 75.1 (Cq), 55.3 (CH₃), 46.1 (CH₂), 39.9 (CH₂), 30.6 (CH₂), 26.3 (CH₂), 22.1 (CH₂), 21.8 (CH₂), 21.7 (CH₃), 19.4 (CH₂), 13.7 (CH₃). **ESI-MS** m/z : 460 [M+Na]⁺, 438 [M+H]⁺.

5-(4-methylbenzyl)-6-(phenylethynyl)-1-tosyl-1,2,3,4-tetrahydropyridine, 8l



Synthesised according to the general procedure. Off-white solid, 53% (2-steps), **mp** 144–146 °C (*n*-Pr₂O). **R_f** 0.44 (7/3 PE/Et₂O). **¹H NMR** (600 MHz) δ (ppm): 7.83–7.81 (m, 2H), 7.38–7.36 (m, 2H), 7.31–7.28 (m, 3H), 7.22 (d, 2H, $J = 8.0$ Hz), 7.10–7.05 (m, 4H), 3.69–3.66 (m, 2H), superimposed to 3.66 (s, 2H), 2.40 (s, 3H), 2.32 (s, 3H), 1.99 (t, 2H, $J = 6.9$ Hz), 1.65–1.60 (m, 2H). **¹³C NMR** (150 MHz) δ (ppm): 143.4 (Cq), 137.8 (Cq), 136.5 (Cq), 136.4 (Cq), 136.0 (Cq), 131.6 (CH), 129.6 (CH), 129.3 (CH), 128.7 (CH), 128.5 (CH), 128.4 (CH), 127.7 (CH), 123.1 (Cq), 117.4 (Cq), 93.9 (Cq), 84.9 (Cq), 46.2 (CH₂), 40.7 (CH₂), 26.7 (CH₂), 21.7 (CH₂), 21.7 (CH₃), 21.2 (CH₃). **ESI-MS** m/z : 464 [M+Na]⁺, 442 [M+H]⁺.

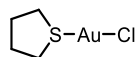
6-ethynyl-5-(4-methoxybenzyl)-1-tosyl-1,2,3,4-tetrahydropyridine, **8a'**



The terminal alkyne was obtained in the gold-catalysed reaction, when the catalyst failed to convert it to the hydroarylation product. Yellow oil. *R_f* 0.13 (9/1 PE/EtOAc). **¹H NMR** (600 MHz) δ (ppm): 7.80–7.78 (m, 2H), 7.26 (d, 2H, *J* = 8.0 Hz), 7.09–7.07 (m, 2H), 6.81–6.79 (m, 2H), 3.79 (s, 3H), 3.58 (s, 2H) superimposed to 3.58–3.56 (m, 2H), 3.28 (s, 1H), 2.42 (s, 3H), 1.91 (t, 2H, *J* = 6.8 Hz), 1.55–1.52 (m, 2H). **¹³C NMR** (150 MHz) δ (ppm): 158.3 (Cq), 143.6 (Cq), 138.8 (Cq), 137.3 (Cq), 131.3 (Cq), 129.7 (CH), 129.6 (CH), 127.7 (CH), 116.4 (Cq), 119.9 (CH), 81.9 (CH), 78.8 (Cq), 55.4 (CH₃), 46.1 (CH₂), 40.0 (CH₂), 26.4 (CH₂), 21.7 (CH₃), 21.2 (CH₂). **ESI-MS** *m/z*: 404 [M+Na]⁺, 382 [M+H]⁺.

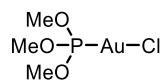
Synthesis of Au(I) complexes

chloro(tetrahydrothiophene)gold(I)^[27]



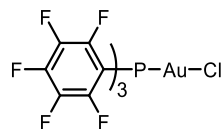
To 0.1 M a solution of HAuCl₄ (1.0 eq, 0.2 mmol) in EtOH, tetrahydrothiophene (6.0 eq) was added, resulting in the immediate precipitation of [(THT)AuCl] as a white solid. The mixture was stirred for 10 min, then it was filtered and the solid was washed with cold EtOH and dried under reduced pressure. White solid, 88% yield. **¹H NMR** (200 MHz) δ (ppm): 3.61–3.25 (br s, 4H), 2.37–1.96 (br s, 4H).

chloro(trimethylphosphite)gold(I)^[28]



To a 0.1 M suspension of [(THT)AuCl] (1.0 eq) in THF, trimethylphosphite (1.0 eq) was added. The mixture was stirred for 1 h at room temperature in the dark, then the volatiles were removed under reduced pressure. The resulting solid was solubilized again in THF, pentane was added and the mixture was kept at –18 °C overnight; the desired gold complex crystallised as a white solid (84% yield). **¹H NMR** (600 MHz) δ (ppm): 3.74 (d, 9H, *J* = 14.0 Hz).

chloro[tris(2,3,4,5,6-pentafluorophenyl)phosphine]gold(I)^[29]



To a 0.1 M solution of [(THT)AuCl] (1.0 eq) in DCM, pentafluorophenylphosphine (1.0 eq) was added. The mixture was stirred for 2 h at room temperature in the dark, then the volatiles were removed under reduced pressure. The resulting solid was solubilized again in DCM, pentane was added and the mixture was kept at –18 °C overnight; the desired gold complex crystallised as a white solid (81% yield). **¹⁹F NMR** (564 MHz) δ (ppm): –127.4 (s), –140.5 (s), –155.8 (s). **³¹P NMR** (242 MHz) δ (ppm): –32.6 (m).

Computational methods

All stationary points on the energy hypersurface, *i.e.* minima and first order saddle points, corresponding to transition structures (TS), were determined by gradient procedures within the Density Functional Theory (DFT) and making use of the M06. Reactants, transition

structures, and intermediates have been optimised in the gas phase with the 6-31G(d) basis set whereas, for Au only, the SDD effective core potential was used. The nature of the critical points was checked by vibrational analysis. The energies were then refined by single-point energy computations with def2TZVP basis set, using the polarizable continuum model (PCM). This theory level is indicated as M06/def2TZVP-PCM//M06/6-31G(d). Since the experimental part of the work was carried out in the liquid phase, solvent (1,2-dichloroethane) was simulated using the polarized continuum method, within the SMD and IEF-PCM schemes. The M06/6-31G(d) thermochemical corrections were added to the M06/def2TZVP PCM relative energies to obtain the Gibbs free energies. According to the experimental section, the Gibbs free energies reported, were estimated at T = 353 K. Quantum mechanical calculations were carried out by using the GAUSSIAN09 system of programs. Ultrafine integration grid and two-electron integral accuracy of 10-12 were used in all the computations.

Crystallography

Single-crystal data for **9a** were collected with a Gemini R Ultra diffractometer with graphite-monochromated Mo-K α radiation ($\lambda = 0.71073$) by the ω -scan method. Cell parameters were retrieved with the CrysAlisPro software and the same program was used to perform data reduction with corrections for Lorentz and polarizing effects. Scaling and absorption corrections were applied through the CrysAlisPro multiscan technique. The structure for **9a** was solved with Direct Methods. All structures have been refined with full-matrix least-squares techniques on F^2 with SHELXL-14 using the program Olex2. All non-hydrogen atoms were refined anisotropically. Hydrogen atoms were calculated and riding on the corresponding bonded atoms. The graphics of the crystal structure has been generated using Mercury 3.9. CCDC code 1962707 contains the supplementary crystallographic data for **9a**.

References

- [1] a) E. G. Occhiato, *Mini Rev. Org. Chem.* **2004**, *1*, 149-162; b) E. G. Occhiato, S. Dina, C. Prandi, *Heterocycles* **2010**, *80*, 697-724; c) C. Prandi, E. G. Occhiato, *Pest Manag. Sci.* **2019**, *75*, 2385-2402.
- [2] a) E. G. Occhiato, C. Prandi, A. Ferrali, A. Guarna, A. Deagostino, P. Venturello, *J. Org. Chem.* **2002**, *67*, 7144-7146; b) E. G. Occhiato, C. Prandi, A. Ferrali, A. Guarna, P. Venturello, *J. Org. Chem.* **2003**, *68*, 9728-9741; c) P. Larini, A. Guarna, E. G. Occhiato, *Org. Lett.* **2006**, *8*, 781-784; d) A. Deagostino, P. Larini, E. G. Occhiato, L. Pizzuto, C. Prandi, P. Venturello, *J. Org. Chem.* **2008**, *73*, 1941-1945; e) L. Bartali, A. Guarna, P. Larini, E. G. Occhiato, *Eur. J. Org. Chem.* **2007**, *2007*, 2152-2163.
- [3] a) L. Bartali, A. Casini, A. Guarna, E. G. Occhiato, D. Scarpi, *Eur. J. Org. Chem.* **2010**, *2010*, 5831-5840; b) D. Scarpi, L. Bartali, A. Casini, E. G. Occhiato, *Eur. J. Org. Chem.* **2012**, *2012*, 2597-2605.
- [4] a) C. Bhattacharya, P. Bonfante, A. Deagostino, Y. Kapulnik, P. Larini, E. G. Occhiato, C. Prandi, P. Venturello, *Org. Biomol. Chem.* **2009**, *7*, 3413-3420; b) C. Prandi, E. G. Occhiato, S. Tabasso, P. Bonfante, M. Novero, D. Scarpi, M. E. Bova, I. Miletto, *Eur. J. Org. Chem.* **2011**, *2011*, 3781-3793.
- [5] E. G. Occhiato, C. Prandi, A. Ferrali, A. Guarna, *J. Org. Chem.* **2005**, *70*, 4542-4545.
- [6] a) A. Oppedisano, C. Prandi, P. Venturello, A. Deagostino, G. Goti, D. Scarpi, E. G. Occhiato, *J. Org. Chem.* **2013**, *78*, 11007-11016; b) D. Scarpi, S. Begliomini, C. Prandi, A. Oppedisano, A. Deagostino, E. Gómez-Bengoa, B. Fiser, E. G. Occhiato, *Eur. J. Org. Chem.* **2015**, *2015*, 3251-3265.
- [7] S. Nejrotti, G. Prina Cerai, A. Oppedisano, A. Maranzana, E. G. Occhiato, D. Scarpi, A. Deagostino, C. Prandi, *Eur. J. Org. Chem.* **2017**, *2017*, 6228-6238.
- [8] a) M. Petrović, D. Scarpi, B. Fiser, E. Gómez-Bengoa, E. G. Occhiato, *Eur. J. Org. Chem.* **2015**, *2015*, 3943-3956. See also: b) D. Scarpi, M. Petrovic, B. Fiser, E. Gómez-Bengoa, E. G. Occhiato, *Org. Lett.* **2016**, *18*, 3922-3925; c) A. Rinaldi, M. Petrović, S. Magnolfi, D. Scarpi, E. G. Occhiato, *Org. Lett.* **2018**, *20*, 4713-4717.
- [9] a) C. Shu, C.-B. Chen, W.-X. Chen, L.-W. Ye, *Org. Lett.* **2013**, *15*, 5542-5545; b) C. Shu, L. Li, C. B. Chen, H. C. Shen, L. W. Ye, *Chem. Asian J.* **2014**, *9*, 1525-1529.
- [10] a) V. Sridharan, P. A. Suryavanshi, J. C. Menendez, *Chem. Rev.* **2011**, *111*, 7157-7259; b) J. D. Scott, R. M. Williams, *Chem. Rev.* **2002**, *102*, 1669-1730; c) A. R. Katritzky, S. Rachwal, B. Rachwal, *Tetrahedron* **1996**, *52*, 15031-15070.
- [11] A. Poloukhine, V. Rassadin, A. Kuzmin, V. V. Popik, *J. Org. Chem.* **2010**, *75*, 5953-5962.
- [12] S. Samala, G. Singh, R. Kumar, R. S. Ampapathi, B. Kundu, *Angew. Chem. Int. Ed.* **2015**, *54*, 9564-9567.
- [13] R. Adam, J. R. Cabrero-Antonino, A. Spannenberg, K. Junge, R. Jackstell, M. Beller, *Angew. Chem. Int. Ed.* **2017**, *56*, 3216-3220.
- [14] X. Chen, J. T. Merrett, P. W. Hong Chan, *Org. Lett.* **2018**, *20*, 1542-1545.
- [15] B. W. Boal, A. W. Schammel, N. K. Garg, *Org. Lett.* **2009**, *11*, 3458-3461.
- [16] Carried out at M06/aug-cc-pVTZ//M06/6-31+G(d) level of calculation. All calculations presented in this chapter were performed in collaboration with prof. Andrea Maranzana, University of Torino.
- [17] a) T.-Y. Yue, W. A. Nugent, *J. Am. Chem. Soc.* **2002**, *124*, 13692-13693; b) X. Liu, Z. Han, Z. Wang, K. Ding, *Angew. Chem. Int. Ed.* **2014**, *53*, 1978-1982.

- [18] An electron-withdrawing group is required on nitrogen to form the corresponding vinyl triflate (see ref. 1a).
- [19] A. Orsini, A. Vitèrisi, A. Bodlenner, J.-M. Weibel, P. Pale, *Tetrahedron Lett.* **2005**, *46*, 2259-2262.
- [20] Hydration was indeed observed by Ye, see ref. 9a.
- [21] M. G. Menkir, S.-L. Lee, *Catal. Sci. Technol.* **2017**, *7*, 6026-6041.
- [22] G. C. Levy, *Acc. Chem. Res.* **1973**, *6*, 161-169.
- [23] A. R. Modarresi-Alam, H. A. Amirazizi, H. Bagheri, H.-R. Bijanzadeh, E. Kleinpeter, *J. Org. Chem.* **2009**, *74*, 4740-4746.
- [24] X-ray analysis were performed in collaboration with dr. Emanuele Priola, University of Torino.
- [25] a) A. B. Smith III, T. A. Rano, N. Chida, G. A. Sulikowski, J. L. Wood, *J. Am. Chem. Soc.* **1992**, *114*, 8008-8022; b) W. Closson, S. Ji, S. Schulenberg, *J. Am. Chem. Soc.* **1970**, *92*, 650-657.
- [26] W. Delong, W. Lanying, W. Yongling, S. Shuang, F. Juntao, Z. Xing, *Eur. J. Org. Chem.* **2017**, *130*, 286-307.
- [27] M. J. Harper, E. J. Emmett, J. F. Bower, C. A. Russell, *J. Am. Chem. Soc.* **2017**, *139*, 12386-12389.
- [28] C. E. Strasser, S. Cronje, H. Schmidbaur, H. G. Raubenheimer, *J. Organomet. Chem.* **2006**, *691*, 4788-4796.
- [29] A. Tlahuext-Aca, M. N. Hopkinson, R. A. Garza-Sanchez, F. Glorius, *Chem. Eur. J.* **2016**, *22*, 5909-5913.

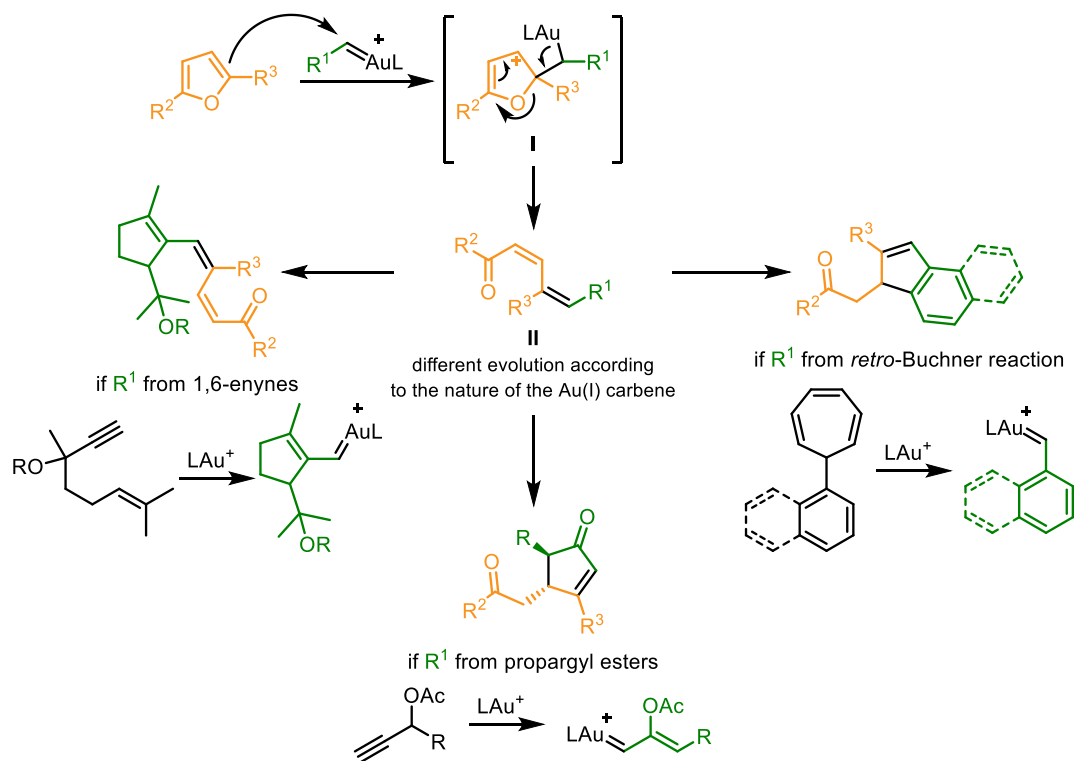
Chapter 3: Gold(I)-catalysed divergent reactivity of furan-ynes with *N*-oxides

The results presented in this chapter are not published yet.

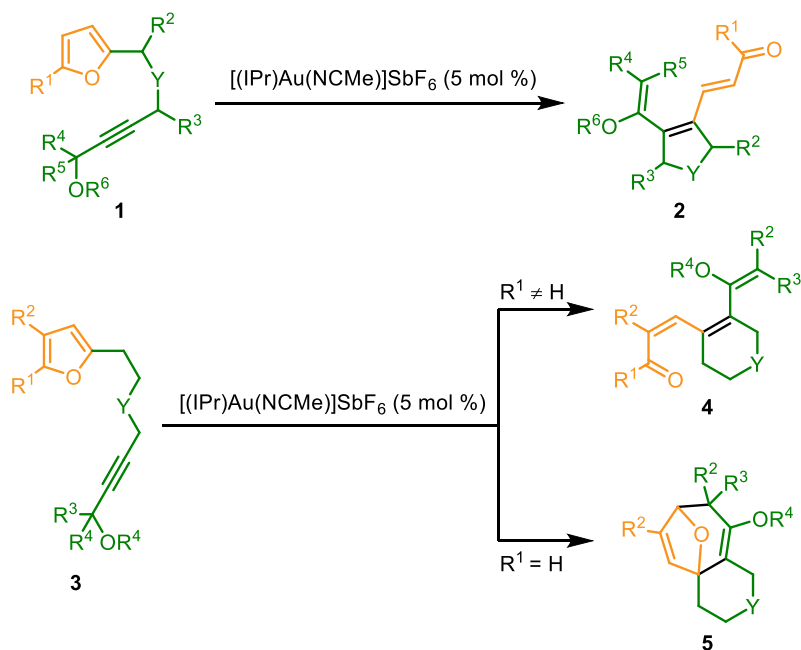
3.1 Reactions of furans with gold(I) carbenes

The application of gold catalysis to furans features a long and successful history. By virtue of their nucleophilicity, furan rings are privileged candidates for reactions with π -systems activated by the coordination of gold.^[1] As introduced in Section 1.3.2, the synthesis of phenols from alkyne-tethered furans (“furan-ynes”) represented one of the first ever studied methodologies in modern gold catalysis and opened the way to a wide array of synthetic opportunities.

A peculiar common feature in most reaction pathways involving furans, under conditions of gold catalysis, is represented by their propensity to undergo ring opening, thus allowing to easily access a considerable structural diversity. This characteristic has also been exploited in combination with the chemistry of Au(I) carbenes. In 2014 Echavarren reported the intermolecular reactions of furans with carbenes generated by rearrangement of propargyl esters, cycloisomerisation of 1,6-enynes and *retro*-Buchner reaction (Scheme 3.1, see also Scheme 1.4).^[2] The work highlighted a common reaction pathway, involving the attack of the furan onto the electrophilic gold(I) carbene; the key intermediate **I** then undergoes formal 1,2-elimination through ring opening and demetalation, affording intermediate **II** which evolves towards different products according to the nature of the starting carbene. The reactions were efficiently catalysed by NHC and Buchwald phosphine Au(I) complexes. An intramolecular version of the methodology, employing a propargyl ester tether as the gold carbene source, was afterwards studied by Tang and Shi. The work investigated how structural variations on substrates **1** and **3** allowed to disclose the synthesis of 5- and 6-membered heterocyclic skeletons **2** and **4** decorated with an extended unsaturated system, as well as oxygen-bridged tricyclic structures **5** (Scheme 3.2).^[3]

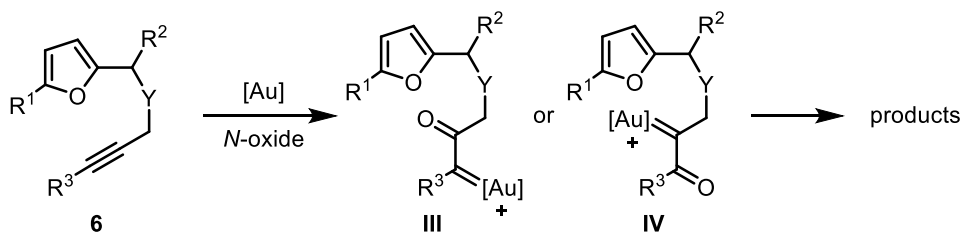


Scheme 3.1 Intermolecular reactions of furans with three types of Au(I) carbenes.



Scheme 3.2 Intramolecular reactions of furans with Au(I) carbenes generated from the rearrangement of propargyl esters.

Based on these previously reported results, we wanted to investigate the possibility to react the furan ring with a further type of Au(I) carbenes, *i.e.* α -oxo gold(I) carbenes. The functionalisation of aromatic rings *via* this chemistry has been briefly discussed in Section 1.3.3. We envisaged that treating a furan-yne substrate **6** with a pyridine or quinoline *N*-oxide would lead to the formation of the desired reactive intermediate **III** or **IV**, depending on the regioselectivity of the nucleophilic attack (Scheme 3.3). Further evolution of the gold(I) carbene, either by reaction with the furan ring or through other possible pathways, would eventually afford the final products.



Scheme 3.3 Planning the application of gold(I) catalysis with *N*-oxides to furan-ynes.

3.2 Study of the reaction conditions

3.2.1 Optimisation of the divergent reactivity

We started our investigation by studying the reactivity of furan-yne **6a**, bearing a 5-methylfuran ring and a phenyl-substituted alkyne moiety (Table 3.1), in the presence of 5 mol % of the [(IPr)Au(NTf₂)] complex and 1.2 equivalents of 2,6-dichloropyridine *N*-oxide **A**, in 1,2-dichloroethane as the solvent, at room temperature (Table 3.1, entry 1). Under these conditions, we observed the complete consumption of the starting material and the clean formation of the 6-membered dihydropyridone **7a** as the only reaction product in 81% yield after 6 hours (Table 3.1, entry 1). The structure of **7a** was unequivocally identified through X-Ray diffraction (Figure 3.1). We then varied the gold(I) catalyst, keeping the same oxidant. With the phosphite gold complex [((2,4-^tBu₂C₆H₃O)₃P)AuCl], in combination with AgNTf₂ as the chloride scavenger, two other products were observed, apart from **7a**: the 5-membered dihydropyrrole **8a** and the furan enone **9a** (entry 2). However, the yields of all three products were low. Discouraging results were obtained also with triaryl and trialkyl phosphine ligands on the gold atom (entries 3–5). On the other hand, high yields of **7a** were observed with Buchwald phosphine Au(I) chloride complexes, activated by AgNTf₂ (entries 6–7), while the cationic counterpart [(JohnPhos)Au(NCMe)]SbF₆ revealed to be less effective (entry 8).

Table 3.1 Study of the reaction conditions.^a

Reaction scheme: **6a** $\xrightarrow{[Au], Ox, DCE, rt}$ **7a**, **8a**, or **9a**.

Catalysts A-G: **A** (1,3-dichloro-5-methylimidazolium), **B** (1-methyl-2,3-dihydro-1H-benzimidazolium), **C** (1,3-dibromo-5-methylimidazolium), **D** (1,3-dichloro-5-nitroimidazolium), **E** (1-methylimidazolium), **F** (1-methyl-3-nitroimidazolium), **G** (1-methyl-3-carboximidazolium).

entry	catalyst	Ox	time	yield (%) ^b		
				7a (E/Z)	8a (E/Z)	9a
1	[(IPr)Au(NTf ₂)]	A	6 h	81 (12/88)	–	–
2	[((2,4- ^t Bu ₂ C ₆ H ₃ O) ₃ P)AuCl]/AgNTf ₂	A	6 h	15 (0/100)	6 (0/100)	11
3	[(Ph ₃ P)AuCl]/AgNTf ₂	A	6 h	–	–	–
4	[((<i>p</i> -CF ₃ Ph) ₃ P)AuCl]/AgNTf ₂	A	6 h	23 (0/100)	6 (0/100)	8
5	[(Et ₃ P)AuCl]/AgNTf ₂	A	6 h	–	–	–
6	[(JohnPhos)AuCl]/AgNTf ₂	A	6 h	77 (6/94)	–	–
7	[(^t BuXPhos)AuCl]/AgNTf ₂	A	6 h	67 (10/90)	–	–
8	[(JohnPhos)Au(NCMe)]SbF ₆	A	6 h	40 (25/75)	–	–
9	[(MorDalPhos)Au(NCMe)]SbF ₆	A	6 h	54 (15/85)	–	–
10	[(IMes)AuCl]/AgNTf ₂	A	6 h	47 (13/87)	–	2
11	[(IPr)Au(NTf ₂)]	B	6 h	–	30 (0/100)	60
12	[(IPr)Au(NTf ₂)]	C	6 h	48 (10/90)	–	–
13	[(IPr)Au(NTf ₂)]	D	6 h	56 (14/86)	17 (0/100)	27
14	[(IPr)Au(NTf ₂)]	E	6 h	–	–	22
15	[(IPr)Au(NTf ₂)]	F	6 h	68 (1/99)	–	–
16	[(IPr)Au(NTf ₂)]	G	6 h	–	–	–
17	[(IPr)Au(NTf ₂)]	F	20 h	96 (2/98)	–	–
18	[(MorDalPhos)Au(NCMe)]SbF ₆	B	20 h	–	4 (0/100)	85 ^c
19	[((2,4- ^t Bu ₂ C ₆ H ₃ O) ₃ P)AuCl]/AgNTf ₂	B	20 h	–	13 (0/100)	29
20	[(JohnPhos)AuCl]/AgNTf ₂	B	20 h	–	15 (0/100)	60
21	[(C ₆ F ₅) ₃ P)AuCl]/AgNTf ₂	B	20 h	–	4 (0/100)	11

^a All reactions were performed at rt with 0.1 mmol **7a**, 0.12 mmol Ox, 0.005 mmol Au(I) complex and, when specified, 0.005 mmol Ag(I) salt, in 1.0 ml of DCE. ^b Determined by ¹H NMR at 600 MHz, using *n*-heptane as internal standard. ^c 74% isolated yield.

Again, lower yields of **7a** were obtained with the bidentate ligand MorDalPhos (Figure 3.2) and with the NHC complex [(IMes)AuCl] (entries 9–10). The reaction proceeds with a good stereoselectivity for the configuration of the exocyclic C-C double bond in **7a** and **8a**, observing a general preference for the *Z* isomer, with a *E/Z* ratio ranging from 0/100 (entries 2 and 4) to 25/75 (entry 8).

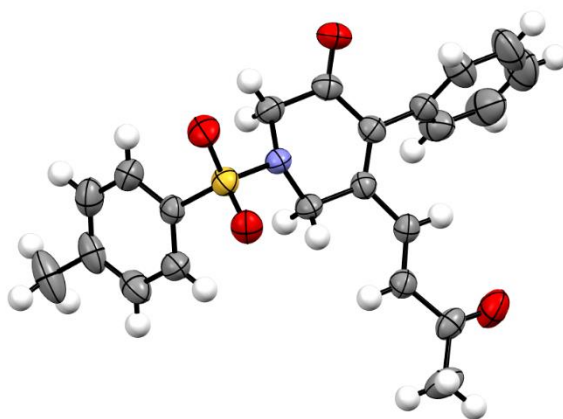


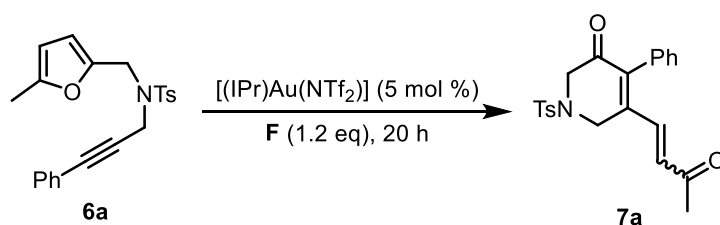
Figure 3.1 Crystal structure of **7a**.

The screening of various gold(I) complexes, with **A** as the *N*-oxide, showed that the best yield of **7a** was obtained with [(IPr)Au(NTf₂)] (Table 3.1, entry 1), so we decided to test different oxidants, in combination with this catalyst. With 8-methylquinoline *N*-oxide **B**, the formation of **7a** was completely suppressed in favour of a 1:2 ratio of **8a** and **9a** (entry 11). Other *N*-oxides were either less selective (**D**, entry 13) or less active (entries 12, 14–17) in converting the substrate **6a** into one of the three possible reaction products. However, 4-nitropyridine *N*-oxide **F** afforded **7a** in 68% yield after 6 hours, with an almost complete selectivity for the *Z* isomer (entry 15); interestingly, in this case a 25% yield of unreacted starting material was detected in the reaction mixture. The high diastereoselectivity observed with this oxidant prompted us to perform again the reaction for longer times; we found that in 20 hours the starting material was completely consumed and **7a** was formed in 96% yield, with a 2/98 *E/Z* ratio (entry 17). We then considered the outcome of the reaction with **B** and [(IPr)Au(NTf₂)] (entry 11) and we deemed it worthwhile to further explore the reactivity of this oxidant with different gold(I) complexes. With [(MorDalPhos)Au(NCMe)]SbF₆ an almost complete product selectivity was observed, with a 85% yield of the furan enone **9a** (entry 18, 74% yield of isolated product). Other complexes were less effective and, more

importantly, none of them was able to direct the selectivity towards dihydropyrrole **8a**, for which the best result remains the 30% yield with [(IPr)Au(NTf₂)] and **B** (Table 3.1, entry 11).

Turning our attention back to product **7a**, we tried to isolate it in a pure form from the 96% NMR yield, 2/98 *E/Z* ratio, of entry 17 (Table 3.1). However, we immediately realized that (*Z*)-**7a** was not stable over time, as it tended to isomerise to the *E* form. Based on this, we decided to try to orient the synthesis directly towards a total selectivity for (*E*)-**7a**. As shown in Table 3.2, we maintained the best conditions from the above-described screening, and we at first increased the reaction temperature to 80 °C, obtaining a slight improvement in the *E/Z* ratio, but with a lower overall yield (Table 3.2, entry 1).

Table 3.2 Optimisation of the *E/Z* ratio in the synthesis of **7a**.



entry	T (°C)	solvent	additive	yield % of 7a (<i>E/Z</i>) ^a
1	80 °C	DCE	–	66 (23/77)
2	rt	DCE	TFA (2.0 eq)	73 (16/84)
3	rt	DCE	<i>p</i> -TsOH (2.0 eq)	43 (100/0)
4	rt	DCE	MsOH (2.0 eq)	58 (100/0)
5	rt	CHCl ₃	–	63 (3/97)
6	rt	HFIP	–	–
7	rt	DCE	MsOH (2.0 eq) ^b	94 (17/83)
8	rt	DCE	<i>p</i> -TsOH (2.0 eq) ^b	89 (11/89)
9	rt	DCE	TfOH (2.0 eq) ^b	–
10	rt	DCE	MsOH (5.0 eq) ^b	80 ^c (100/0)
11	rt	DCE	I ₂ (one crystal) ^b	21 (86/14)

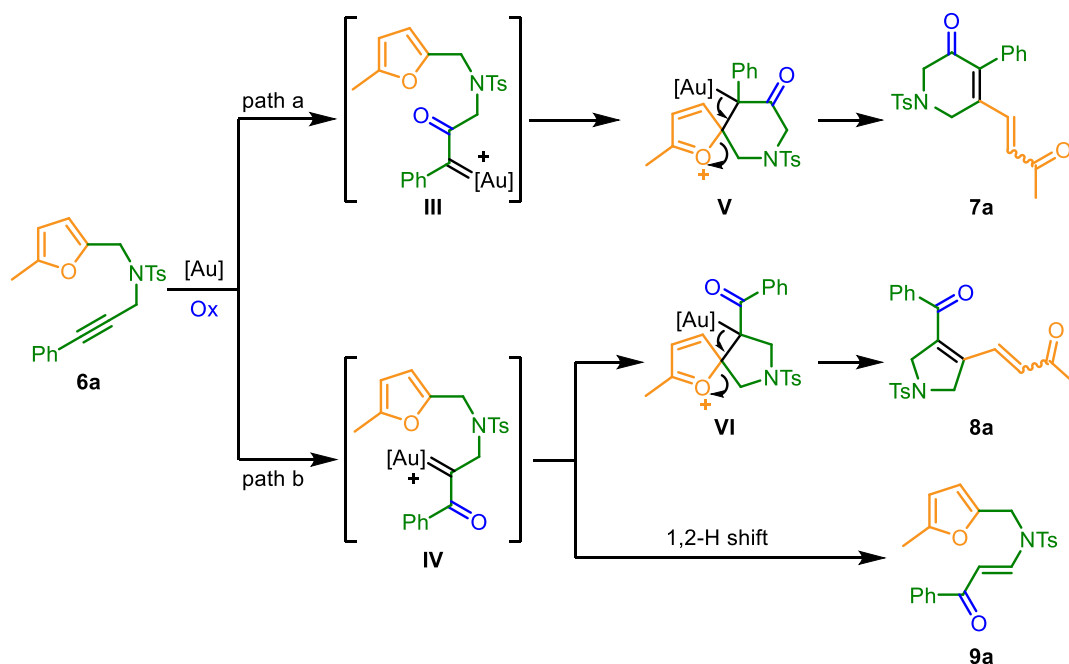
^a Determined by ¹H NMR at 600 MHz, using *n*-heptane as internal standard. ^b Added after 20 h, then stirred for one additional hour. ^c 72% isolated yield.

Changing our approach, we decided to add a Brønsted acid to the reaction mixture, such as trifluoroacetic acid (entry 2), *p*-toluenesulfonic acid (entry 3) or methanesulfonic acid (entry 4). Interestingly, the latter two were able to induce complete selectivity towards (*E*)-**7a**, but again with reduced yields. Also attempts to employ more acidic solvents, such as CHCl₃ and 1,1,1,3,3,3-hexafluoroisopropanol (entries 5–6) met with failure. We attributed the decrease of the yield, in the presence of a Brønsted acid, to the possible degradation of the starting material **6a**.

To avoid it, we decided to add the acid to the reaction mixture only at the end of the gold(I)-catalysed step, *i.e.* after 20 hours: under these conditions, with MsOH and *p*-TsOH, the yield remained high, but again with an unsatisfying *E/Z* ratio (entries 7–8), while a stronger acid, such as trifluoromethanesulfonic acid, completely degraded the product (entry 9). Eventually, we found a viable solution by increasing the amount of MsOH up to 5.0 equivalents, obtaining a still high 80% NMR yield (72% isolated) of *E*-**7a** (entry 10). Additionally, we also attempted to raise the *E/Z* ratio by the addition of I_2 , as previously reported,^[4] but without success (entry 11).

3.2.2 Mechanistic hypothesis

A plausible mechanistic picture for the formation of products **7a**, **8a** and **9a** is depicted in Scheme 3.4. Upon activation of the alkyne moiety in substrate **6a** by the Au(I) complex, the attack of the *N*-oxide onto the C1 atom of the triple bond leads to α -oxo gold(I) carbene **III**, which then undergoes cyclisation through nucleophilic attack by the furan ring, affording the spirocyclic intermediate **V** (path a, Scheme 3.4). A final elimination step eventually determines the opening of the furan ring and the formation of the endocyclic double bond, leading to the formation of **7a**.



Scheme 3.4 Possible mechanistic pathways in the gold(I)-catalysed reaction of furan-yne **6a** with *N*-oxides.

Based on the results presented in Table 3.1 and Table 3.2, the *Z* isomer is likely first formed, and then converted into (*E*)-**7a**. If the regioselectivity of the first step is switched, the spirocyclic intermediate **VI** is formed upon attack of the furan onto Au(I) carbene **IV** (path b, Scheme 3.4). Then, elimination affords the final product **8a** in the same way as described for **7a**. Again, the *Z* isomer is probably formed in the reactions mechanism, and can subsequently be converted into *E*-**8a**. Moreover, the α -oxo gold(I) carbene intermediate **IV** may also undergo a different reaction pathway, through a 1,2-H shift involving the neighbouring CH₂ group.^[5] This mechanism would lead to the formation of the furan enone **9a**. As previously reported, this reactivity selectively provides the newly formed C-C double bond in the *E* configuration, as was also confirmed by our results. At this point, it should be pointed out that the best selectivity for **9a** was obtained with the gold(I) complex [(MorDalPhos)Au(NCMe)]SbF₆ (Table 3.1, entry 18). The ligand MorDalPhos has been reported to temper the electrophilicity of the Au(I) carbene through double coordination from both the P and the N atom (Figure 3.2).^[6] This is in line with what was observed in our case, as the less electrophilic carbene should be less prone to get attacked by the nucleophilic furan ring, and thus more available to selectively undergo 1,2-H shift. However, when we tried to employ more electrophilic Au(I) complexes, we could not confirm our hypothesis, as we did not observe an enhancement of the selectivity towards **8a** (Table 3.1, entries 19 and 21).

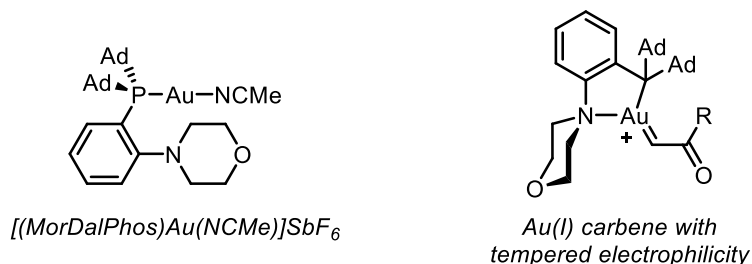
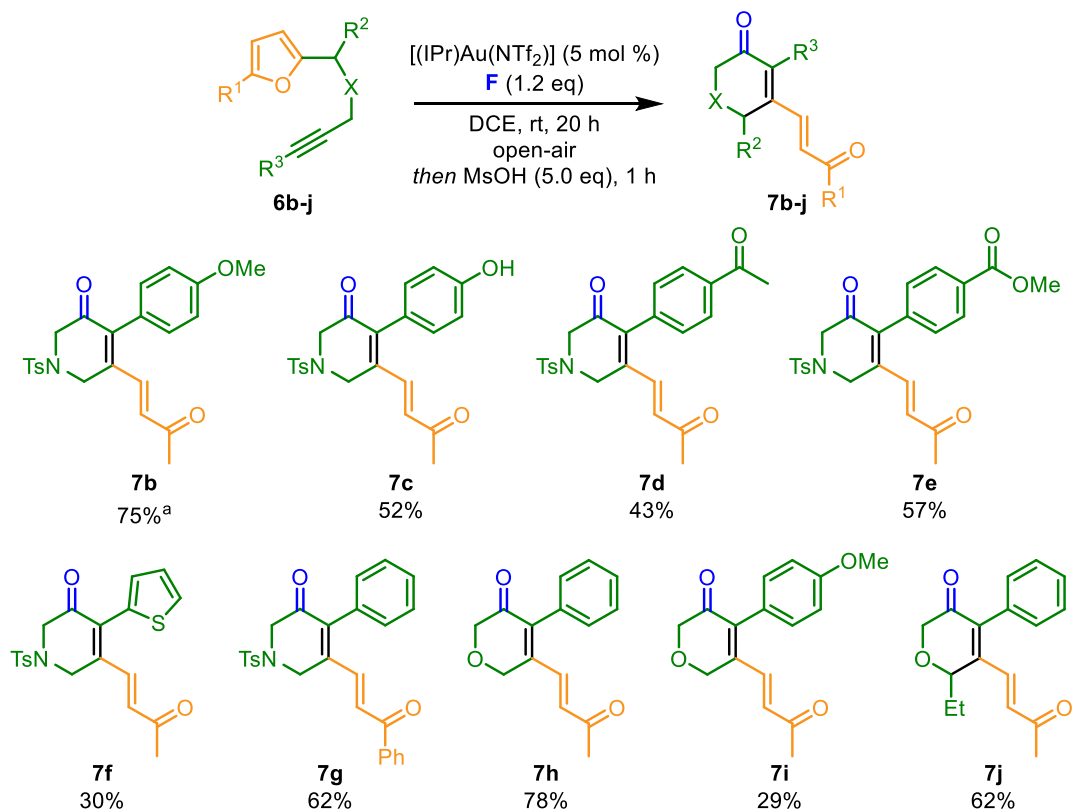


Figure 3.1 The coordination by the *N* atom tempers the electrophilicity of Au(I) carbenes with MorDalPhos ligand.^[6]

3.3 Reaction substrate scope

The study on the divergent reactivity of furan-yne **6a** with *N*-oxides, in the presence of a gold(I) catalyst, allowed us to identify the suitable conditions for the selective synthesis of dihydropyridone **7a** (Table 3.2, entry 10) and furan enone **9a** (Table 3.1, entry 19), while the best results in terms of the yield of dihydropyrrole **8a** were limited to a 30% NMR yield (Table 3.1, entry 11) and still need some further optimisation to obtain a clean and selective access to this molecular scaffold.

We then decided to synthesise a series of furan-ynes **6b-j**, by varying the substitution pattern on the furan ring and on the alkyne side arm. These substrates were reacted under the optimised conditions for the dihydropyridone synthesis, *i.e.* with $[(\text{IPr})\text{Au}(\text{NTf}_2)]$ as the gold(I) complex, 4-nitropyridine *N*-oxide as the oxidant, in DCE at room temperature for 20 hours, followed by the addition of 5.0 equivalents of MsOH and further stirring for 1 hour.



Scheme 3.5 Early reaction substrate scope for the gold(I)-catalysed synthesis of dihydropyridones. ^a Isolated yields. All products were in *E* configuration.

The results of the study on the substrate scope are reported in Scheme 3.5. It should be noted that further extension of the reaction scope is still under investigation. The alkyne terminus of the substrate was varied by choosing aromatic rings with different substituents: the methodology proved to be compatible with electron-donating (**7b-c**) and electron-withdrawing (**7d-e**) functionalities, and the heteroaromatic thiophene ring was also tolerated (**7f**). The methyl group in the furan ring was successfully replaced with a phenyl (**7g**), and the *N*-Ts linker with an *O* linker (**7h-i**). Dihydropyridone **7j**, bearing a substituent on the heterocyclic ring, was also synthesised.

3.4 Conclusion

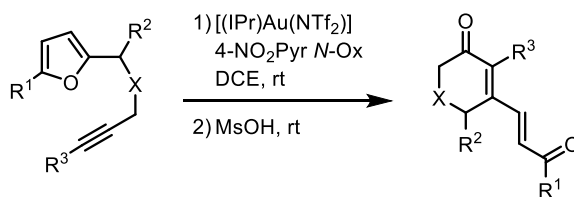
The study of the reactivity of furan-ynes with *N*-oxides, in the presence of a gold(I) catalyst, has revealed an intriguing divergent mechanistic picture, with the formation of three possible heterocyclic scaffolds, a dihydropyridone, a dihydropyrrole and a furan, each of them with different pendant functional groups. The outcome of the reaction was controlled by the choice of the gold(I) complex and the *N*-oxide. The best conditions for selectively synthesising the dihydropyridone scaffold were thus identified, allowing also for a complete *E* diastereoselectivity of the C-C double bond in the side arm. The substrate scope of the dihydropyridone synthesis has been extended in different directions, and several electrophilic and nucleophilic functional groups proved to be tolerated. Further investigation on the substrate applicability of this methodology is ongoing, as well as possible synthetic manipulations of the dihydropyridone scaffold. Moreover, the possibility of performing the reaction in its intermolecular version is currently under investigation. The furan enone product was also selectively obtained in high yield. Both reactions were performed under mild conditions, at room temperature and without the exclusion of air and moisture. Unfortunately, we have not been able yet to find the appropriate conditions to orient the reaction towards the dihydropyrrole product, which still remains as a secondary product, with a 30% NMR yield, in the synthesis of the furan enone. Further optimisation in this direction is under study.

3.5 Experimental section

General information

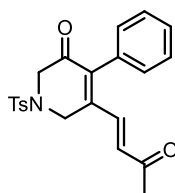
Flasks and all equipment used for the generation and reaction of moisture-sensitive compounds were dried by electric heat gun under nitrogen. Unless specified, all reagents were used as received without further purifications. Anhydrous THF was obtained by distillation over LiAlH₄, followed by distillation over Na-benzophenone. Flash column chromatography was performed over silica gel (40–63 μm, 230–400 mesh); *R_f* values refer to TLC carried out on silica gel plates. ¹H NMR and ¹³C NMR spectra were recorded on a Jeol ECZR600, in CDCl₃ or in CD₃OD, using residual solvent peak as an internal reference (CHCl₃, ¹H: 7.26 ppm, ¹³C: 77.16 ppm; CH₃OH, ¹H: 3.34 ppm, ¹³C: 49.86 ppm). Multiplicity is reported as follows: s (singlet), d (doublet), t (triplet), q (quartet), quin (quintet), sext (sextet), m (multiplet), br (broad). GC-MS spectra were recorded at an ionizing voltage of 70 eV. HRMS analysis were run on a high resolving power hybrid mass spectrometer (HRMS) Orbitrap Fusion (Thermo Scientific, Rodano, Italy), equipped with an a ESI ion source. The samples were analysed in acetonitrile solution using a syringe pump at a flow rate of 5 μL/min. The tuning parameters adopted for the ESI source were: source voltage 4.0 kV. The heated capillary temperature was maintained at 275°C. The mass accuracy of the recorded ions (vs. the calculated ones) was ±2.5 mmu (milli-mass units).

General procedure for gold(I)-catalysed synthesis of dihydropyridones



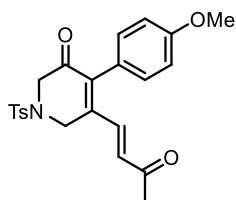
A solution of the furan-yne substrate (1.0 eq, 0.2 mmol) and 4-nitropyridine *N*-oxide (1.2 eq) in DCE (0.1 M with respect to the furan-yne) was prepared, then $[(IPr)Au(NTf_2)]$ (0.05 eq) was added and the mixture was stirred at room temperature for 20 h. Then, MsOH (5.0 eq) was added and the mixture was stirred at room temperature for 1 h. A few drops of Et₃N were added and the solvent was evaporated under reduced pressure. The crude product was purified by flash column chromatography to afford pure dihydropyridones **7** as the product.

(*E*)-5-(3-oxobut-1-en-1-yl)-4-phenyl-1-tosyl-1,6-dihydropyridin-3(2H)-one, **7a**



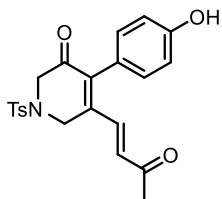
Synthesised according to the general procedure. Yellow solid, 72% yield, mp 176–177 °C (decomposition). R_f 0.21 (75/25 PE/EtOAc). **¹H NMR** (600 MHz, CDCl₃) δ (ppm): 7.73–7.69 (m, 2H), 7.39–7.34 (m, 5H), 7.03 (d, 1H, $J = 16.6$ Hz), 6.87–6.84 (m, 2H), 6.46 (d, 1H, $J = 16.6$ Hz), 4.31 (s, 2H), 4.04 (s, 2H), 2.44 (s, 3H), 2.19 (s, 3H). **¹³C NMR** (150 MHz, CDCl₃) δ (ppm): 197.3 (Cq), 190.4 (Cq), 144.9 (Cq), 144.1 (Cq), 141.4 (Cq), 137.9 (CH), 133.4 (Cq), 132.2 (CH), 131.3 (Cq), 130.5 (CH), 130.4 (CH), 129.2 (CH), 128.3 (CH), 127.8 (CH), 53.3 (CH₂), 45.1 (CH₂), 28.0 (CH₃), 21.7 (CH₃).

(*E*)-4-(4-methoxyphenyl)-5-(3-oxobut-1-en-1-yl)-1-tosyl-1,6-dihydropyridin-3(2H)-one, **7b**



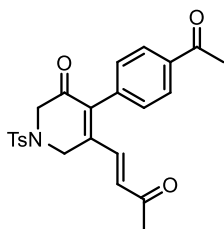
Synthesised according to the general procedure. Yellow solid, 75% yield, mp 150–153 °C (decomposition). R_f 0.24 (7/3 PE/EtOAc). **¹H NMR** (600 MHz, CDCl₃) δ (ppm): 7.69 (d, 2H, $J = 8.3$ Hz), 7.35 (d, 2H, $J = 8.1$ Hz), 7.09 (d, 1H, $J = 16.6$ Hz), 6.90–6.87 (m, 2H), 6.82–6.79 (m, 2H), 6.45 (d, 1H, $J = 16.6$ Hz), 4.29 (s, 2H), 4.03 (s, 2H), 3.83 (s, 3H), 2.44 (s, 3H), 2.22 (s, 3H). **¹³C NMR** (150 MHz, CDCl₃) δ (ppm): 197.4 (Cq), 190.7 (Cq), 160.3 (Cq), 144.8 (Cq), 143.5 (Cq), 140.9 (Cq), 138.2 (CH), 133.3 (Cq), 132.0 (CH), 131.8 (CH), 130.4 (CH), 127.8 (CH), 123.3 (Cq), 113.8 (CH), 55.4 (CH₃), 53.3 (CH₂), 45.2 (CH₂), 28.1 (CH₃), 21.7 (CH₃).

(E)-4-(4-hydroxyphenyl)-5-(3-oxobut-1-en-1-yl)-1-tosyl-1,6-dihydropyridin-3(2H)-one, **7c**



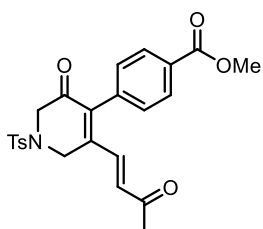
Synthesised according to the general procedure. Yellow solid, 52% yield, mp 170–174 °C (decomposition). **R_f** 0.25 (9/1 DCM/EtOAc). **¹H NMR** (600 MHz, CD₃OD) δ (ppm): 7.74–7.72 (m, 2H), 7.42 (d, 2H, *J* = 7.9 Hz), 7.07 (d, 1H, *J* = 16.4 Hz), 6.78–6.75 (m, 2H), 6.69 (d, 1H, *J* = 16.4 Hz), 6.64–6.62 (m, 2H), 4.51 (s, 2H), 4.17 (s, 2H), 2.45 (s, 3H), 2.24 (s, 3H), 2.19 (s, 3H). **¹³C NMR** (150 MHz, CD₃OD) δ (ppm): 200.5 (Cq), 193.7 (Cq), 160.2 (Cq), 146.9 (Cq), 145.9 (Cq), 143.0 (Cq), 140.2 (CH), 136.9 (Cq), 134.1 (CH), 133.4 (CH), 132.3 (CH), 129.6 (CH), 124.6 (Cq), 116.5 (CH), 55.2 (CH₂), 47.1 (CH₂), 29.1 (CH₃), 22.3 (CH₃).

(E)-4-(4-acetylphenyl)-5-(3-oxobut-1-en-1-yl)-1-tosyl-1,6-dihydropyridin-3(2H)-one, **7d**



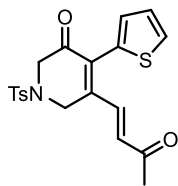
Synthesised according to the general procedure. White solid, 43% yield, mp 161–164 °C (decomposition). **R_f** 0.24 (6/4 PE/EtOAc). **¹H NMR** (600 MHz, CDCl₃) δ (ppm): 7.96–7.93 (m, 2H), 7.71 (d, 2H, *J* = 8.3 Hz), 7.37 (d, 2H, *J* = 8.0 Hz), 6.96 (d, 1H, *J* = 16.4 Hz) superimposed to 6.98–6.95 (m, 2H), 6.51 (d, 1H, *J* = 16.4 Hz), 4.34 (s, 2H), 4.06 (s, 2H), 2.62 (s, 3H), 2.45 (s, 3H), 2.22 (s, 3H). **¹³C NMR** (150 MHz, CDCl₃) δ (ppm): 197.6 (Cq), 196.9 (Cq), 190.0 (Cq), 145.0 (Cq), 144.8 (Cq), 140.4 (Cq), 137.4 (Cq), 136.9 (CH), 136.2 (Cq), 133.4 (Cq), 132.7 (CH), 130.8 (CH), 130.5 (CH), 128.2 (CH), 127.8 (CH), 53.2 (CH₂), 45.1 (CH₂), 28.4 (CH₃), 26.8 (CH₃), 21.7 (CH₃).

methyl *(E)*-4-(3-oxo-5-(3-oxobut-1-en-1-yl)-1-tosyl-1,2,3,6-tetrahydropyridin-4-yl)benzoate, **7e**



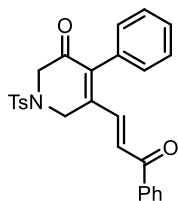
Synthesised according to the general procedure. Light orange solid, 57% yield, mp 186–191 °C (decomposition). **R_f** 0.21 (65/35 PE/EtOAc). **¹H NMR** (600 MHz, CDCl₃) δ (ppm): 8.04–8.02 (m, 2H), 7.71–7.69 (m, 2H), 7.36 (d, 2H, *J* = 8.0 Hz), 6.95 (d, 1H, *J* = 16.6 Hz) superimposed to 6.94–6.92 (m, 2H), 6.50 (d, 1H, *J* = 16.5 Hz), 4.34 (s, 2H), 4.06 (s, 2H), 3.93 (s, 3H), 2.45 (s, 3H), 2.20 (s, 3H). **¹³C NMR** (150 MHz, CDCl₃) δ (ppm): 197.0 (Cq), 190.0 (Cq), 166.6 (Cq), 145.0 (Cq), 144.8 (Cq), 140.4 (Cq), 137.0 (CH), 136.0 (Cq), 133.4 (Cq), 132.7 (CH), 130.7 (Cq), 130.6 (CH), 130.5 (CH), 129.5 (CH), 127.8 (CH), 53.2 (CH₂), 52.5 (CH₃), 45.1 (CH₂), 28.2 (CH₃), 21.7 (CH₃).

(E)-5-(3-oxobut-1-en-1-yl)-4-(thiophen-2-yl)-1-tosyl-1,6-dihydropyridin-3(2H)-one, **7f**



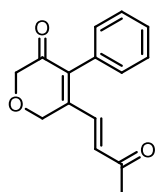
Synthesised according to the general procedure. Yellow solid, 30% yield, mp 146-148 (Et₂O, decomposition). *R_f* 0.23 (7/3 PE/EtOAc). **¹H NMR** (600 MHz, CDCl₃) δ (ppm): 7.70-7.67 (m, 2H), 7.52 (dd, 1H, *J* = 5.2, 1.2 Hz), 7.36 (d, 1H, *J* = 16.5 Hz), 7.32 (d, 2H, *J* = 8.0 Hz), 7.06 (dd, 1H, *J* = 5.1, 3.6 Hz), 6.81 (dd, 1H, *J* = 3.6, 1.2 Hz), 6.55 (d, 1H, *J* = 16.5 Hz), 4.31 (s, 2H), 4.1 (s, 2H), 2.39 (s, 3H), 2.29 (s, 3H). **¹³C NMR** (150 MHz, CDCl₃) δ (ppm): 197.3 (Cq), 189.9 (Cq), 144.9 (Cq), 143.9 (Cq), 138.0 (CH), 134.4 (Cq), 133.2 (Cq), 132.4 (CH), 131.8 (CH), 131.1 (Cq), 130.5 (CH), 130.4 (CH), 127.7 (CH), 126.7 (CH), 53.3 (CH₂), 45.7 (CH₂), 28.3 (CH₃), 21.7 (CH₃).

(E)-5-(3-oxo-3-phenylprop-1-en-1-yl)-4-phenyl-1-tosyl-1,6-dihydropyridin-3(2H)-one, **7g**



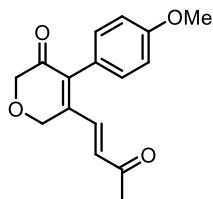
Synthesised according to the general procedure. Yellow solid, 62% yield, mp 175-178 °C (decomposition). *R_f* 0.23 (8/2 PE/EtOAc). **¹H NMR** (600 MHz, CDCl₃) δ (ppm): 7.92 (d, 2H, *J* = 7.2 Hz), 7.72 (d, 2H, *J* = 8.3 Hz), 7.64-7.60 (m, 1H), 7.51 (t, 2H, *J* = 7.8 Hz), 7.37-7.34 (m, 5H), 7.29 (d, 2H, *J* = 1.3 Hz), 6.82 (dd, 2H, *J* = 7.7, 1.6 Hz), 4.49 (s, 2H), 4.11 (s, 2H), 2.44 (s, 3H). **¹³C NMR** (150 MHz, CDCl₃) δ (ppm): 190.6 (Cq), 189.3 (Cq), 144.9 (Cq), 144.1 (Cq), 141.5 (Cq), 139.2 (CH), 137.2 (Cq), 133.7 (CH), 133.7 (Cq), 131.3 (Cq), 130.5 (CH), 130.5 (CH), 129.1 (CH), 129.0 (CH), 128.7 (CH), 128.3 (CH), 127.8 (CH), 127.7 (CH), 53.3 (CH₂), 45.2 (CH₂), 21.7 (CH₃).

(E)-5-(3-oxobut-1-en-1-yl)-4-phenyl-2H-pyran-3(6H)-one, **7h**



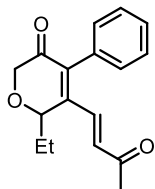
Synthesised according to the general procedure. Yellow solid, 78% yield, mp 104-106 °C (Et₂O). *R_f* 0.44 (6/4 PE/EtOAc). **¹H NMR** (600 MHz, CDCl₃) δ (ppm): 7.46-7.41 (m, 3H), 7.20-7.17 (m, 2H) superimposed to 7.15 (d, 1H, *J* = 16.7 Hz), 6.32 (d, 1H, *J* = 16.7 Hz), 4.72 (s, 2H), 4.34 (s, 2H), 2.19 (s, 3H). **¹³C NMR** (150 MHz, CDCl₃) δ (ppm): 197.6 (Cq), 193.2 (Cq), 146.6 (Cq), 140.1 (Cq), 137.5 (CH), 132.0 (CH), 131.3 (Cq), 130.7 (CH), 129.1 (CH), 128.4 (CH), 72.5 (CH₂), 65.6 (CH₂), 27.6 (CH₃).

(E)-4-(4-methoxyphenyl)-5-(3-oxobut-1-en-1-yl)-2H-pyran-3(6H)-one, **7i**



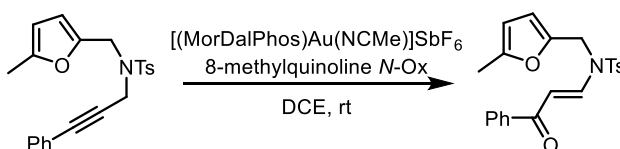
Synthesised according to the general procedure. Yellow solid, 29% yield. *R_f* 0.35 (75/25 PE/EtOAc). **¹H NMR** (600 MHz, CDCl₃) δ (ppm): 7.21 (d, 1H, *J* = 16.8 Hz), 7.15-7.12 (m, 2H), 6.98-6.95 (m, 2H), 6.32 (d, 1H, *J* = 16.7 Hz), 4.70 (s, 2H), 4.33 (s, 2H), 3.86 (s, 3H), 2.21 (s, 3H). **¹³C NMR** (150 MHz, CDCl₃) δ (ppm): 197.7 (Cq), 193.6 (Cq), 160.3 (Cq), 145.0 (Cq), 139.7 (Cq), 137.9 (CH), 132.3 (CH), 131.6 (CH), 123.4 (Cq), 113.9 (CH), 72.6 (CH₂), 65.7 (CH₂), 55.5 (CH₃), 27.7 (CH₃).

(E)-6-ethyl-5-(3-oxobut-1-en-1-yl)-4-phenyl-2H-pyran-3(6H)-one, **7j**



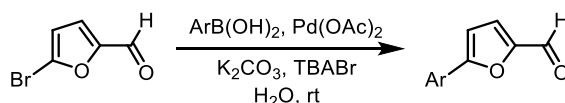
Synthesised according to the general procedure. Yellow oil, 62% yield. R_f 0.12 (9/1 PE/EtOAc). $^1\text{H NMR}$ (600 MHz, CDCl_3) δ (ppm): 7.34–7.27 (m, 3H), 7.07–7.04 (m, 2H), 6.29 (dd, 1H, $J = 12.2, 1.6$ Hz), 6.10 (d, 1H, $J = 12.2$ Hz), 4.75–4.72 (m, 1H), 4.42 (d, 1H, $J = 16.4$ Hz), 4.32 (dd, 1H, $J = 16.4, 1.3$ Hz), 2.08 (s, 3H), 1.79–1.73 (m, 2H), 1.03 (t, 3H, $J = 7.4$ Hz). $^{13}\text{C NMR}$ (150 MHz, CDCl_3) δ (ppm): 197.7 (Cq), 193.3 (Cq), 156.9 (Cq), 136.8 (CH), 134.9 (Cq), 133.2 (Cq), 130.1 (CH), 129.6 (CH), 128.1 (CH), 128.1 (CH), 77.2 (CH), 70.5 (CH_2), 30.9 (CH_3), 25.9 (CH_2), 10.1 (CH_3).

Synthesis of (E)-4-methyl-*N*-((5-methylfuran-2-yl)methyl)-*N*-(3-oxo-3-phenylprop-1-en-1-yl)benzenesulfonamide, **9a**



A solution of the furan-yne substrate (1.0 eq, 0.2 mmol) and 8-methylquinoline *N*-oxide (1.2 eq) in DCE (0.1 M with respect to the furan-yne) was prepared, then [(MorDalPhos)Au(NCMe)]SbF₆ (0.05 eq) was added and the mixture was stirred at room temperature for 20 h. Then, a few drops of Et₃N were added and the solvent was evaporated under reduced pressure. The crude product was purified by flash column chromatography to afford pure vinyl ketone **9a** as the product. White solid, 74% yield, mp 127–128 °C (EtOAc). R_f 0.20 (9/1 PE/EtOAc). $^1\text{H NMR}$ (600 MHz, CDCl_3) δ (ppm): 8.26 (d, 1H, $J = 13.6$ Hz), 7.88–7.85 (m, 2H), 7.71 (d, 2H, $J = 8.4$ Hz), 7.54–7.51 (m, 1H), 7.46–7.42 (m, 2H), 7.29 (d, 2H, $J = 8.0$ Hz), 6.50 (d, 1H, $J = 13.6$ Hz), 6.07 (d, 1H, $J = 3.1$ Hz), 5.85–5.84 (m, 1H), 4.74 (s, 2H), 2.42 (s, 3H), 2.07 (d, 3H, $J = 1.1$ Hz). $^{13}\text{C NMR}$ (150 MHz, CDCl_3) δ (ppm): 189.4 (Cq), 152.4 (Cq), 146.0 (Cq), 144.9 (Cq), 142.6 (CH), 138.7 (Cq), 135.7 (Cq), 132.5 (CH), 130.1 (CH), 128.6 (CH), 128.2 (CH), 127.6 (CH), 110.7 (CH), 106.7 (CH), 104.0 (CH), 43.3 (CH_2), 21.7 (CH_3), 13.5 (CH_3).

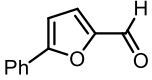
General procedure for the Suzuki coupling of 5-bromo-2-furaldehyde^[7]



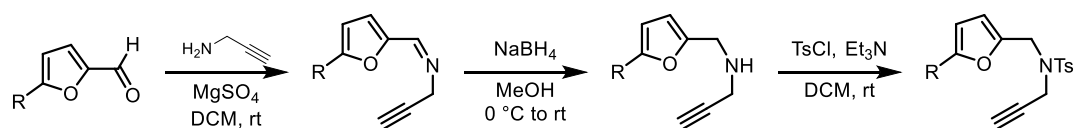
Into a flask, 2-bromofuraldehyde (1.0 eq, 15 mmol), arylboronic acid (1.1 eq), palladium(II) acetate (0.02 eq), potassium carbonate (2.5 eq) and tetrabutylammonium bromide (1.0 eq) were added, then deionized H₂O (0.5 M with respect to 2-bromofuraldehyde) was added and the mixture was vigorously stirred for 2 h at room temperature. Then, the mixture was extracted three times with EtOAc; the combined organic layers were dried over anhydrous

Na₂SO₄, filtered and the volatiles were evaporated under reduced pressure. The crude product was purified by flash column chromatography to obtain the pure 5-aryl substituted furfural.

5-phenylfuran-2-carbaldehyde^[8]

 Synthesised according to the general procedure. Yellow oil, 75% yield. **R_f** 0.46 (9/1 PE/EtOAc). **¹H NMR** (600 MHz, CDCl₃) δ (ppm): 9.66 (s, 1H), 7.85–7.82 (m, 2H), 7.47–7.44 (m, 2H), 7.42–7.39 (m, 1H), 7.33 (d, 1H, *J* = 3.7 Hz), 6.85 (d, 1H, *J* = 3.7 Hz). **GC-MS** *m/z* (%): 172 [M]⁺ (100), 171 (45), 115 (77).

General procedure for the synthesis of terminal alkynes with N-Ts linker^[9]

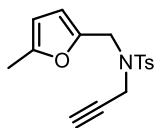


To a 1.0 M solution of furfuraldehyde (1.0 eq, 10–20 mmol) in DCM, MgSO₄ (1.1 eq) and propargylamine (1.0 eq) were added and the mixture was stirred at room temperature for 24–48 h (GC-MS monitoring). The mixture was filtered over silica with EtOAc and the volatiles were evaporated under reduced pressure to obtain the crude imine, which was used for the next step without further purification.

To a 1.0 M solution of the crude furanyl imine in MeOH, NaBH₄ (1.0 eq) was added portionwise at 0 °C. The mixture was allowed to reach room temperature and stirred for 5–10 min (GC-MS monitoring) until complete conversion. Then, MeOH was evaporated to half of the initial volume under reduced pressure. Water was added and the mixture was extracted three times with EtOAc; the combined organic layers were dried over Na₂SO₄, filtered and the volatiles were evaporated under reduced pressure to obtain the crude amine, which was used for the next step without further purification.

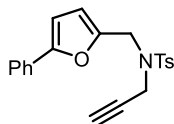
To a 1.0 M solution of the crude amine in DCM, Et₃N (1.0 eq) was added, then *p*-toluenesulfonyl chloride (1.0 eq) was added portionwise and the mixture was stirred at room temperature overnight. Then, water was added and the mixture was extracted three times with DCM; the combined organic layers were dried over Na₂SO₄, filtered and the volatiles were evaporated under reduced pressure. The crude product was purified by flash column chromatography to obtain the pure *N*-Ts product.

*4-methyl-N-((5-methylfuran-2-yl)methyl)-N-(prop-2-yn-1-yl)benzenesulfonamide*⁹¹



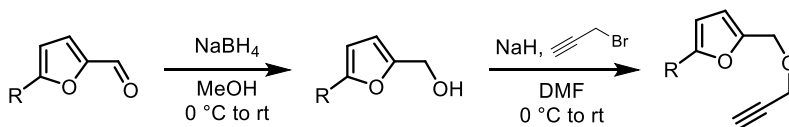
Synthesised according to the general procedure. White solid, 63% yield (3-steps). **R_f** 0.31 (9/1 PE/EtOAc). **¹H NMR** (600 MHz, CDCl₃) δ (ppm): 7.75–7.73 (m, 2H), 7.30–7.28 (m, 2H), 6.16 (d, 1H, *J* = 3.0 Hz), 5.86 (dq, 1H, *J* = 3.0 Hz, 1.0 Hz), 4.37 (s, 2H), 4.02 (d, 2H, *J* = 2.5 Hz), 2.43 (s, 3H), 2.20 (d, 3H, *J* = 1.0 Hz), 2.05 (t, 1H, *J* = 2.5 Hz). **GC-MS** *m/z* (%): 303 [M]⁺ (3), 148 (100), 147 (36), 120 (77), 95 (82), 91 (42).

4-methyl-N-((5-phenylfuran-2-yl)methyl)-N-(prop-2-yn-1-yl)benzenesulfonamide



Synthesised according to the general procedure. White solid, 64% yield (3-steps), mp 89–91 °C (Et₂O). **R_f** 0.38 (9/1 PE/EtOAc). **¹H NMR** (600 MHz, CDCl₃) δ (ppm): 7.76–7.74 (m, 2H), 7.56–7.54 (m, 2H), 7.37–7.34 (m, 2H), 7.28–7.24 (m, 3H), 6.55 (d, 1H, *J* = 3.3 Hz), 6.37 (d, 1H, *J* = 3.3 Hz), 4.52 (s, 2H), 4.09 (d, 2H, *J* = 2.5 Hz), 2.38 (s, 3H), 2.11 (t, 1H, *J* = 2.5 Hz). **¹³C NMR** (150 MHz, CDCl₃) δ (ppm): 154.5 (Cq), 148.2 (Cq), 143.8 (Cq), 136.2 (Cq), 130.5 (Cq), 129.7 (CH), 128.7 (CH), 127.8 (CH), 127.7 (CH), 123.9 (CH), 112.3 (CH), 105.7 (CH), 76.7 (Cq), 74.1 (CH), 43.1 (CH₂), 36.5 (CH₂), 21.6 (CH₃).

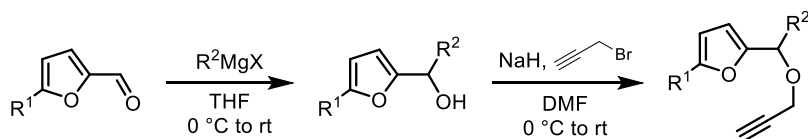
General procedure A for the synthesis of terminal alkynes with O linker^[10]



To a 1.0 M solution of furfuraldehyde (1.0 eq, 10 mmol) in MeOH, NaBH₄ (1.0 eq) was added portionwise at 0 °C. The mixture was allowed to reach room temperature and stirred overnight. Then, MeOH was evaporated to half of the initial volume under reduced pressure. Water was added and the mixture was extracted three times with DCM; the combined organic layers were dried over Na₂SO₄, filtered and the volatiles were evaporated under reduced pressure to obtain the crude furfuryl alcohol, which was used for the next step without further purification.

To a 1.0 M solution of the crude furfuryl alcohol in anhydrous DMF, at 0 °C under N₂ atmosphere, NaH (1.5 eq) was added portionwise. The mixture was stirred at 0 °C for 15 min, then propargyl bromide (1.5 eq) was added and the mixture was allowed to reach room temperature and stirred overnight. Then, the mixture was cooled down to 0 °C, water was added and the mixture was extracted three times with DCM; the combined organic layers were washed three times with water, dried over anhydrous Na₂SO₄, filtered and the volatiles were removed under reduced pressure. The crude product was purified by flash column chromatography to obtain the pure *O*-propargyl product.

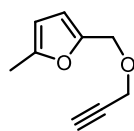
General procedure B for the synthesis of terminal alkynes with O linker^[11]



To a 0.5 M solution of furfuraldehyde (1.0 eq, 10 mmol) in anhydrous THF, at 0 °C under N₂ atmosphere, a solution of Grignard reagent (1.2 eq) was added. The mixture was allowed to reach room temperature and stirred for 1–2 h (GC-MS monitoring). Then, a saturated NH₄Cl solution was added and the mixture was extracted three times with DCM; the combined organic layers were dried over Na₂SO₄, filtered and the volatiles were evaporated under reduced pressure to obtain the crude furyl alcohol, which was used for the next step without further purification.

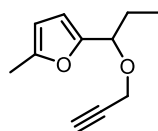
To a 1.0 M solution of the crude furanyl alcohol in anhydrous DMF, at 0 °C under N₂ atmosphere, NaH (1.5 eq) was added portionwise. The mixture was stirred at 0 °C for 15 min, then propargyl bromide (1.5 eq) was added and the mixture was allowed to reach room temperature and stirred overnight. Then, the mixture was cooled down to 0 °C, water was added and the mixture was extracted three times with DCM; the combined organic layers were washed three times with water, dried over anhydrous Na₂SO₄, filtered and the volatiles were removed under reduced pressure. The crude product was purified by flash column chromatography to obtain the pure *O*-propargyl product.

2-methyl-5-((prop-2-yn-1-yloxy)methyl)furan^[10]



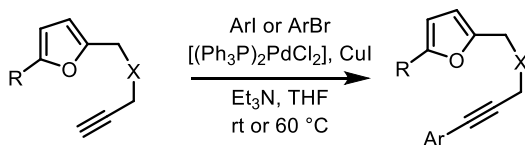
Synthesised according to the general procedure A. Pale yellow oil, 67% yield (2-steps). *R_f* 0.18 (99/1 PE/EtOAc). ¹H NMR (600 MHz, CDCl₃) δ (ppm): 6.25 (dd, 1H, *J* = 3.0, 0.6 Hz), 5.92 (dq, 1H, *J* = 3.1 Hz, 1.1 Hz), 4.50 (s, 2H), 4.16 (d, 2H, *J* = 2.4 Hz), 2.45 (d, 3H, *J* = 2.4 Hz), 2.29 (d, 3H, *J* = 1.0 Hz). **GC-MS** *m/z* (%): 150 [M]⁺ (30), 110 (21), 95 (100).

2-methyl-5-(1-(prop-2-yn-1-yloxy)propyl)furan^[11]



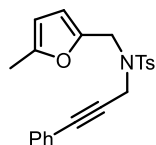
Synthesised according to the general procedure B with EtMgBr. Yellow oil, 46% yield (2-steps). *R_f* 0.29 (98/2 PE/EtOAc). ¹H NMR (600 MHz, CDCl₃) δ (ppm): 6.17 (d, 1H, *J* = 3.0 Hz), 5.89 (dq, 1H, *J* = 3.1, 1.0 Hz), 4.34 (t, 1H, *J* = 7.1 Hz), 4.13 (dd, 1H, *J* = 15.8, 2.4 Hz), 3.95 (dd, 1H, *J* = 15.8, 2.4 Hz), 2.38 (t, 1H, *J* = 2.4 Hz), 2.27 (d, 3H, *J* = 1.0 Hz), 1.95–1.81 (m, 2H), 0.90 (t, 3H, *J* = 7.5 Hz). **GC-MS** *m/z* (%): 178 [M]⁺ (5), 149 (100), 123 (38), 120 (24), 109 (36), 91 (22), 77 (33), 43 (41).

General procedure for the Sonogashira coupling^[12]



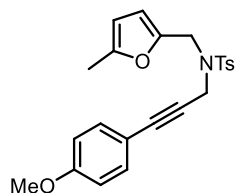
In a vial under N₂ atmosphere, a 2.0 M solution of the terminal alkyne (1.0 eq, 1.0–2.0 mmol) in anhydrous THF was prepared. The aryl iodide or aryl bromide (1.5 eq) and Et₃N (2.0 eq) were added and the mixture was degassed for 10–15 min. Then, [(Ph₃P)₂PdCl₂] (0.02 eq) and CuI (0.04 eq) were added and the mixture was stirred at room temperature (for ArI) or at 60 °C (for ArBr) overnight. After that time, a saturated NH₄Cl solution was added and the mixture was extracted three times with EtOAc; the combined organic layers were dried over Na₂SO₄, filtered and the volatiles were removed under reduced pressure. The crude product was purified by flash column chromatography to obtain the pure aryl alkyne.

4-methyl-N-((5-methylfuran-2-yl)methyl)-N-(3-phenylprop-2-yn-1-yl)benzenesulfonamide, 6a



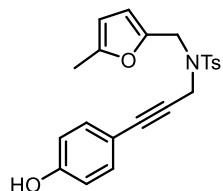
Synthesised according to the general procedure at rt with PhI. White solid, 68% yield, mp 81–83 °C (Et₂O). *R_f* 0.17 (95/5 PE/EtOAc). **¹H NMR** (600 MHz, CDCl₃) δ (ppm): 7.78 (d, 2H, *J* = 8.2 Hz), 7.31–7.23 (m, 5H), 7.09 (d, 2H, *J* = 8.1 Hz), 6.20 (d, 1H, *J* = 2.8 Hz), 5.88 (d, 1H, *J* = 2.0 Hz), 4.42 (s, 2H), 4.24 (s, 2H), 2.34 (s, 3H), 2.22 (s, 3H). **¹³C NMR** (150 MHz, CDCl₃) δ (ppm): 153.0 (Cq), 146.7 (Cq), 143.6 (Cq), 136.2 (Cq), 131.7 (CH), 129.6 (CH), 128.5 (CH), 128.3 (CH), 128.0 (CH), 122.4 (Cq), 111.2 (CH), 106.4 (CH), 85.9 (Cq), 81.9 (Cq), 43.4 (CH₂), 37.1 (CH₂), 21.6 (CH₃), 13.7 (CH₃). **HRMS** (ESI) *m/z*. calcd. for C₂₂H₂₁NO₃SNa⁺ 402.1134, found 402.1127.

N-(3-(4-methoxyphenyl)prop-2-yn-1-yl)-4-methyl-N-((5-methylfuran-2-yl)methyl)benzenesulfonamide, 6b



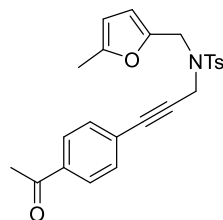
Synthesised according to the general procedure at rt with *p*-iodoanisole. White solid, 69% yield, mp 92–94 °C (Et₂O). *R_f* 0.28 (9/1 PE/EtOAc). **¹H NMR** (600 MHz, CDCl₃) δ (ppm): 7.79–7.77 (m, 2H), 7.27–7.25 (m, 2H), 7.06–7.03 (m, 2H), 6.79–6.76 (m, 2H), 6.19 (d, 1H, *J* = 3.0 Hz), 5.87 (dq, 1H, *J* = 3.0, 1.0 Hz), 4.41 (s, 2H), 4.22 (s, 2H), 3.80 (s, 3H), 2.36 (s, 3H), 2.22 (d, 3H, *J* = 0.9 Hz). **¹³C NMR** (150 MHz, CDCl₃) δ (ppm): 159.8 (Cq), 153.0 (Cq), 146.8 (Cq), 143.5 (Cq), 136.3 (Cq), 133.2 (CH), 129.6 (CH), 128.0 (CH), 114.5 (Cq), 113.9 (CH), 111.1 (CH), 106.4 (CH), 85.8 (Cq), 80.4 (Cq), 55.4 (CH₃), 43.3 (CH₂), 37.2 (CH₂), 21.6 (CH₃), 13.7 (CH₃). **HRMS** (ESI) *m/z*. calcd. for C₂₃H₂₃NO₄SNa⁺ 432.1240, found 432.1230.

N-(3-(4-hydroxyphenyl)prop-2-yn-1-yl)-4-methyl-*N*-((5-methylfuran-2-yl)methyl)benzenesulfonamide, **7c**



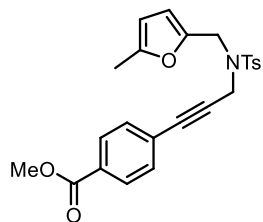
Synthesised according to the general procedure at rt with *p*-iodophenol. White solid, 60% yield, mp 100–103 °C (DCM/pentane). *R_f* 0.27 (8/2 PE/EtOAc). **¹H NMR** (600 MHz, CDCl₃) δ (ppm): 7.79 (m, 2H), 7.27–7.24 (m, 2H), 7.01–6.98 (m, 2H), 6.73–6.70 (m, 2H), 6.19 (d, 1H, *J* = 3.1 Hz), 5.87 (dd, 1H, *J* = 3.0, 1.0 Hz), 5.03 (br s, 1H), 4.41 (s, 2H), 4.21 (s, 3H), 2.36 (s, 3H), 2.22 (s, 3H). **¹³C NMR** (150 MHz, CDCl₃) δ (ppm): 156.1 (Cq), 153.0 (Cq), 146.7 (Cq), 143.7 (Cq), 136.1 (Cq), 133.3 (CH), 129.6 (CH), 128.0 (CH), 115.4 (CH), 114.5 (Cq), 111.2 (CH), 106.4 (CH), 85.9 (Cq), 80.2 (Cq), 43.2 (CH₂), 37.2 (CH₂), 21.6 (CH₃), 13.7 (CH₃).

N-(3-(4-acetylphenyl)prop-2-yn-1-yl)-4-methyl-*N*-((5-methylfuran-2-yl)methyl)benzenesulfonamide, **6d**



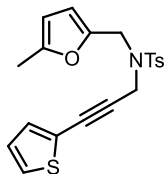
Synthesised according to the general procedure at rt with 4'-iodoacetophenone. White solid, 73% yield, mp 91–93 °C (Et₂O). *R_f* 0.32 (8/2 PE/EtOAc). **¹H NMR** (600 MHz, CDCl₃) δ (ppm): 7.85–7.83 (m, 2H), 7.79–7.77 (m, 2H), 7.28–7.25 (m, 2H), 7.19–7.16 (m, 2H), 6.18 (d, 1H, *J* = 3.0 Hz), 5.88 (dq, 1H, *J* = 3.0, 1.0 Hz), 4.42 (s, 2H), 4.26 (s, 2H), 2.59 (s, 3H), 2.35 (s, 3H), 2.21 (s, 3H). **¹³C NMR** (150 MHz, CDCl₃) δ (ppm): 197.3 (Cq), 153.1 (Cq), 146.6 (Cq), 143.7 (Cq), 136.5 (Cq), 136.2 (Cq), 131.8 (CH), 129.7 (CH), 128.2 (CH), 128.0 (CH), 127.2 (Cq), 111.2 (CH), 106.5 (CH), 85.6 (Cq), 85.0 (Cq), 43.6 (CH₂), 37.1 (CH₂), 26.7 (CH₃), 21.6 (CH₃), 13.7 (CH₃).

methyl 4-(3-((4-methyl-*N*-((5-methylfuran-2-yl)methyl)phenyl)sulfonamido)prop-1-yn-1-yl)benzoate, **6e**



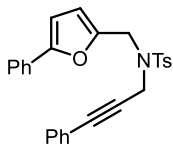
Synthesised according to the general procedure at rt with methyl *p*-iodobenzoate. White solid, 85% yield, mp 133–135 °C (Et₂O). *R_f* 0.26 (9/1 PE/EtOAc). **¹H NMR** (600 MHz, CDCl₃) δ (ppm): 7.93–7.90 (m, 2H), 7.79–7.76 (m, 2H), 7.26–7.24 (m, 2H), 7.15–7.13 (m, 2H), 6.19 (d, 1H, *J* = 3.1 Hz), 5.89–5.87 (dq, 1H, *J* = 3.1, 1.2 Hz), 4.42 (s, 2H), 4.25 (s, 2H), 3.92 (d, 3H, *J* = 0.7 Hz), 2.34 (s, 3H), 2.21 (s, 3H). **¹³C NMR** (150 MHz, CDCl₃) δ (ppm): 166.5 (Cq), 153.1 (Cq), 146.6 (Cq), 143.7 (Cq), 136.1 (Cq), 131.6 (CH), 129.8 (Cq), 129.7 (CH), 129.4 (CH), 128.0 (CH), 127.0 (Cq), 111.2 (CH), 106.5 (CH), 85.1 (Cq), 85.1 (Cq), 52.4 (CH₃), 43.6 (CH₂), 37.1 (CH₂), 21.6 (CH₃), 13.7 (CH₃). **HRMS** (ESI) *m/z*. calcd. for C₂₄H₂₃NO₅SN⁺ 460.1189, found 460.1180.

4-methyl-N-((5-methylfuran-2-yl)methyl)-N-(3-(thiophen-2-yl)prop-2-yn-1-yl)benzenesulfonamide, **6f**



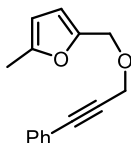
Synthesised according to the general procedure at 60 °C with 2-bromothiophene. White solid, 43% yield, mp 87–89 °C (Et₂O). *R_f* 0.34 (9/1 PE/EtOAc). **¹H NMR** (600 MHz, CDCl₃) δ (ppm): 7.79–7.76 (m, 2H), 7.30–7.27 (m, 2H), 7.21 (dd, 1H, *J* = 5.1, 1.2 Hz), 6.25 (dd, 1H, *J* = 3.6, 1.2 Hz), 6.92 (dd, 1H, *J* = 5.2, 3.6 Hz), 6.19 (d, 1H, *J* = 3.0 Hz), 5.88 (dq, 1H, *J* = 3.0, 1.0 Hz), 4.39 (s, 2H), 4.25 (s, 2H), 2.38 (s, 3H), 2.22 (d, 3H, *J* = 1.1 Hz). **¹³C NMR** (150 MHz, CDCl₃) δ (ppm): 153.1 (Cq), 146.6 (Cq), 143.7 (Cq), 136.0 (Cq), 132.4 (CH), 129.7 (CH), 127.9 (CH), 127.4 (CH), 126.9 (CH), 122.3 (Cq), 111.2 (CH), 106.5 (CH), 85.9 (Cq), 79.1 (Cq), 43.5 (CH₂), 37.3 (CH₂), 21.7 (CH₃), 13.7 (CH₃).

4-methyl-N-((5-phenylfuran-2-yl)methyl)-N-(3-phenylprop-2-yn-1-yl)benzenesulfonamide, **7g**



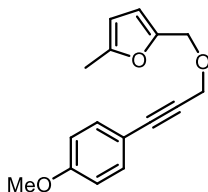
Synthesised according to the general procedure at rt with PhI. White solid, 81% yield, 110–111 °C (CHCl₃). *R_f* 0.41 (9/1 PE/EtOAc). **¹H NMR** (600 MHz, CDCl₃) δ (ppm): 7.80 (d, 2H, *J* = 8.3 Hz), 7.60–7.58 (m, 2H), 7.35 (t, 2H, *J* = 7.7 Hz), 7.31–7.29 (m, 1H), 7.26–7.22 (m, 5H), 7.12 (dd, 2H, *J* = 8.3, 1.2 Hz), 6.56 (d, 1H, *J* = 3.3 Hz), 6.41 (d, 1H, *J* = 3.3 Hz), 4.56 (s, 2H), 4.31 (s, 2H), 2.32 (s, 3H). **¹³C NMR** (150 MHz, CDCl₃) δ (ppm): 154.5 (Cq), 148.3 (Cq), 143.7 (Cq), 136.1 (Cq), 131.7 (CH), 130.6 (Cq), 129.7 (CH), 128.7 (Cq), 128.6 (CH), 128.3 (CH), 127.9 (CH), 127.7 (CH), 123.9 (CH), 122.3 (Cq), 112.3 (CH), 105.8 (CH), 86.0 (Cq), 81.9 (Cq), 43.5 (CH₂), 37.5 (CH₂), 21.5 (CH₃).

2-methyl-5-(((3-phenylprop-2-yn-1-yl)oxy)methyl)furan, **6h**



Synthesised according to the general procedure at rt with PhI. Colourless oil, 74% yield. *R_f* 0.21 (99/1 PE/EtOAc). **¹H NMR** (600 MHz, CDCl₃) δ (ppm): 7.48–7.44 (m, 2H), 7.34–7.30 (m, 3H), 6.28 (d, 1H, *J* = 3.0 Hz), 5.94 (dq, 1H, *J* = 3.0, 1.0 Hz), 4.56 (s, 2H), 4.39 (s, 2H), 2.30 (d, 3H, *J* = 0.8 Hz). **¹³C NMR** (150 MHz, CDCl₃) δ (ppm): 153.1 (Cq), 149.2 (Cq), 131.9 (CH), 128.6 (CH), 128.4 (CH), 122.8 (Cq), 111.2 (CH), 106.4 (CH), 86.6 (Cq), 85.0 (Cq), 63.5 (CH₂), 57.6 (CH₂), 13.7 (CH₃).

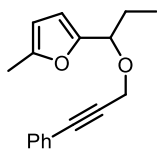
2-(((3-(4-methoxyphenyl)prop-2-yn-1-yl)oxy)methyl)-5-methylfuran, **7i**



Synthesised according to the general procedure at rt with *p*-iodoanisole. Colourless oil, 66% yield. *R_f* 0.28 (96/4 PE/EtOAc). **¹H NMR** (600 MHz, CDCl₃) δ (ppm): 7.41–7.38 (m, 2H), 6.86–6.83 (m, 2H), 6.27 (d, 1H, *J* = 3.0 Hz), 5.93 (dd, 1H, *J* = 3.1, 1.0 Hz), 4.55 (s, 2H), 4.38 (s, 2H), 3.81 (s, 3H), 2.29 (s, 3H). **¹³C NMR** (150 MHz, CDCl₃) δ (ppm): 159.8

(Cq), 153.1 (Cq), 149.3 (Cq), 133.4 (CH), 114.9 (Cq), 114.0 (CH), 111.2 (CH), 106.4 (CH), 86.6 (Cq), 83.5 (Cq), 63.4 (CH₂), 57.7 (CH₂), 55.4 (CH₃), 13.8 (CH₃).

2-methyl-5-(1-((3-phenylprop-2-yn-1-yl)oxy)propyl)furan, 7j



Synthesised according to the general procedure at rt with PhI. Colourless oil, 76% yield. *R_f* 0.34 (99/1 PE/EtOAc). **¹H NMR** (600 MHz, CDCl₃) δ (ppm): 7.45–7.42 (m, 2H), 7.32–7.29 (m, 3H), 6.22 (d, 1H, *J* = 3.0 Hz), 5.93–5.91 (m, 1H), 4.42 (t, 1H, *J* = 7.1 Hz), 4.36 (d, 1H, *J* = 15.8 Hz), 4.21 (d, 1H, *J* = 15.8 Hz), 2.28 (d, 3H, *J* = 0.9 Hz), 2.00–1.85 (m, 2H), 0.93 (t, 3H, *J* = 7.5 Hz). **¹³C NMR** (150 MHz, CDCl₃) δ (ppm): 152.3 (Cq), 151.6 (Cq), 131.8 (CH), 128.4 (CH), 128.3 (CH), 122.9 (Cq), 109.9 (CH), 106.0 (CH), 85.9 (Cq), 85.6 (Cq), 75.3 (CH), 56.3 (CH₂), 27.1 (CH₂), 13.7 (CH₃), 10.3 (CH₃).

References

- [1] a) M. E. Muratore, A. M. Echavarren, *Gold-catalyzed hydroarylation of alkynes* in *PATAI'S Chemistry of Functional Groups* (Ed.: Wiley), **2009**, pp. 1-96; b) M. S. Kirillova, F. M. Miloserdov, A. M. Echavarren, *Hydroarylation of Alkynes using Cu, Ag, and Au Catalysts* in *Catalytic Hydroarylation of Carbon-Carbon Multiple Bonds* (Ed.: Wiley), **2017**, pp. 217-303; c) N. Ahlsten, X. C. Cambeiro, G. J. Perry, I. Larrosa, *C-H Functionalisation of Heteroaromatic Compounds via Gold Catalysis* in *Au-Catalyzed Synthesis and Functionalization of Heterocycles*, Springer, **2016**, pp. 175-226.
- [2] D. Lebœuf, M. Gaydou, Y. Wang, A. M. Echavarren, *Org. Chem. Front.* **2014**, *1*, 759-764.
- [3] J. M. Yang, X. Y. Tang, M. Shi, *Chem. Eur. J.* **2015**, *21*, 4534-4540.
- [4] E. Brambilla, V. Pirovano, M. Giannangeli, G. Abbiati, A. Caselli, E. Rossi, *Org. Chem. Front.* **2019**, *6*, 3078-3084.
- [5] a) B. Lu, C. Li, L. Zhang, *J. Am. Chem. Soc.* **2010**, *132*, 14070-14072; b) S. Nejrotti, G. Prina Cerai, A. Oppedisano, A. Maranzana, E. G. Occhiato, D. Scarpì, A. Deagostino, C. Prandi, *Eur. J. Org. Chem.* **2017**, *2017*, 6228-6238.
- [6] K. Ji, Z. Zheng, Z. Wang, L. Zhang, *Angew. Chem. Int. Ed.* **2015**, *54*, 1245-1249.
- [7] J. C. Bussolari, D. C. Rehorn, *Org. Lett.* **1999**, *1*, 965-967.
- [8] B. Martín-Matute, C. Nevado, D. J. Cárdenas, A. M. Echavarren, *J. Am. Chem. Soc.* **2003**, *125*, 5757-5766.
- [9] S. Carrettin, M. C. Blanco, A. Corma, A. S. K. Hashmi, *Adv. Synth. Catal.* **2006**, *348*, 1283-1288.
- [10] A. S. K. Hashmi, T. Hengst, C. Lothschütz, F. Rominger, *Adv. Synth. Catal.* **2010**, *352*, 1315-1337.
- [11] A. S. K. Hashmi, T. Häffner, W. Yang, S. Pankajakshan, S. Schäfer, L. Schultes, F. Rominger, W. Frey, *Chem. Eur. J.* **2012**, *18*, 10480-10486.
- [12] J. Jouha, F. Buttard, M. Lorion, C. Berthonneau, M. Khouili, M.-A. Hiebel, G. Guillaumet, J.-F. o. Brière, F. Suzenet, *Org. Lett.* **2017**, *19*, 4770-4773.

Chapter 4: Bifunctional ligands for the silver-free activation of gold(I) chloride complexes

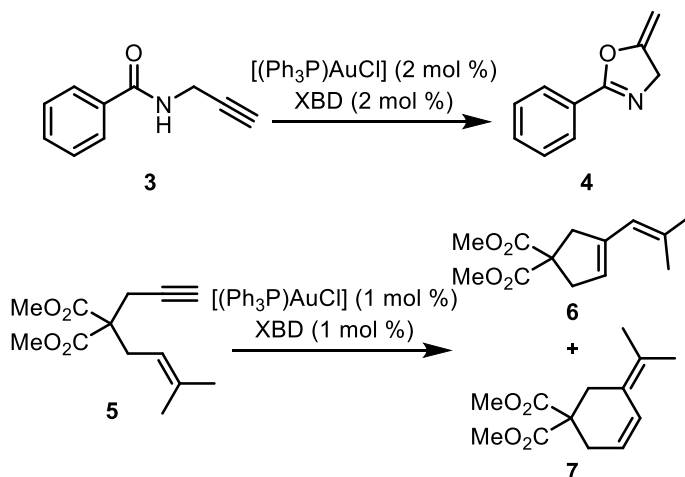
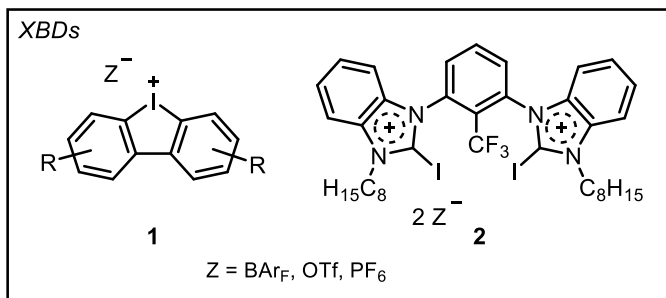
The work presented in this chapter was performed during a visiting period of three months in the group of prof. Antonio Echavarren at the Institute of Chemical Research of Catalonia (ICIQ) in Tarragona, Spain. The results are not published yet.

4.1 Silver-free activation of Au(I) complexes

As discussed in Section 1.1.2, the presence of a silver co-catalyst in gold(I) catalysis, employed as a chloride scavenger to activate the gold(I) chloride complex [LAuCl] by anion metathesis, is often non-innocent and can interfere beyond the mere role of activator. Nevertheless, the addition of AgX still remains the most popular method adopted in the development of new Au(I)-catalysed reactions. It should be noted that overcoming the use of silver(I) salts, which are often hygroscopic and light-sensitive, would also represent an improvement in terms of atom economy and costs of the catalytic system.^[1]

Gandon reported that Cu(I) and Cu(II) salts of the required low coordinating anions efficiently activated phosphine, phosphite and NHC gold(I) chloride complexes for a number of Au(I)-catalysed reactions, including cycloisomerisation of 1,6-enynes, hydroarylation, Conia-ene reaction and hydrofunctionalisations. The use of Cu salts was meant to enable a gradual anion metathesis, which in the case of Ag(I) salts is rapidly driven by the precipitation of AgCl, thus slowing down the catalyst decomposition by maintaining a reservoir of the stable [LAuCl] species. The strategy allowed for superior performances, compared to the corresponding Ag(I) salts, with Au loadings as low as 0.1 mol %.^[2]

Advances in the activation of gold(I) chloride complexes without any metal salt additive have also been made. A recent study took advantage of halogen bonding between the chloride ligand and halogen bond donors (XBDs) such as iodonium derivatives **1** and bis(benzimidazolium) compound **2** (Scheme 4.1). Catalysis tests run on two benchmark reactions, *i.e.* the cyclisation of propargyl amide **3** into oxazoline **4** and the cycloisomerisation of 1,6-enyne **5**, showed that [(Ph₃P)AuCl] was successfully activated by an equimolar amount of **1** or **2**, while it did not display any catalytic activity in the absence of the XBD.^[3]



Scheme 4.1 Halogen bond donors **1** and **2** and their application in the Au(I)-catalysed cyclisation of propargyl amide **3** and 1,6-enyne **5**.

The possibility of activating [LAuCl] complexes by hydrogen bonding was first studied by Gung from a computational point of view. The investigation took into account the abstraction of the chloride anion by hydrogen bond donors (HBDs) such as urea, thiourea and substituted squaramides. The results showed that the abstraction becomes favourable only if the geometry of the HBD allows for a multi-dentate coordination of the chloride. However, the authors pointed out that they had not considered specific interactions of the solvent molecules with the substrate, which could play an important role, having employed a polarizable continuum model (PCM) to simulate the reaction medium.^[4]

Hydrogen bonding was later successfully exploited by Gabbaï with his bifunctional phosphine gold(I) complex **8** bearing a trifluoroacetamide group (Figure 4.1). Spectroscopic data and interatomic distances in the crystal structure accounted for the presence of a hydrogen bond interaction between the amide and the chloride, with the complex involved in a monomer-dimer equilibrium in solution. Complex **8** was again tested in the cyclisation of **3** and was found to be catalytically active without any additive, even if the yields were modest. Furthermore, **8** failed

in promoting two other Au(I)-catalysed reactions, *i.e.* the hydroamination of acetylene with *p*-toluidine and the cycloisomerisation of 1,6-enyne **5**.^[5]

On these premises, we envisaged that the introduction of a HBD moiety such as urea, thiourea or squaramide on triaryl or dialkyl aryl phosphines could make these phosphines effective bifunctional ligands for silver-free gold catalysis. In this design, the HBD would act as an intramolecular chloride scavenger, as represented in Figure 4.1. In particular, I worked on the synthesis and evaluation of the catalytic activity of Au(I) chloride complexes with triaryl phosphines bearing urea and thiourea functional groups.

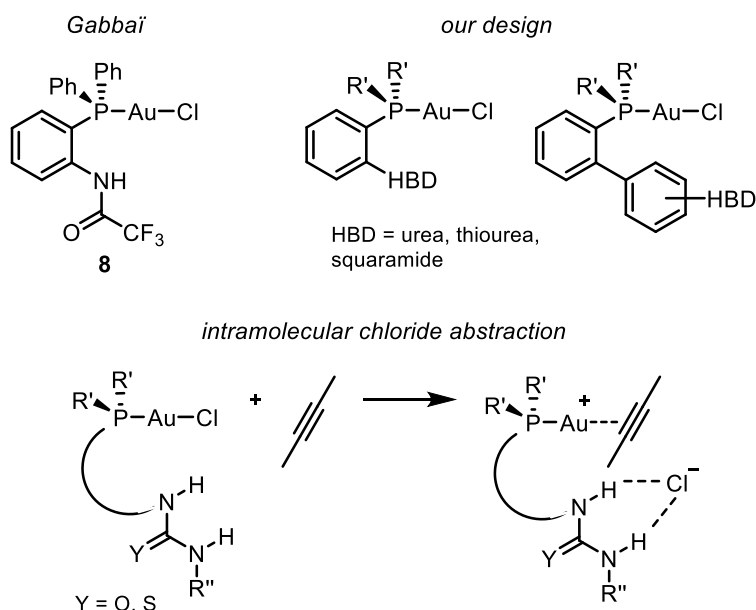


Figure 4.1 Bifunctional ligands with HBD moieties for silver-free activation of [LAuCl] complexes.

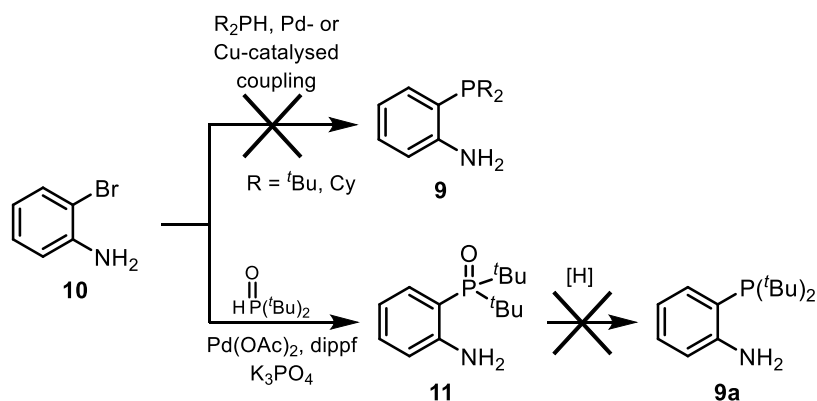
4.2 Synthesis of the complexes

4.2.1 Synthesis of the ligands

The first step of the project was the synthesis of dialkyl aryl phosphines with a urea or thiourea functional group in the *ortho* position of the aromatic ring (**9** in Scheme 4.2). The presence of bulky R groups, such as *tert*-butyl or cyclohexyl, was meant to reduce the conformational freedom of the gold complex and orient the Au–Cl moiety towards the hydrogen bond donor (on this regard, see Section 1.2.2). Unfortunately, the Pd-^[6] or Cu-catalysed^[7] cross-coupling of *o*-bromoaniline **10** with di-*tert*-butyl or dicyclohexylphosphine did not afford the expected product: several attempts with varying conditions mainly gave mixtures of compounds which we

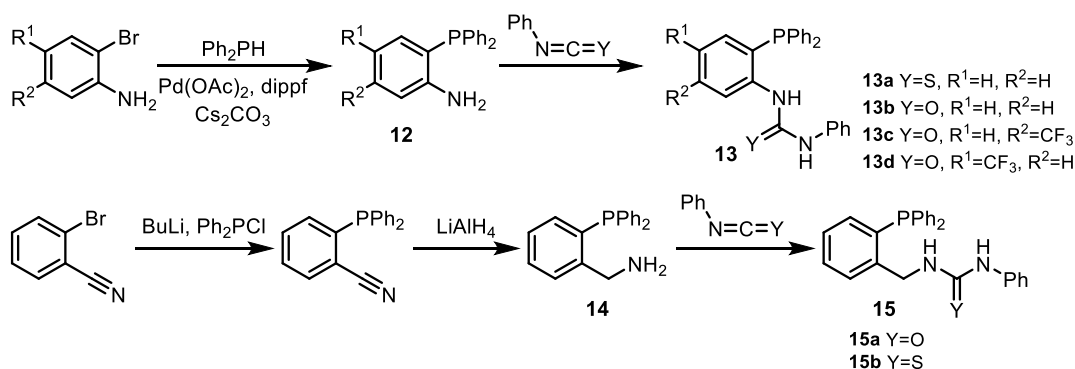
hypothesized to be phosphine oxide derivatives according to their ^{31}P NMR signals (Scheme 4.2). The synthesis of **9** was also unsuccessfully attempted through organolithium chemistry by metal-halogen exchange or directed *ortho*-metalation and subsequent trapping with di-*tert*-butylchlorophosphine.

Since the cross-coupling strategy mainly afforded phosphine oxides instead of phosphines, we decided to synthesise (2-aminophenyl)di-*tert*-butylphosphine oxide **11** by coupling of **10** with di-*tert*-butylphosphine oxide^[8] and subsequently reduce it to the corresponding phosphine (Scheme 4.2). However, attempts with several reducing agents were again met with failure.^[9]



Scheme 4.2 Attempted synthesis of *o*-aminophenyl dialkyl phosphines **9**.

Since phosphines **9** proved to be an elusive synthetic target, we turned our attention to more stable triphenylphosphines and employed diphenylphosphine as a coupling partner to obtain *o*-aminophenyl derivatives **12**,^[6] which were then reacted with phenyl isocyanate or isothiocyanate to eventually afford the desired bifunctional ligands **13** (Scheme 4.3). We also extended the library of urea and thiourea phosphines by reaction of the benzylamino derivatives **14** with phenyl isocyanate and isothiocyanate, obtaining ligands **15**.



Scheme 4.3 Synthesis of bifunctional urea and thiourea phosphine ligands.

4.2.2 Complexation

Aniline (thio)urea phosphines **13** and benzylamine (thio)urea phosphines **15** were reacted with the gold precursor [(DMS)AuCl] in DCM to obtain the corresponding gold(I) chloride complexes (Figure 4.2, see also Scheme 1.1). The NMR characterization of thiourea complexes [(**13a**)AuCl] and [(**15b**)AuCl] was troublesome due to the presence of broad peaks, probably because of a secondary labile coordination of the S atom to the metal center. On the other hand, aniline urea complexes [(**13b–d**)AuCl] could not be obtained in a pure form. For this reason, we decided to test those ligands by generating the Au(I) complex *in situ* during the catalysis.

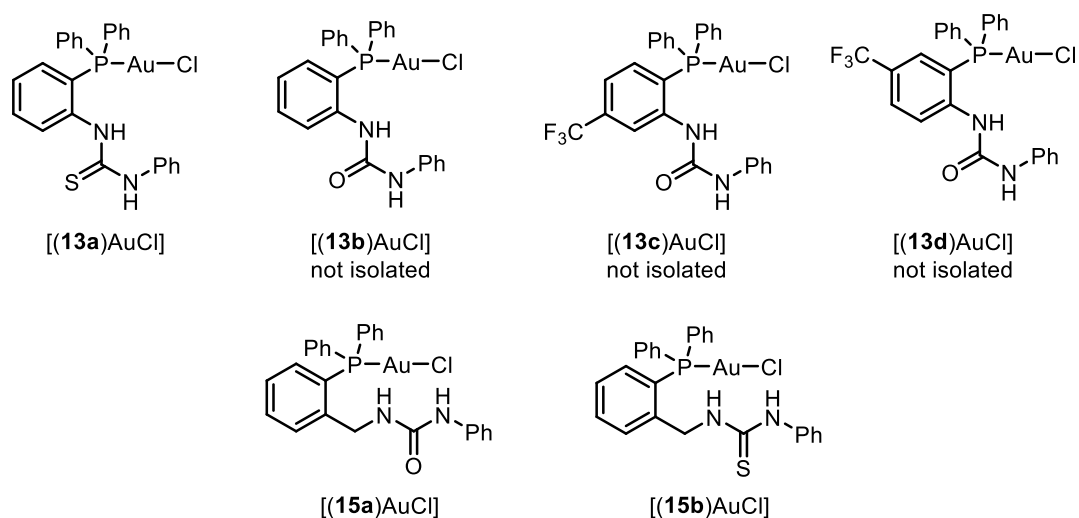


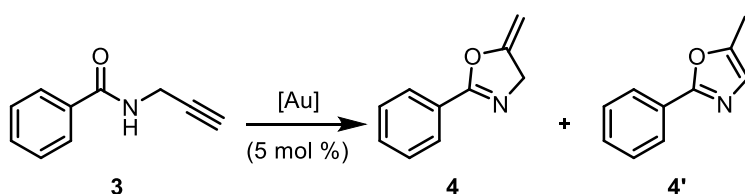
Figure 4.2 Gold(I) chloride complexes with bifunctional ligands **13** and **15**.

4.3 Preliminary results on catalytic activity

The first reaction chosen as a benchmark to test our new complexes was the cyclisation of propargyl benzamide **3**, affording oxazoline **4** or its aromatic isomer, oxazole **4'**, as possible products.^[3, 5, 10] The reactions were performed in three different solvents: chloroform, methanol and α,α,α -trifluorotoluene. Preliminary results are highlighted in Table 4.1. The general observation is that the complexes are active catalysts for the reaction, suggesting that the abstraction of the chloride ligand by intramolecular H bond may be effective. The best yields of product **4** were obtained with the benzylamine urea phosphine complex [(**15a**)AuCl] in MeOH (Table 4.1, entry 9) and with the CF₃-substituted aniline urea phosphine **13c** in CHCl₃ (entry 3) and MeOH (entry 4), by generating the gold

complex *in situ*. The higher activity of Au(I) complexes of **13c**, compared to aniline urea **13b** (entry 2), may be attributed to the increased HBD character of the electron-poor urea **13c**, featuring a CF₃ group in the *meta* position. By comparison, ligand **13d**, in which the CF₃ group is in *para* to the urea moiety, showed reduced yields of **4** (entries 6–7). Thiourea complexes [(**13a**)AuCl] and [(**15b**)AuCl] were less effective in promoting the reaction (entries 1, 10–11). We also performed the reaction in the presence of the gold precursor [(DMS)AuCl] alone, to verify a possible interference in the reactions in which the complexes were generated *in situ*. Indeed, we observed that [(DMS)AuCl] is not active in MeOH (entry 13) and displays very low activity in PhCF₃ (entry 14), while a 43% yield of oxazole **4'** was obtained in chloroform (entry 12).

Table 4.1 Catalysis tests for the oxazoline synthesis.^a



entry	catalyst	solvent	yield of 4 ^b	yield of 4' ^b
1	[(13a)AuCl]	CHCl ₃	12%	11%
2	13b + [(DMS)AuCl]	CHCl ₃	5%	23%
3	13c + [(DMS)AuCl]	CHCl ₃	57%	43%
4	13c + [(DMS)AuCl]	MeOH	46%	–
5	13c + [(DMS)AuCl]	PhCF ₃	15%	9%
6	13d + [(DMS)AuCl]	CHCl ₃	11%	51%
7	13d + [(DMS)AuCl]	MeOH	29%	–
8	[(15a)AuCl]	CHCl ₃	28%	7%
9	[(15a)AuCl]	MeOH	50%	–
10	[(15b)AuCl]	CHCl ₃	18%	15%
11	[(15b)AuCl]	PhCF ₃	13%	–
12	[(DMS)AuCl]	CHCl ₃	–	43%
13	[(DMS)AuCl]	MeOH	–	–
14	[(DMS)AuCl]	PhCF ₃	3%	5%
15	13c	CHCl ₃	–	–
16	13d	CHCl ₃	–	–

^a All reactions were performed at room temperature, under Ar atmosphere and in the dark, for a time of 24 h. ^b Determined by ¹H NMR at 300 or 400 MHz, using *n*-dodecane as internal standard.

We hypothesized that the activity of [(DMS)AuCl] could be linked to the formation of gold nanoparticles or AuCl in the reaction medium. The interference of [(DMS)AuCl] may then account for the formation of **4'** in entries 2, 3 and 6. However, further investigation involving the isolation of pure [(**13c**)AuCl] and [(**13d**)AuCl] is required to clarify this aspect. Control experiments, performed with the best ligands **13c** and **13d** in the absence of gold (entries 15–16) and confirmed that the metal is essential for the catalysis, since no conversion was observed.

4.4 Conclusion

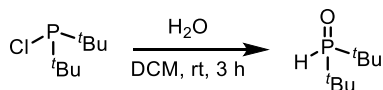
The synthesis of bifunctional (thio)urea phosphine ligands featuring the hydrogen bond donor moiety in the *ortho* position to the phosphine has been achieved. Preliminary results show that gold(I) complexes bearing this class of ligands are active in the Au(I)-catalysed cyclisation of propargyl benzamide to oxazoline without the addition of a co-catalyst. Future work should aim to better understand the role of the hydrogen bond donor in the catalysis, as the acidity of the urea moiety may also be involved in accelerating the protodeauration step. Furthermore, the isolation of pure Au complexes instead of their generation *in situ* would eliminate the interference of the gold precursor [(DMS)AuCl]. Finally, testing the bifunctional ligands in other gold(I)-catalysed transformations would give a more complete picture on the generality of this approach.

4.5 Experimental section

General information

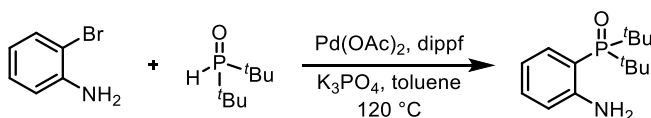
Flasks and all equipment used for the generation and reaction of air or moisture sensitive compounds were dried by electric heater gun under vacuum and filled with argon. Anhydrous solvents were dried by passing through an activated alumina column on a PureSolv™ solvent purification system. Flash column chromatography was performed over silica gel (40–63 μm, 230–400 mesh); *R_f* values refer to TLC carried out on silica gel plates. ¹H NMR and ¹³C NMR spectra were recorded on BrukerAvance Ultrashield NMR spectrometers (300 MHz, 400 MHz, 500 MHz), in CDCl₃ or in (CD₃)₂SO, using residual solvent peak as an internal reference (CHCl₃, ¹H: 7.26 ppm, ¹³C: 77.16 ppm; (CH₃)₂SO, ¹H: 2.54 ppm, ¹³C: 40.45 ppm). Multiplicity is reported as follows: s (singlet), d (doublet), t (triplet), q (quartet), quin (quintet), sext (sextet), m (multiplet), br (broad). GC-MS spectra were recorded at an ionizing voltage of 70 eV. Mass spectra were recorded on MicroTOF Focus or Maxis Impact spectrometers (both from Bruker Daltonics).

Synthesis of di-*tert*-butylphosphine oxide^[11]



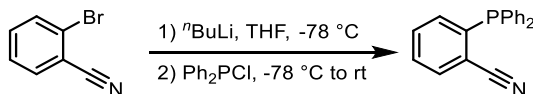
To a solution of di-*tert*-butylchlorophosphine (1.0 eq, 5.0 mmol) in anhydrous DCM (0.25 M), under Ar atmosphere, water (1.1 eq) was added. The mixture was stirred at room temperature until complete disappearance of the starting material (3 h, ³¹P NMR monitoring), then the volatiles were removed under reduced pressure to afford pure product as a white solid. Quantitative yield. **¹H NMR** (400 MHz, CDCl₃) δ (ppm): 6.19 (d, 1H, *J* = 446.9 Hz), 1.36 (d, 18H, *J* = 16.1 Hz). **³¹P{¹H} NMR** (161 MHz, CDCl₃) δ (ppm): 76.1.

Synthesis of (2-aminophenyl)di-*tert*-butylphosphine oxide, **11**^[6]



A vial under Ar atmosphere was charged with 2-bromoaniline (1.1 eq), Pd(OAc)₂ (0.05 eq), dippf (0.06 eq), K₃PO₄ (2.0 eq), di-*tert*-butylphosphine oxide (1.0 eq, 3.0 mmol) and toluene (0.5 M). Then, the vial was sealed and stirred at 120 °C. After one night, another 0.05 eq of Pd(OAc)₂ and 0.06 eq of dippf were added and the mixture was stirred at 120 °C until complete disappearance of the starting material (³¹P NMR monitoring). Then, the volatiles were removed under reduced pressure and the crude product was purified by flash column chromatography to afford pure product as an off-white solid. 38% yield, **mp** 180–181 °C (EtOAc). *R_f* 0.20 (1/1 DCM/EtOAc). **¹H NMR** (500 MHz, CDCl₃) δ (ppm): 7.22 (ddd, 1H, *J* = 10.6, 8.1, 1.6 Hz), 7.19–7.14 (m, 1H), 6.59–6.55 (m, 2H), 5.89 (br s, 2H), 1.32 (d, 18H, *J* = 13.5 Hz). **¹³C NMR** (125 MHz, CDCl₃) δ (ppm): 154.9 (Cq, d, *J* = 2.3 Hz), 132.2 (CH, d, *J* = 2.4 Hz), 131.8 (CH, d, *J* = 10.4 Hz), 117.5 (CH, d, *J* = 7.4 Hz), 114.9 (CH, d, *J* = 11.3 Hz), 108.7 (Cq, d, *J* = 81.6 Hz), 37.6 (CH, d, *J* = 59.2 Hz), 27.2 (CH₃). **³¹P{¹H} NMR** (202 MHz, CDCl₃) δ (ppm): 65.4.

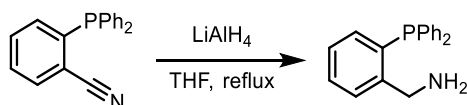
Synthesis of 2-(diphenylphosphino)benzonitrile^[12]



Into a Schlenk tube under Ar atmosphere, 2-bromobenzonitrile (1.0 eq, 5.0 mmol) was added and dissolved in anhydrous THF (0.25 M). The solution was cooled down to –78 °C and *n*-BuLi (1.1 eq, 2.5 M solution in hexane) was slowly added. The mixture was stirred at –78 °C for 1 h, then chlorodiphenylphosphine (1.0 eq) was slowly added and the mixture was stirred at –78 °C for 1 h. After that time, the mixture was allowed to reach room temperature and stirred until complete consumption of the starting material (1.5 h, GC-MS and TLC monitoring). Then, water (15 ml) and Et₂O (20 ml) were added and the mixture

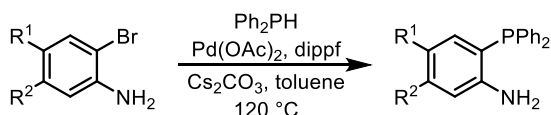
was extracted three times with 15 ml of Et₂O; the combined organic layers were dried over anhydrous Na₂SO₄, filtered and the volatiles were removed under reduced pressure. The crude product was purified by flash column chromatography to afford pure product as a yellow solid. 60% yield. *R_f* 0.53 (9/1 CyH/EtOAc). ¹H NMR (400 MHz, CDCl₃) δ (ppm): 7.71 (ddd, 1H, *J* = 7.4, 3.2, 1.5), 7.47 (td, 1H, *J* = 7.6, 1.6 Hz), 7.44–7.35 (m, 7H), 7.34–7.28 (m, 4H). ³¹P{¹H} NMR (161 MHz, CDCl₃) δ (ppm): –5.4. GC-MS *m/z*(%): 287 [M]⁺ (100), 286 (61), 208 (24), 183 (45).

Synthesis of (2-(diphenylphosphino)phenyl)methanamine, 14^[13]



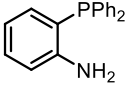
Into a two-neck flask, equipped with a condenser, under Ar atmosphere, LiAlH₄ (1.1 eq) was added. Then, anhydrous THF (12 ml) was added and the resulting mixture was stirred for 10 min at room temperature. A solution of 2-(diphenylphosphino)benzonitrile (1.0 eq, 3.0 mmol) in anhydrous THF (8 ml) was slowly added and the mixture was stirred at reflux for 4 h. After that time, the mixture was cooled down to 0 °C and the residual LiAlH₄ was quenched with ice. A 1 M solution of NaOH (30 ml) was added and the mixture was extracted three times with EtOAc. The combined organic layers were washed with 1 M NaOH (15 ml) and water (15 ml), dried over anhydrous Na₂SO₄, filtered and the volatiles were removed under vacuum. The crude product was purified by flash column chromatography to afford pure product as a yellow solid. 66% yield. *R_f* 0.15 (96/2/2 DCM/EtOAc/Et₃N). ¹H NMR (400 MHz, CDCl₃) δ (ppm): 7.46–7.42 (m, 1H), 7.38–7.31 (m, 6H), 7.30–7.24 (m, 5H), 7.16 (td, 1H, *J* = 7.4, 1.4 Hz), 6.88 (ddd, 1H, *J* = 7.8, 4.7, 1.4 Hz), 4.02 (d, 2H, *J* = 1.7 Hz). ³¹P{¹H} NMR (161 MHz, CDCl₃) δ (ppm): –12.8.

General procedure for coupling between aryl bromides and phosphines^[6]

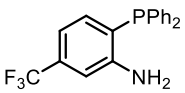


A vial under Ar atmosphere was charged with the aryl bromide (1.0 eq, 2.0–4.0 mmol), Pd(OAc)₂ (0.05 eq), dippf (0.06 eq) and Cs₂CO₃ (2.0 eq). Anhydrous toluene (0.5 M), previously degassed, was added and the mixture was stirred for 15 min at room temperature, then the phosphine (1.1 eq) was added and the mixture was stirred at 120 °C until complete consumption of the starting material (usually 20 h, GC-MS and ³¹P NMR monitoring). Then, the mixture was cooled down to room temperature and the volatiles were removed under reduced pressure. The crude product was purified by flash column chromatography to afford the pure triaryl phosphine.

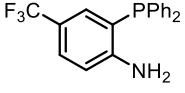
2-(diphenylphosphino)aniline, **12a**^[9b]

 Synthesised according to the general procedure. White solid, 62% yield. **R_f** 0.45 (9/1 CyH/EtOAc + 0.1% Et₃N). **¹H NMR** (400 MHz, CDCl₃) δ (ppm): 7.37–7.29 (m, 10H), 7.18 (ddd, 1H, *J* = 8.0, 7.2, 1.7 Hz), 6.79–6.74 (m, 1H), 6.72–6.66 (m, 2H), 4.14 (s, 2H). **³¹P{¹H} NMR** (161 MHz, CDCl₃) δ (ppm): –17.3. **GC-MS** *m/z* (%): 277 [M]⁺ (100), 276 (59), 198 (70), 183 (29).

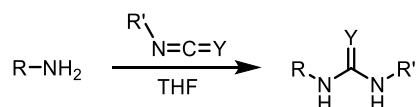
2-(diphenylphosphino)-5-(trifluoromethyl)aniline, **12c**

 Synthesised according to the general procedure. White solid, 64% yield, **mp** 126–128 °C (CyH). **R_f** 0.40 (9/1 CyH/EtOAc + 0.1% Et₃N). **¹H NMR** (500 MHz, CDCl₃) δ (ppm): 7.41–7.35 (m, 6H), 7.34–7.29 (m, 4H), 6.91–6.87 (m, 2H), 6.82 (dd, 1H, *J* = 7.7, 5.2 Hz), 4.28 (s, 2H). **¹³C NMR** (125 MHz, CDCl₃) δ (ppm): 149.7 (d, *J* = 19.9 Hz, Cq), 134.7 (d, *J* = 2.4 Hz, CH), 134.4 (d, *J* = 7.4 Hz, Cq), 133.9 (d, *J* = 19.5 Hz, CH), 132.4 (q, *J* = 32.1 Hz, Cq), 129.4 (CH), 129.0 (d, *J* = 7.3 Hz, CH), 124.2 (q, *J* = 272.7, Cq), 124.1 (d, *J* = 11.8 Hz, Cq), 115.0–114.9 (m, CH), 111.7 (quin, *J* = 3.8 Hz, CH). **³¹P{¹H} NMR** (202 MHz, CDCl₃) δ (ppm): –17.4 Hz. **¹⁹F NMR** (376 MHz, CDCl₃) δ (ppm): –63.2 (s). **HRMS** (APCI, positive mode) *m/z*: calcd. for [C₁₉H₁₆F₃NP]⁺ 346.0967, found 346.0969.

2-(diphenylphosphino)-4-(trifluoromethyl)aniline, **12d**

 Synthesised according to the general procedure. Colourless oil, 78% yield. **R_f** 0.44 (9/1 CyH/EtOAc + 0.1% Et₃N). **¹H NMR** (500 MHz, CDCl₃) δ (ppm): 7.40–7.34 (m, 7H), 7.34–7.29 (m, 4H), 7.01 (dd, 1H, *J* = 5.6, 2.2 Hz), 6.70 (dd, 1H, *J* = 8.4, 5.0 Hz), 4.42 (br s, 2H). **¹³C NMR** (125 MHz, CDCl₃) δ (ppm): 152.4 (d, *J* = 18.8 Hz, Cq), 134.4 (d, *J* = 7.5 Hz, Cq), 133.8 (d, *J* = 19.4 Hz, CH), 131.5 (quin, *J* = 4.0 Hz, CH), 129.4 (CH), 129.0 (d, *J* = 7.0 Hz, CH), 127.6 (q, *J* = 3.6 Hz, CH), 124.8 (q, *J* = 271.0 Hz, Cq), 120.5 (qd, *J* = 32.3, 2.3 Hz, Cq), 119.5 (d, *J* = 11.6 Hz, Cq), 114.8 (d, *J* = 2.3 Hz, CH). **³¹P{¹H} NMR** (202 MHz, CDCl₃) δ (ppm): –17.1 Hz. **¹⁹F NMR** (376 MHz, CDCl₃) δ (ppm): –61.4 (s). **HRMS** (APCI, positive mode) *m/z*: calcd. for [C₁₉H₁₆F₃NP]⁺ 346.0967, found 346.0966.

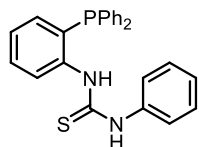
General procedure for the synthesis of ureas and thioureas



To a solution of the aniline or amine (1.0 eq, 0.5 mmol) in anhydrous THF (0.1 M), under Ar atmosphere, the isocyanate or isothiocyanate (1.1 eq) was added and the mixture was stirred at the appropriate temperature until complete consumption of the starting material (usually 16–24 h, TLC monitoring). Then, the volatiles were removed under reduced

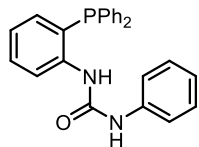
pressure and the crude product was purified by flash column chromatography to afford the pure urea or thiourea.

1-(2-(diphenylphosphino)phenyl)-3-phenylthiourea, **13a**



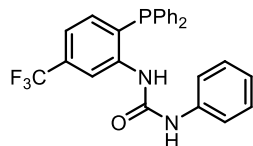
Synthesised according to the general procedure at room temperature for a reaction time of 18 h. White solid, 80% yield, **mp** 133–135 °C (CHCl₃). **R_f** 0.50 (DCM). **¹H NMR** (500 MHz, CDCl₃) δ (ppm): 7.78 (dd, 1H, *J* = 8.0, 4.3 Hz), 7.74 (br s, 1H), 7.69 (s, 1H), 7.39 (td, 1H, *J* = 7.7, 1.6 Hz), 7.36–7.29 (m, 6H), 7.28–7.20 (m, 7H), 7.17 (t, 1H, *J* = 7.9 Hz), 7.12–7.09 (m, 2H), 6.83 (ddd, 1H *J* = 7.7, 4.1, 1.5 Hz). **¹³C NMR** (125 MHz, CDCl₃) δ (ppm): 180.3 (Cq), 141.0 (d, *J* = 20.3 Hz, Cq), 136.6 (Cq), 135.2 (d, *J* = 9.3 Hz, Cq), 134.3 (d, *J* = 19.9 Hz, CH), 133.9 (CH), 130.0 (CH), 129.9 (CH), 129.6 (CH), 129.2 (d, *J* = 7.3 Hz, CH), 128.1 (d, *J* = 2.1 Hz, CH), 127.8 (CH), 127.6 (CH), 125.8 (CH). **³¹P{¹H} NMR** (202 MHz, CDCl₃) δ (ppm): –13.8. **HRMS** (ESI, negative mode) calcd. for [C₂₅H₂₀N₂PS][–] 411.1090, found 411.1086.

1-(2-(diphenylphosphino)phenyl)-3-phenylurea, **13b**



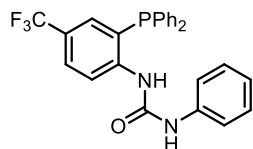
Synthesised according to the general procedure at room temperature for a reaction time of 18 h. White solid, 77% yield, **mp** 164–166 °C (CHCl₃). **R_f** 0.25 (DCM). **¹H NMR** (500 MHz, CDCl₃) δ (ppm): 7.96 (dd, 1H, *J* = 8.3, 3.0 Hz), 7.39–7.29 (m, 8H), 7.26–7.21 (m, 6H), 7.18–7.15 (m, 2H), 7.10–7.03 (m, 2H), 6.88 (dd, 1H, *J* = 7.8, 3.1 Hz), 6.74 (s, 1H). **¹³C NMR** (125 MHz, CDCl₃) δ (ppm): 153.4 (Cq), 141.5 (d, *J* = 18.3 Hz, Cq), 137.8 (Cq), 134.9 (Cq), 134.0 (CH), 133.9 (d, *J* = 19.0 Hz, CH), 130.4 (CH), 129.3 (d, *J* = 2.8 Hz, CH), 128.9 (CH), 128.9 (CH), 124.8 (CH), 124.5 (CH), 123.3 (CH), 121.9 (CH), 120.5 (Cq). **³¹P{¹H} NMR** (202 MHz, CDCl₃) δ (ppm): –16.9 Hz. **HRMS** (ESI, negative mode) *m/z*: calcd. for [C₂₅H₂₀N₂OP][–] 395.1319, found 395.1317.

1-(2-(diphenylphosphino)-5-(trifluoromethyl)phenyl)-3-phenylurea, **13c**



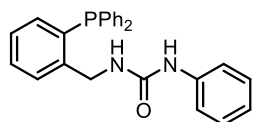
Synthesised according to the general procedure at 60 °C for a reaction time of 24 h. White solid, 59% yield, **mp** 98–100 °C (CHCl₃). **R_f** 0.24 (9/1 CyH/EtOAc). **¹H NMR** (500 MHz, CDCl₃) δ (ppm): 8.45 (dd, 1H, *J* = 4.3, 1.7 Hz), 7.42–7.34 (m, 7H), 7.31–7.27 (m, 2H), 7.24–7.13 (m, 8H), 6.94 (dd, 1H, *J* = 8.0, 4.4 Hz), 6.40 (br s, 1H). **¹³C NMR** (125 MHz, CDCl₃) δ (ppm): 152.9 (Cq), 142.1 (d, *J* = 18.3 Hz, Cq), 137.2 (Cq), 134.3 (d, *J* = 2.1 Hz, CH), 133.8 (d, *J* = 19.4 Hz, CH), 133.7 (d, *J* = 6.5 Hz, Cq), 132.3 (q, *J* = 32.5 Hz, Cq), 130.9 (d, *J* = 12.7 Hz, Cq), 129.8 (CH), 129.6 (CH), 129.1 (d, *J* = 7.4 Hz, CH), 124.0 (q, *J* = 272.8 Hz, Cq), 125.2 (CH), 122.6 (CH), 120.4–120.3 (m, CH), 128.7 (CH). **³¹P{¹H} NMR** (202 MHz, CDCl₃) δ (ppm): –17.4. **¹⁹F NMR** (376 MHz, CDCl₃) δ (ppm): –63.0 (s). **HRMS** (ESI, positive mode) *m/z*: calcd. for [C₂₆H₂₁F₃N₂OP]⁺ 465.1338, found 465.1338.

1-(2-(diphenylphosphino)-4-(trifluoromethyl)phenyl)-3-phenylurea, 13d



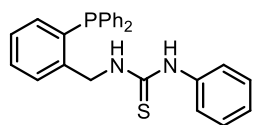
Synthesised according to the general procedure at 65 °C for a reaction time of 20 h. White solid, 60% yield, **mp** 203–205 °C (CHCl₃). **R_f** 0.18 (9/1 CyH/EtOAc). **¹H NMR** (500 MHz, CDCl₃) δ (ppm): 8.33 (dd, 1H, *J* = 8.7, 4.3 Hz), 7.61 (d, 1H, *J* = 8.4 Hz) superimposed to 7.57 (d, 1H, *J* = 8.1 Hz), 7.44–7.33 (m, 6H), 7.30 (t, 2H, *J* = 7.7 Hz), 7.23–7.14 (m, 7H), 7.13–7.09 (m, 1H), 6.37 (br s, 1H). **¹³C NMR** (125 MHz, CDCl₃) δ (ppm): 152.7 (Cq), 144.9 (d, *J* = 17.0 Hz, Cq), 137.0 (Cq), 133.7 (d, *J* = 19.4 Hz, CH), 133.5 (d, *J* = 6.2 Hz, Cq), 130.9–130.8 (m, CH), 129.8 (CH), 129.7 (CH), 129.2 (d, *J* = 7.3 Hz, CH), 127.5 (q, *J* = 3.2 Hz, CH), 126.3 (d, *J* = 13.2 Hz, Cq), 125.7 (m, Cq), 125.4 (CH), 124.1 (q, *J* = 272.1 Hz, Cq), 122.7 (CH), 121.0 (d, *J* = 1.9 Hz, CH). **³¹P{¹H} NMR** (202 MHz, CDCl₃) δ (ppm): –17.8. **¹⁹F NMR** (376 MHz, CDCl₃) δ (ppm): –62.3 (s). **HRMS** (ESI, positive mode) *m/z*: calcd. for [C₂₆H₂₁F₃N₂OP]⁺ 465.1338, found 465.1343.

1-(2-(diphenylphosphino)benzyl)-3-phenylurea, 15a



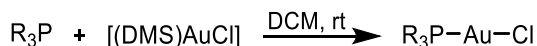
Synthesised according to the general procedure at room temperature for a reaction time of 18 h. White solid, 94% yield, **mp** 179–181 °C (CHCl₃). **R_f** 0.15 (DCM). **¹H NMR** (500 MHz, CDCl₃) δ (ppm): 7.48 (ddd, 1H, *J* = 7.7, 4.5, 1.3 Hz), 7.37–7.29 (m, 7H), 7.26–7.20 (m, 6H), 7.20–7.13 (m, 3H), 6.18 (s, 1H), 5.14 (t, 1H, *J* = 6.0 Hz), 4.60 (dd, 2H, *J* = 6.0, 1.3 Hz). **¹³C NMR** (125 MHz, CDCl₃) δ (ppm): 155.4 (Cq), 134.2 (d, *J* = 24.1 Hz, Cq), 138.6 (Cq), 136.2 (d, *J* = 8.9 Hz, Cq), 135.5 (d, *J* = 13.8 Hz, Cq), 134.0 (d, *J* = 19.7 Hz, CH), 133.9 (CH), 129.6 (CH), 129.5 (CH), 129.3 (CH), 129.1 (CH), 126.9 (d, *J* = 7.0 Hz, CH), 128.0 (CH), 123.7 (CH), 120.8 (CH), 43.4 (d, *J* = 21.1 Hz, CH₂). **³¹P{¹H} NMR** (202 MHz, CDCl₃) δ (ppm): –12.6. **HRMS** (ESI, positive mode) *m/z*: calcd. for [C₂₆H₂₃N₂NaOP]⁺ 433.1440, found 433.1442.

1-(2-(diphenylphosphino)benzyl)-3-phenylthiourea, 15b



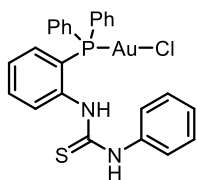
Synthesised according to the general procedure at room temperature for a reaction time of 40 h. White solid, 87% yield, **mp** 137–139 °C (CHCl₃). **R_f** 0.67 (DCM). **¹H NMR** (500 MHz, CDCl₃) δ (ppm): 7.61 (br s, 1H), 7.58 (ddd, 1H, *J* = 7.7, 4.4, 1.3 Hz), 7.37–7.27 (m, 9H), 7.26–7.23 (m, 1H), 7.22–7.14 (m, 5H), 7.08 (dd, 2H, *J* = 7.3, 1.7 Hz), 6.89 (ddd, 1H, *J* = 7.7, 4.6, 1.4 Hz), 6.62 (br s, 1H), 5.04 (d, 2H, *J* = 5.8 Hz). **¹³C NMR** (125 MHz, CDCl₃) δ (ppm): 180.6 (Cq), 141.7 (d, *J* = 24.2 Hz, Cq), 136.1 (Cq), 135.9 (d, *J* = 6.0 Hz, Cq), 135.8 (Cq), 134.0 (CH), 133.9 (d, *J* = 19.6 Hz, CH), 130.3 (CH), 130.1 (d, *J* = 5.4 Hz, CH), 129.6 (CH), 129.1 (CH), 128.8 (d, *J* = 7.0 Hz, CH), 128.3 (CH), 127.3 (CH), 125.2 (CH), 48.2 (d, *J* = 20.1, CH₂). **³¹P{¹H} NMR** (202 MHz, CDCl₃) δ (ppm): –12.7. **HRMS** (APCI, positive mode) *m/z*: calcd. for [C₂₆H₂₄N₂PS]⁺ 437.1392, found 437.1396.

General procedure for the synthesis of gold(I) chloride complexes



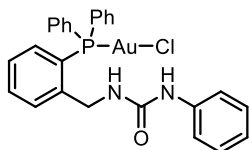
A flask was charged with the phosphine ligand (1.0 eq, 0.1–0.2 mmol) and [(DMS)AuCl] (1.05 eq), then HPLC grade dichloromethane (0.1 M) was added and the mixture was stirred at room temperature, using aluminium foil to protect from light. When the reaction was complete (^{31}P NMR check, usually in 1 h), the volatiles were removed under reduced pressure and the crude gold(I) chloride complex was either purified by trituration or used without further purification. The complexes were stored in the fridge under air, protected from light with aluminium foil.

chloro[1-(2-(diphenylphosphino)phenyl)-3-phenylthiourea] gold(I), [(**13a**)AuCl]



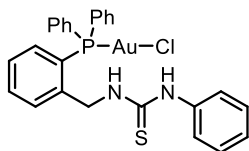
Synthesised according to the general procedure. The compound was deemed pure enough to be used without further purification (incomplete characterization). White solid, 99% yield, **mp** 160–165 °C (decomposition). **HRMS** (ESI, positive mode) m/z : calcd. for $[C_{25}H_{21}AuN_2PS]^+$ 609.0823, found 609.0847.

chloro[1-(2-(diphenylphosphino)benzyl)-3-phenylurea] gold(I), [(**15a**)AuCl]



Synthesised according to the general procedure. Purified by trituration with acetonitrile. White solid, 54% yield, **mp** 208 °C (decomposition). 1H NMR (500 MHz, $CDCl_3$) δ (ppm): 7.66 (ddd, 1H, $J = 7.9, 5.0, 1.3$ Hz), 7.55–7.44 (m, 11H), 7.29–7.26 (m, 2H), 7.24–7.19 (m, 3H), 6.98 (tt, 1H, $J = 7.3, 1.3$ Hz), 6.77–6.72 (m, 2H), 5.47 (t, 1H, $J = 6.0$ Hz), 4.59 (d, 2H, $J = 5.9$ Hz). ^{13}C NMR (125 MHz, $CDCl_3$) δ (ppm): 153.4 (Cq), 143.1 (d, $J = 10.8$ Hz, Cq), 138.7 (Cq), 134.6 (d, $J = 14.0$ Hz, CH), 133.4 (d, $J = 7.7$ Hz, CH), 132.5 (d, $J = 2.5$ Hz, CH), 131.0 (d, $J = 9.0$ Hz, CH), 129.7 (d, $J = 12.1$ Hz, CH), 129.1 (CH), 127.9 (d, $J = 10.1$ Hz, CH), 127.9 (d, $J = 63.9$ Hz, Cq), 125.9 (d, $J = 58.6$ Hz, Cq), 123.3 (CH), 120.1 (CH), 42.9 (d, $J = 12.0$ Hz, CH_2). $^{31}P\{^1H\}$ NMR (202 MHz, $CDCl_3$) δ (ppm): 28.7. **HRMS** (ESI, positive mode) m/z : calcd. for $[C_{26}H_{23}AuClN_2NaOP]^+$ 665.0794, found 665.0789.

chloro[1-(2-(diphenylphosphino)benzyl)-3-phenylthiourea] gold(I), [(**15b**)AuCl]



Synthesised according to the general procedure. Purified by trituration with dichloromethane (incomplete characterization). White solid, quantitative yield, **mp** 190–196 °C (decomposition). **HRMS** (ESI, positive mode) m/z : calcd. for $[C_{26}H_{23}AuN_2PS]^+$ 623.0980, found 623.0979.

References

- [1] Two reviews on silver-free gold(I) catalysis: a) H. Schmidbaur, A. Schier, *Z. Naturforsch.* **2011**, *66b*, 329-350; b) A. Franchino, M. Montesinos-Graner, A. M. Echavarren, *Bull. Chem. Soc. Jpn.*, doi: doi.org/10.1246/bcsj.20200358
- [2] a) A. Guérinot, W. Fang, M. Sircoglou, C. Bour, S. Bezzenine-Lafollée, V. Gandon, *Angew. Chem. Int. Ed.* **2013**, *52*, 5848-5852; b) W. Fang, M. Presset, A. Guerinot, C. Bour, S. Bezzenine-Lafollée, V. Gandon, *Chem. Eur. J.* **2014**, *20*, 5439-5446.
- [3] J. Wolf, F. Huber, N. Erochok, F. Heinen, V. Guerin, C. Legault, S. Kirsch, S. M. Huber, *Angew. Chem. Int. Ed.* **2020**.
- [4] B. W. Gung, S. C. Schlitzer, *Tetrahedron Lett.* **2015**, *56*, 5043-5047.
- [5] S. Sen, F. P. Gabbaï, *Chem. Commun.* **2017**, *53*, 13356-13358.
- [6] M. Murata, S. L. Buchwald, *Tetrahedron* **2004**, *60*, 7397-7403.
- [7] D. Gelman, L. Jiang, S. L. Buchwald, *Org. Lett.* **2003**, *5*, 2315-2318.
- [8] J. Chrzanowski, D. Krasowska, M. Urbaniak, L. Sieroń, P. Pokora-Sobczak, O. M. Demchuk, J. Drabowicz, *Eur. J. Org. Chem.* **2018**, *2018*, 4614-4627.
- [9] a) Y. Li, L.-Q. Lu, S. Das, S. Pisiewicz, K. Junge, M. Beller, *J. Am. Chem. Soc.* **2012**, *134*, 18325-18329; b) Y. Li, S. Das, S. Zhou, K. Junge, M. Beller, *J. Am. Chem. Soc.* **2012**, *134*, 9727-9732; c) K. Damian, M. L. Clarke, C. J. Cobley, *J. Mol. Catal. A Chem.* **2008**, *284*, 46-51; d) S. Sowa, M. Stankevič, A. Flis, K. M. Pietrusiewicz, *Synthesis* **2018**, *50*, 2106-2118.
- [10] a) A. S. K. Hashmi, J. P. Weyrauch, W. Frey, J. W. Bats, *Org. Lett.* **2004**, *6*, 4391-4394; b) J. P. Weyrauch, A. S. K. Hashmi, A. Schuster, T. Hengst, S. Schetter, A. Littmann, M. Rudolph, M. Hamzic, J. Visus, F. Rominger, *Chem. Eur. J.* **2010**, *16*, 956-963.
- [11] K. A. Smoll, W. Kaminsky, K. I. Goldberg, *Organometallics* **2017**, *36*, 1213-1216.
- [12] L. Zhang, F. Yang, G. Tao, L. Qiu, Z. Duan, F. Mathey, *Eur. J. Inorg. Chem.* **2017**, *2017*, 2355-2362.
- [13] J. P. Cahill, F. M. Bohnen, R. Goddard, C. Krüger, P. J. Guiry, *Tetrahedron: Asymmetry* **1998**, *9*, 3831-3839.

Chapter 5: Deep eutectic solvents in organic synthesis

The sustainability of a chemical process may be improved from different points of view, among which the choice of the solvent certainly plays a substantial role. This is particularly true for organic synthesis, since the solvent usually represents the great majority of the raw material produced in such chemical processes.^[1] Volatile organic compounds (VOCs) have been and still are the most widespread solvents for organic transformations. As is well established, VOCs are in general harmful for both human health and the environment, they are flammable and come from non-renewable sources. Several efforts have been made in the last decades to find suitable alternatives to conventional solvents in organic synthesis, and remarkable advances have come from the use of water, supercritical fluids, neat conditions and ionic liquid, among the others.^[2]

A new class of solvents that have emerged at the beginning of the century are deep eutectic solvents (DESs). Their physicochemical properties and their potentially green features, as well as their active influence on the course of many reactions, have been able to rise the interest of several research groups and organic chemistry in DES is nowadays a widespread field of investigation.

In the present chapter an overview of the characteristics of DESs and of their application in organic synthesis will be provided.

5.1 Deep eutectic solvents: general features

5.1.1 Composition

Deep eutectic solvents are defined in a general way as mixtures of two or more components, having a melting point of the mixture significantly lower than those of the components alone, and usually liquid at room temperature.^[3] DESs were initially considered as a new class of ionic liquids (ILs), and indeed they share with ILs some features, such as the negligible vapor pressure, high viscosities and the possibility of tuning their properties by an appropriate design. However, this classification has been overcome and DESs and ILs should be regarded as two separate types of solvents. While ILs are molten salts, *i.e.* single ionic compounds of one cation and one anion, DESs are mixtures of more than one compound.^[4]

The components constituting a DES are small organic molecules able to interact through hydrogen bonding. In most cases the mixture is composed by a Brønsted or Lewis acid acting as hydrogen bond donor (HBD) and a Brønsted or Lewis base acting as hydrogen bond acceptor (HBA). The role of HBA is often played by the halide anion of quaternary ammonium salts, among which choline chloride (ChCl) stands out (Figure 5.1). In his seminal work from 2003,^[5] Abbott reported

that mixing ChCl, which has a melting point of 303 °C, with urea as HBD (mp 134 °C) in 1:2 molar ratio^[6] resulted in the formation of a liquid with a mp of 12 °C.^[7] Other common HBDs are short-chain polyols, such as glycerol, carboxylic acids, sugars and even water. Metal halides, such as ZnCl₂, FeCl₃, CrCl₃ and others, can also be combined with organic molecules to form DESs.^[3, 8]

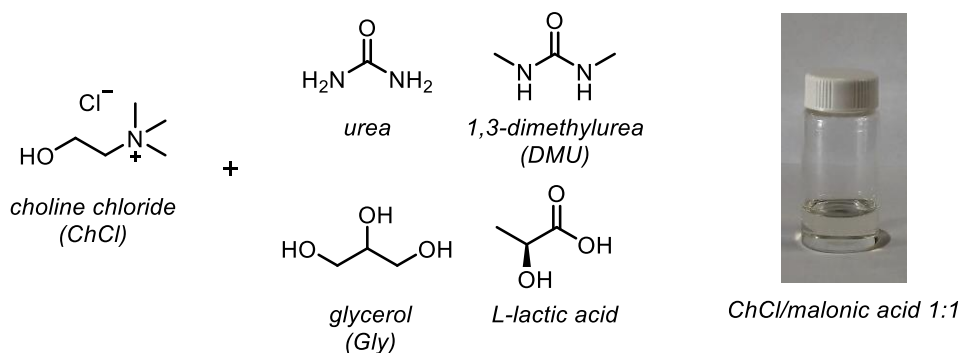


Figure 5.1 Examples of the most common DESs components: choline chloride as HBA and some HBDs. A picture of the DES composed by ChCl (mp 303 °C) and malonic acid (mp 136 °C) in 1:1 molar ratio.

Hydrogen bonding interactions strongly characterize the nature of deep eutectic solvents. The significant lowering in the melting point of the mixture, compared to its single components, has indeed been attributed to the formation of a network of hydrogen bonds between the components.^[3b, 8b]

More recently, the concept of natural deep eutectic solvent (NaDES) has been proposed. In 2011 Verpoorte observed that a small number of primary metabolites, such as carboxylic acids, choline, sugars and some amino acids are found in unexpected high amounts in a wide number of living organisms. The hypothesis put forward was that these compounds could be employed by the organism to form eutectic mixtures that would serve as reaction media for the biosynthesis of non-water-soluble molecules.^[9] It has also been proposed that NaDESs may be involved in the resistance of some organisms to low temperatures and drought.^[10] Taking inspiration from nature, several eutectic mixtures of bio-derived compounds have been prepared, studied and employed for different applications.^[11] Among those, also hydrophobic DESs based on terpenes or fatty acids have been reported.^[12] The term NaDES is thus generally intended to designate deep eutectic solvents composed only by naturally occurring compounds.

5.1.2 Green credentials

Deep eutectic solvents have emerged as an alternative to conventional solvents and an improvement in terms of sustainability, often in comparison with ionic liquids. The first appealing difference between DESs and ILs is that the latter are synthesised by chemical reactions, *e.g.* alkylation of imidazole for the imidazolium-based ones. The synthetic steps imply the use of solvents and reagents for reaction, extraction and purification, and disposal of the waste material, which is often non-biodegradable, is required.^[13] By comparison, the preparation of a DES is much simpler and cleaner: the components are mixed and stirred under heating (often 60–100 °C) until a clear liquid is formed and no further purification is generally required. The method is intrinsically 100% atom-economic. Alternatively, it is also possible to dissolve the components in water and obtain the eutectic mixture by evaporation of water under reduced pressure.

Among the reasons why deep eutectic solvents are diffusely considered as green solvents is their supposed low toxicity. Similarly to ILs, DESs display negligible vapour pressure, resulting in a low risk for atmospheric pollution and low flammability. On the other hand, a substantial difference is found in the intrinsic safety of many DES components, which are often biocompatible, towards human health. It should be noted that this does not necessarily imply a low toxicity of their combination in the eutectic mixture. Two studies by Hayyan revealed a higher toxicity of the considered DESs towards brine shrimp *Artemia salina*, compared to solutions of their single components.^[14] The opposite effect was observed by Yang on another aquatic organism, *Hydra sinensis*.^[15] Up to now, evaluations of DES toxicity have been performed on microorganisms, human cell lines, plants and mice, and the results suggest that the initial assumption of DESs as “biocompatible solvents” still needs deeper investigation.^[16] Anyway, they appear to be safer than conventional solvents and ionic liquids, particularly when their components are essential ingredients of cellular metabolism.^[17] Furthermore, applications of DESs as media for drug solubilization and administration have already been tested.^[18]

In order to evaluate the sustainability of deep eutectic solvents, their whole lifecycle should be considered. On this matter, NaDESs certainly constitute an attractive option, since their components come from potentially renewable sources and often are biodegradable. Biodegradability is a relevant issue, as it reduces not only the impact on human health and the environment, but also the costs for waste disposal. Studies employing the closed bottle test, a standard method in which the substrate is added to aerobic aqueous medium inoculated with wastewater microorganisms, indicated several DESs as “readily biodegradable”.^[16a-d]

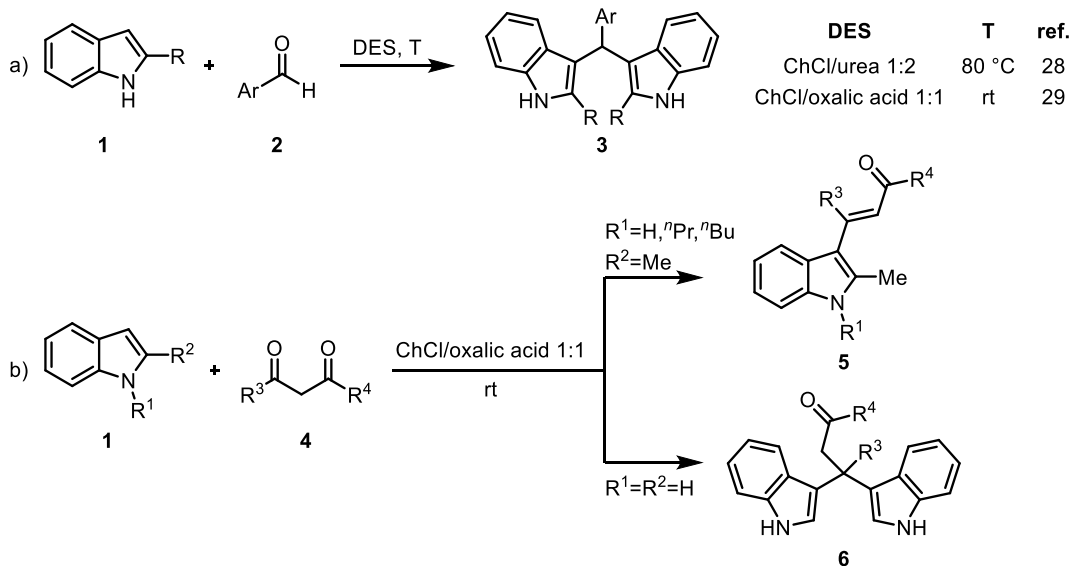
5.2 Deep eutectic solvents in organic synthesis

Alongside with the investigation on their fundamental physicochemical properties, applications of deep eutectic solvents have been studied in several fields, including metal and metal oxide processing,^[3a, 19] fuel industry,^[20] extractions of bioactive compounds^[21] or for analytical applications,^[22] biomass treatment,^[23] DNA and RNA preservation,^[24] solubilization of gases,^[25] including CO₂.^[26] In organic chemistry, the introduction of DESs as new possible reaction media not only has prompted the research towards revisiting a large number of reactions under more sustainable conditions, but has also disclosed novel reactivities and synthetic possibilities.^[27] In general terms, it has been highlighted that DESs can have an active role in promoting organic transformations, thus going beyond the mere function of reaction medium. There are several examples of organic reactions that, when run in a deep eutectic solvent, show higher yields or allow for milder conditions or for the elimination of catalysts and additives. In fact, this active effect is an emerging property of the eutectic mixture and has been largely attributed to the supramolecular hydrogen bond network that characterizes the DES structure.

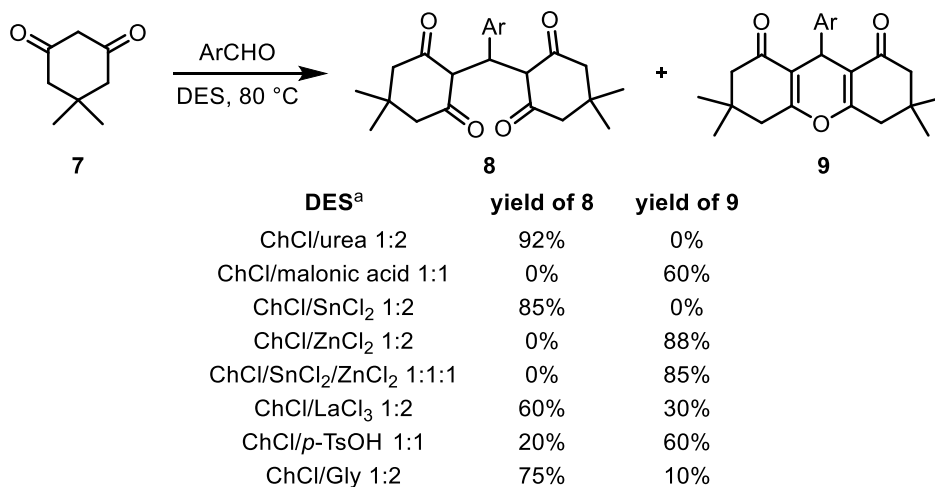
5.2.1 Acid- and base-catalysed reactions

The double role of solvent and promoter/catalyst of a DES is particularly evident with reactions that are catalysed by acids and bases. The case partially matches with the definition of organocatalysis, *i.e.* catalysis by small organic molecules. The choice of the right components of the eutectic mixture, especially the HBD, is often crucial for the outcome of the reaction, as it allows to tune the acid-base character of the melt.

Carbonyl derivatives were successfully activated towards the attack of electron-rich aryl rings, such as indoles **1**, for the synthesis of bis(indolyl)methanes **3** (Scheme 5.1, a). The reaction was promoted by the ChCl/urea 1:2 (mol mol⁻¹) deep eutectic solvent on a wide range of aromatic aldehydes **2** and afforded excellent yields at 80 °C. However, ketones were not reactive under these conditions.^[28] Switching the HBD component from urea to oxalic acid allowed to perform the reaction at room temperature, while keeping the yields unchanged.^[29] The ChCl/oxalic acid 1:1 DES was employed by the same authors to extend the reaction scope to ketones. When 1,3-diketones **4** were reacted with indoles, α,β -unsaturated or β,β -bis(indolyl) carbonyl compounds **5** and **6** were obtained through single or double attack respectively, depending on the indole substitution pattern (Scheme 5.1, b).^[30] Other alkylations of indoles with aldehydes or ketones in DESs were also reported.^[31]



Scheme 5.1 Reactions of aldehydes (a) and 1,3-diketones (b) with indoles in deep eutectic solvents.

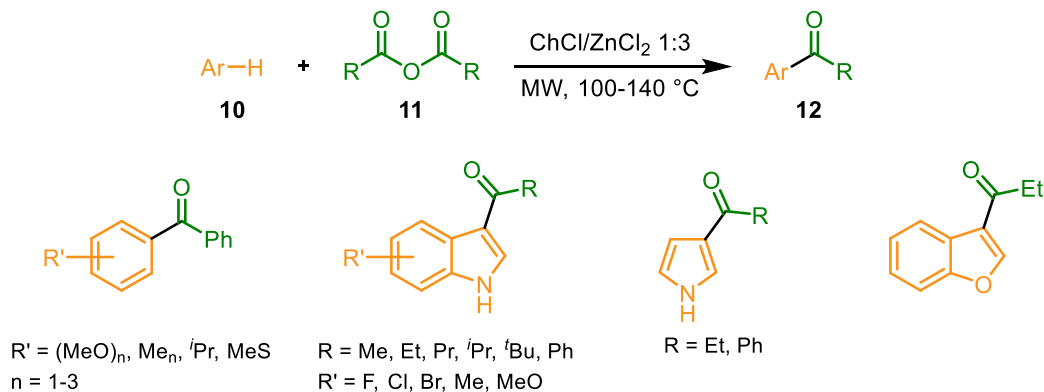


Scheme 5.2 Condensation of dimedone with aromatic aldehydes in DESs (Gly = glycerol).
^a For the chemoselectivity study, Ar = Ph.

Carbonyl compounds were employed not only as electrophiles in reactions assisted by deep eutectic solvents, but the chemistry of enols was also explored. For example, the Mannich-type synthesis of β -aniline carbonyl derivatives^[32] and the Perkin reaction^[33] were successfully performed employing ChCl/ZnCl₂ 1:2 (in water) and ChCl/urea 1:2 respectively. The chemoselective synthesis of hexahydroxanthenediones **8** or tetraketones **9** from dimedone **7** was achieved by Azizi with DESs based on choline chloride combined with either organic molecules

or transition metal chlorides. The chemoselectivity was dictated by the choice of the DES components (Scheme 5.2).^[34]

Other examples of acid-catalysed transformations that have been performed in DESs are the Fischer indole synthesis, studied by Abbott in $\text{ChCl}/\text{ZnCl}_2$ 1:2^[35] and by König in L-tartaric acid/DMU 30:70 (weight ratio),^[36] and Friedel-Crafts acylations and alkylations.^[37] In particular, carboxylic acid anhydrides **11** were employed as acylating agents in $\text{ChCl}/\text{ZnCl}_2$ 1:3 with a wide variety of electron-rich arenes **10** in a chemo- and regioselective manner under microwave irradiation (Scheme 5.3).^[37a]



Scheme 5.3 Reaction scope of the Friedel-Crafts acylation in $\text{ChCl}/\text{ZnCl}_2$ 1:3.

5.2.2 Transition metal-catalysed reactions

The first examples of transition metal catalysis in deep eutectic solvents came from the work of König, who reported Ru-catalysed hydrogenation, Cu-catalysed azide alkyne cycloaddition, and Pd-catalysed Stille, Suzuki, Heck and Sonogashira cross-couplings.^[38] The reactions were performed in binary DESs composed of a sugar and urea or DMU, or in ternary systems analogous to the previous ones, with the addition of NH_4Cl as the third component. Later, Capriati reported the Cu-catalysed Ullman amine synthesis and the Pd-catalysed aminocarbonylation, Suzuki and Sonogashira coupling of aryl halides in ChCl/urea 1:2 and ChCl/Gly 1:2.^[39] Interestingly, Pd catalysis was carried out in most cases without the use of any ligand, and in some cases the presence of a ligand was even detrimental to the reaction yield. It appears that the transposition of Pd-catalysed methodologies in DESs as reaction media requires a new ligand design, as commonly employed phosphines are often not suitable for these unconventional solvents. The group of Ramón addressed the issue and found a valuable alternative in the cationic pyridinium-based phosphines, previously reported by Alcarazo.^[40] The 2-(dicyclohexylphosphino)-1-phenylpyridinium **13** proved an efficient and general ligand for the Suzuki, Heck, Sonogashira and C-S bond coupling reactions in various

DESs (Figure 5.2), with catalyst loadings in the range 0.1-1%. The yields were significantly improved by the use of **13**, compared to both Pd(II) salts alone or with common trialkyl or triarylphosphines as ligands.^[41]

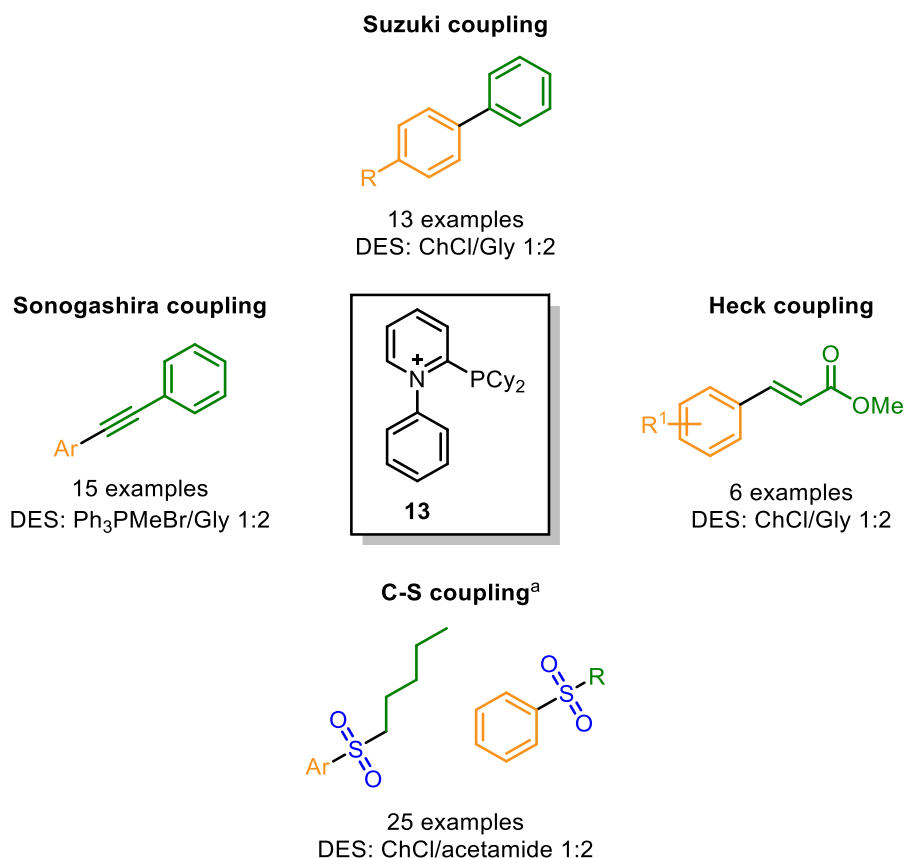


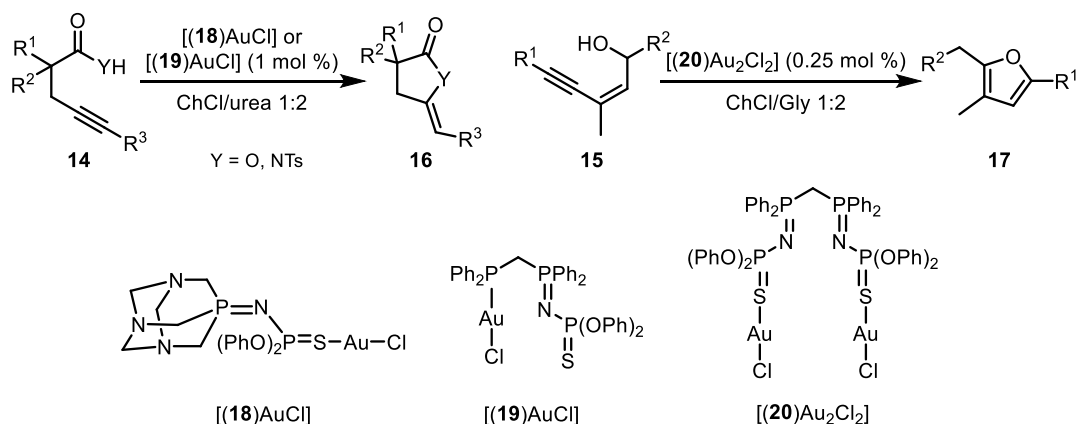
Figure 5.2 Application of pyridinium phosphine **13** in Pd-catalysed reactions in DESs.

^a Na₂S₂O₅ as SO₂ source.

By contrast, the Pd-catalysed C-H activation of thiophene derivatives in ChCl/urea 1:2 was successfully achieved by Farinola with (*o*-MeOPh)₃P as the ligand and [Pd₂(dba)₃] as the metal source.^[42]

Deep eutectic solvents have also been employed by García-Álvarez for gold(I)-catalysed transformations. The intramolecular reactions of *O*- and *N*-containing alkynes **14–15** were performed in ChCl/urea 1:2 and ChCl/Gly 1:2 with iminophosphorane ligands **18–20** (Scheme 5.4), previously developed by the same research group for reactions of various transition metals in water and ionic liquids.^[43] The reactivity of common phosphine and NHC gold(I) complexes was not investigated. Interestingly, the gold(I) chloride complexes did not require activation by silver(I) salts (see Chapters 1 and 4); this may be attribute to hydrogen bonding

interactions with the DES matrix. The same complexes were then employed, in deep eutectic solvents, in combination with biocatalysis.^[44]



Scheme 5.4 Gold catalysis in deep eutectic solvents.

5.2.3 Operational aspects

The physicochemical properties and the chemical behaviour of deep eutectic solvents influence the laboratory practices that are adopted in the use of these solvents.

A first relevant feature for organic synthesis is viscosity. In analogy with ionic liquids, DESs often exhibit high viscosities, as exemplified by Table 5.1. The values are in the range of 10^1 – 10^3 cP; by comparison, dichloromethane (0.45 cP at 20 °C), toluene (0.59 cP), ethyl acetate (0.46 cP) and other common organic solvents are much less viscous.

Table 5.1 Viscosity of some DESs determined by NMR diffusion at 25 °C.^[45]

DES components		ratio	viscosity (cP) ^a
ChCl	Gly	1:2	259
ChCl	ethylene glycol	1:2	37
ChCl	urea	1:2	750
ChCl	malonic acid	1:1	1124

^a cP = g s⁻¹ cm⁻¹

The viscosity of DESs has been attributed to the hydrogen bonding network that characterizes the melt. The chemical nature of the components is also important, because their volume determines the availability of holes in the structure of the fluid, which allow suitable motion.^[3a, 46] This parameter is significant for the application of DESs in organic synthesis, because it influences the ability to ensure

proper mechanical stirring to the reaction mixture. The stirring may be crucial for the outcome of the reaction, since the organic substrates, particularly the most nonpolar ones, are in some cases not completely soluble in the polar DES medium. However, it should be noted that the viscosity of DESs is often highly dependent on the temperature: for example, the value for ChCl/malonic acid 1:1 decreases to 342 at 40 °C and to 161 cP at 55 °C.^[45, 47] The viscosity may also be influenced by the water content in the eutectic mixture.^[48]

When working with deep eutectic solvents, a central aspect is represented by the procedure employed for the work-up at the end of the reaction. From this point of view, this class of solvents appears to be particularly appealing, because the components of the DES are usually water-soluble. The addition of water disrupts the structure of the eutectic mixture and the components are dissolved into the aqueous layer, into which the organic product of the reaction is often insoluble. Thus, in optimal conditions a solid organic product can precipitate and be collected by simple filtration or, if it is an oil, form a separate layer. This procedure not only allows to avoid the use of extraction solvents, but also enables the recycle of the DES. Indeed, evaporation of water restores the eutectic mixture, that can be used for another reaction cycle, usually up to 3-5 consecutive runs.

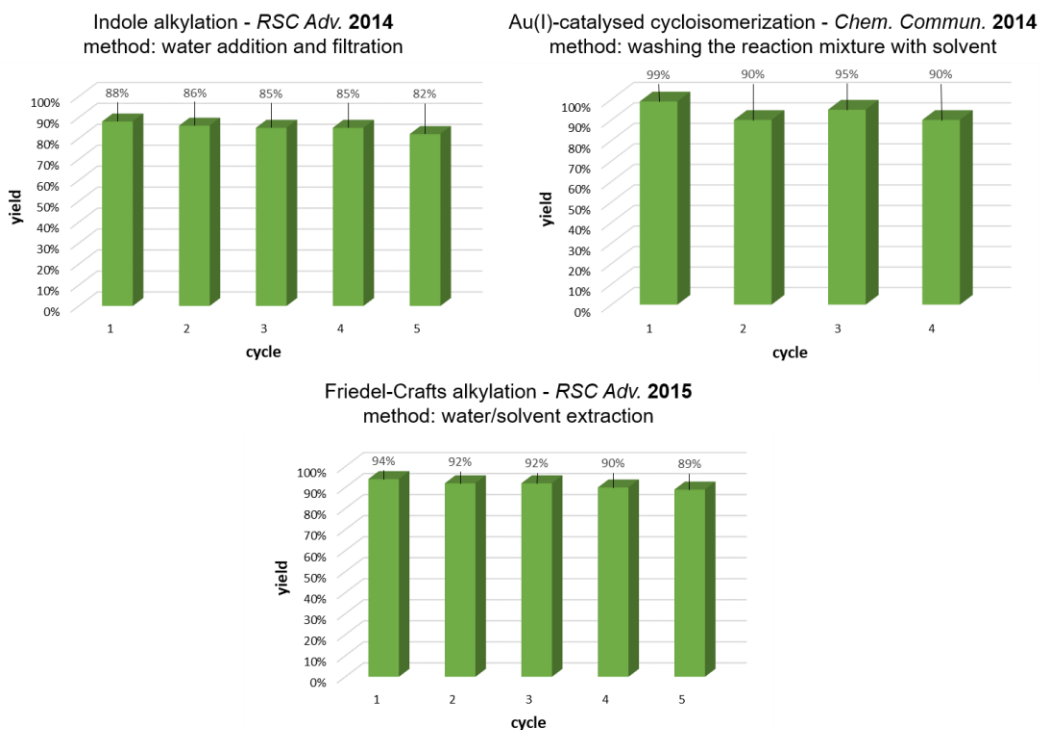


Figure 5.3 Product yields in the recycling of the DES with three different methods in the indole alkylation,^[30] Au(I)-catalysed cycloisomerisation^[43a] and Friedel-Crafts alkylation.^[37b]

The possibility of recycling the DES has been reported in a wide number of cases, among which many of those presented in Sections 5.2.1 and 5.2.2, as exemplified by Figure 5.3. It should be noted that other recycling procedures are also feasible: extracting the product directly from the reaction mixture, by washing with an organic solvent (*e.g.* diethyl ether) able to dissolve the product but not the DES components; performing a classical water/organic solvent extraction, followed by evaporation of the aqueous layer to restore the DES.

References

- [1] F. Roschangar, J. Colberg, P. J. Dunn, F. Gallou, J. D. Hayler, S. G. Koenig, M. E. Kopach, D. K. Leahy, I. Mergelsberg, J. L. Tucker, *Green Chem.* **2017**, *19*, 281-285.
- [2] a) C. J. Clarke, W.-C. Tu, O. Levers, A. Brohl, J. P. Hallett, *Chem. Rev.* **2018**, *118*, 747-800; b) J. H. Clark, S. J. Tavener, *Org. Process Res. Dev.* **2007**, *11*, 149-155; c) R. A. Sheldon, *Green Chem.* **2005**, *7*, 267-278; d) B. H. Lipshutz, F. Gallou, S. Handa, *ACS Sust. Chem. Eng.* **2016**, *4*, 5838-5849.
- [3] a) E. L. Smith, A. P. Abbott, K. S. Ryder, *Chem. Rev.* **2014**, *114*, 11060-11082; b) Q. Zhang, K. D. O. Vigier, S. Royer, F. Jérôme, *Chem. Soc. Rev.* **2012**, *41*, 7108-7146.
- [4] M. A. Martins, S. P. Pinho, J. A. Coutinho, *J. Solution Chem.* **2019**, *48*, 962-982.
- [5] A. P. Abbott, G. Capper, D. L. Davies, R. K. Rasheed, V. Tambyrajah, *Chem. Commun.* **2003**, 70-71.
- [6] All DESs composition are reported as molar ratios throughout the whole thesis, unless otherwise specified.
- [7] It should be pointed out that a glass transition temperature, rather than a melting point, is used in several cases to describe the solid-liquid transition of DESs. Throughout this thesis, the term "melting point" will be used to include both behaviours.
- [8] a) C. Ruß, B. König, *Green Chem.* **2012**, *14*, 2969-2982; b) M. Francisco, A. van den Bruinhorst, M. C. Kroon, *Angew. Chem. Int. Ed.* **2013**, *52*, 3074-3085.
- [9] Y. H. Choi, J. van Spronsen, Y. Dai, M. Verberne, F. Hollmann, I. W. Arends, G.-J. Witkamp, R. Verpoorte, *Plant Physiol.* **2011**, *156*, 1701-1705.
- [10] A. Gertrudes, R. Craveiro, Z. Eltayari, R. L. Reis, A. Paiva, A. R. C. Duarte, *ACS Sust. Chem. Eng.* **2017**, *5*, 9542-9553.
- [11] a) Y. Dai, J. van Spronsen, G.-J. Witkamp, R. Verpoorte, Y. H. Choi, *Anal. Chim. Acta* **2013**, *766*, 61-68; b) Y. Liu, J. B. Friesen, J. B. McAlpine, D. C. Lankin, S.-N. Chen, G. F. Pauli, *J. Nat. Prod.* **2018**, *81*, 679-690; c) H. Vanda, Y. Dai, E. G. Wilson, R. Verpoorte, Y. H. Choi, *C. R. Chimie* **2018**, *21*, 628-638; d) A. Paiva, R. Craveiro, I. Aroso, M. Martins, R. L. Reis, A. R. C. Duarte, *ACS Sust. Chem. Eng.* **2014**, *2*, 1063-1071.
- [12] a) C. Florindo, L. C. Branco, I. M. Marrucho, *ChemSusChem* **2019**, *12*, 1549-1559; b) D. J. van Osch, C. H. Dietz, J. van Spronsen, M. C. Kroon, F. Gallucci, M. van Sint Annaland, R. Tuinier, *ACS Sust. Chem. Eng.* **2019**, *7*, 2933-2942; c) B. D. Ribeiro, C. Florindo, L. C. Iff, M. A. Coelho, I. M. Marrucho, *ACS Sust. Chem. Eng.* **2015**, *3*, 2469-2477; d) N. Schaeffer, M. A. Martins, C. M. Neves, S. P. Pinho, J. A. Coutinho, *Chem. Commun.* **2018**, *54*, 8104-8107.
- [13] M. Deetlefs, K. R. Seddon, *Green Chem.* **2010**, *12*, 17-30.
- [14] a) M. Hayyan, M. A. Hashim, A. Hayyan, M. A. Al-Saadi, I. M. AlNashef, M. E. Mirghani, O. K. Saheed, *Chemosphere* **2013**, *90*, 2193-2195; b) M. Hayyan, M. A. Hashim, M. A. Al-Saadi, A. Hayyan, I. M. AlNashef, M. E. Mirghani, *Chemosphere* **2013**, *93*, 455-459.
- [15] Q. Wen, J.-X. Chen, Y.-L. Tang, J. Wang, Z. Yang, *Chemosphere* **2015**, *132*, 63-69.
- [16] a) Z. Yang, *Toxicity and Biodegradability of Deep Eutectic Solvents and Natural Deep Eutectic Solvents in Deep Eutectic Solvents: Synthesis, Properties, and Applications* (Ed.: Wiley), **2019**, pp. 43-60; b) B.-Y. Zhao, P. Xu, F.-X. Yang, H. Wu, M.-H. Zong, W.-Y. Lou, *ACS Sust. Chem. Eng.* **2015**, *3*, 2746-2755; c) K. Radošević, M. C. Bubalo, V. G. Srček, D. Grgas, T. L. Dragičević, I. R. Redovniković, *Ecotoxicol.*

- Environ. Saf.* **2015**, *112*, 46-53; d) I. Juneidi, M. Hayyan, M. A. Hashim, *RSC Adv.* **2015**, *5*, 83636-83647; e) R. F. Frade, S. Simeonov, A. A. Rosatella, F. Siopa, C. A. Afonso, *Chemosphere* **2013**, *92*, 100-105; f) X.-D. Hou, Q.-P. Liu, T. J. Smith, N. Li, M.-H. Zong, *PLOS ONE* **2013**, *8*.
- [17] a) B. Kudłak, K. Owczarek, J. Namieśnik, *Environ. Sci. Pollut. Res.* **2015**, *22*, 11975-11992; b) Y. P. Mbous, M. Hayyan, W. F. Wong, C. Y. Looi, M. A. Hashim, *Sci. Rep.* **2017**, *7*, 1-14.
- [18] a) M. Faggian, S. Sut, B. Perissutti, V. Baldan, I. Grabnar, S. Dall'Acqua, *Molecules* **2016**, *21*, 1531; b) S. Sut, M. Faggian, V. Baldan, G. Poloniato, I. Castagliuolo, I. Grabnar, B. Perissutti, P. Brun, F. Maggi, D. Voinovich, *Molecules* **2017**, *22*, 1921; c) S. N. Pedro, M. G. Freire, C. S. Freire, A. J. Silvestre, *Expert Opin. Drug Del.* **2019**, *16*, 497-506.
- [19] J. Richter, M. Ruck, *Molecules* **2020**, *25*, 78.
- [20] a) H. Zhao, G. A. Baker, *J. Chem. Technol. Biotechnol.* **2013**, *88*, 3-12; b) M. F. B. Majid, H. F. B. M. Zaid, C. F. Kait, K. Jumbri, L. C. Yuan, S. Rajasuriyan, *J. Mol. Liq.* **2020**, 112870.
- [21] a) M. H. Zainal-Abidin, M. Hayyan, A. Hayyan, N. S. Jayakumar, *Anal. Chim. Acta* **2017**, *979*, 1-23; b) M. C. Bubalo, S. Vidović, I. R. Redovniković, S. Jokić, *Food Bioprod. Process.* **2018**, *109*, 52-73; c) Y. Dai, J. Van Spronsen, G.-J. Witkamp, R. Verpoorte, Y. H. Choi, *J. Nat. Prod.* **2013**, *76*, 2162-2173.
- [22] M. de los Ángeles Fernández, J. Boiteux, M. Espino, F. J. Gomez, M. F. Silva, *Anal. Chim. Acta* **2018**, *1038*, 1-10.
- [23] a) X. Tang, M. Zuo, Z. Li, H. Liu, C. Xiong, X. Zeng, Y. Sun, L. Hu, S. Liu, T. Lei, *ChemSusChem* **2017**, *10*, 2696-2706; b) P. Kalhor, K. Ghandi, *Molecules* **2019**, *24*, 4012; c) A. Satlewal, R. Agrawal, S. Bhagia, J. Sangoro, A. J. Ragauskas, *Biotechnol. Adv.* **2018**, *36*, 2032-2050.
- [24] a) H. Zhao, *J. Chem. Technol. Biotechnol.* **2015**, *90*, 19-25; b) H. Tateishi-Karimata, N. Sugimoto, *Nucleic Acids Res.* **2014**, *42*, 8831-8844.
- [25] a) Y. Marcus, *Monatsh. Chem.* **2018**, *149*, 211-217; b) Y. Chen, X. Han, Z. Liu, D. Yu, W. Guo, T. Mu, *ACS Sust. Chem. Eng.* **2020**, *8*, 5410-5430.
- [26] a) S. Sarmad, J. P. Mikkola, X. Ji, *ChemSusChem* **2017**, *10*, 324-352; b) Y. Zhang, X. Ji, X. Lu, *Renew. Sust. Energy Rev.* **2018**, *97*, 436-455.
- [27] a) S. T. Handy, *Deep eutectic solvents in organic synthesis in Ionic Liquids—Current State of the Art* (ed: IntechOpen), **2015**; b) M. Obst, B. König, *Eur. J. Org. Chem.* **2018**, *2018*, 4213-4232; c) D. A. Alonso, A. Baeza, R. Chinchilla, G. Guillena, I. M. Pastor, D. J. Ramón, *Eur. J. Org. Chem.* **2016**, *2016*, 612-632; d) P. Liu, J.-W. Hao, L.-P. Mo, Z.-H. Zhang, *RSC Adv.* **2015**, *5*, 48675-48704; e) N. Guajardo, C. R. Mueller, R. Schrebler, C. Carlesi, P. Dominguez de Maria, *ChemCatChem* **2016**, *8*, 1020-1027; f) S. Khandelwal, Y. K. Tailor, M. Kumar, *J. Mol. Liq.* **2016**, *215*, 345-386.
- [28] S. Handy, N. M. Westbrook, *Tetrahedron Lett.* **2014**, *55*, 4969-4971.
- [29] U. N. Yadav, G. S. Shankarling, *J. Mol. Liq.* **2014**, *191*, 137-141.
- [30] A. K. Sanap, G. S. Shankarling, *RSC Adv.* **2014**, *4*, 34938-34943.
- [31] a) A. Kumar, R. D. Shukla, D. Yadav, L. P. Gupta, *RSC Adv.* **2015**, *5*, 52062-52065; b) N. Azizi, Z. Manocheri, *Res. Chem. Intermed.* **2012**, *38*, 1495-1500.
- [32] F. Keshavarzipour, H. Tavakol, *Catal. Lett.* **2015**, *145*, 1062-1066.
- [33] P. M. Pawar, K. J. Jarag, G. S. Shankarling, *Green Chem.* **2011**, *13*, 2130-2134.
- [34] N. Azizi, S. Dezfooli, M. M. Hashemi, *C. R. Chimie* **2013**, *16*, 997-1001.

- [35] R. C. Morales, V. Tambyrajah, P. R. Jenkins, D. L. Davies, A. P. Abbott, *Chem. Commun.* **2004**, 158-159.
- [36] S. Gore, S. Baskaran, B. König, *Org. Lett.* **2012**, *14*, 4568-4571.
- [37] a) P. H. Tran, H. T. Nguyen, P. E. Hansen, T. N. Le, *RSC Adv.* **2016**, *6*, 37031-37038; b) A. Wang, P. Xing, X. Zheng, H. Cao, G. Yang, X. Zheng, *RSC Adv.* **2015**, *5*, 59022-59026; c) B. Yuan, Y. Li, F. Yu, X. Li, C. Xie, S. Yu, *Catal. Lett.* **2018**, *148*, 2133-2138; d) X. Jin, A. Wang, H. Cao, S. Zhang, L. Wang, X. Zheng, X. Zheng, *Res. Chem. Intermed.* **2018**, *44*, 5521-5530.
- [38] a) G. Imperato, S. Höger, D. Lenoir, B. König, *Green Chem.* **2006**, *8*, 1051-1055; b) G. Imperato, R. Vasold, B. König, *Adv. Synth. Catal.* **2006**, *348*, 2243-2247; c) F. Ilgen, B. König, *Green Chem.* **2009**, *11*, 848-854.
- [39] a) F. Messa, S. Perrone, M. Capua, F. Tolomeo, L. Troisi, V. Capriati, A. Salomone, *Chem. Commun.* **2018**, *54*, 8100-8103; b) G. Dilauro, S. M. García, D. Tagarelli, P. Vitale, F. M. Perna, V. Capriati, *ChemSusChem* **2018**, *11*, 3495-3501; c) A. F. Quivelli, P. Vitale, F. M. Perna, V. Capriati, *Front. Chem.* **2019**, *7*, 723; d) F. Messa, G. Dilauro, F. M. Perna, P. Vitale, V. Capriati, A. Salomone, *ChemCatChem* **2020**.
- [40] H. Tinnermann, C. Wille, M. Alcarazo, *Angew. Chem. Int. Ed.* **2014**, *53*, 8732-8736.
- [41] a) X. Maset, A. Khoshnood, L. Sotorrios, E. Gómez-Bengoá, D. A. Alonso, D. J. Ramón, *ChemCatChem* **2017**, *9*, 1269-1275; b) X. Maset, G. Guillena, D. J. Ramón, *Chem. Eur. J.* **2017**, *23*, 10522-10526.
- [42] A. Punzi, D. I. Coppi, S. Matera, M. A. Capozzi, A. Operamolla, R. Ragni, F. Babudri, G. M. Farinola, *Org. Lett.* **2017**, *19*, 4754-4757.
- [43] a) M. J. Rodríguez-Álvarez, C. Vidal, J. Díez, J. García-Álvarez, *Chem. Commun.* **2014**, *50*, 12927-12929; b) C. Vidal, L. Merz, J. García-Álvarez, *Green Chem.* **2015**, *17*, 3870-3878; c) M. J. Rodríguez-Álvarez, C. Vidal, S. Schumacher, J. Borge, J. García-Álvarez, *Chem. Eur. J.* **2017**, *23*, 3425-3431.
- [44] M. a. J. Rodríguez-Álvarez, N. s. Ríos-Lombardía, S. r. Schumacher, D. Pérez-Iglesias, F. Morís, V. Cadierno, J. García-Álvarez, J. González-Sabín, *ACS Catal.* **2017**, *7*, 7753-7759.
- [45] C. D'Agostino, R. C. Harris, A. P. Abbott, L. F. Gladden, M. D. Mantle, *Phys. Chem. Chem. Phys.* **2011**, *13*, 21383-21391.
- [46] a) A. P. Abbott, R. C. Harris, K. S. Ryder, *J. Phys. Chem. B* **2007**, *111*, 4910-4913; b) A. P. Abbott, G. Capper, S. Gray, *ChemPhysChem* **2006**, *7*, 803-806.
- [47] J. N. Al-Dawsari, A. Bessadok-Jemai, I. Wazeer, S. Mokraoui, M. A. AlMansour, M. K. Hadj-Kali, *J. Mol. Liq.* **2020**, 113127.
- [48] a) C. Ma, A. Laaksonen, C. Liu, X. Lu, X. Ji, *Chem. Soc. Rev.* **2018**, *47*, 8685-8720; b) A. Yadav, S. Trivedi, R. Rai, S. Pandey, *Fluid Phase Equilib.* **2014**, *367*, 135-142.

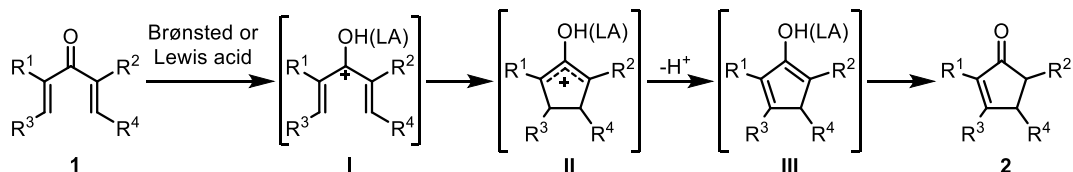
Chapter 6: The Nazarov cyclisation in natural deep eutectic solvents

Part of the results presented in this chapter are published in *Green Chem.* **2020**, *22*, 110-117.

6.1 The Nazarov cyclisation

6.1.1 General features

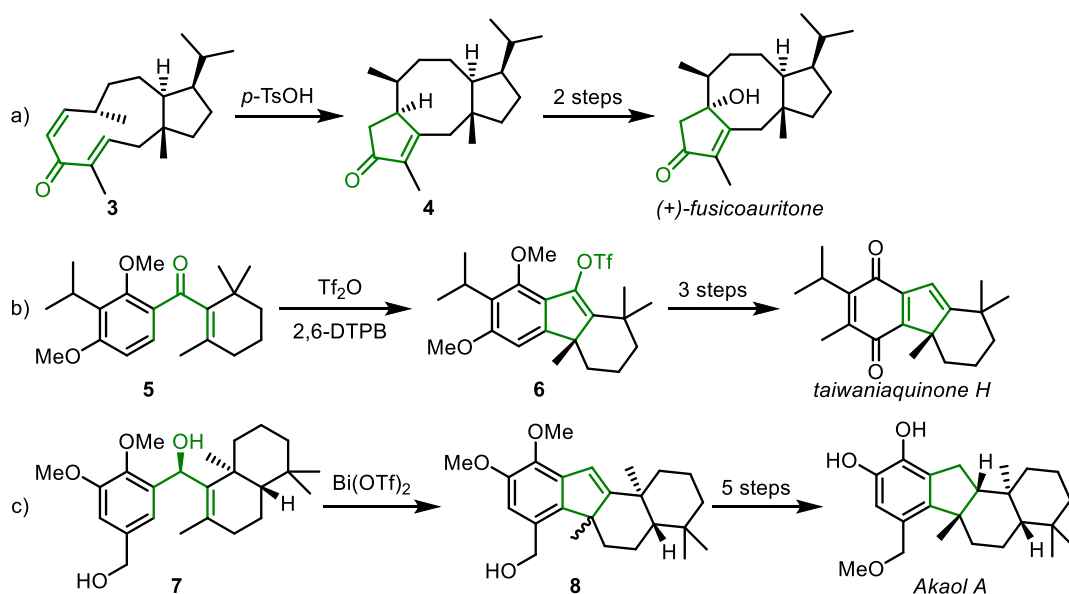
The Nazarov cyclisation is an electrocyclic reaction that converts α,α' -divinyl ketones **1** into cyclopentenones **2** in the presence of a Brønsted or Lewis acid as a catalyst (Scheme 6.1). The transformation was first reported by Nazarov in 1941 as a side reaction in the hydration of dienyne catalysed by HgSO_4 and H_2SO_4 . Its mechanism involves the activation of the carbonyl moiety by the acid catalyst to form pentadienyl cation intermediate **I**, which undergoes ring closure through a 4π -conrotatory electrocycloisomerisation to oxyallyl cation **II**. The reaction is ended by β -elimination and cleavage of the acid catalyst, affording cyclopentenone **2** as the final product.^[1]



Scheme 6.1 General mechanism of the Nazarov cyclisation.

Since its discovery, the Nazarov cyclisation has been extensively studied by several research groups, becoming a truly effective and versatile tool for synthetic chemists. Its success relies not only on the opportunity to access the cyclopentenone motif, which is itself of great value in total synthesis, but also on the remarkable variety of alternative versions of this reaction that have been proposed throughout the years. On one hand, advances in the generation of the key pentadienyl cation intermediate **I** have extended the repertoire of substrates, beyond classical dienones **1**, from which the Nazarov cyclisation can be performed. Such examples include ethers, allenes, diketones, enynes, propargyl esters, among others.^[2] On the other hand, the transformation has been deeply studied in its regio- and stereoselectivity. These two crucial features can be controlled through the electronic and steric properties of the substituents in the starting material, as well as by the use of chiral catalysts, be they chiral Brønsted acids or metal complexes with asymmetric ligands.^[3] For all these reasons, the Nazarov cyclisation has been

successfully applied to several total synthesis of natural and pharmaceutically active compounds.^[3c, 4] To report some examples, the cyclopentenone core featured in derivatives such as (+)-fusicoauritone was obtained by the late-stage cyclisation of intermediate **3**, catalysed by *p*-TsOH (Scheme 6.2, a).^[5] In a more general way, the Nazarov cyclisation represents a tool for the introduction of 5-membered rings. The synthetic manipulation of the Nazarov product **6** successfully afforded taiwaniaquinoids, a family of East Asian conifers metabolites, among which taiwaniaquinone H, bearing a cyclopentadiene moiety (Scheme 6.2, b).^[6] The cyclopenta-fused tetracyclic structure of Akaol A was obtained by the Lewis acid-catalysed Nazarov cyclisation of aryl vinyl carbinol **7**, followed by hydrogenation of the double bond.^[7]



Scheme 6.2 Examples of the application of the Nazarov cyclisation in total synthesis.

6.1.2 Improving sustainability of the Nazarov cyclisation

As discussed in the previous Section, the Nazarov cyclisation represents a powerful synthetic tool and has been employed in several total synthesis. The wide diffusion of this reaction justifies the interest in developing modern methodologies to address its sustainability, which still presents some drawbacks. Indeed, the Brønsted acids used as promoters are usually strong acids (*i.e.* TFA, MsOH, TfOH), which are toxic and corrosive; moreover, they are often required in stoichiometric or super-stoichiometric amount. When Lewis acids are employed, either main-groups Lewis acids or transition metals, it should be pointed out that these are in many cases air- and moisture-sensitive and require strictly controlled conditions,

besides their often high cost. A third issue is represented by the solvent of the reaction: the Nazarov cyclisation is, in the great majority of cases, performed in VOCs, among which chlorinated solvents constitute a predominant part.^[8]

Up to now, the number of studies on more sustainable conditions for the Nazarov cyclisation is not as high as one would expect, given the relevance of this reaction in synthesis. On the side of the solvent, few examples report on the Nazarov cyclisations under neat conditions or through micellar catalysis in water, using sodium dodecylbenzenesulfonate as surfactant and InBr_3 as the promoter of the reaction.^[9] On the side of the catalyst system, improvements include the development of less toxic and/or recyclable promoters. As an example, a solid acid such as phosphomolybdic acid was employed as a heterogeneous catalyst for the mild and selective Nazarov cyclisation of several dienone substrates, with good selectivities in the presence of acid-labile functional groups; the catalyst loading was as low as 0.5 mol %. Furthermore, the authors showed that supporting the acid on SiO_2 resulted in increased efficiency of the process, by significative reduction of the reaction times, and allowed for the recycling of the catalyst system up to 4 cycles.^[10]

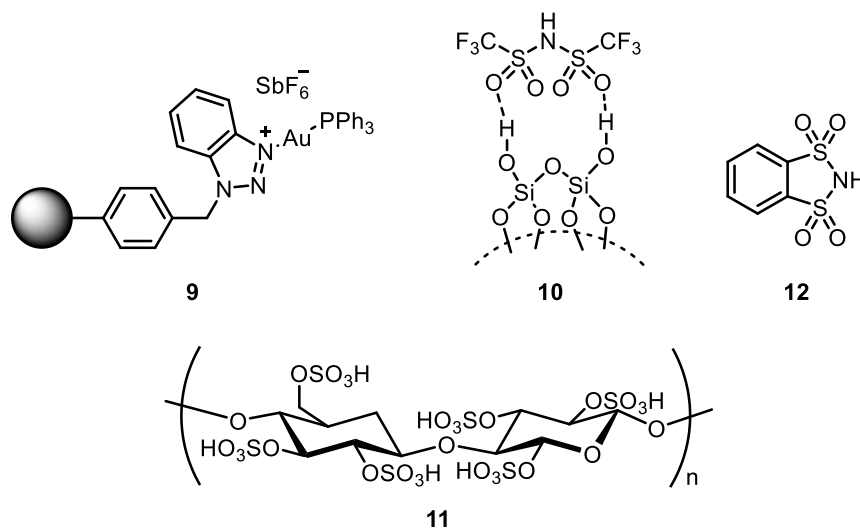


Figure 6.1 Examples of more sustainable heterogeneous and homogeneous catalysts for the Nazarov cyclisation.

The strategy of anchoring the catalyst to a solid support was also applied to a polystyrene-supported triazole Au(I) complex **9**^[11] and SiO_2 -supported trifluoromethanesulfonimide **10**, this latter in combination with flow technique in a reaction column (Figure 6.1).^[12] A similar concept inspired the design of a cellulose-based catalyst, in which the polysaccharide was modified by functionalization of the -OH groups with a sulfonic acid moiety **11**. Recovery of the catalyst system by simple filtration allowed also in this case its reuse, up to 6 cycles.^[13] On the other

hand, more sustainable catalysis under homogeneous conditions was envisaged with *o*-benzenedisulfonimide **12**, which was separated during the work-up procedure by virtue of its water solubility, allowing for its full recovery (Figure 6.1).^[14]

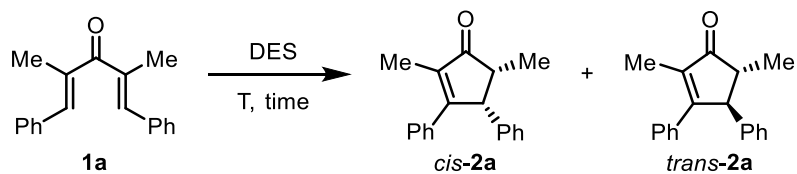
On these bases, we envisaged that deep eutectic solvents could offer a viable alternative to both conventional solvents and catalysts for the Nazarov cyclisation. As discussed in Section 5.2.1, DESs are active reaction media, effective in promoting several acid- and base-catalysed transformations. The aim of our study was to verify whether eutectic mixtures, in which one of the two components is a carboxylic acid, could be able to act as promoters for the Nazarov cyclisation. The use of naturally occurring weak acids would allow for a mild catalysis in a potentially renewable solvent system, displaying low toxicity and good biodegradability (see Section 5.1.2). Furthermore, we envisioned the possibility of recovering the NaDES at the end of the reaction and restoring it for other reaction cycles, thus further improving the green character of the methodology.

6.2 Study of the reaction conditions

We started our investigation on the Nazarov cyclisation in natural deep eutectic solvents by choosing the symmetrical dienone **1a** as the model substrate.^[15] We tested several NaDESs composed of choline chloride (ChCl) and carboxylic acids, represented in Figure 6.2, evaluating their ability to convert **1a** into cyclopentenone **2a** (Table 6.1). ChCl/L-(+)-lactic acid in 1:2 molar ratio was found to be ineffective in promoting the reaction at room temperature, even after 24 h (Table 6.1, entry 1), while with ChCl/oxalic acid 1:1 a 30% yield of **2a** was observed after 16 h (entry 2). Raising the temperature to 60 °C resulted in a significant improvement of the yield up to 91% (entry 3). We then tested other NaDESs based on carboxylic acids, such as L-(-)-malic acid, citric acid and L-(+)-tartaric acid, but in these cases the yields were lower (entries 4–6). On the other hand, with malonic acid (entry 7) and maleic acid (entry 8) as the HBD component of the eutectic mixture, product **2a** was obtained in good yields of 92% and 87% respectively. ChCl/*p*-toluenesulfonic acid (TsOH) in 1:2 molar ratio was also tested, affording a yield up to 99% (entry 9). Since TsOH is not a bio-derived compound, ChCl/TsOH is formally not a NaDES, however its toxicity and biodegradability were found to be comparable to those of the other acid-based NaDESs.^[16] Two NaDESs in which the HBA component is betaine (entry 11) or L-proline (entry 12), instead of ChCl, were found to be ineffective in promoting the reaction. We then performed some control experiments, at first with a DES not containing an acid, such as ChCl/H₂O 1:2 (entry 13), and with a polar protic organic solvent, such as EtOH

(entry 14). In both cases, no conversion into **2a** was observed, indicating that an acid-containing DES is required.

Table 6.1 Study of the reaction conditions for the Nazarov cyclisation of **1a**.^a



entry	solvent	T (°C)	time	yield ^b	<i>cis/trans</i> ^c
1	ChCl/L-(+)-lactic acid 1:2	rt	24 h	traces	–
2	ChCl/oxalic acid dihydrate 1:1	rt	16 h	30%	57/43
3	ChCl/oxalic acid dihydrate 1:1	60	16 h	91%	14/86
4	ChCl/L-(–)-malic acid/H ₂ O 1:1:2	60	16 h	22%	26/74 ^e
5	ChCl/citric acid 1:1 + 2% H ₂ O	60	16 h	36%	67/33
6	ChCl/L-(+)-tartaric acid 1:1 + 2% H ₂ O	80 ^d	16 h	67%	17/83 ^e
7	ChCl/malonic acid 1:1	60	16 h	92%	17/83
8	ChCl/maleic acid 1:1	60	16 h	87%	16/84
9	ChCl/TsOH monohydrate 1:2	60	16 h	99%	15/85
10	ChCl/R-(–)-mandelic acid 1:1	60	16 h	59%	20/80 ^e
11	betaine/malonic acid 1:2	60	16 h	–	–
12	L-proline/oxalic acid dihydrate 1:1	60	16 h	–	–
13	ChCl/H ₂ O 1:2	60	16 h	–	–
14	EtOH	60	16 h	–	–
15	EtOH (10 eq malonic acid)	60	16 h	33%	24/76
16	DCE (10 eq malonic acid)	60	16 h	traces	–
17	H ₂ O (10 eq malonic acid)	60	16 h	23%	30/70

^a All reactions were performed with 0.2 mmol of **1a** and 1.0 g of DES. ^b Yields of isolated products. ^c Determined by ¹H NMR analysis of purified compounds. ^d Higher temperature was required due to the viscosity of the medium. ^e 0% enantiomeric excess.

To get further insight into the activity of NaDESs in the Nazarov cyclisation, the acidic component alone, malonic acid, was tested in polar and apolar solvents such as ethanol (entry 15), 1,2-dichloroethane (entry 16) and water (entry 17). The low yield obtained, compared with the corresponding DES (entry 7), suggested that the activity is a property arising from the eutectic mixture rather than deriving from the acidic component *per se*.

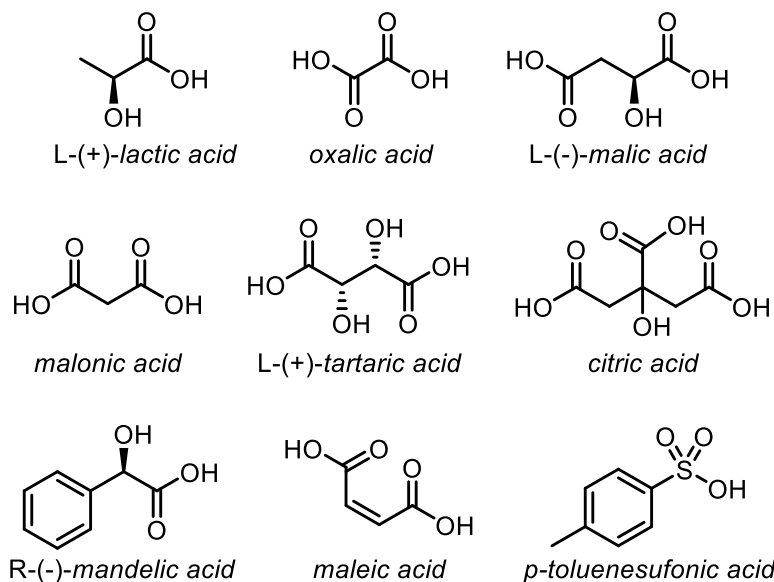


Figure 6.2 Acids used to form eutectic mixtures in combination with choline chloride.

The results reported in Table 6.1 can be analysed taking into consideration the pK_a of the acidic component of the various NaDESs, since the nature of the HBA component, ChCl, is fixed. Excluding the strong acid TsOH, three NaDESs were very effective, *i.e.* those containing malonic acid (pK_a 2.83), oxalic acid (1.23) and maleic acid (1.93). On the other hand, with L-(-)-malic acid (3.40) and citric acid (2.92) low yields were obtained, while with L-(+)-tartaric acid (2.99) and R-(-)-mandelic acid (3.41) intermediate performances were observed, affording **2a** in 67% and 59% yield respectively.^[17] It can be observed that these data do not account for a direct correlation between the pK_a of the acid and the yield of the corresponding NaDES in the Nazarov cyclisation. Indeed, it has already been argued that the acid/base behaviour of a DES can differ from that of its components alone, mainly due to the tight intermolecular interactions arising in the eutectic mixture. On this matter, a recent study highlighted that the temperature may also play a crucial role in affecting the acidity of a DES. Interestingly, a significant drop in the pH of ChCl/oxalic acid 1:1 and ChCl/malonic acid 1:1 was observed by raising the temperature from 20 °C to 60 °C.^[18] This is in line with our results, which showed comparable yields of **2a** at 60 °C for these two NaDESs, despite the different pK_a values of their HBD components (1.23 for oxalic acid and 2.83 for malonic acid).

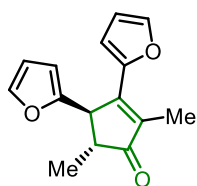
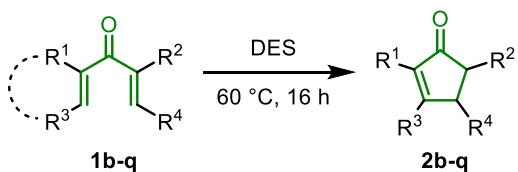
From the point of view of the *cis/trans* selectivity of the reaction, no diastereoselectivity was observed at room temperature (Table 6.1, entry 2), while at 60 °C a preference for the *trans* isomer of **2a** was generally ascertained. The best values lie around a *cis/trans* ratio of 15/85 and are observed with ChCl/oxalic

acid (entry 3), ChCl/malonic acid (entry 7), ChCl/maleic acid (entry 8) and ChCl/TsOH (entry 9), which are also those which afforded the best yields. In one case only, *i.e.* with ChCl/citric acid, the selectivity was in favour of *cis*-**2a** (entry 5). The relationship between the nature of the eutectic mixture and the diastereoselectivity can not be easily inferred: a model to fit the experimental data should take into account the interactions of the substrate with the components of the DES, considering also its supramolecular structure, during the multiple key activation steps of the reaction mechanism. Further computational and physicochemical investigation is required for a better elucidation of these aspects. However, it should be noted that no enantioselectivity was induced when NaDESs composed of chiral carboxylic acids were employed (entries 4, 6 and 10).

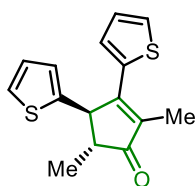
6.3 Reaction substrate scope

To study the substrate scope for the Nazarov cyclisation, the three best performing NaDESs among those presented in Table 6.1 were chosen, *i.e.* ChCl/malonic acid, ChCl/oxalic acid and ChCl/TsOH. Our approach was to always test the milder acid, malonic acid, first, and move to the other two only if it was not possible to achieve full conversion.

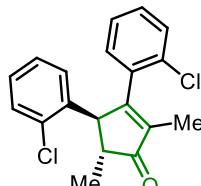
The different types of Nazarov products obtained are represented in Scheme 6.3. Symmetrical dienones bearing electron-rich as well as electron-poor aryl rings were successfully cyclised to the corresponding cyclopentenones **2b–e** with very good yields. Almost complete diastereoselectivity was observed in the case of sterically encumbered 2-chlorophenyl and 2,6-dichlorophenyl substituted products **2d** and **2e**. We then studied the reactivity of dienones embedded in a heterocyclic structure, because of the synthetic value of the opportunity to access heteropolycyclic molecular scaffolds. Indole cyclopentenones **2f–h** were obtained in 78–93% yields, and similar results were observed for dihydropyran derivatives **2i–o**. Remarkably, aryl vinyl ketones, which are less prone to undergo the cyclisation due to the transient dearomatisation required in the reaction mechanism, were successfully converted into the Nazarov products **2p** and **2q**.^[19]



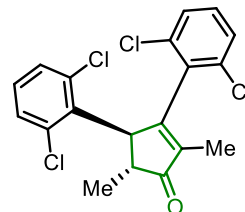
ChCl/oxalic acid 1:1
95%, dr 71/29



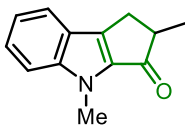
ChCl/malonic acid 1:1
83%, dr 56/44



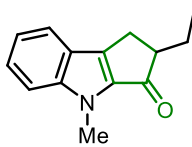
ChCl/TsOH 1:2
89%, dr 97/3



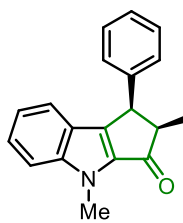
ChCl/TsOH 1:2
84%, dr 97/3



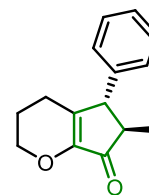
ChCl/oxalic acid 1:1
93%



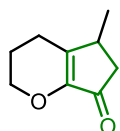
ChCl/oxalic acid 1:1
78%



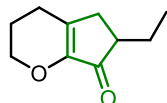
ChCl/malonic acid 1:1
80%, dr 60/40



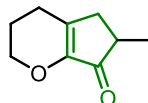
ChCl/malonic acid 1:1
82%, dr 77/23



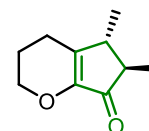
ChCl/malonic acid 1:1
84%



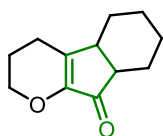
ChCl/malonic acid 1:1
85%



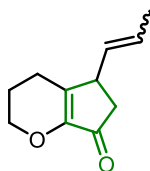
ChCl/malonic acid 1:1
94%



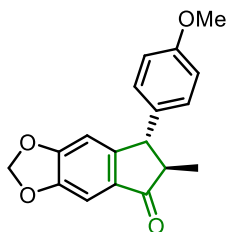
ChCl/malonic acid 1:1
95%, dr 86/14



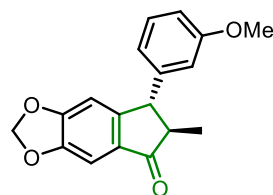
ChCl/malonic acid 1:1
82%



ChCl/malonic acid 1:1
91%



ChCl/TsOH 1:2
83%, dr 89/11



ChCl/TsOH 1:2
74%, dr 94/6

Scheme 6.3 Substrate scope. All reactions were performed with 0.5 mmol of substrate in 2.5 g of DES. Yields refer to isolated products. The diastereoisomeric ratios were determined by ^1H NMR.

We then tried to further extend the reaction scope by applying our conditions to other substrates, represented in Figure 6.3, for which the Nazarov cyclisation has never been reported. The indolyl phenyl ketone **1r** and the 1,3-dimethylindole derivative **1s** failed to convert into the corresponding cyclopentenone with all the three best NaDESs tested: the starting material was recovered unaltered. In the case of 7-azaindole derivative **1t**, some conversion was observed with ChCl/TsOH as the reaction medium, but the yield was low, and we considered not worthwhile to further investigate the reactivity of this substrate.

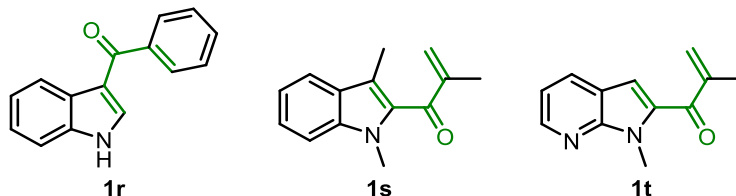


Figure 6.3 Substrates that failed to deliver the corresponding Nazarov product.

6.4 Recycling of the eutectic mixture

Having assessed the best conditions and the reaction substrate scope for the Nazarov cyclisation in deep eutectic solvents, we focused our attention on a central aspect in developing sustainable methodologies, which is the recyclability of the reaction solvent system.

At first, we studied the recycling of ChCl/malonic acid 1:1 in the cyclisation of dienone **1a**, at a concentration of 0.2 mmol/g (*i.e.* 0.2 mmol of substrate *per* g of NaDES). As discussed in Section 5.2.3, several procedures have been employed in the literature to separate the product from the eutectic mixture and restore the latter for another reaction cycle. In our case, we found that the addition of water at the end of the reaction induced the complete precipitation of product **2a**, while the NaDES components were dissolved in the aqueous phase. Filtration allowed to recover the solid organic product, while evaporation of water under reduced pressure allowed to restore the NaDES, which was used for another reaction cycle without further manipulation (Figure 6.6). This procedure allowed to run the Nazarov cyclisation for two cycles without any significant drop in the yield, and with an acceptable drop to 70% up to the fourth cycle (Figure 6.4). When we tried to recycle the NaDES for the fifth run, we observed a significantly lower yield.

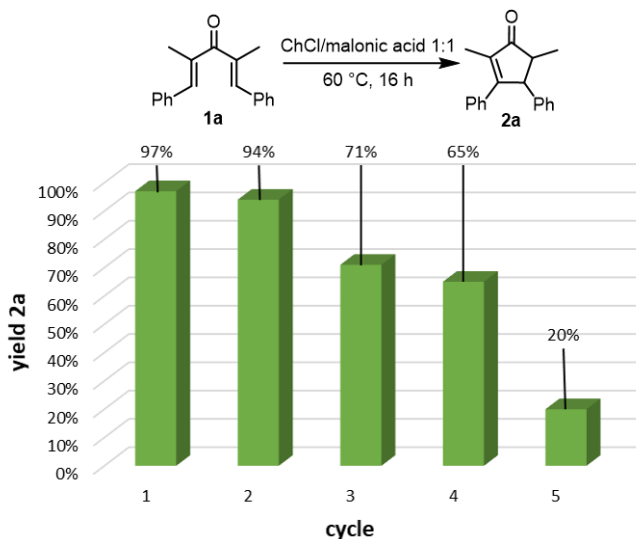


Figure 6.4 Recycling of ChCl/malonic 1:1 for the Nazarov cyclisation of **1a**. Yields determined by ^1H NMR with CH_3NO_2 as internal standard.

Since the activity of the NaDES is related to the intermolecular interactions that occur between its components and with the substrate, we tried to shed better light on the features of the eutectic mixture after every reaction cycle by ^1H NMR spectroscopy. After recovering the NaDES from the aqueous layer (Figure 6.6), a sample was introduced into a closed capillary, which was put into an NMR tube and surrounded with deuterated solvent to acquire the spectrum.

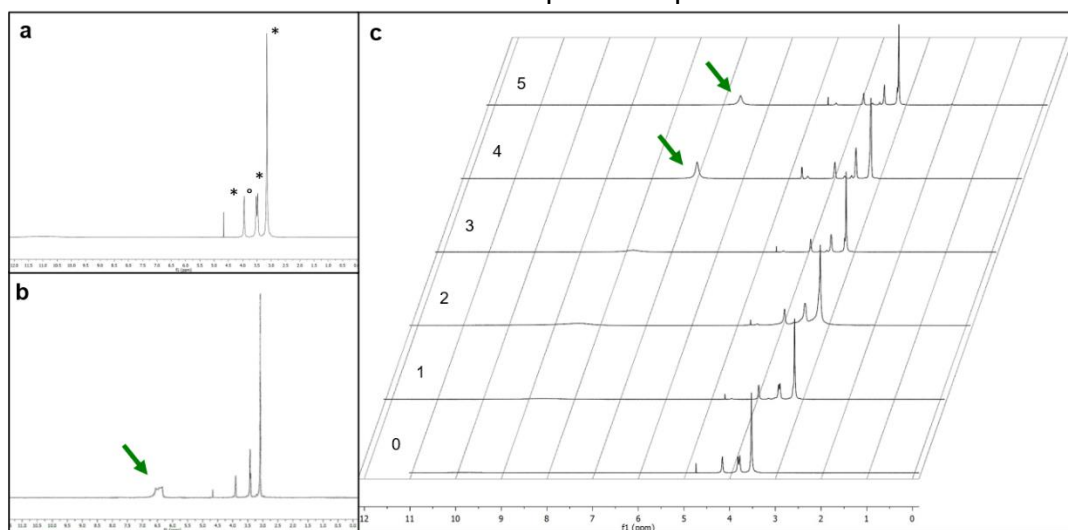


Figure 6.5 ^1H NMR spectra of ChCl/malonic acid NaDES. a) Freshly prepared ($^*\text{ChCl}$, $^*\text{malonic acid}$). b) Freshly prepared, with addition of 10% w/w H_2O . c) After the first (1), second (2), third (3), fourth (4) and fifth (5) cycle.

In Figure 6.5, a, the ^1H NMR spectrum of freshly prepared ChCl/malonic acid 1:1 shows the peaks attributable to ChCl (*) at 4.1 (2H), 3.4 (2H) and 3.1 (9H) ppm, while at 3.5 ppm lies the CH_2 group of malonic acid. The COOH proton is involved in the network of intermolecular H bonds and is barely detectable as a broad signal at 10-11 ppm. In Figure 6.5, b, the spectrum of the same NaDES, to which 10% w/w H_2O was added, is reported. In this case, a signal at around 7 ppm can be attributed to the water present in the structure of the eutectic mixture. In Figure 6.5, c, the spectra of ChCl/malonic acid after every reaction cycle are reported. The structure of the NaDES remains substantially unchanged after the first cycle (Figure 6.5, c, 1), compared to the freshly prepared one (Figure 6.5, c, 0); in these cases, yields of **2a** of 94% and 97% respectively were obtained (see Figure 6.4). Starting from the NaDES recovered from the second cycle, a broad signal around 8 ppm starts to appear and becomes progressively more evident after the fourth and fifth cycle, shifting towards 7 ppm. The presence of some other minor peaks might indicate that the constituents of the DES are partially decomposed.^[20] Comparing the spectrum of the NaDES after the fourth reaction cycle, which is almost inactive (20% yield of **2a**), with the spectrum of ChCl/malonic acid + 10% w/w H_2O , it appears that the fall in the performance in the Nazarov cyclisation is correlated with the presence of water entrapped in the structure of the eutectic mixture, which can not be removed by simple evaporation under reduced pressure. This could affect the properties of the solvent system and have a detrimental effect on its ability to convert the substrate **1a**. However, further physicochemical investigation is needed to fully characterize the consequences of the recycling procedure on the structure and activity of the eutectic mixture.

The positive results of the recycling experiments prompted us to further increase the efficiency of the process, with a view to its scalability. At first, we aimed to reduce the amount of NaDES employed for the reaction, finding the highest concentration at which the yield remained unaltered at 1.0 mmol/g, provided that the substrate was well dispersed in the medium and the stirring of the mixture was effective. This concentration was applied to a gram-scale experiment, with 1.05 g (4.0 mmol) of **1a** in 4.0 g of NaDES. The recycling procedure was applied to restore the eutectic mixture, as previously described, and to run a second reaction cycle with 4.0 mmol of **1a** (Figure 6.6). To minimize the waste, the water recovered from the evaporation under reduced pressure was used again for the second cycle. The overall process afforded 2.01 g of cyclopentenone **2a**, and employed only 4.0 g of ChCl/malonic acid. To quantify the green credentials of the protocol, the E-factor parameter could be calculated according to the following equation:^[21]

$$e - factor = \frac{g \text{ DES} + g \text{ H}_2\text{O}}{g \text{ 2a}} = \frac{4 \text{ g} + 35 \text{ g}}{2 \text{ g}} = 19.5$$

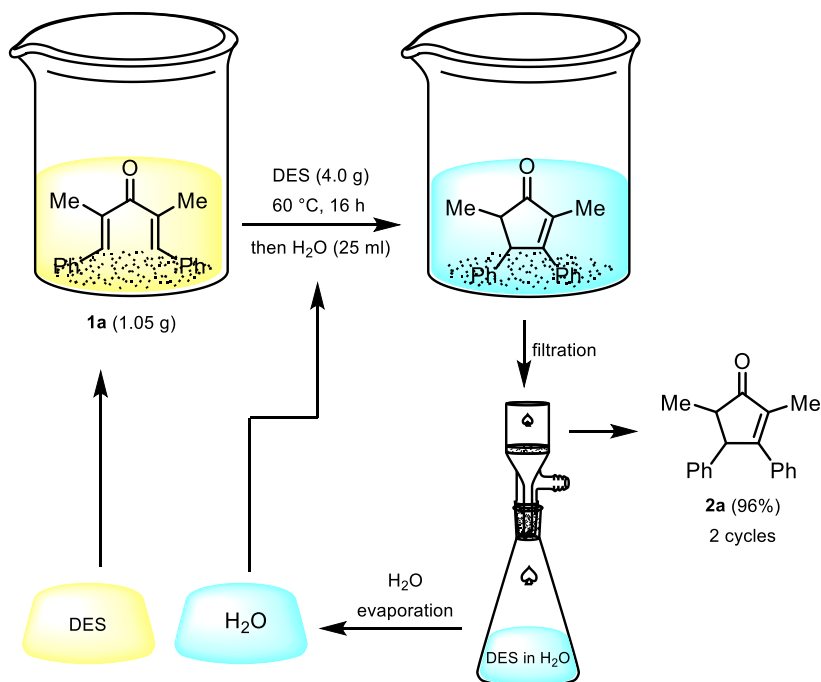


Figure 6.6 Two-cycles, gram-scale reaction.

6.5 Conclusion

Our investigation showed the feasibility of the Nazarov cyclisation in natural deep eutectic solvents, with high yields for different classes of dienone substrates. Remarkably, the emerging properties of the eutectic mixture enables an effective catalysis by weak carboxylic acids, which are normally considered as not active in promoting the reaction: the use of strong mineral acids is thus avoided, with advantages under the point of view of safety and sustainability. Moreover, an easy and practical recovery procedure allows for the recycle of the active solvent system up to 4 cycles with a tolerable loss in the reaction yield in the 3rd and 4th cycle.

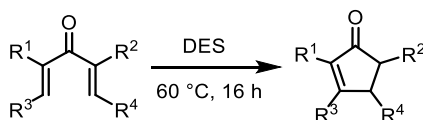
To improve our understanding of the actual catalytic mechanisms active during the transposition of acid-catalysed reactions into deep eutectic solvents, such as the Nazarov cyclisation, physicochemical as well as theoretical investigation is still needed. However, our results are in line with a growing body of literature in pointing towards a specific effect of eutectic mixtures in promoting this kind of reactions.

6.6 Experimental section

General information

Flasks and all equipment used for the generation and reaction of moisture-sensitive compounds were dried by electric heat gun under nitrogen. Unless specified, all reagents were used as received without further purifications. Anhydrous THF was obtained by distillation over LiAlH₄, followed by distillation over Na-benzophenone; benzaldehyde was distilled under vacuum. Flash column chromatography was performed over silica gel (40–63 μm, 230–400 mesh); *R_f* values refer to TLC carried out on silica gel plates. ¹H NMR and ¹³C NMR spectra were recorded on a Jeol ECZR600, in CDCl₃, using residual solvent peak as an internal reference (CHCl₃, ¹H: 7.26 ppm, ¹³C: 77.16 ppm). NMR spectra of DESs were recorded in a capillary tube, using D₂O as locking solvent. Multiplicity is reported as follows: s (singlet), d (doublet), t (triplet), q (quartet), quin (quintet), sext (sextet), m (multiplet), br (broad). GC-MS spectra were recorded at an ionizing voltage of 70 eV.

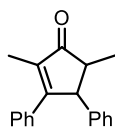
General procedure for the Nazarov cyclisation in DES



A vial was charged with the dienone substrate (0.2–0.5 mmol), then the DES (5 g per mmol of substrate) was added and the mixture was stirred at 60 °C for 16 h. Water was added and the mixture was extracted three times with cyclopentyl methyl ether (CPME); the combined organic layers were dried over anhydrous Na₂SO₄, filtered and the solvent was evaporated under reduced pressure. When required, the crude product was purified by flash column chromatography.

Procedure for DES recycling: a vial was charged with the dienone **1a** (1.0–4.0 mmol), then ChCl/malonic acid 1:1 (5 g or 1 g per mmol of substrate) was added and the mixture was stirred at 60 °C for 16 h. Water was added, causing the precipitation of the product. The solid product was recovered by filtration, while water was evaporated under reduced pressure to afford the eutectic mixture, which was used for the next reaction cycle.

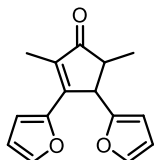
2,5-dimethyl-3,4-diphenylcyclopent-2-en-1-one, **2a**^[22]



Synthesised according to the general procedure with ChCl/malonic acid 1:1. White solid, 92% yield, *trans/cis* ratio 83/17. *R_f* 0.25 (9/1 PE/Et₂O). **trans-2a** ¹H NMR (600 MHz) δ (ppm): 7.34–7.24 (m, 5H), 7.23–7.19 (m, 2H), 7.15–7.11 (m, 1H), 7.09–7.06 (m, 2H), 3.98 (quin, 1H, *J* = 2.2 Hz), 2.41 (qd, 1H, *J* = 7.3, 2.8 Hz), 2.03 (d, 3H, *J* = 2.0 Hz), 1.36 (d, 3H, *J* = 7.5 Hz). ¹³C NMR (150 MHz) δ (ppm): 211.1 (Cq), 167.2 (Cq), 142.2 (Cq), 136.9 (Cq), 135.3 (Cq), 129.1 (CH), 128.9 (CH), 128.5 (CH), 128.4 (CH), 127.7 (CH), 126.8 (CH), 56.5 (CH), 51.4 (CH), 15.4 (CH₃), 10.3 (CH₃). **GC-MS** *m/z* (%): 262 [M]⁺ (100), 247 (88), 219 (38), 115 (36). **cis-2a** ¹H NMR (600 MHz)

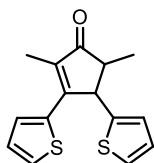
δ (ppm): 7.40–7.37 (m, 2H), 7.34–7.24 (m, 4H), 7.24–7.19 (m, 2H), 7.18–7.16 (m, 1H), 7.00 (br s, 1H), 4.63–4.60 (m, 1H), 2.92 (quin, 1H, $J = 7.4$ Hz), 2.09 (d, 3H, $J = 1.7$ Hz), 0.76 (d, 3H, $J = 7.5$ Hz). **^{13}C NMR** (150 MHz) δ (ppm): 211.6 (Cq), 166.4 (Cq), 139.3 (Cq), 137.1 (Cq), 135.9 (Cq), 129.1 (CH), 128.5 (CH), 128.5 (CH), 128.4 (CH), 127.7 (CH), 127.0 (CH), 52.7 (CH), 45.6 (CH), 12.4 (CH₃), 10.4 (CH₃). **GC-MS** m/z (%): 262 (100), 247 (92), 219 (40), 115 (40).

*3,4-di(furan-2-yl)-2,5-dimethylcyclopent-2-en-1-one, 2b*²²¹



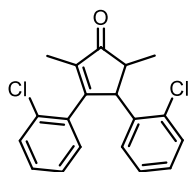
Synthesised according to the general procedure with ChCl /oxalic acid 1:1. Orange solid, 95% yield, *trans/cis* ratio 71/29. R_f 0.18 (9/1 PE/Et₂O). ***trans-2b*** **^1H NMR** (600 MHz) δ (ppm): 7.55 (d, 1H, $J = 1.4$ Hz), 7.29–7.28 (m, 1H), 6.56 (d, 1H, $J = 3.4$ Hz), 6.46–6.44 (m, 1H), 6.28 (dd, 1H, $J = 3.1, 1.7$ Hz), 6.10 (d, 1H, $J = 3.1$ Hz), 3.96–3.94 (m, 1H), 2.54 (qd, 1H, $J = 7.4, 2.8$ Hz), 2.15 (d, 3H, $J = 1.7$ Hz), 1.30 (d, 3H, $J = 7.6$ Hz). **^{13}C NMR** (150 MHz) δ (ppm): 209.6 (Cq), 154.9 (Cq), 151.0 (Cq), 150.6 (Cq), 144.9 (CH), 144.8 (CH), 133.5 (Cq), 114.8 (CH), 112.2 (CH), 110.5 (CH), 106.3 (CH), 47.5 (CH), 47.1 (CH), 16.2 (CH₃), 10.1 (CH₃). **GC-MS** m/z (%): 242 [M]⁺ (100), 227 (29). ***cis-2b*** **^1H NMR** (600 MHz) δ (ppm): 7.54 (d, 1H, $J = 1.4$ Hz), 7.28–7.27 (m, 1H), 6.59 (d, 1H, $J = 3.4$ Hz), 6.46–6.44 (m, 1H), 6.36 (dd, 1H, $J = 3.1, 2.1$ Hz), 6.03 (d, 1H, $J = 3.1$ Hz), 4.57 (d, 1H, $J = 7.2$ Hz), 2.83–2.77 (m, 1H), 2.17 (d, 3H, $J = 1.7$ Hz), 0.88 (d, 3H, $J = 7.6$ Hz). **^{13}C NMR** (150 MHz) δ (ppm): 209.8 (Cq), 153.5 (Cq), 151.3 (Cq), 150.5 (Cq), 144.9 (CH), 141.8 (CH), 133.8 (Cq), 114.4 (CH), 112.2 (CH), 110.4 (CH), 107.9 (CH), 44.9 (CH), 43.5 (CH), 11.5 (CH₃), 10.1 (CH₃). **GC-MS** m/z (%): 242 [M]⁺ (100), 227 (29).

*2,5-dimethyl-3,4-di(thiophen-2-yl)cyclopent-2-en-1-one, 2c*²²¹



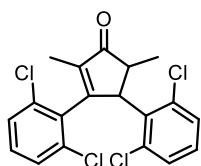
Synthesised according to the general procedure with ChCl /malonic acid 1:1. White solid, 83% yield, *trans/cis* ratio 56/44. R_f 0.20 (9/1 PE/Et₂O). ***trans-2c*** **^1H NMR** (600 MHz) δ (ppm): 7.52–7.49 (m, 1H), 7.29 (d, 1H, $J = 3.8$ Hz), 7.15–7.12 (m, 1H), 7.07–7.04 (m, 1H), 6.92–6.89 (m, 1H), 6.86 (d, 1H, $J = 3.4$ Hz), 4.24 (br s, 1H), 2.49 (qd, 1H, $J = 7.4$ Hz, 2.4 Hz), 2.16 (d, 3H, $J = 1.7$ Hz), 1.34 (d, 3H, $J = 7.6$ Hz). **^{13}C NMR** (150 MHz) δ (ppm): 209.3 (Cq), 157.5 (Cq), 146.6 (Cq), 138.1 (Cq), 133.9 (Cq), 130.4 (CH), 130.0 (CH), 127.7 (CH), 127.1 (CH), 124.8 (CH), 124.4 (CH), 51.8 (CH), 51.2 (CH), 16.4 (CH₃), 10.6 (CH₃). **GC-MS** m/z (%): 274 [M]⁺ (100), 259 (57), 231 (37). ***cis-2c*** **^1H NMR** (600 MHz) δ (ppm): 7.52–7.49 (m, 1H), 7.36 (d, 1H, $J = 3.4$ Hz),), 7.15–7.12 (m, 1H), 7.07–7.04 (m, 1H), 6.92–6.89 (m, 1H), 6.78 (d, 1H, $J = 3.1$ Hz), 4.85 (d, 1H, $J = 7.2$ Hz), 2.87 (quin, 1H, $J = 7.2$ Hz), 2.18 (d, 3H, $J = 1.4$ Hz), 0.89 (d, 3H, $J = 7.6$ Hz). **^{13}C NMR** (150 MHz) δ (ppm): 209.4 (Cq), 157.7 (Cq), 143.6 (Cq), 138.6 (Cq), 133.7 (Cq), 129.9 (CH), 129.9 (CH), 127.7 (CH), 127.1 (CH), 126.2 (CH), 124.4 (CH), 47.4 (CH), 46.0 (CH), 11.3 (CH₃), 10.5 (CH₃). **GC-MS** m/z (%): 274 [M]⁺ (100), 259 (55), 231 (38).

3,4-bis(2-chlorophenyl)-2,5-dimethylcyclopent-2-en-1-one, 2d^[22]



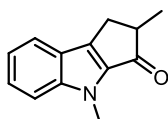
Synthesised according to the general procedure with ChCl/TsOH 1:2. White solid, 89% yield, *trans/cis* ratio 97/3. **R_f** 0.24 (9/1 PE/Et₂O). **trans-2d** **¹H NMR** (600 MHz) δ (ppm): 7.33 (d, 1H, *J* = 8.3 Hz), 7.22 (d, 1H, *J* = 7.6 Hz), 7.18–7.10 (m, 4H), 7.06–7.02 (m, 2H), 4.74 (br s, 1H), 2.53 (br s, 1H), 1.77 (s, 3H), 1.41 (d, 3H, *J* = 6.9 Hz). **¹³C NMR** (150 MHz) δ (ppm): 210.2 (Cq), 165.7 (Cq), 139.8 (Cq), 138.6 (Cq), 134.7 (Cq), 134.3 (Cq), 132.4 (Cq), 130.0 (CH), 129.8 (CH), 129.8 (CH), 129.8 (CH), 129.3 (CH), 128.2 (CH), 127.3 (CH), 126.6 (CH), 53.3 (CH), 50.8 (CH), 15.7 (CH₃), 9.8 (CH₃). **GC-MS** *m/z* (%): 332 [M+2]⁺ (65), 330 [M]⁺ (98), 317 (66), 315 (100), 297 (23), 295 (65), 269 (27), 267 (79), 232 (30), 202 (31), 115 (56).

3,4-bis(2,6-dichlorophenyl)-2,5-dimethylcyclopent-2-en-1-one, 2e^[22]



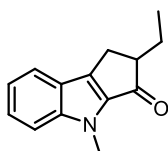
Synthesised according to the general procedure with ChCl/TsOH 1:2. White solid, 84% yield, *trans/cis* ratio 97/3. **R_f** 0.41 (9/1 PE/Et₂O). **trans-2e** **¹H NMR** (600 MHz) δ (ppm): 7.34 (dd, 1H, *J* = 7.9, 1.4 Hz), 7.20–7.12 (m, 4H), 7.04 (t, 1H, *J* = 7.9 Hz), 5.13–5.11 (m, 1H), 3.21 (qd, 1H, *J* = 7.4, 1.2 Hz), 1.68 (d, 3H, *J* = 1.7 Hz), 1.39 (d, 3H, *J* = 7.6 Hz). **¹³C NMR** (150 MHz) δ (ppm): 211.6 (Cq), 160.6 (Cq), 141.0 (Cq), 137.1 (Cq), 136.8 (Cq), 134.4 (Cq), 133.7 (Cq), 133.2 (Cq), 133.1 (Cq), 130.5 (CH), 130.2 (CH), 128.8 (CH), 128.4 (CH), 128.2 (CH), 52.6 (CH), 45.4 (CH), 18.1 (CH₃), 9.3 (CH₃). **GC-MS** *m/z* (%): 402 [M+4]⁺ (35), 400 [M+2]⁺ (69), 398 [M]⁺ (54), 387 (25), 385 (51), 383 (39), 365 (46), 363 (48), 339 (32), 337 (97), 335 (100), 302 (40), 300 (61), 151 (30), 149 (47), 115 (37), 113 (32).

2,4-dimethyl-1,4-dihydrocyclopenta[b]indol-3(2H)-one, 2f^[23]



Synthesised according to the general procedure with ChCl/oxalic acid 1:1. Beige solid, 93% yield. **R_f** 0.13 (95/5 PE/EtOAc). **¹H NMR** (600 MHz) δ (ppm): 7.70–7.68 (m, 1H), 7.42 (ddd, 1H, *J* = 8.3, 6.9, 1.2 Hz), 7.38–7.36 (m, 2H), 7.17 (ddd, 1H, *J* = 7.9, 6.9, 1.0 Hz), 3.92 (s, 3H), 3.33 (dd, 1H, *J* = 16.7, 6.4 Hz), 3.07–3.02 (m, 1H), 2.65 (dd, 1H, *J* = 16.5, 2.4 Hz), 1.37 (d, 3H, *J* = 7.6 Hz). **¹³C NMR** (150 MHz) δ (ppm): 198.1 (Cq), 145.2 (Cq), 143.1 (Cq), 138.2 (Cq), 126.9 (CH), 123.2 (Cq), 121.9 (CH), 120.3 (CH), 111.1 (CH), 47.6 (CH₃), 30.3 (CH), 28.8 (CH₂), 17.4 (CH₃). **GC-MS** *m/z* (%): 199 [M]⁺ (94), 184 (100), 171 (34), 170 (43).

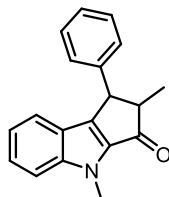
2-ethyl-4-methyl-1,4-dihydrocyclopenta[b]indol-3(2H)-one, 2g^[23]



Synthesised according to the general procedure with ChCl/oxalic acid 1:1. White solid, 78% yield. **R_f** 0.21 (95/5 PE/EtOAc). **¹H NMR** (600 MHz) δ (ppm): 7.70 (d, 1H, *J* = 8.3 Hz), 7.44–7.40 (m, 1H), 7.38–7.36 (m, 1H), 7.18 (ddd, 1H, *J* = 7.9, 6.9, 1.0 Hz), 3.92 (s, 3H), 3.24 (dd, 1H, *J* = 16.7, 6.4 Hz), 2.94 (dddd, 1H, *J* = 9.0, 6.5, 4.1, 2.2 Hz), 2.74 (dd, 1H, *J* = 16.7,

2.2 Hz), 2.05–1.98 (m, 1H), 1.66–1.58 (m, 1H), 1.03, (t, 3H, $J = 7.4$ Hz). **^{13}C NMR** (150 MHz) δ (ppm): 197.4 (Cq), 145.1 (Cq), 143.5 (Cq), 138.8 (Cq), 126.8 (CH), 123.2 (Cq), 121.9 (CH), 120.3 (CH), 111.1 (CH), 54.3 (CH₃), 30.22 (CH), 26.0 (CH₂), 25.1 (CH₂), 11.6 (CH₃). **GC-MS** m/z (%): 275 [M]⁺ (100), 260 (39), 246 (43), 232 (74).

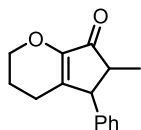
2,4-dimethyl-1-phenyl-1,4-dihydrocyclopenta[b]indol-3(2H)-one, 2h^[24]



Synthesised according to the general procedure with ChCl/malonic acid 1:1. Pale yellow solid, 80% yield, *trans/cis* ratio 40/60. **R_f** 0.21 (95/5 PE/EtOAc).

trans-2h ^1H NMR (600 MHz) δ (ppm): 7.43–7.40 (m, 2H), 7.38–7.36 (m, 1H), 7.34–7.22 (m, 4H), 7.10–7.05 (m, 2H), 4.80 (d, 1H, $J = 6.5$ Hz), 4.00 (s, 3H), 3.42–3.36 (m, 1H), 0.86 (d, 3H, $J = 7.6$ Hz). **^{13}C NMR** (150 MHz) δ (ppm): 197.4 (Cq), 145.3 (Cq), 144.5 (Cq), 139.9 (Cq), 138.7 (Cq), 129.1 (CH), 128.9 (CH), 128.3 (CH), 127.4 (CH), 126.9 (CH), 126.8 (CH), 122.9 (Cq), 122.5 (CH), 120.4 (CH), 111.1 (CH), 52.5 (CH₃), 43.7 (CH), 30.3 (CH), 14.1 (CH₃). **GC-MS** m/z (%): 275 [M]⁺ (100), 260 (37), 246 (46), 232 (78). **cis-2h ^1H NMR** (600 MHz) δ (ppm): 7.43–7.40 (m, 2H), 7.34–7.22 (m, 5H), 7.10–7.05 (m, 2H), 4.14 (d, 1H, $J = 3.1$ Hz), 3.99 (s, 3H), 2.87 (qd, 1H, $J = 7.4, 2.9$ Hz), 1.48 (d, 3H, $J = 7.6$ Hz). **^{13}C NMR** (150 MHz) δ (ppm): 196.6 (Cq), 145.2 (Cq), 144.1 (Cq), 142.3 (Cq), 138.3 (Cq), 129.1 (CH), 128.9 (CH), 128.3 (CH), 127.4 (CH), 127.0 (CH), 126.8 (CH), 122.7 (Cq), 122.3 (CH), 120.5 (CH), 111.1 (CH), 58.9 (CH₃), 48.5 (CH), 30.3 (CH), 15.4 (CH₃). **GC-MS** m/z (%): 275 [M]⁺ (100), 260 (39), 246 (43), 232 (74).

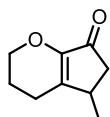
6-methyl-5-phenyl-3,4,5,6-tetrahydrocyclopenta[b]pyran-7(2H)-one, 2i^[25]



Synthesised according to the general procedure with ChCl/malonic acid 1:1. White oil, 82% yield, *trans/cis* ratio 77/23. **R_f** 0.28 (8/2 PE/EtOAc). **trans-2i**

^1H NMR (600 MHz) δ (ppm): 7.36–7.32 (m, 2H), 7.27–7.25 (m, 1H), 7.15–7.12 (m, 2H), 4.17–4.14 (m, 2H), 3.35 (q, 1H, $J = 1.9$ Hz), 2.25 (qd, 1H, $J = 7.4, 2.3$ Hz), 2.10 (td, 2H, $J = 6.6, 1.8$ Hz), 2.00–1.88 (m, 2H), 1.27 (t, 3H, $J = 7.4$ Hz). **^{13}C NMR** (150 MHz) δ (ppm): 202.7 (Cq), 150.8 (Cq), 145.4 (Cq), 141.2 (Cq), 129.1 (CH), 127.4 (CH), 127.3 (CH), 67.0 (CH₂), 53.3 (CH), 49.4 (CH), 22.1 (CH₂), 21.6 (CH₂), 15.0 (CH₃). **cis-2i ^1H NMR** (600 MHz) δ (ppm): 7.33–7.30 (m, 2H), 7.27–7.24 (m, 1H), 7.03 (d, 2H, $J = 7.2$ Hz), 4.22 (ddd, 1H, $J = 10.3, 6.5, 3.4$ Hz), 4.19–4.15 (m, 1H), 4.02 (d, 1H, $J = 6.5$ Hz), 2.79–2.73 (m, 1H), 2.19 (t, 2H, $J = 6.2$ Hz), 2.00–1.88 (m, 2H), 0.69 (d, 3H, $J = 7.6$ Hz). **^{13}C NMR** (150 MHz) δ (ppm): 203.1 (Cq), 151.7 (Cq), 145.0 (Cq), 138.7 (Cq), 129.1 (CH), 128.6 (CH), 127.2 (CH), 67.2 (CH₂), 48.9 (CH), 43.4 (CH), 22.6 (CH₂), 21.8 (CH₂), 12.4 (CH₃).

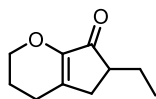
5-methyl-3,4,5,6-tetrahydrocyclopenta[b]pyran-7(2H)-one, 2j^[26]



Synthesised according to the general procedure with ChCl/malonic acid 1:1. Pale yellow oil, 84% yield. **^1H NMR** (600 MHz) δ (ppm): 4.13–4.08 (m, 1H), 4.05–4.00 (m, 1H), 2.74–2.68 (m, 1H), 2.59 (dd, $J = 18.6, 6.2$ Hz, 1H), 2.41 (dt, $J =$

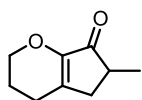
18.9, 6.9 Hz, 1H), 2.19 (dt, $J = 18.6, 5.9$ Hz, 1H), 1.96–1.90 (m, 3H), 1.14 (d, $J = 6.9$ Hz, 3H). **^{13}C NMR** (150 MHz) δ (ppm): 200.2 (Cq), 150.6 (Cq), 149.7 (Cq), 66.8 (CH₂), 41.6 (CH₂), 32.1 (CH), 21.9 (CH₂), 21.5 (CH₂), 19.3 (CH₃). **GC-MS** m/z (%): 152 [M]⁺ (97), 137 (100), 124 (25), 109 (31), 81 (44).

6-ethyl-3,4,5,6-tetrahydrocyclopenta[b]pyran-7(2H)-one, 2k^[25]



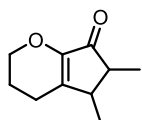
Synthesised according to the general procedure with ChCl/malonic acid 1:1. White oil, 83% yield. **^1H NMR** (600 MHz) δ (ppm): 4.09–4.02 (m, 2H), 2.57 (ddt, $J = 17.4, 6.3, 1.7$ Hz, 1H), 2.31 (t, $J = 6.4$ Hz, 2H), 2.27–2.22 (m, 1H), 2.09 (dq, $J = 17.4, 1.9$ Hz, 1H), 1.94–1.89 (m, 2H), 1.84–1.77 (m, 1H), 1.41–1.33 (m, 1H), 0.90 (t, $J = 7.4$ Hz, 3H). **^{13}C NMR** (150 MHz) δ (ppm): 203.0 (Cq), 150.7 (Cq), 144.4 (Cq), 66.8 (CH₂), 44.8 (CH), 32.8 (CH₂), 24.4 (CH₂), 24.1 (CH₂), 21.7 (CH₂), 11.2 (CH₃). **GC-MS** m/z (%): 166 [M]⁺ (40), 138 (100), 110 (22), 95 (15).

6-methyl-3,4,5,6-tetrahydrocyclopenta[b]pyran-7(2H)-one, 2l^[25]



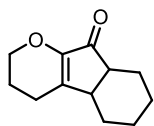
Synthesised according to the general procedure with ChCl/malonic acid 1:1. Pale yellow oil, 94% yield. **^1H NMR** (600 MHz) δ (ppm): 4.11–4.06 (m, 2H), 2.68 (ddt, 1H, $J = 17.4, 6.4, 1.6$ Hz), 2.40–2.34 (m, 1H), 2.33–2.30 (m, 2H), 2.02 (dq, 1H; $J = 17.4, 1.8$ Hz), 1.96–1.91 (m, 2H), 1.17 (d, 3H, $J = 7.5$ Hz). **^{13}C NMR** (150 MHz) δ (ppm): 203.7 (Cq), 150.3 (Cq), 140.1 (Cq), 66.9 (CH₂), 38.1 (CH), 35.0 (CH₂), 24.1 (CH₂), 21.7 (CH₂), 16.6 (CH₃). **GC-MS** m/z (%): 152 [M]⁺ (100), 137 (43), 109 (20), 96 (24), 95 (26), 81 (20), 68 (31), 67 (36).

5,6-dimethyl-3,4,5,6-tetrahydrocyclopenta[b]pyran-7(2H)-one, 2m^[25]



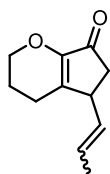
Synthesised according to the general procedure with ChCl/malonic acid 1:1. Pale yellow oil, 95% yield, *trans/cis* ratio 86/14. ***trans*-2m** **^1H NMR** (600 MHz) δ (ppm): 4.11–4.08 (m, 1H), 4.07–4.03 (m, 1H), 2.43–2.36 (m, 1H), 2.27–2.22 (m, 1H), 2.22–2.15 (m, 1H), 1.94 (quin, $J = 5.8$ Hz, 2H), 1.90–1.85 (m, 1H), 1.17 (t, $J = 7.3$ Hz, 3H), 1.16 (d, $J = 7.0$ Hz, 3H). **^{13}C NMR** (150 MHz) δ (ppm): 202.8 (Cq), 149.6 (Cq), 147.6 (Cq), 66.7 (CH₂), 47.4 (CH), 41.4 (CH), 21.7 (CH₂), 21.7 (CH₂), 17.9 (CH₃), 14.8 (CH₃). **GC-MS** m/z (%): 166 [M]⁺ (49), 151 (100), 95 (23) 67 (20). ***cis*-2m** **^1H NMR** (600 MHz) δ (ppm): 4.16–4.12 (m, 1H), 4.03–3.99 (m, 1H), 2.84–2.78 (m, 1H), 2.51–2.46 (m, 1H), 2.43–2.36 (m, 1H), 2.22–2.15 (m, 1H), 1.94 (quin, $J = 5.8$ Hz, 2H), 1.08 (d, $J = 7.6$ Hz, 3H), 1.04 (d, $J = 7.3$ Hz, 3H). **^{13}C NMR** (150 MHz) δ (ppm): 203.4 (Cq), 150.0 (Cq), 148.9 (Cq), 66.9 (CH₂), 42.2 (CH), 36.2 (CH), 22.1 (CH₂), 21.7 (CH₂), 14.9 (CH₃), 11.3 (CH₃). **GC-MS** m/z (%): 166 [M]⁺ (57), 151 (100), 95 (25), 67 (23)

3,4,4b,5,6,7,8,8a-octahydroindeno[2,1-*b*]pyran-9(2*H*)-one, **2n**^[25]



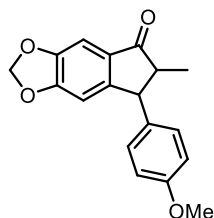
Synthesised according to the general procedure with ChCl/malonic acid 1:1. Pale yellow oil, 83% yield. *R_f* 0.20 (8/2 PE/EtOAc). **¹H NMR** (600 MHz) δ (ppm): 4.12–4.08 (m, 1H), 4.05–4.01 (m, 1H), 2.73–2.69 (m, 1H), 2.40 (q, 1H, *J* = 6.4 Hz), 2.38–2.32 (m, 1H), 2.45–2.19 (m, 1H), 1.98–1.86 (m, 3H), 1.84–1.78 (m, 1H), 1.72–1.64 (m, 1H), 1.51–1.43 (m, 2H), 1.40–1.28 (m, 2H), 1.19–1.14 (m, 1H). **¹³C NMR** (150 MHz) δ (ppm): 203.0 (Cq), 150.4 (Cq), 148.4 (Cq), 67.0 (CH₂), 43.9 (CH), 37.7 (CH), 29.8 (CH₂), 26.8 (CH₂), 22.1 (CH₂), 21.8 (CH₂), 20.6 (CH₂), 20.5 (CH₂). **GC-MS** *m/z* (%): 192 [M]⁺ (100), 164 (68), 149 (25), 138 (24), 136 (24), 135 (42), 79 (33).

5-(prop-1-en-1-yl)-3,4,5,6-tetrahydrocyclopenta[*b*]pyran-7(2*H*)-one, **2o**^[25]



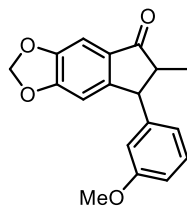
Synthesised according to the general procedure with ChCl/malonic acid 1:1. Pale yellow oil, 91% yield. *R_f* 0.19 (8/2 PE/EtOAc). (*E*)-**2o** **¹H NMR** (600 MHz) δ (ppm): 5.63–5.55 (m, 1H), 5.15 (ddq, 1H, *J* = 14.8, 9.0, 1.5 Hz), 4.11–4.04 (m, 2H), 3.20 (t, 1H, *J* = 7.2 Hz), 2.62 (dd, 1H, *J* = 18.8, 6.4 Hz), 2.34 (dt, 1H, *J* = 18.9, 6.4 Hz), 2.16 (dt, 2H, *J* = 19.6, 6.9 Hz), 1.93–1.90 (m, 2H), 1.68 (d, 3H, *J* = 6.5, 1.7 Hz). **¹³C NMR** (150 MHz) δ (ppm): 200.0 (Cq), 151.0 (Cq), 147.5 (Cq), 131.6 (CH), 127.8 (CH), 66.9 (CH₂), 41.3 (CH), 40.4 (CH₂), 22.4 (CH₂), 21.6 (CH₂), 17.9 (CH₃). **GC-MS** *m/z* (%): 178 [M]⁺ (100), 163 (85), 150 (46), 135 (67), 91 (30), 79 (62).

7-(4-methoxyphenyl)-6-methyl-6,7-dihydro-5*H*-indeno[5,6-*d*][1,3]dioxol-5-one, **2p**^[19]



Synthesised according to the general procedure with ChCl/TsOH 1:2. Colourless oil, 83% yield, *trans/cis* ratio 89/11. *R_f* 0.26 (9/1 PE/EtOAc). ***trans*-2p** **¹H NMR** (600 MHz) δ (ppm): 7.13 (s, 1H), 7.08–7.05 (m, 2H), 6.88–6.85 (m, 2H), 6.54 (s, 1H), 6.03 (s, 2H), 3.84 (d, 1H, *J* = 4.5 Hz), 3.80 (s, 3H), 2.57 (qd, 1H, *J* = 7.3, 4.5 Hz), 1.32 (d, 3H, *J* = 7.3 Hz). **¹³C NMR** (150 MHz) δ (ppm): 206.0 (Cq), 158.8 (Cq), 154.5 (Cq), 154.0 (Cq), 148.7 (Cq), 134.9 (Cq), 120.9 (Cq), 129.0 (CH), 114.4 (CH), 105.8 (CH), 102.3 (CH₂), 102.0 (CH), 55.4 (CH₃), 54.0 (CH), 53.0 (CH), 14.5 (CH₃). **GC-MS** *m/z* (%): 296 [M]⁺ (94), 281 (100),

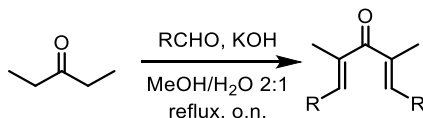
7-(3-methoxyphenyl)-6-methyl-6,7-dihydro-5*H*-indeno[5,6-*d*][1,3]dioxol-5-one, **2q**^[19]



Synthesised according to the general procedure with ChCl/TsOH 1:2. Colourless oil, 74% yield, *trans/cis* ratio 96/4. *R_f* 0.28 (9/1 PE/EtOAc). ***trans*-2p** **¹H NMR** (600 MHz) δ (ppm): 7.25 (t, 1H, *J* = 8.0 Hz), 7.14 (s, 1H), 6.82 (ddd, 1H, *J* = 8.3, 2.6, 0.8 Hz), 6.74 (br d, 1H, *J* = 7.7 Hz), 6.68–6.67 (m, 1H), 6.58 (s, 1H), 6.05 (s, 2H), 3.87 (d, 1H, *J* = 4.4 Hz), 3.78 (s, 3H), 2.62 (qd, 1H, *J* = 7.3, 4.4 Hz), 1.34 (d, 3H, *J* = 7.3 Hz). **¹³C NMR** (150 MHz) δ (ppm): 205.9 (Cq), 160.2 (Cq), 154.6 (Cq), 153.6 (Cq), 148.8 (Cq), 144.6 (Cq), 131.0 (Cq), 130.0 (CH), 120.4 (CH), 114.0 (CH), 112.2 (CH), 105.9 (CH), 102.4 (CH₂),

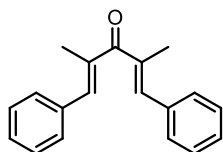
102.2 (CH), 55.4 (CH₃), 53.8 (CH), 53.7 (CH), 14.8 (CH₃). **GC-MS** *m/z* (%): 296 [M]⁺ (100), 281 (52).

General procedure for the aldol condensation of 3-pentanone and aldehydes^[22]



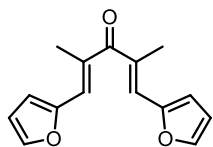
3-Pentanone (1.0 eq, 10–20 mmol) was mixed with the aldehyde (2.5 eq) and the mixture was added to a flask already containing KOH (2.5 eq) in 2:1 MeOH/H₂O (1.0 M towards 3-pentanone). The mixture was stirred at reflux overnight, then it was cooled down. A 1.0 M solution of HCl was added until the pH was 7. The mixture was extracted three times with DCM; the combined organic layers were dried over anhydrous Na₂SO₄, filtered and the solvent was evaporated under reduced pressure. The crude product was recrystallised with MeOH to afford pure dienone.

(1E,4E)-2,4-dimethyl-1,5-diphenylpenta-1,4-dien-3-one, **1a**^[22]



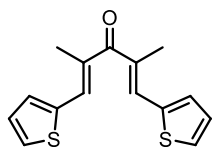
Synthesised according to the general procedure. White solid, 45% yield. **¹H NMR** (600 MHz) δ (ppm): 7.45–7.39 (m, 8H), 7.35–7.32 (m, 2H), 7.22–7.20 (m, 2H), 2.21 (d, 6H, *J* = 1.6 Hz). **GC-MS** *m/z* (%): 262 [M]⁺ (60), 247 (18), 144 (17), 116 (100), 115 (62).

(1E,4E)-1,5-di(furan-2-yl)-2,4-dimethylpenta-1,4-dien-3-one, **1b**^[22]



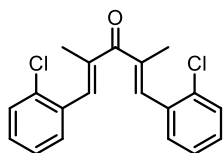
Synthesised according to the general procedure. Yellow solid, 45% yield. **¹H NMR** (600 MHz) δ (ppm): 7.54 (d, 2H, *J* = 1.8 Hz), 2.27 (s, 2H), 6.61 (d, 2H, *J* = 3.4 Hz), 6.52 (dd, 2H, *J* = 3.6, 1.8 Hz), 2.25 (d, 6H, *J* = 1.3 Hz). **GC-MS** *m/z* (%): 242 [M]⁺ (100), 227 (10), 106 (24), 77 (45).

(1E,4E)-2,4-dimethyl-1,5-di(thiophen-2-yl)penta-1,4-dien-3-one, **1c**^[22]



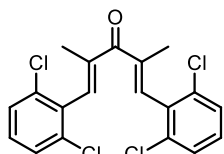
Synthesised according to the general procedure. Yellow solid, 49% yield. **¹H NMR** (600 MHz) δ (ppm): 7.52 (d, 2H, *J* = 5.0 Hz), 7.36 (s, 2H), 7.25 (d, 2H, *J* = 3.7 Hz), 7.13 (dd, 2H, *J* = 5.1, 3.6 Hz), 2.28 (d, 6H, *J* = 1.3 Hz). **GC-MS** *m/z* (%): 274 [M]⁺ (100), 259 (64), 231 (32), 151 (30), 123 (40), 122 (74).

(1*E*,4*E*)-1,5-bis(2-chlorophenyl)-2,4-dimethylpenta-1,4-dien-3-one, **1d**^[22]



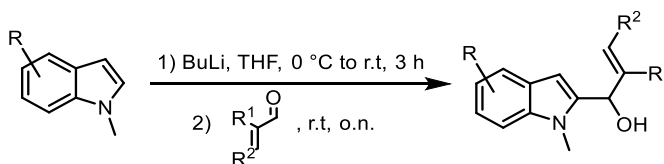
Synthesised according to the general procedure. White solid, 75% yield. **¹H NMR** (600 MHz) δ (ppm): 7.44 (dd, 2H, $J = 7.7, 1.5$ Hz), 7.41 (s, 2H), 7.40 (dd, 2H, $J = 7.6, 1.9$ Hz), 7.33–7.36 (m, 4H), 2.07 (d, 6H, $J = 1.5$ Hz). **GC-MS** m/z (%): 294 (22), 236 (45), 234 (100).

(1*E*,4*E*)-1,5-bis(2,6-dichlorophenyl)-2,4-dimethylpenta-1,4-dien-3-one, **1e**^[22]



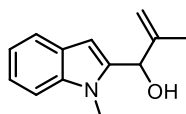
Synthesised according to the general procedure. White solid, 55% yield. **¹H NMR** (600 MHz) δ (ppm): 7.37 (d, 4H, $J = 8.2$ Hz), 7.27–7.26 (m, 2H), 7.23 (t, 2H, $J = 8.1$ Hz), 1.86 (d, 6H, $J = 1.4$ Hz). **GC-MS** m/z (%): 402 [M+4]⁺ (9), 400 [M+2]⁺ (18), 398 [M]⁺ (14), 367 (33), 365 (95), 363 (100), 177 (58), 150 (44), 149 (82), 115 (80).

General procedure for the synthesis of indole alcohols^[23]



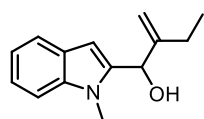
A solution of *N*-methylindole (1.0 eq, 1.0–5.0 mmol) in anhydrous THF (0.6 M), in a Schlenk flask under N₂ atmosphere, was cooled down to 0 °C. *n*-BuLi (1.2 eq, 2.5 M solution in hexane) was added and the mixture was stirred at room temperature for 3 h. Then, the α,β -unsaturated aldehyde (1.1 eq) was added and the mixture was stirred at room temperature overnight. After that time, the mixture was cooled down again to 0 °C and a saturated NH₄Cl solution was added. The mixture was extracted three times with Et₂O; the combined organic layers were dried over anhydrous Na₂SO₄, filtered and the solvent was evaporated under reduced pressure. The crude product was purified by flash column chromatography to afford pure indole alcohol.

2-methyl-1-(1-methyl-1*H*-indol-2-yl)prop-2-en-1-ol^[23]



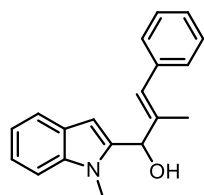
Synthesised according to the general procedure. Pale yellow oil, 74% yield. **R_f** 0.23 (9/1 PE/EtOAc). **¹H NMR** (600 MHz) δ (ppm): 7.58 (d, 1H, $J = 7.9$ Hz), 7.32 (dd, 1H, $J = 8.3, 1.0$ Hz), 7.24–7.21 (m, 1H), 7.12–7.08 (m, 1H), 6.44 (s, 1H), 5.34 (d, 1H, $J = 4.8$ Hz), 5.25–5.24 (m, 1H), 5.12 (q, 1H, $J = 1.5$ Hz), 3.78 (s, 3H), 1.99 (d, 1H, $J = 5.0$ Hz), 1.77 (s, 3H). **GC-MS** m/z (%): 201 [M]⁺ (54), 184 (100), 183 (46), 168 (35), 132 (40), 117 (28).

1-(1-methyl-1H-indol-2-yl)-2-methylenebutan-1-ol^[23]



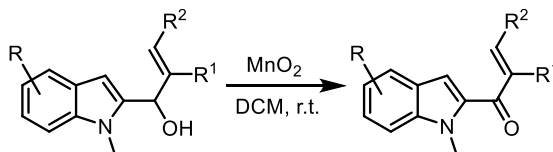
Synthesised according to the general procedure. Yellow oil, 50% yield. **R_f** 0.19 (9/1 PE/EtOAc). **¹H NMR** (600 MHz) δ (ppm): 7.58 (d, 1H, J = 7.7 Hz), 7.31 (d, 1H, J = 8.3 Hz), 7.24–7.21 (m, 1H), 7.12–7.09 (m, 1H), 6.43 (s, 1H), 5.38 (d, 1H, J = 4.7 Hz), 5.29–5.28 (m, 1H), 5.14–5.12 (m, 1H), 3.76 (s, 3H), 2.15–2.07 (m, 1H), 2.07–2.00 (m, 1H) superimposed to 2.00 (d, 1H, J = 5.0 Hz), 1.06 (t, 3H, J = 7.3 Hz). **GC-MS** m/z (%): 215 [M]⁺ (67), 198 (100), 182 (41), 144 (40), 132 (62), 117 (34).

(E)-2-methyl-1-(1-methyl-1H-indol-2-yl)-3-phenylprop-2-en-1-ol^[24]



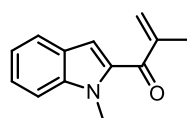
Synthesised according to the general procedure. White solid, 93% yield. **R_f** 0.32 (85/15 PE/EtOAc). **¹H NMR** (600 MHz) δ (ppm): 7.60 (dd, 1H, J = 7.9 Hz, 1.0 Hz), 7.38–7.32 (m, 5H), 7.27–7.21 (m, 2H), 7.12–7.09 (m, 1H), 7.82–7.80 (m, 1H), 6.51 (s, 1H), 5.48 (d, 1H, J = 4.8 Hz), 3.82 (s, 3H), 2.09 (d, 1H, J = 4.9 Hz), 1.90 (d, 3H, J = 1.4 Hz). **GC-MS** m/z (%): 277 [M]⁺ (27), 260 (34), 259 (100), 244 (66).

General procedure for the oxidation of indole alcohols to indole dienones^[25]



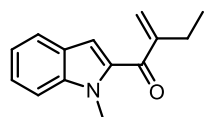
To a solution of indole alcohol (1.0 eq, 1.0–3.0 mmol) in DCM (0.1 M towards the substrate), stirring at room temperature, 12 eq of MnO₂ were added portionwise (approximately 2 eq every 10 min). Then, the mixture was filtered through a celite pad and the solvent was evaporated under reduced pressure. The crude product was purified by flash column chromatography to afford pure indole dienone.

2-methyl-1-(1-methyl-1H-indol-2-yl)prop-2-en-1-one, **1f**^[23]



Synthesised according to the general procedure. Pale yellow solid, 73% yield. **R_f** 0.68 (9/1 PE/EtOAc). **¹H NMR** (600 MHz) δ (ppm): 7.69–7.67 (m, 1H), 7.41–7.37 (m, 2H), 7.16 (ddd, 1H, J = 7.9, 6.2, 1.7 Hz), 7.10–7.09 (m, 1H), 4.02 (s, 3H), 2.10–2.09 (m, 3H). **GC-MS** m/z (%): 199 [M]⁺ (100), 184 (26), 171 (42), 158 (40), 156 (34), 144 (48), 89 (76).

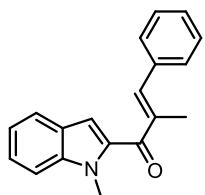
1-(1-methyl-1H-indol-2-yl)-2-methylenebutan-1-one, **1g**^[23]



Synthesised according to the general procedure. Yellow oil, 86% yield. **R_f** 0.77 (9/1 PE/EtOAc). **¹H NMR** (600 MHz) δ (ppm): 7.68 (dt, 1H, J = 7.9, 1.1 Hz), 7.41–7.37 (m, 2H), 7.16 (ddd, 1H, J = 7.9, 6.1, 1.7 Hz), 7.10 (s, 1H), 5.80 (d, 1H, J = 1.0 Hz), 5.74 (q, 1H, J = 1.5 Hz), 4.04 (s,

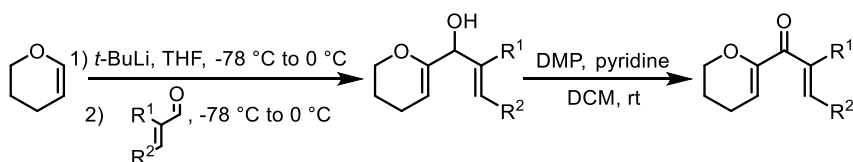
3H), 2.53–2.49 (m, 2H), 1.14 (t, 3H, $J = 7.4$ Hz). **GC-MS** m/z (%): 213 $[M]^+$ (100), 198, (46), 184 (26), 170 (55), 159 (42), 144 (60), 131 (34), 89 (67).

(*E*)-2-methyl-1-(1-methyl-1*H*-indol-2-yl)-3-phenylprop-2-en-1-one, **1h**^[24]



Synthesised according to the general procedure. Yellow solid, 70% yield. **R_f** 0.66 (9/1 PE/EtOAc). **¹H NMR** (600 MHz) δ (ppm): 7.68 (dt, 1H, $J = 8.3, 1.1$ Hz), 7.50–7.49 (m, 1H), 7.48–7.41 (m, 5H), 7.40–7.37 (m, 1H), 7.37–7.34 (m, 1H), 7.17 (ddd, 1H, $J = 8.0, 6.8, 1.3$ Hz), 7.08 (d, 1H, $J = 0.8$ Hz), 4.04 (s, 3H), 2.29 (d, 3H, $J = 1.4$ Hz). **GC-MS** m/z (%): 275 $[M]^+$ (100), 260 (29), 232 (30), 89 (35).

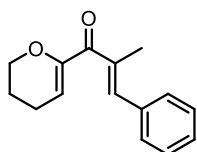
General procedure for the synthesis of dihydropyranyl dienones^[25]



A solution of 3,4-dihydropyran (1.0 eq, 5.0 mmol) in anhydrous THF (1.0 M) was cooled down to -78 °C. *t*-BuLi (1.1 eq, 1.7 M solution in pentane) was added dropwise and the mixture was allowed to warm to 0 °C and stirred for 30 min at that temperature. Then, the mixture was cooled down again to -78 °C and the α,β -unsaturated aldehyde (1.1 eq) was added. The mixture was allowed to warm to 0 °C and it was stirred for 10 min, then H_2O was added and the mixture was extracted three times with EtOAc; the combined organic layers were dried over anhydrous Na_2SO_4 , filtered and the solvent was evaporated under reduced pressure. The crude product was used directly for the subsequent oxidation.

To a solution of Dess-Martin periodinane (1.1 eq) in DCM (0.3 M towards the substrate), pyridine (5.0 eq) was added. The mixture was stirred for 5 min, then the alcohol substrate (1.0 eq, crude from the previous step) in solution of DCM was added. The mixture was stirred for 30 min, then a 3 M NaOH solution was added and the mixture was stirred for 10 min before extracting three times with DCM. The combined organic layers were washed with brine, dried over anhydrous Na_2SO_4 , filtered and the solvent was evaporated under reduced pressure. The crude product was purified by flash column chromatography to afford pure pyranal dienone.

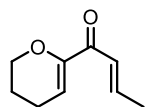
1-(3,4-dihydro-2*H*-pyran-6-yl)-2-methyl-3-phenylprop-2-en-1-one, **1i**^[25]



Synthesised according to the general procedure. Colourless oil, 39% yield (2-steps). **R_f** 0.36 (9/1 PE/EtOAc). **¹H NMR** (600 MHz) δ (ppm): 7.42–7.38 (m, 4H), 7.34–7.31 (m, 1H), 7.25–7.24 (m, 1H), 5.83 (t, 1H, $J = 4.2$ Hz), 4.18–4.16 (m, 2H), 2.26 (td, 2H, $J = 6.4, 4.2$ Hz), 2.14 (d, 3H, $J =$

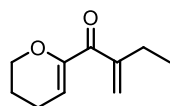
1.4 Hz), 1.94–1.90 (m, 2H). **GC-MS** m/z (%): 228 [M]⁺ (79), 227 (34), 213 (38), 200 (84), 199 (39), 129 (30), 117 (62), 115 (100), 91 (37).

1-(3,4-dihydro-2H-pyran-6-yl)but-2-en-1-one, 1j^[26]



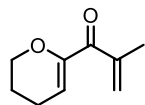
Synthesised according to the general procedure. Pale yellow oil, 37% yield (2-steps). **¹H NMR** (600 MHz) δ (ppm): 7.00 (dq, 1H, $J = 15.4, 6.9$ Hz), 6.67 (dq, 1H, $J = 15.3, 1.7$ Hz), 6.00 (t, 1H, $J = 4.3$ Hz), 4.11–4.08 (m, 2H), 2.23–2.20 (m, 2H), 1.90 (dd, 3H, $J = 6.9$ Hz, 1.7 Hz), 1.87–1.83 (m, 2H). **GC-MS** m/z (%): 152 [M]⁺ (33), 137 (31), 124 (25), 83 (13), 68 (100), 55 (22).

1-(3,4-dihydro-2H-pyran-6-yl)-2-methylenebutan-1-one, 1k^[25]



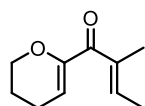
Synthesised according to the general procedure. Pale yellow oil, 35% yield (2-steps). **¹H NMR** (600 MHz) δ (ppm): 5.86 (t, 1H, $J = 4.2$ Hz), 5.58 (q, 1H, $J = 1.1$ Hz), 5.54 (q, 1H, $J = 1.5$ Hz), 4.13–4.10 (m, 2H), 2.35 (qt, 2H, $J = 7.6, 1.4$ Hz), 2.25–2.21 (m, 2H), 1.89–1.85 (m, 2H), 1.03 (t, 3H, $J = 7.5$ Hz). **GC-MS** m/z (%): 166 [M]⁺ (88), 123 (28), 111 (27), 83 (32), 55 (100).

1-(3,4-dihydro-2H-pyran-6-yl)-2-methylprop-2-en-1-one, 1l^[25]



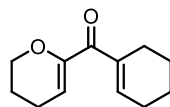
Synthesised according to the general procedure. Colourless oil, 26% yield (2-steps). **R_f** 0.45 (8/2 PE/EtOAc). **¹H NMR** (600 MHz) δ (ppm): 5.84 (t, 1H, $J = 4.2$ Hz), 5.65 (quin, 1H, $J = 1.0$ Hz), 5.62 (quin, 1H, $J = 1.5$ Hz), 4.12–4.09 (m, 2H), 2.21 (td, 2H, $J = 6.4, 4.2$ Hz), 1.93 (dd, 3H, $J = 1.6, 1.0$ Hz), 1.88–1.84 (m, 2H). **GC-MS** m/z (%): 152 [M]⁺ (100), 137 (10), 124 (35), 111 (24), 83 (24), 69 (73), 68 (24), 55 (80), 41 (72).

1-(3,4-dihydro-2H-pyran-6-yl)-2-methylbut-2-en-1-one, 1m^[25]



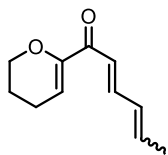
Synthesised according to the general procedure. Colourless oil, 31% yield (2-steps). **R_f** 0.50 (8/2 PE/EtOAc). **¹H NMR** (600 MHz) δ (ppm): 6.50–6.45 (m, 1H), 5.61 (t, 1H, $J = 4.2$ Hz), 4.09–4.06 (m, 2H), 2.18 (td, 2H, $J = 6.4, 4.1$ Hz), 1.87–1.82 (m, 2H), 1.81–1.78 (m, 6H). **GC-MS** m/z (%): 166 [M]⁺ (37), 151 (100), 138 (28), 123 (22), 83 (47), 55 (88).

cyclohex-1-en-1-yl(3,4-dihydro-2H-pyran-6-yl)methanone, 1n^[25]



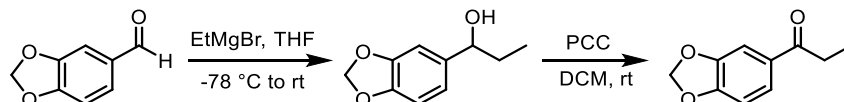
Synthesised according to the general procedure. Colourless oil, 24% yield (2-steps). **R_f** 0.20 (8/2 PE/EtOAc). **¹H NMR** (600 MHz) δ (ppm): 6.70–6.67 (m, 1H), 5.66 (t, 1H, $J = 4.2$ Hz), 4.10–4.07 (m, 2H), 2.28–2.24 (m, 2H), 2.23–2.17 (m, 4H), 1.88–1.83 (m, 2H), 1.66–1.57 (m, 4H). **GC-MS** m/z (%): 192 [M]⁺ (100), 164 (80), 163 (30), 149 (31), 136 (33), 135 (46), 109 (46), 108 (28), 81 (86), 79 (88), 77 (30), 55 (55), 53 (40).

1-(3,4-dihydro-2H-pyran-6-yl)hexa-2,4-dien-1-one, **1o**^[25]



Synthesised according to the general procedure. Colourless oil, 28% yield (2-steps). *R_f* 0.40 (8/2 PE/EtOAc). (**E**)-**1o** ¹H NMR (600 MHz) δ (ppm): 7.33–7.28 (m, 1H), 6.62 (d, 1H, *J* = 15.1 Hz), 6.25–6.16 (m, 2H), 5.99 (t, 1H, *J* = 4.3 Hz), 4.10–4.07 (m, 2H), 2.22–2.19 (m, 2H), 1.86–1.82 (m, 5H). **GC-MS** *m/z* (%): 178 [M]⁺ (65), 163 (100), 135 (50), 95 (70), 67 (64).

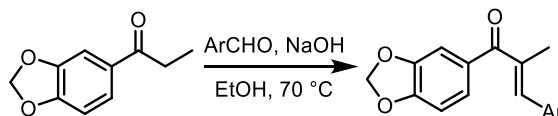
Synthesis of 1-(benzo[d][1,3]dioxol-5-yl)propan-1-one^[27]



A solution of piperonal (1.0 eq, 15 mmol) in anhydrous THF (0.3 M) was cooled down to -78 °C. EtMgBr (1.5 eq, 3.0 M solution in Et₂O) was added dropwise and the mixture was stirred for 30 min at that temperature. Then, the mixture was allowed to warm to room temperature. A 10% AcOH solution was added and the mixture was extracted three times with Et₂O; the combined organic layers were washed with water, dried over anhydrous Na₂SO₄, filtered and the solvent was evaporated under reduced pressure. The crude product was used directly for the subsequent oxidation.

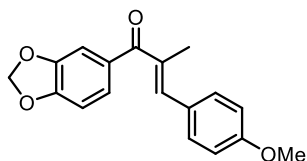
To a solution of the alcohol (1.0 eq) in DCM (0.25 M), pyridinium chlorochromate (1.3 eq) was added portionwise. The mixture was stirred until complete consumption of the starting material (GC-MS, 6 h), then it was filtered through a pad of celite and a pad of MgSO₄. The solvent was evaporated under reduced pressure to afford crude product, which was purified by flash column chromatography to afford pure ketone. White solid, 57% yield (2-steps). *R_f* 0.46 (9/1 PE/EtOAc) ¹H NMR (600 MHz) δ (ppm): 7.56 (dd, 1H, *J* = 8.2, 1.7 Hz), 7.44 (d, 1H, *J* = 1.7 Hz), 6.84 (d, 1H, *J* = 8.2 Hz), 6.03 (s, 2H), 2.92 (q, 2H, *J* = 7.2 Hz), 1.20 (t, 3H, *J* = 7.3 Hz). **GC-MS** *m/z* (%): 178 [M]⁺ (28), 149 (100), 121 (21).

General procedure for the synthesis of aryl vinyl ketones^[19]



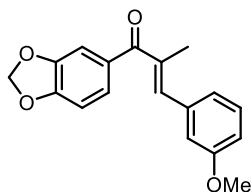
To a solution of NaOH (2.0 eq) in EtOH (0.5 M towards the substrate) the substrate (1.0 eq, 2.0 mmol) and the aldehyde (1.0 eq) were added and the mixture was stirred at 70 °C for 2–3 h. Then, a 1 M HCl solution was added and the mixture was extracted three times with EtOAc; the combined organic layers were dried over anhydrous Na₂SO₄, filtered and the solvent was evaporated under reduced pressure. The crude product was purified by flash column chromatography to afford pure aryl vinyl ketone as the product.

1-(benzo[d][1,3]dioxol-5-yl)-3-(4-methoxyphenyl)-2-methylprop-2-en-1-one, 1p^[19]



Synthesised according to the general procedure. White solid, 53% yield. **R_f** 0.25 (9/1 PE/EtOAc). **¹H NMR** (600 MHz) δ (ppm): 7.41–7.39 (m, 2H), 7.24 (dd, 1H, $J = 8.0, 1.7$ Hz), 7.28 (d, 1H, $J = 1.7$ Hz), 7.09 (br s, 1H), 6.95–6.92 (m, 2H), 6.85 (d, 1H, $J = 8.1$ Hz), 6.05 (s, 2H), 3.85 (s, 3H), 2.25 (d, 3H, $J = 1.4$ Hz). **GC-MS** m/z (%): 296 [M]⁺ (100), 295 (28), 281 (39), 188 (38), 149 (55), 121 (28).

1-(benzo[d][1,3]dioxol-5-yl)-3-(3-methoxyphenyl)-2-methylprop-2-en-1-one, 1q^[19]



Synthesised according to the general procedure. White solid, 49% yield. **R_f** 0.29 (9/1 PE/EtOAc). **¹H NMR** (600 MHz) δ (ppm): 7.38 (dd, 1H, $J = 8.1, 1.7$ Hz), 7.34–7.31 (m, 2H), 7.07 (br s, 1H), 7.01 (br d, 1H, $J = 7.5$ Hz), 6.93 (t, 1H, $J = 2.1$ Hz), 6.89 (br d, 1H, $J = 8.3$ Hz), 6.86 (d, 1H, $J = 8.1$ Hz), 6.05 (s, 2H), 3.83 (s, 3H), 2.24 (d, 3H, $J = 1.5$ Hz). **GC-MS** m/z (%): 296 [M]⁺ (100), 295 (29), 281 (22), 265 (24), 149 (64), 121 (21).

Preparation of the deep eutectic solvents

All the DESs were prepared according to literature procedures. The general procedure involves mixing of the two (or three) components of the mixture and stirring at a certain temperature until a clear homogeneous liquid is formed. Then, the mixture is stirred for another 20–30 min and finally cooled down to room temperature.

DES	mp (lit.)	T of preparation	reference
ChCl/malonic acid 1:1	10 °C	60 °C	[28]
ChCl/oxalic acid dihydrate 1:1	–40 °C ^a	60 °C	[29]
ChCl/citric acid 1:1	69 °C	100 °C	[28]
ChCl/maleic acid 1:1	not reported	100 °C	[30]
ChCl/L-(+)-lactic acid 1:2	–67 °C ^a	60 °C	[31]
ChCl/L-(-)-malic acid/H ₂ O 1:1:2	–71 °C ^a	80 °C	[32]
ChCl/L-(+)-tartaric acid 1:1	47 °C	100 °C	[33]
ChCl/TsOH monohydrate 1:2	12 °C	60 °C	[20]
ChCl/R-(-)-mandelic acid 1:1	not reported	60 °C	[34]
betaine/malonic acid 1:2	not reported	90 °C	[35]
L-proline/oxalic acid dihydrate 1:1	–14.5 °C	60 °C	[33]
ChCl/H ₂ O 1:2	not reported	60 °C	[36]

^a glass transition temperature (T_g)

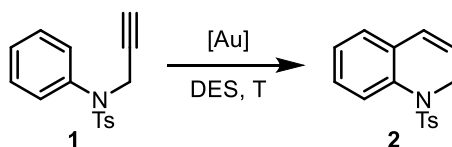
References

- [1] a) K. L. Habermas, S. E. Denmark, T. K. Jones, *Org. React.* **2004**, *45*, 1-158; b) M. A. Tius, *Eur. J. Org. Chem.* **2005**, *2005*, 2193-2206; c) D. R. Wenz, J. Read de Alaniz, *Eur. J. Org. Chem.* **2015**, *2015*, 23-37.
- [2] a) W. T. Spencer III, T. Vaidya, A. J. Frontier, *Eur. J. Org. Chem.* **2013**, *2013*, 3621-3633; b) M. A. Tius, *Chem. Soc. Rev.* **2014**, *43*, 2979-3002.
- [3] a) N. Shimada, C. Stewart, M. A. Tius, *Tetrahedron* **2011**, *67*, 5851; b) T. Vaidya, R. Eisenberg, A. J. Frontier, *ChemCatChem* **2011**, *3*, 1531-1548; c) A. Frontier, C. Collison, **2005**; d) H. Pellissier, *Tetrahedron* **2005**, *27*, 6479-6517.
- [4] M. G. Vinogradov, O. V. Turova, S. G. Zlotin, *Org. Biomol. Chem.* **2017**, *15*, 8245-8269.
- [5] D. R. Williams, L. A. Robinson, C. R. Nevill, J. P. Reddy, *Angew. Chem. Int. Ed.* **2007**, *46*, 915-918.
- [6] G. Liang, Y. Xu, I. B. Seiple, D. Trauner, *J. Am. Chem. Soc.* **2006**, *128*, 11022-11023.
- [7] B. N. Kakde, N. Kumar, P. K. Mondal, A. Bisai, *Org. Lett.* **2016**, *18*, 1752-1755.
- [8] Out of 3110 "Reactions" results on Reaxys, 1408 are performed in DCM, 335 in DCE, 186 in chloroform, 364 in toluene. Data obtained in October 2020.
- [9] a) F. Dhoro, M. A. Tius, *J. Am. Chem. Soc.* **2005**, *127*, 12472-12473; b) S. Wang, R. William, K. K. G. E. Seah, X.-W. Liu, *Green Chem.* **2013**, *15*, 3180-3183.
- [10] K. Murugan, S. Srimurugan, C. Chen, *Chem. Commun.* **2010**, *46*, 1127-1129.
- [11] W. Cao, B. Yu, *Adv. Synth. Catal.* **2011**, *353*, 1903-1907.
- [12] Y. Shimoda, H. Yamamoto, *Tetrahedron Lett.* **2015**, *56*, 3090-3092.
- [13] Z. Daneshfar, A. Rostami, *RSC Adv.* **2015**, *5*, 104695-104707.
- [14] M. Barbero, S. Cadamuro, A. Deagostino, S. Dughera, P. Larini, E. G. Occhiato, C. Prandi, S. Tabasso, R. Vulcano, P. Venturello, *Synthesis* **2009**, *2009*, 2260-2266.
- [15] P. Yates, N. Yoda, W. Brown, B. Mann, *J. Am. Chem. Soc.* **1958**, *80*, 202-205.
- [16] a) B.-Y. Zhao, P. Xu, F.-X. Yang, H. Wu, M.-H. Zong, W.-Y. Lou, *ACS Sust. Chem. Eng.* **2015**, *3*, 2746-2755. See also: b) M. Amere, J. Blanchet, M.-C. Lasne, J. Rouden, *Tetrahedron Lett.* **2008**, *49*, 2541-2545.
- [17] R. Williams, W. Jencks, F. Westheimer, *pKa data compiled by R. Williams*. Available online: https://www.chem.wisc.edu/areas/reich/pkatable/pKa_compilation-1-Williams.pdf, **2004**.
- [18] A. Skulcova, A. Russ, M. Jablonsky, J. Sima, *BioResources* **2018**, *13*, 5042-5051.
- [19] X. Zhou, Y. Zhao, Y. Cao, L. He, *Adv. Synth. Catal.* **2017**, *359*, 3325-3331.
- [20] N. R. Rodriguez, D. Salvachúa, R. Katahira, B. Black, N. Cleveland, M. Reed, H. Smith, E. Baidoo, J. Keasling, B. Simmons, *ACS Sustainable Chem. Eng.* **2019**, *5*, 8171-8180.
- [21] R. A. Sheldon, *Pure Appl. Chem.* **2000**, *72*, 1233-1246. 25 g of H₂O were employed for dissolving the DES at the end of the reaction and rinsing; 15 g out 25 g of H₂O were recovered from the evaporation and used for the same purpose in the second cycle.
- [22] Z. Daneshfar, A. Rostami, *RSC Adv.* **2015**, *5*, 104695-104707.
- [23] G.-P. Wang, M.-Q. Chen, S.-F. Zhu, Q.-L. Zhou, *Chem. Sci.* **2017**, *8*, 7197-7202.
- [24] L. Süsse, M. Vogler, M. Mewald, B. Kemper, E. Irran, M. Oestreich, *Angew. Chem. Int. Ed.* **2018**, *57*, 11441-11444.
- [25] G. Liang, S. N. Gradl, D. Trauner, *Org. Lett.* **2003**, *5*, 4931-4934.
- [26] K. Murugan, S. Srimurugan, C. Chen, *Chem. Commun.* **2010**, *46*, 1127-1129.

- [27] A. Joncour, A. Décor, S. Thoret, A. Chiaroni, O. Baudoin, *Angew. Chem. Int. Ed.* **2006**, *45*, 4149-4152.
- [28] A. P. Abbott, D. Boothby, G. Capper, D. L. Davies, R. K. Rasheed, *J. Am. Chem. Soc.* **2004**, *126*, 9142-9147.
- [29] M. Francisco, A. van den Bruinhorst, M. C. Kroon, *Angew. Chem. Int. Ed.* **2013**, *52*, 3074-3085.
- [30] Y. H. Choi, J. van Spronsen, Y. Dai, M. Verberne, F. Hollmann, I. W. Arends, G.-J. Witkamp, R. Verpoorte, *Plant Physiol.* **2011**, *156*, 1701-1705.
- [31] M. Francisco, A. van den Bruinhorst, L. F. Zubeir, C. J. Peters, M. C. Kroon, *Fluid Phase Equilib.* **2013**, *340*, 77-84.
- [32] Y. Dai, J. van Spronsen, G.-J. Witkamp, R. Verpoorte, Y. H. Choi, *Anal. Chim. Acta* **2013**, *766*, 61-68.
- [33] D. A. Alonso, A. Baeza, R. Chinchilla, G. Guillena, I. M. Pastor, D. J. Ramón, *Eur. J. Org. Chem.* **2016**, *2016*, 612-632.
- [34] H. Matsumiya, T. Hara, *Biomass and Bioenergy* **2015**, *72*, 227-232.
- [35] F. Cardellini, M. Tiecco, R. Germani, G. Cardinali, L. Corte, L. Roscini, N. Spreti, *RSC Adv.* **2014**, *4*, 55990-56002.
- [36] C. Vidal, J. García-Álvarez, A. Hernán-Gómez, A. R. Kennedy, E. Hevia, *Angew. Chem. Int. Ed.* **2014**, *53*, 5969-5973.

Appendix: Gold(I)-catalysed hydroarylation reactions in deep eutectic solvents

In Section 5.2.2, the recent developments on gold(I) catalysis in deep eutectic solvents have been presented. The group of García-Álvarez successfully employed mono- and dinuclear iminophosphorane gold(I) complexes to promote *N*- and *O*-cyclisation reactions in DESs, without the need of a silver(I) co-catalyst as chloride scavenger.^[1] However, more common and commercially available Au(I) complexes were not considered in those studies. We thus wanted to investigate the possibility to perform the Au(I)-catalysed intramolecular hydroarylation of *N*-propargyl-*N*-tosylaniline **1** in DESs (Scheme A.1), through activation of commercial [LAuCl] complexes by the H-bonding interactions of the eutectic mixture. As introduced in Section 1.3.1, the hydroarylation of substrate **1** is a known reaction that was studied under classical conditions, obtaining good results with various Au(I) complexes.^[2]



Conditions

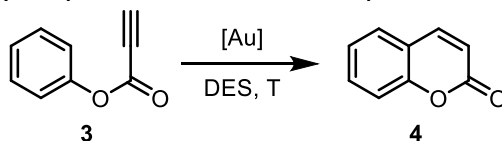
- [Au] = [(Ph₃P)AuCl] or [((2,4-^tBu₂C₆H₃O)₃P)AuCl] or [(JohnPhos)AuCl] or [(IPr)Au(NTf₂)]
DES = ChCl/Gly 1:2 or ChCl/urea 1:2 or ChCl/H₂O 1:2
room temperature or 60 °C
- [Au] = [(Ph₃P)AuCl] or [((2,4-^tBu₂C₆H₃O)₃P)AuCl] or [(JohnPhos)AuCl] or [(IPr)Au(NTf₂)]
DES = ChCl/Gly 1:2 or ChCl/urea 1:2 or ChCl/H₂O 1:2
100 μl CPME or toluene
room temperature or 60 °C
- [Au] = [(Ph₃P)AuCl] or [((2,4-^tBu₂C₆H₃O)₃P)AuCl] or [(JohnPhos)AuCl] or [(IPr)AuCl] or [(*p*-CF₃Ph)₃P)AuCl]
DES = ChCl/malonic acid 1:1 or thymo/menthol 1:1 or thymol/capric acid 0.3:0.7
room temperature

Scheme A.1 Screening of conditions for the gold(I)-catalysed hydroarylation of **1**.

General conditions: 0.1 mmol **1**, 0.005 mmol [Au], 0.5 g of DES, 16 h. The conversion was evaluated by ¹H NMR at 600 MHz using *n*-heptane as internal standard.

We started our investigation with a first set of reactions in which **1** was mixed with different combinations of Au(I) complexes and deep eutectic solvents. The DESs employed were ChCl/Gly in 1:2 molar ratio, ChCl/urea 1:2 e ChCl/H₂O 1:2 (Scheme A.1, a). After 16 hours at room temperature, no conversion was observed, and the starting material was recovered unaltered. Raising the temperature to 60 °C did not change the outcome of the reaction. It ought to be noted that not only

gold(I) chloride complexes were inactive in promoting the reaction, but also [(IPr)Au(NTf₂)] afforded 0% conversion under these conditions. Since both the substrate and the Au(I) catalyst appeared to be slightly soluble in the considered DESs, we envisaged that the addition of a co-solvent could be beneficial to the outcome of the reaction. Conversely, when we added cyclopentyl methyl ether or toluene to the reaction mixture (Scheme A.1, b), no improvements were detected in terms of conversion, which remained 0%. At last, we tested other DESs such as the acidic ChCl/malonic acid 1:1 and the hydrophobic thymol/menthol 1:1 and thymol/capric acid 0.3:0.7 (Scheme A.1, c).^[3] In these cases too, the conversion of **1** into the expected bicyclic product **2** did not take place.



Conditions

[Au] = [(Ph₃P)AuCl] or [((2,4-^tBu₂C₆H₃O)₃P)AuCl] or [(JohnPhos)AuCl] or [(JohnPhos)Au(NCMe)]SbF₆
 DES = ChCl/Gly 1:2 or ChCl/urea 1:2 or ChCl/H₂O 1:2
 room temperature

Scheme A.2 Screening of conditions for the gold(I)-catalysed hydroarylation of **3**.
 General conditions: 0.1 mmol **3**, 0.005 mmol [Au], 0.5 g of DES, 16 h. The conversion was evaluated by ¹H NMR at 600 MHz using *n*-heptane as internal standard.

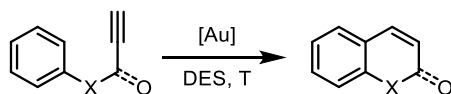
We then tested a similar substrate, *i.e.* phenyl propiolate **3**, which should undergo hydroarylation into 2H-chromen-2-one **4** (Scheme A.2).^[4] Compared to **1**, the alkyne moiety in **3** is expected to be more electrophilic because of the conjugation with the carboxylic group. Unfortunately, when we reacted substrate **3** under the conditions described in Scheme A.2, we only observed cleavage of the ester functionality, as the sole product of the reaction was phenol. We did not perform any further catalytic test on this substrate.

Based on these negative results, we reasoned that the possible explanation for the lack of reactivity in the gold(I)-catalysed hydroarylation of **1** could reside either in the low solubility of the Au(I) complexes in DESs, or in the fact that maybe the eutectic mixture is actually not able to activate the gold(I) chloride by hydrogen bonding interaction, as initially envisaged. Indeed, it is possible that the iminophosphorane complexes reported by García-Álvarez are active as chlorides independently from the solvent in which the reaction is performed. It should also be noted that, compared to García-Álvarez's studies, we employed weaker nucleophiles, such as aryl rings, instead of *O*- and *N*-nucleophiles. Further investigation is required to verify whether more polar or cationic ligands on the

gold(I) complex would enable the reaction to take place, either because of their increased solubility or electrophilicity. On this regard, the pyridinium phosphine Au(I) complexes developed by Alcarazo will be tested.^[5]

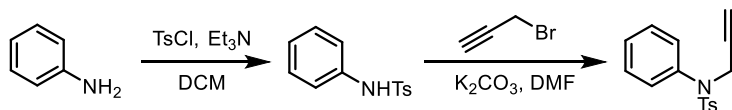
Experimental section

Catalysis tests



Into a vial, *N*-propargyl-*N*-tosylaniline **1** or phenyl propiolate **3** (1.0 eq, 0.1 mmol) and the Au(I) complex (0.05 eq) were added. Then, 0.5 g of DES were added and the mixture was stirred at room temperature or at 60 °C for 16 h. Then, CDCl₃ (1.0 ml) and *n*-heptane (0.2 mmol) were added, the mixture was stirred for 10-30 s and a sample was taken for ¹H NMR analysis.

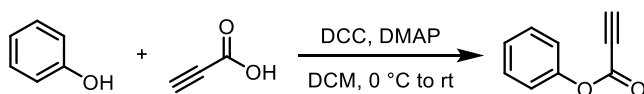
Synthesis of *N*-propargyl-*N*-tosylaniline, **1**^[6]



A solution of aniline (1.0 eq, 5.0 mmol) and triethylamine (1.5 eq) in DCM (0.2 M) was cooled down to 0 °C, then *p*-toluenesulfonyl chloride (1.2 eq) was slowly added and the mixture was stirred at rt for 1 h. Then, a 1.0 M solution of HCl was added and the mixture was extracted three times with DCM. The combined organic layers were washed three times with a 1.0 M solution of NaOH and discarded. The basic aqueous layers were combined and neutralized with a 1.0 M solution of HCl, then the organic product was extracted three times with DCM. The combined organic layers were dried over anhydrous Na₂SO₄, filtered and the solvent evaporated under reduced pressure to afford *N*-tosylaniline as the product.

N-tosylaniline (1.0 eq) and K₂CO₃ (2.0 eq) were dissolved in DMF (0.4 M) and propargyl bromide (1.5 eq) was slowly added. The mixture was stirred overnight, then a 1.0 M solution of HCl was added and the mixture was extracted three times with Et₂O; the combined organic layers were dried over anhydrous Na₂SO₄, filtered and the solvent was evaporated under reduced pressure. The crude product was purified by flash column chromatography to afford pure *N*-propargyl-*N*-tosylaniline **3** as the product. White solid. *R*_f 0.33 (6/4 PE/DCM). ¹H NMR (600 MHz, CDCl₃) δ (ppm): 7.56–7.53 (m, 2H), 7.34–7.30 (m, 3H), 7.25–7.21 (m, 4H), 4.44 (d, 2H, *J* = 2.5 Hz), 2.42 (s, 3H), 2.16 (t, 1H, *J* = 2.5 Hz). GC-MS *m/z* (%): 286 [M]⁺ (13), 285 (71), 220 (32), 182 (52), 155 (21), 130 (100), 129 (63), 103 (56), 91 (80), 77 (69), 65 (25).

Synthesis of phenyl propiolate, **3**⁷¹



To a solution of phenol (1.0 eq, 10 mmol) and propiolic acid (1.1 eq) in anhydrous DMF (12 ml), at 0 °C in a three-neck flask under N₂ atmosphere, a solution of *N,N'*-dicyclohexylcarbodiimide (1.1 eq) and *N,N*-dimethylaminopyridine (0.01 eq) in anhydrous DMF (12 ml) was added. The mixture was allowed to warm up to room temperature and was then stirred overnight. Then, the mixture was filtered over celite and the volatiles were removed under reduced pressure. The crude product was purified by flash column chromatography to afford pure phenyl propiolate **4**. Colourless liquid. *R_f* 0.36 (95/5 PE/Et₂O). ¹H NMR (600 MHz, CDCl₃) δ (ppm): 7.43–7.39 (m, 2H), 7.29–7.26 (m, 1H), 7.17–7.14 (m, 3H), 3.07 (s, 1H). GC-MS *m/z* (%): 146 [M]⁺ (46), 145 (26), 128 (54), 94 (40), 90 (100), 53 (67), 65 (27), 39 (23).

References

- [1] a) M. J. Rodríguez-Álvarez, C. Vidal, J. Díez, J. García-Álvarez, *Chem. Commun.* **2014**, *50*, 12927-12929; b) C. Vidal, L. Merz, J. García-Álvarez, *Green Chem.* **2015**, *17*, 3870-3878. See also: c) M. J. Rodríguez-Álvarez, C. Vidal, S. Schumacher, J. Borge, J. García-Álvarez, *Chem. Eur. J.* **2017**, *23*, 3425-3431.
- [2] a) C. Nevado, A. M. Echavarren, *Chem. Eur. J.* **2005**, *11*, 3155-3164; b) R. S. Menon, A. D. Findlay, A. C. Bissember, M. G. Banwell, *J. Org. Chem.* **2009**, *74*, 8901-8903; c) D. Ding, T. Mou, M. Feng, X. Jiang, *J. Am. Chem. Soc.* **2016**, *138*, 5218-5221; d) T. Vacala, L. P. Bejcek, C. G. Williams, A. C. Williamson, P. A. Vadola, *J. Org. Chem.* **2017**, *82*, 2558-2569.
- [3] N. Schaeffer, M. A. Martins, C. M. Neves, S. P. Pinho, J. A. Coutinho, *Chem. Commun.* **2018**, *54*, 8104-8107.
- [4] a) A. Cervi, P. Aillard, N. Hazeri, L. Petit, C. L. Chai, A. C. Willis, M. G. Banwell, *J. Org. Chem.* **2013**, *78*, 9876-9882; b) A. C. Shaikh, S. Shalini, R. Vaidhyanathan, M. V. Mane, A. K. Barui, C. R. Patra, Y. Venkatesh, P. R. Bangal, N. T. Patil, *Eur. J. Org. Chem.* **2015**, *2015*, 4860-4867.
- [5] a) H. Tinnermann, C. Wille, M. Alcarazo, *Angew. Chem. Int. Ed.* **2014**, *53*, 8732-8736; b) M. Alcarazo, *Chem. Eur. J.* **2014**, *20*, 7868-7877; c) H. Tinnermann, L. D. Nicholls, T. Johannsen, C. Wille, C. Golz, R. Goddard, M. Alcarazo, *ACS Catal.* **2018**, *8*, 10457-10463.
- [6] E. Richmond, J. Moran, *J. Org. Chem.* **2015**, *80*, 6922-6929.
- [7] N. Coles, M. Mahon, R. Webster, *Chem. Commun.* **2018**, *54*, 10443-10446.



Università degli Studi di Torino

Doctoral School of the University of Torino

PhD Programme in Chemical and Materials Sciences, XXXIII cycle

**Lewis and Brønsted acid-catalysed synthetic transformations: new
avenues for C-C bond formation**

Candidate: **Stefano Nejrotti**

Supervisor: Prof. **Cristina Prandi**

Jury Members: Prof. **Vittorio Pace**
Università degli Studi di Torino
Dipartimento di Chimica

Prof. **Elisabetta Rossi**
Università degli Studi di Milano
Dipartimento di Scienze Farmaceutiche

Prof. **Antonio M. Echavarren**
Institut Català d'Investigació Química

Head of the Doctoral School: Prof. Alberto Rizzuti

PhD Programme Coordinator: Prof. Bartolomeo Civalleri

Torino, 2021